

**Integrating texture analysis and innovative modelling approaches for
capturing morphological diversities and dynamics of informal settlements
in Durban metropolitan area, South Africa**

Dadirai Matarira

217081922

**A thesis submitted in the fulfilment for the Degree of Doctor of Philosophy
in Environmental Sciences, under the School of Agricultural, Earth and
Environmental Sciences, University of KwaZulu-Natal.**

Supervisors: Professor Onesimo Mutanga

Professor Maheshvari Naidu

Westville, South Africa

December 2022

Abstract

Fast-growing urbanization trend is resulting in rampant social inequalities in most cities of the developing world. These inequalities are manifesting most clearly in the burgeoning and spread of informal settlements. With an estimated 1 billion informal settlement inhabitants worldwide, the United Nations has mandated member states to prioritize alleviation of living conditions for the urban poor in these deprived living spaces. In order to achieve their objectives, comprehensive information on the exact locations and dimensions of informal settlements is of vital importance. However, there is global lack of systematic empirical spatial documentation of the informal settlements. Diversities in their dynamic patterns and morphological appearances across locales or within the same geographical location present challenges in their semantic abstraction. Durban city is characterized by rapidly expanding and spatially heterogeneous informal settlement landscape. Although attempts have been made to map informal settlements in the city, there is paucity of documented research on comprehensive empirical investigation of informal settlements' spatial patterns and dynamics, and potential links between processes and patterns for Durban metropolitan area. The study could aid impact evaluation of intervention policies and assessment of environmental consequences, with implications on urban sustainability management and planning. Given this background, this study sought to exploit integration of various innovative mapping approaches with texture analysis to localize morphologic variations in informal settlement features as well as their dynamics in Durban Metropolitan area, South Africa. To attain this, five objectives were set. The initial objective brought forth a synopsis of texture analysis approaches in modelling informal settlements. The study examined factors such as algorithms, sensors, feature selection as well as scale of analysis. The results of the review confirmed progress in literature in the use of texture analysis. However, scant studies were observed in sub-Saharan Africa, with South African studies only concentrated in Johannesburg. Results also indicated underutilization of Sentinel-2A in mapping informal settlements. The second objective sought to exploit the potential of pan sharpening Sentinel-2A imagery for enhanced abstraction of morphologically varied informal settlements. Pan sharpening techniques were exploited on Sentinel-2A to make the most of the spectral resolution of Sentinel-2A data and the high spatial resolution of the 10 m bands. Higher spectral and spatial resolution of pan sharpened Sentinel-2A, integrated with image texture led to the highest informal settlement detection accuracy, with the best results achieved using Gram Schmidt algorithm (F-score-95.2%; Overall accuracy 91.8%). However, there remained a challenge of misidentification between informal settlements and formal areas

due to morphological similarity between informal settlements and other formal areas in Durban. The third objective developed an automated informal settlement mapping framework using Google Earth Engine (GEE) cloud computing, and assessed the relative value of various spectral and textural feature sets in characterizing spatial distribution of dynamic informal settlements in a complex and heterogeneous Durban landscape. Results indicated that random forest (RF) classification algorithm within the GEE was able to capture the diversities of informal settlements better than in studies that used classical image processing software. The spectral bands and texture features' model achieved highest accuracy level of 94%, whilst addition of spectral indices decreased classification accuracy. The fourth objective explored object-based image classification in GEE, using high resolution PlanetScope imagery for informal settlement mapping. Fusion of PlanetScope, Sentinel-2, and Sentinel-1 data was investigated using object-based image analysis approach within the GEE platform. The convenience of simple non-iterative clustering (SNIC) algorithm within the GEE, for segmentation, was explored in the context of informal settlement mapping. Results indicated higher levels of accuracy (F-score 94%, Overall accuracy, 95%) compared to other similar studies that used classical image processing softwares for object-based image analysis. Exploiting advantages of integrating sensors as well as cloud computing capabilities of GEE yielded added value to the characterization of informal settlement diversities in Durban. The final objective was to systematically analyse informal settlement growth patterns and related land cover/ land use transitions, between 2015 and 2021, using intensity analysis approach. The study involved linking of informal settlement growth patterns to processes. The results revealed a net increase (3%) in informal settlement area of coverage. Intensity analysis at category level indicated that informal settlements' gain was more active than the loss, with gain intensity of 72% against uniform intensity of 26%. The settlements avoided water. The transition level revealed systematic transition between informal settlement class and other urban class. The systematic process was found to be mainly influenced by South African government's restructuring initiatives in the form of upgrading programmes aimed at improving conditions in the deprived areas.

Different sets of experiments and different data inputs employed in the study presented relative merits of various mapping approaches in providing more nuanced extraction of informal settlement extents and dynamics. However, the study confirmed that complexities remain in urban environments that complicate applicability of approaches for informal settlement mapping. Grey level co-occurrence matrix (GLCM) image texture coupled with robustness and

operationalization of GEE cloud computing platform presented enhanced potential in capturing inherent complexities of informal settlements. Even so, the results of mapping remain contingent upon various factors ranging from image spatial resolution, fragmentation of landscape under investigation, intricate relations between land cover categories, and the selection of pertinent textural features. An approach that precisely captures diversities of urban deprivation pockets, through integration of field surveys, would be crucial for promoting research on socio-ecological dynamics, urban sustainability, urban risk management as well as informed decision making.

Keywords: Urbanization, unplanned settlements, texture analysis, mapping, Google Earth Engine, Durban

Preface

This study was conducted in the School of Agricultural, Earth and Environmental Sciences, University of KwaZulu-Natal, Westville, South Africa, under the supervision of Professor Onesimo Mutanga and Professor Maheshvari Naidu from January 2020 to December 2022.

I declare that the current work represents my own ideas and has never been submitted to any other academic institutions. Acknowledgment has been duly made for statements originating from other authors.

Dadirai Matarira

Signed



..... Date 03/12/2022...

1. Professor Onesimo Mutanga (Supervisor) Signed



ate 03/12/2022.....

2. Professor Maheshvari (Co-Supervisor)

Signe



Date...04/12/2022...

Declaration 1: Plagiarism

I, Dadirai Matarira declare that:

1. The research reported in this dissertation is my original work unless otherwise indicated.
2. This dissertation has not been submitted for the attainment of a degree or examination purposes at another university.
3. This dissertation does not contain any data, graphics, and other information from other persons unless duly acknowledged.
4. This dissertation does not contain other persons' writings unless duly acknowledged as such. In cases where written sources have been cited;
 - a. Their words have been paraphrased and general information attributed to them has been referenced.
 - b. Where exact words have been used, they were placed inside quotation marks and referenced.
5. This dissertation does not contain text, graphics, and or tables directly copied and pasted from the internet unless otherwise sources were duly acknowledged within the content of this dissertation.

Signed..........

Date: ...03/12/22.....

Declaration 2: List of Publications and Manuscripts

1. **Matarira, D.,** Mutanga, O., & Naidu, M. (2022). Texture analysis approaches in modelling informal settlements: a review. *Geocarto International*, 37(26), 13451-13478, doi:10.1080/10106049.2022.2082541
2. **Matarira, D.,** Mutanga, O., & Naidu, M. (2022). Performance evaluation of pansharpening Sentinel 2A imagery for informal settlement identification by spectral-textural features. *Transactions of the Royal Society of South Africa*, 1-14. doi:10.1080/0035919x.2022.2144538
3. **Matarira, D.,** Mutanga, O., & Naidu, M. (2022). Google Earth Engine for Informal Settlement Mapping: A Random Forest Classification Using Spectral and Textural Information. *Remote Sensing*, 14(20). doi:10.3390/rs14205130
4. **Matarira, D.,** Mutanga, O., Naidu, M., & Vizzari, M. (2022). Object-Based Informal Settlement Mapping in Google Earth Engine Using the Integration of Sentinel-1, Sentinel-2, and PlanetScope Satellite Data. *Land*, 12(1). doi:10.3390/land12010099
5. **Matarira, D.,** Mutanga, O., Naidu, M., Mushore, T. D., & Vizzari, M. (2023). Characterizing Informal Settlement Dynamics Using Google Earth Engine and Intensity Analysis in Durban Metropolitan Area, South Africa: Linking Pattern to Process. *Sustainability*, 15(3). doi:10.3390/su15032724

Dedication

To
my late husband, Caxton

I have now completed the race. The race you boldly convinced me to begin. Your endless emotional and financial support have finally borne fruit. You always believed in me even when the journey was proving difficult. It's unfortunate you didn't manage to witness the end of it. You were going to be very proud of me. I thank you so much for having to look after the kids when I had to be fully involved. A selfless man.

To Tavonga and Tadiwa, thank you my babies for enduring my absence under very difficult circumstances. Thank you Tavo for looking after your brother in my absence. You are a great girl.

“To God Be the Glory”

Acknowledgements

First and foremost, all glory and honour to God, the Almighty, for all the blessings and guidance from the beginning of this journey to the end of it. I will keep trusting him for my future.

I would like to thank my esteemed supervisors, Prof. Onesimo Mutanga and Prof. Maheshvari Naidu, for their invaluable supervision, and tutelage during the course of my Ph.D. degree. This degree would not have been accomplished without their unwavering support and vital guidance. I am extremely grateful for their patience, motivation, scientific direction, invaluable critical comments, and mentorship until I managed to scientifically reason and eventually write well. I feel proud to have been under your supervision. I'd like to thank the UKZN-funded Big Data for Science and Society Project (BDSS) for the funding opportunity to undertake my studies. My gratitude extends to the NRF Chair in Land use Planning and Management (Grant no. 84157), for their generous financial support.

I am deeply grateful to Professor Vizzari for his kind help and treasured support in my research. Prof Odindi, thank you very much for your guidance and tremendous support throughout. I also acknowledge and give warmest thanks to my friends and colleagues in the Department; Dr Terrence Mushore, Dr Garikai Membele, Upenyu Mupfiga, Pride Mafuratidze, Collins, Dr Trylee Matongera, Dr Odebiri Omosalewa, Mthembeni Mngadi, Dr Tsitsi Bangira, Prof Timothy Dube, Dr Mbulisi Sibanda. Thank you very much for your academic support and encouragement throughout. To my LAN mates and colleagues, Pindile, Dudu, Anita, Adeola, Amanda, Xolile, Khaya and Samantha, I thank you for the cherished time we spent. Dr Henry Ndaimani, Dr Samuel Kusangaya, Samantha Kachuta, Sharon, Simbai, and Sam Radebe, I thank you very much for your support.

My appreciation also goes to my friends, Blessing Mangere, Shumi Machekanyanga, Rebecca Gono, Regina, Quincy, Mrs Mhazo, Tariro Saburi, Nancy Mahachi, Sithokozile Chamisa, Esnath Madziyauswa, and Mrs Bwanya for your collective efforts in parenting my kids in my absence, as I pursued my Ph.D. Thank you for looking after them and for your constant prayers and support. To Josephine Hapazari and family, I can't thank you enough. May God richly bless you. Mrs Makhanye, you are the best. To Joyce Mlay, thank you my sister for your support.

To my mother, sisters, Mukai, Vongai, Lucia, my uncle George Matizanadzo, Pride Matizanadzo and Mitchy, Sheila Matizanadzo, thank you for your support and encouragement during my study. God bless you all.

Table of Contents

Abstract.....	i
Preface.....	iv
Declaration 1: Plagiarism.....	v
Declaration 2: List of Publications and Manuscripts.....	vi
Dedication.....	vii
Acknowledgements.....	viii
Table of Contents.....	x
List of Tables.....	xiv
List of Figures.....	xv
List of Acronyms.....	xvii
CHAPTER ONE:.....	1
1.1 Introduction.....	1
1.2. Aim and objectives.....	7
1.3. Description of the study site.....	8
1.4. General structure of the thesis.....	9
CHAPTER TWO: LITERATURE REVIEW.....	12
2.1. Introduction.....	13
2.1.1. Conceptualizing informal settlements.....	14
2.1.1.1. Definitions.....	14
2.1.1.2. Morphology of informal settlement landscape.....	15
2.2. Satellite image texture analysis and informal settlement identification.....	16
2.3. Literature search methods.....	18
2.4. Meta-Data analysis.....	20
2.5. Results.....	20
2.5.1. Geographic location of texture analysis studies.....	20
2.5.2. Trends in texture analysis based on published articles.....	21
2.5.3. Satellite data types and texture analysis.....	22
2.5.4. Texture analysis approaches for the identification of informal settlements.....	23
2.5.5. Spatial analysis of informal settlement mapping studies.....	28
2.5.6. Texture feature selection.....	30
2.6. Comparison studies.....	30
2.6.1. Comparing methodological performance.....	30
2.6.2. Comparison of used classifiers.....	31

2.7. Effect of window size in informal settlement extraction	33
3. Discussion of results, gaps in knowledge and future directions	33
3.1. Geographic distribution of case studies	33
3.2. Application of texture analysis approaches for informal settlement modelling	36
3.2.1. Performance of texture analysis approaches in informal settlement mapping	36
3.2.2. Multiscale analysis.....	37
3.2.3. Application of machine learning in texture based informal settlement detection.	39
3.2.4. Spatial analysis of texture analysis algorithms	40
3.2.5. Effect of feature selection on classification	40
3.2.6. Comparisons between countries	41
3.3. Integrating texture analysis and socio-economic data	43
3.4. Limitations of texture analysis in informal settlement identification	44
3.5. Conclusion	44
3.6. Summary	45
CHAPTER THREE:	47
3.1. Introduction.....	48
3.2. Methods and Materials.....	51
3.2.1. Data and pre-processing.....	51
3.3. Methods.....	52
3.3.1. Pansharpening methods	53
3.3.2. Performance evaluation of the pan-sharpened images.....	56
3.3.3. Separability analysis	57
3.3.4. Texture feature extraction and analysis	57
3.3.5. Image classification	59
3.3.6. Accuracy assessment	60
3.4. Experimental Results	60
3.4.1. Establishing optimum window size	60
3.4.2. Spectral quality	61
3.4.3. Pan sharpening and interclass separability	61
3.4.4. Image classification results	63
3.5. Discussion	67
3.6. Conclusion	69
3.7. Summary	70
CHAPTER FOUR:.....	71
4.1. Introduction.....	73

4.2. Materials and Methods.....	77
4.2.1. Datasets	77
4.2.2. Methods.....	78
4.2.3. Feature Extraction	79
4.2.3.1. Spectral Features	79
4.2.3.2. GLCM Textural Features	80
4.2.4. Feature Combinations	81
4.2.5. Random Forest Classification	82
4.2.6. Variable Importance.....	83
4.2.7. Accuracy Assessment, Classification Comparison, and Statistical Testing	83
4.2.7.1 Pixel-Based Accuracy Assessment	83
4.2.7.2. Patch-Based Accuracy Assessment	84
4.2.7.3. Regression between Extracted Informal Settlement Areas and Ground Truth Data ..	85
4. 3. Results.....	86
4.3.1. Evaluation and Comparative Analysis of Classification Results.....	86
4.3.1.1. Visual Analysis of Different Feature Input Models.....	86
4.3.1.2. Accuracy Assessment and Analysis.....	87
4.3.1.3. Importance of Features for Informal Settlement Mapping	89
4.3.1.4. Feature Subset Evaluation.....	90
4.3.1.5. Patch-Based Accuracy Assessment	91
4.4. Discussion	94
4.5. Conclusions.....	97
CHAPTER FIVE:	99
5.1. Introduction.....	101
5.2. Methodology	105
5.2.2. Image segmentation with SNIC	107
5.2.3. Texture analysis	108
5.2.4. Object based Image Classification.....	109
5.2.6. Feature Importance Assessment	111
5.3. Results.....	111
5.3.1. Accuracy assessment of the LULC map.....	111
5.3.2. Relative contribution of input variables in RF classification.....	114
5.5. Conclusion	119
5.6. Summary	119
CHAPTER SIX:.....	120

6.1. Introduction.....	121
6.2. Materials and methods	125
6.2.1 Study area.....	125
6.2.2. Data collection and pre processing	128
6.2.3. Object based image classification	128
6.2.4. Land-Cover Transition Matrix	129
6.2.5. Intensity Analysis.....	129
6.2.5.1 Category level analysis	130
6.2.5.2 Transition level analysis	131
6.3. Results.....	132
6.3.1. Observed Patterns of LULC Change Dynamics	132
6.3.2. Intensity analysis.....	135
6.3.2.1. Category level	135
6.3.2.2. Transition level	136
6.4. Discussion	139
6.5. Conclusion	143
CHAPTER SEVEN:	145
7.1. Introduction.....	145
7.2. Conclusions.....	146
7.3. Challenges and Recommendations for the future	148
References.....	150

List of Tables

Table 2.1. Commonly used GLCM texture metrics and expected values for informal settlement areas	17
Table 2.2. Studies with well documented classifiers and accuracy levels.....	23
Table 2.3. Strengths and limitations of various texture analysis methods for informal settlement identification.....	26
Table 2.4. Studies of ISs in India using texture-based approaches classified by texture descriptor.....	29
Table 2.5. Studies of ISs in South Africa using texture-based approaches classified by texture descriptor.....	30
Table 3.2. Image texture measures derived from Sentinel-2A imagery for informal settlement extraction.....	58
Table 3.3. LULC classes	59
Table 3.4. Quantitative assessment of performance of pansharpening methods	61
Table 3.5. Classification results for the resampled and pan sharpened images.....	64
Table 3.6. Classification results for the 4 classification scenarios	65
Table 4.1. Image feature sets that were extracted from Sentinel 2A imagery.	79
Table 4.2. Spectral indices selected for research.	80
Table 4.3. Producer accuracy (%), user accuracy (%), average F-scores and standard deviation for different feature input models.	87
Table 4.4. Two sample <i>t</i> -tests for the mapping of informal settlements and their <i>p</i> values. ...	89
Table 4.5. Two sample <i>t</i> -tests for all variables vs feature subsets for feature input models. ..	91
Table 4.6. Spatial accuracy assessment results for area-based classification.	92
Table 5.1. Texture metrics computed using GLCM	108
Table 5.2. The optical, SAR, spectral and textural features applied to the classifications in this study	109
Table 5.3. The definitions of LULC classes	110
Table 5.4. Confusion matrix derived from LULC classification	113
Table 6.2. Summary of LULC map accuracies (%) for 2015 and 2021	133

List of Figures

Figure 1.1. Location of the study area	9
Figure 2.1a-e. Some examples of tree bark different textures. Sources: (Fekri-Ershad, 2020); (Baykal, 2019).....	18
Figure 2.2. The number of published articles for informal settlement mapping	19
Figure 2.3. Country level distribution of texture analysis studies for IS identification.....	21
Figure 2.4. Number of published articles from 2005 to 2021 (The dotted line indicates the trend line).....	22
Figure 2.5. Satellite data used for texture based informal settlement modelling.....	23
Figure 2.6. Studies that have used texture analysis approaches	25
Figure 2.7. Number of publications per year for GLCM.....	26
Figure 2.8. Frequency of classifiers.....	32
Figure 2.9. Overall accuracy of RF vs SVM	32
Figure 3.1. Technical flow chart.....	53
Figure 3.2. The structure of pansharpening procedure	56
Figure 3.3. Coefficient of variation curve using the mean feature for informal settlement classes	60
Figure 3.4. TDSI values for class pairs involving informal settlements.....	62
Figure 3.6. Classification results for the pan sharpened images.....	64
Figure 3.7. Classification results for the four classification scenarios	65
Figure 3.8. LULC map showing informal settlements for part of Durban Metro	66
Figure 4.1. Research workflow chart.....	78
Figure 4.2. Ground truth samples of informal settlements (A-G (red)).....	85
Figure 4.3. LULC maps obtained using different feature combinations from (a) Txts, (b) SIs, (c) SIs + Txts, (d) SBs + SIs + Txts (e) SBs + SIs, (f) SBs, (g) SBs + Txts.	87
Figure 4.4. Feature importance scores of the 10 most important features for the image combinations.....	90
Figure 4.5. Classified informal settlement patch areas (A-G (black)) for models (a) SBs, (b) SIs, (c)Txts, (d) SBs + SIs, (e) SBs + Txts, (f) SIs + Txts, (g) SBs + SIs + Txts, and corresponding ground truth polygons (A-G (red)).....	92
Figure 5.1. Workflow chart of the methodology	105
Figure 5.2. Comparison of results of informal settlements and LULC classification (a) and visual appearance of sample informal settlements on an RGB image (b) (circled in red)	112
Figure 5.3. Classified informal settlement patch areas against ground truth patch extents...	114
Figure 5.4. Importance assessment of LULC classification features.....	114
Figure 5.5. (a) shows misclassified informal settlement patches that on the ground (b) are commercial buildings. The black rectangles, (c) and (d), indicate misclassification of bare land (d) as informal settlement (c)(red patch). The red rectangle indicates missed informal settlement (c) that exists on the ground (d).....	117
Figure 6.1. Study area selected in KwaZulu-Natal province (a), within Durban Metropolis (b), South Africa. (c) is the overview of the area obtained with an RGB PlanetScope imagery, in UTM/WGS84 plane coordinate	126
Figure 6.3. (a) LULC map for 2015; and (b) LULC map for 2021.	133
Figure 6.4. Areal changes of land use categories in the study area from 2015 to 2021	134

Figure 6.5. (a) The category loss map; and (b) the category gain map for the time interval 2015 to 2021.	135
Figure 6.6. Intensity Analysis for category-level changes for each land category during the time interval 2015-2021	136
Figure 6.7. (a) Maps of land transitions to informal settlements, and (b) transitions from informal settlement for the 2015-2021 time period	137
Figure 6.8. Intensity of the observed transitions (a) given the gross gain of informal settlement, (b) gross gain of other urban, (c) gross gain of bare land, and (d) gross gain of vegetation.....	138
Figure 6.9. A representation of variation of uniform transition intensity of informal settlement during the 2015–2021time interval.....	139

List of Acronyms

ANN	Artificial Neural Network
BT	Brovey Transform
CART	Classification and Regression Trees
CBERS-4	China-Brazil Earth Resources Satellite
CNN	Convolutional Neural Networks
CS	Component substitution
DMP	Differential Morphological Profiles
DK-DCNN	Dilated kernel- based deep convolutional neural network
ENVI	Environment for visualizing images
ESRI	Environmental Systems Research Institute
ETM	Enhanced Thematic Mapper
FCNs	Deep fully convolutional networks
GEE	Google Earth Engine
GEOBIA	Geographical Object-Based Image Analysis
GLCM	Grey-level co-occurrence matrix
GS	Gram-Schmidt
IHS	Intensity, Hue, and Saturation
IS	Informal Settlement
LBP	Local Binary Patterns
LDA	Linear Discriminant Analysis
LR	Linear Regression
LSR	Line Support Regions
LULC	Land use/land cover change
MDM	Minimum Distance to mean Classifier
MKL-SVMs	Multi kernel learning-Support Vector Machines
MM	Mathematical Morphology
MRA	Multi-Resolution Analysis
Msh-Msi-MP	Multi Shape-Multi Size-Morphological Profile
Msh-Msi-MP-GF	Multi Shape-Multi Size-Morphological Profile-Guided Filter
OBIA	Object Based Image Analysis
OOA	Object Oriented Analysis
PAN	Panchromatic
PL	PlanetScope
RF	Random Forest
RGB	Red, Green Blue
RS	Remote Sensing
S1	Sentinel 1
S2	Sentinel 2
SLIC	Simple Linear Iterative Clustering
SM	Simple mean
SNIC	Simple Non-iterative Clustering

SVM	Support Vector Machine
SWIR	Short Wave Infrared
TDSI	Transformed Divergence Separability Index
UN	United Nations
UNDP	United Nations Development Programme
VHR	Very High Resolution

CHAPTER ONE:

General Introduction

1.1 Introduction

‘Slum settlements’, are a growing concern, globally. Mahabir et al. (2016) postulated that they have become almost ubiquitous in most developing countries that often lack infrastructure and resources to control their growth and expansion. Globalization has accelerated urbanized growth without matching capacity to provide the housing infrastructure that sufficiently keeps up with demand, as cities continue to grapple with the influx of people either from rural areas or neighbouring countries (Fox, 2014, Patel et al., 2015, UN-Habitat, 2015). The heterogenous process of urbanisation (Ooi and Phua, 2007) has thus resulted in urbanization of poverty (Zhang, 2016) and huge inequalities, with subsequent shifts in spatial distribution of populations (Balsa-Barreiro et al., 2019). These inequalities have manifested visibly in the mushrooming and growth of “slums” in most urban areas of the global south (Rodriguez Lopez et al., 2017, Wurm et al., 2017b). The increasing development of these deprived areas is one of the most serious humanitarian challenges to sustainable urban development in the developing world (Hofmann et al., 2015, UN-Habitat, 2003). Faced with the mandate to eradicate poverty by 2030, world cities are obliged to ameliorate the lives of the “slum” dwellers as a priority goal in the 2030 Sustainable Development Goals (Fallatah et al., 2022, Pratomo et al., 2017). However, despite their visible growing extents, scholars have argued that lack of adequate information on their morphology, spatial dimensions, and dynamics is the main setback to attaining the vision (Wang et al., 2019c, Badmos et al., 2018). Where the information exists, it frequently displays poor temporal accuracy and consistency (Wang et al., 2019b). “Slum” morphological diversities, coupled with their dynamic nature in space and time (Badmos et al., 2018, Samper et al., 2020) make semantic abstraction of their locations and spatial extents intricate (Gibson et al., 2019, Wang et al., 2019b). With their rapid spread, sometimes covering large extents or scattered pockets within urban areas (Mboga et al., 2017), Hofmann et al. (2008) suggested the need for classification methods that are feasible for complex environments and that provide spatial information in a timely and accurate way. This study contends that there is need for holistic techniques that are reproducible, and that can provide rapid and reliable spatial information with possibility of being updated within certain

time interval to allow monitoring of these dynamic landscapes, as well as informing of policy related to urban area and risk management.

Approximately one billion people live in “slums”, globally (Winter et al., 2020), and projections reveal that the number will increase to two billion by 2030 and three billion by 2050 (UN-Habitat, 2016). The United-Nations (2015) presents the percentage of the urban population living in “slum” conditions as 35% in Southern Asia, 24% in Latin America and the Caribbean and 13% in North Africa. The challenge of “slums” is regarded as acute in sub-Saharan Africa (SSA) where the proportion of the urban population that is residing in these areas of deprivation reaches 62% (UN-Habitat, 2015). For South Africa, estimates suggest that 13.9% of households live in these slums (Nkonki-Mandleni et al., 2021). Kwazulu-Natal province has 25% of the population occupying informal housing (Gibbs et al., 2014). Approximately 13.29% of all households in Durban reside in informal settlements (Statistics, 2016). These estimates of populations are projected to double by 2030 (UN-Habitat, 2016). Jones (2017) proposed that there is need for policies that redress complexities of urbanization particularly in curbing uncontrollable growth of "slums".

The aforementioned estimates of populations are based on UN-Habitat (2003)’s definition that associated “slums” with overcrowding, insecurity of tenure, inadequate provision of basic amenities such as safe water, sanitation and other infrastructure. However, there does not exist a standard definition for “slums” as yet (Fallatah et al., 2018, Persello and Stein, 2017, Samper et al., 2020). There are numerous nomenclatures of “slum settlements” (e.g., squatter settlements, barrios bajos, favelas, shanties, ghettos, unplanned townships or slums) (Winter et al., 2020). The names vary between country to country or within the same country, depending on the context. For instance, when considering tenure status, they are usually denoted as “illegal”, “squatter, or “informal” settlements (Kuffer et al., 2016a). In the context of growth dynamics, they are referred to as “spontaneous” or “irregular” (Kraff et al., 2020), and terms such as “deprived,” “shantytown”, and “sub-standard” explain the socio-economic status of informal settlement dwellers (UN-Habitat, 2015). While some researchers regard informal settlements as synonymous with “slums” (Arimah, 2010, UN-Habitat, 2003), and are often used interchangeably in the literature (Mahabir et al 2016), some scholars regard them as antonymous (Hofmann et al., 2015, Jones, 2017). There are also terminological restrictions from one country to the other (Taubenböck et al., 2018). For instance, the term “slum” is not used in South Africa because of associated negative connotations of a bad area, which is an

incubator of unsociable and criminal activities (Marx and Charlton, 2003a). Although the United Nations continues to use the term “slum”, concerns have been expressed that the term is emotive and pejorative (Ezeh et al., 2017, Gilbert, 2007). Ezeh et al. (2017) further suggests the term ‘informal settlement’ as an alternative. The current study, thus, assumes the term informal settlement.

According to Mahabir et al. (2018), the lack of consensus on the definition of informal settlement could partly be attributed to the diversification of their morphological characteristics worldwide. Morphologies for informal settlements vary across countries, across cities, across informal settlement areas within the same city, or within the same informal settlement landscape (Kuffer et al., 2016b). The factors that drive these morphological miscellanies are anchored in three key types of typologies; object type, land and site characteristics, and the area's temporal dynamics and history (Kuffer et al., 2017). In some countries, for example, Medieval Cairo, informal settlements occupy the urban fringe, often dispersed in agricultural land (Kuffer et al., 2017). In Durban, they characteristically occupy every vacant land, are along rivers and in flood prone areas (Membele et al., 2022b, Williams et al., 2018). Differences in informal settlement morphogenesis also largely explain diversities in morphological layouts of informal settlements from place to place (Kuffer et al., 2017). Morphogenesis explains their characteristics as sometimes an expression of the process of development stage, that is, from being spaced out at infancy stage to closely packed at maturity (Kuffer et al., 2016a, Schmitt et al., 2018), sometimes associated with increasing building size and height. Sometimes, the variations are explained in terms of unique constructional materials. For example, morphology of informal settlements in Jeddah, Saudi Arabia, differ with those in Asia and Africa in that formal and informal settlements’ constructional materials are identical (Fallatah et al., 2019). To the contrary, those in Asia and Africa usually present dissimilar appearance compared to planned residential developments (Shekhar, 2012, Kohli et al., 2016a). Nevertheless, sometimes due to upgrading processes, the morphologies may revamp with time and become decent low-income homes (Mahabir et al., 2018). This supports the assertion that the definition of the term informal settlement can change with time. These dynamic informal settlement morphologies contribute to lack of consensus on the definition of informal settlements (Taubenböck et al., 2018). Differential morphologies also surmise that those informal settlements expand with different spatial patterns and development dynamics (Bren d'Amour et al., 2017). These diversities in morphological layouts as well as absence of an agreed definition of informal settlements makes their mapping inherently complex.

Nonetheless, remote sensing methods build on the premise that informal settlements share specific morphological features that can be recognized in an image (Taubenböck et al., 2018).

Previously, there has been a number of initiatives that were aimed at mapping informal settlements in South Africa. These initiatives included Eskom's SPOT Building Count, and STATSSA dwelling Frame building count (Kemper et al., 2015). Just like in the global context, such survey based approaches have been regarded as costly in terms of resource requirements and time consuming (Kemper et al., 2015). Remote sensing has offered possible solutions to identification and monitoring of the spatial behaviour of informal settlements. Supported by progress in accessibility of very-high-resolution (VHR) data, as well as technological advancements, remote sensing has been an invaluable data source for providing updated, consistent and comprehensive geospatial information with great thematic detail in complex urban environments (Wang et al., 2019b). The capabilities of remote sensing to capture the geography, morphological diversities, and dynamics of informal settlements has been explored in various informal settlement studies (Kuffer et al., 2016b, Persello and Stein, 2017, Prabhu et al., 2021b, Wurm et al., 2017a). However, a plethora of studies have raised concern over drawbacks that are associated with use of high spatial resolution satellite systems, especially when classification is solely based on spectral properties of the image (Ansari et al., 2019a, Duque et al., 2017, Mboga et al., 2017). For instance, multiformity of informal settlement landscapes, fragmented spatial configuration of urban environments, and diverse morphologies of informal settlements (Chen et al., 2015, Mugiraneza et al., 2019, Stark et al., 2020) inhibit accurate depiction of their spatiality (Leonita et al., 2018, Mboga et al., 2017). In order to address shortcomings arising from sole reliance on spectral information, researchers have adopted image processing techniques that are based on information from adjacent pixels (Pelizari et al., 2018).

The surge in use of VHR satellites (Quick bird, World view, Orbview, GeoEye) has been associated with observed increase in utilization of texture analysis for informal settlement mapping (Kuffer et al., 2016b, Wurm et al., 2019). The capability of spatial contextual information in the form of image texture to enhance capturing of informal settlements' diverse morphological characteristics has been emphasized (Kuffer et al., 2016b, Kuffer et al., 2018, Kuffer et al., 2014). Texture analysis refers to a class of mathematical procedures and models that distinguish the spatial variations within imagery, in order to extract information (Armi and Fekri-Ershad, 2019). Numerous studies have explored texture feature algorithms such as grey

level co-occurrence matrix (GLCM) (Kohli et al., 2016b, Kuffer et al., 2016b, Prabhu et al., 2017, Wurm et al., 2017b), local Binary Patterns (LBPs) (Luus et al., 2014, Mdakane and van den Bergh, 2012, van den Bergh, 2011), contourlets (Ansari et al., 2019b), curvelets (Ansari and Buddhiraju, 2019a), and lacunarity (Kit and Lüdeke, 2013, Owen and Wong, 2013a). Several authors have conducted reviews on texture analysis techniques (Hofmann et al., 2015, Kuffer et al., 2016a, Mahabir et al., 2018). These studies mostly stressed the role of remote sensing in informal settlement identification, and gave general overviews of various mapping approaches, but presenting a brief review of texture analysis approaches. Unpacking the application of various image texture features and capabilities of the numerous texture analysis approaches could enhance better understanding of the complexity and dynamism of informal settlements (Kuffer et al., 2016b).

Some studies have taken advantage of innovative approaches such as pan sharpening in texture analysis for informal settlement mapping (Kohli et al., 2016a, Mugiraneza et al., 2019, Owen and Wong, 2013b). For instance, pan sharpened Quickbird image (Kohli et al., 2016a) and pan sharpened Worldview image (Kuffer et al., 2016b) have been used to map informal settlements in Pune (India) and Kigali, Mumbai and Ahmedabad, respectively. In another study Owen and Wong (2013b) pan sharpened Quickbird MS imagery using 0.6m PAN band, employing the rational polynomial coefficients approach in Guatemala. According to Kumar et al. (2014), the availability of high spectral and spatial resolution images is crucial when mapping areas with complex morphologic structures such as urban environment. The aforementioned studies have exploited pan sharpened products of costly, high-resolution imageries, which are not within the financial reach of most institutions in resource constrained nations. Capabilities of pan sharpening freely downloadable Sentinel-2A for capturing the distribution of morphologic informal settlements can also be explored for capturing smaller and lesser-known informal settlements in the diverse Durban landscape. Wurm et al. (2017b) described capturing of small deprivation pockets as compromised when using image texture from only the Sentinel-2A 10 m bands. Thus, pan sharpening Sentinel-2A would exploit the high spatial resolution and high spectral resolution for potential enhancement of informal settlement detection accuracy.

In texture analysis, there are various image processing functions that are undertaken, especially when using grey level co-occurrence matrix (GLCM) algorithm. These steps include calculation of optimum window size, a process involving testing of varied window sizes. Also, calculation of average distance forms an important step in texture-based image classification.

These processes, apart from being time consuming (Graesser et al., 2012), would generate sheer volumes of data which is computationally demanding in terms of processing (Rodriguez-Galiano et al., 2012), especially where classical image-processing software is concerned (Stromann et al., 2019). The traditional image processing platforms may lack the computational capacities to handle the large data processing requirements, thus causing classification complexity (Chen* et al., 2010, Shafizadeh-Moghadam et al., 2021). Also, local computers would require specifications in terms of software and hardware which would, again, have cost implications.

Recent advances in cloud computing, through the development of Google Earth Engine (GEE) has partially reduced challenges involving data preparation, management, processing, and analysis (Kelley et al., 2018, Mananze et al., 2020). Open-access data, as well as a host of data within the GEE, for example, Sentinel-2, Sentinel-1, MODIS and Landsat (Amani et al., 2019b) have presented opportunities for more comprehensive and advanced processing functionality, through data integration (Amani et al., 2017). Google Earth Engine has removed the procedure of downloading a large number of satellite images, feature extraction, and provides data in formats that are ready to use. A plethora of machine learning algorithms as well as image mosaicking techniques within GEE allow combinations of different feature sets, allowing comprehensive mapping. Because of its reliable, broad code applicability, GEE has been leveraged in various environmental applications ranging from crop mapping (Kelley et al., 2018, Shelestov et al., 2017, Teluguntla et al., 2018), wetland mapping (Amani et al., 2019b, Liu et al., 2022), and urban LULC mapping (Hamud et al., 2021, Mugiraneza et al., 2020). Its cloud computing prowess presents the potential for the mapping of high spatial variability of morphological informal settlements in heterogeneous urban landscapes. Recently, the accessibility of high resolution PlanetScope (PL) data within GEE has presented opportunities for implementation of mapping approaches aimed at systematic examination of morphological informal settlements. For instance, its availability within GEE has made geographic object-based image analysis (GEOBIA) implementable within the platform. Earlier studies that demonstrated the potency of object based image analysis (OBIA) in enhancing informal settlement mapping (Fallatah et al., 2020, Fallatah et al., 2022, Kohli et al., 2016a, Shekhar, 2012) have focused on Kohli et al. (2012)'s ontology-based informal settlement characterization, which has been described as complex, tedious, associated with many segmentation and classification tasks, and requiring considerable analysis skills (Kohli et al., 2016a). The numerous processing steps involved in segmentation and classification demand

increased computer capacity (Gorelick et al., 2017). GEE, through the convenience of inbuilt, simple non iterative clustering (SNIC) algorithm, presents potential for OBIA to map spatial morphology of deprivation pockets in complex built up environment, with ease and enhanced speed (Pu et al., 2020). In addition, the inbuilt GLCM algorithm makes texture analysis implementable within the cloud computing platform which, according to Kohli et al. (2013b) is critical in distinguishing between formal and informal areas when using the OBIA technique.

The online-based environmental monitoring platform provides unique capabilities to map informal settlements' morphologic dynamics over time and with precision (Mugiraneza et al., 2020, Tingzon et al., 2020). Kraff et al. (2020) alluded that informal settlement dynamics can only be comprehensively investigated by bridging the gap from static to multi-temporal measurement. As informal settlements continue to change rapidly in response to urbanization, understanding their dynamics in the context of associated land cover/ land use (LULC) transitions would be key in the modelling of future rates of change. United-Nations (2019) expressed the need to understand the dynamics of human settlements as crucial for sustainable development and management of the environment, as well as for effective implementation of settlement policies. Intensity analysis is an approach that presents potential for holistic assessment of informal settlement spatial dynamics through linking patterns with process. Findings of this study could be used to create knowledge repositories which would assist in devising a tailored informal settlement management approach for Durban municipality, especially aimed at addressing the challenges associated with encroachment into flood vulnerable land. Moreover, the findings have potential to reveal insights on better matched solutions, whether in the form of informal settlement management policies or adaptive strategies.

1.2. Aim and objectives

The main aim of this study was to exploit the integration of various innovative mapping approaches with texture analysis to unpack the morphologic variations in informal settlement features in Durban Metropolitan area, South Africa.

To achieve this, the following objectives were set:

1. To provide a synopsis of texture analysis approaches in modelling informal settlements

2. To evaluate the potential of pan sharpening techniques on Sentinel-2A data, and textural features in enhancing informal settlement identification accuracy, in a fragmented urban environment
3. To leverage Google Earth Engine's cloud computing capabilities and advanced data analytic capabilities for accurate capturing of morphological diversities of informal settlements in a heterogeneous urban landscape
4. To exploit Sentinel-1(S1) radar data, Sentinel-2 (S2) and PlanetScope (PL) optical data fusion for more accurate and precise mapping of informal settlements using geographic object-based image analysis (GEOBIA), within Google Earth Engine.
5. To map and systematically analyze informal settlement growth patterns and associated land use/ land cover transitions using intensity analysis approach.

1.3. Description of the study site

The study area (Figure 1.1c) is located in KwaZulu-Natal province, South Africa (Figure 1.1a), and lies within Durban Metropolitan area (Figure 1.1b). Situated in the north-western part of Durban city, the area of study extends to, approximately, 900 ha between longitudes 29.95°E and 29.98°E, and latitudes 29.8°S and 29.83°S. The study area forms part of the Umgeni catchment, lying to the south of the Umgeni River. It covers suburbs such as Clare Estate, Westville, and Reservoir hills. The area includes informal settlements such as Kennedy Road, Quarry Road, New Germany road, Palmiet zone 1, and Foreman Road. The topography of the area is steep and highly undulating, ranging from about 30 m to 120 m above sea level. A humid subtropical climate coupled with a mean annual precipitation exceeding 1000 mm per annum characterize Durban (Williams et al., 2018). Also, warm, wet summers and mild, dry winters describe Durban climate. Most informal settlements in the study area are close to road networks such as Palmiet Road, Clare Road, Quarry Road, and New Germany Road. These roads follow a steep topography and often lead down to Umgeni River. The informal settlements' location on steep slopes, in proximity to road and river networks, coupled with characteristic fragile soils may contribute to their vulnerability to landslides and flood hazards during extreme climatic conditions. Most of the informal settlements are located within 'pockets' of formal settlements or close to prominent institutions or business areas. For example, Reservoir Hills shopping center lies adjacent to the New Germany road informal settlement. Similarly, the University of KwaZulu-Natal, Westville campus, lies at an average

distance of about 1.5 km from the three closest informal settlements. This is reflective of the morphology of informal settlements in Durban, where they capitalize on every inch of urban space in the city. The fact that about 75% of the metropolitan gross housing backlog of 305,000 units represent informal dwellings (Marx and Charlton, 2003b) showing high levels of accommodation crisis in Durban. Moreover, the housing units are constructed using corrugated iron, plastic, timber, and metal sheeting that testify to the poverty and low-income levels of the residents.

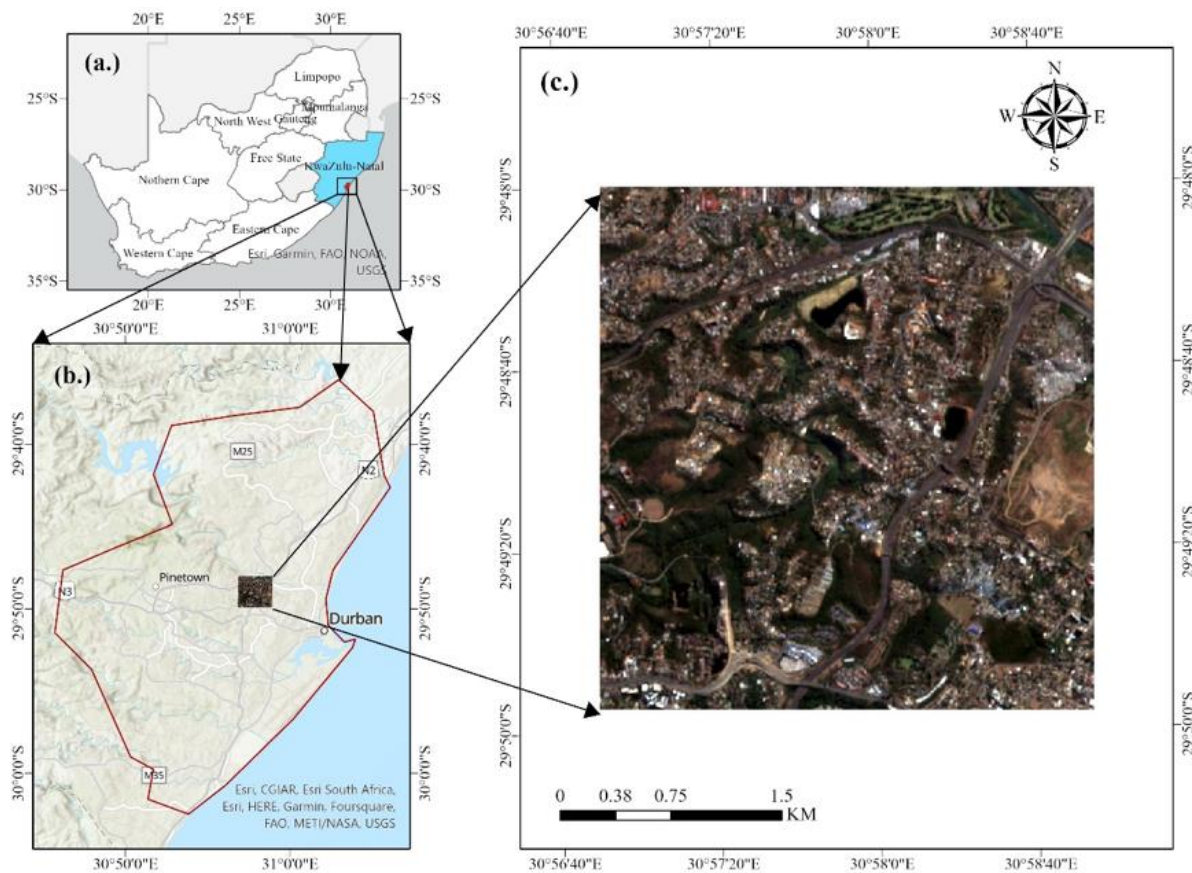


Figure 1.1. Location of the study area

1.4. General structure of the thesis

The thesis comprises seven chapters where chapter 1 forms the introduction and chapter 7 forms the synthesis chapter. Five research papers that answer each of the aforementioned research objectives outlined in section 1.2, also form part of the thesis. The literature review and methodology are entrenched within the mentioned papers.

Chapter Two provides a systematic review of progress of texture analysis in mapping informal settlements. The review presents an investigation of key factors affecting texture-based classification processes in the identification of informal settlements. The factors include sensors, algorithms, scale, classifiers and feature selection methods. Gaps and opportunities were presented, as well as future directions on the application of texture analysis for informal settlement identification.

Chapter Three evaluates the potential of pan sharpening techniques on Sentinel-2A data, and textural features in enhancing informal settlement identification accuracy. Specifically, Sentinel-2A 20 m bands were pan sharpened using 10 m bands to investigate the potency of integrating pan sharpening and image texture in mapping diverse spatial layout of informal settlements.

Chapter Four leverages data analytic tools and available data archives within the GEE cloud computing environment in order to establish a framework that integrates spectral and texture features, as well as random forest classification to enhance capturing of informal settlement morphological diversities. This paper performed a comparison analysis of 7 different feature combinations to investigate their discriminative capabilities in accurately predicting informal settlement locations and extents. Feature combinations including spectral bands, spectral indices and various GLCM texture features were explored.

Chapter Five explored the available high-spatial resolution PlanetScope imagery within the GEE platform, coupled with the convenience of simple non-iterative clustering (SNIC) segmentation algorithm to perform GEOBIA to map spatial morphology of deprivation pockets in complex built up environment of Durban. The study fused data from Sentinel-1(S1) radar data, Sentinel-2 (S2) and PlanetScope (PL) optical data sensors with different spectral characteristics and spatial resolutions for effective abstraction of informal settlement diversity. GLCM algorithm, present within the GEE platform was employed for extraction of image texture features from PL imagery, which were integrated within the classification framework for precise localization of informal settlements in a complex urban landscape.

Chapter Six analyzed spatiotemporal dynamics of informal settlements in relation to triggered LULC changes in part of Durban Metropolis. The study mapped and systematically analyzed transitions in LULC in response to informal settlement growth patterns in Durban Metropolitan area from 2015 to 2021. An object-based image classification, incorporating texture analysis was performed on fused Sentinel -1 and PlanetScope data within the GEE. Further, intensity

analysis approach was utilized to quantitatively investigate inter category transitions, at category, and transition levels so as to enhance comprehension of patterns and processes of change and consequences on the environment. Findings have implications for sustainable urbanization policies and devising of environmentally responsible approaches, especially in rapidly urbanizing cities. The study applied an object-based image classification on PlanetScope imagery within the GEE platform.

CHAPTER TWO: LITERATURE REVIEW

Texture analysis approaches in modelling informal settlements

This chapter is based on:

Matarira, D., Mutanga, O., & Naidu, M. (2022). Texture analysis approaches in modelling informal settlements: a review. *Geocarto International*, 37(26), 13451-13478, doi:10.1080/10106049.2022.2082541

Abstract:

Texture-based informal settlement mapping has gained attention in urban remote sensing research. Numerous studies conducted on the use of texture analysis for informal settlement mapping have investigated wide-ranging sensors, algorithms, scale, classifiers, feature selection methods, and other factors of interest. However, no study has systematically investigated key factors affecting texture-based classification processes. This paper presents a detailed synthesis of scientific progress in texture based informal settlement mapping. Results revealed that grey level co-occurrence matrix was the most popularly used algorithm. Quickbird was the widely used sensor in the mapping of informal settlements using texture analysis approaches. The use of machine-learning classifiers, particularly, support vector machine and random forest yielded, comparatively, high accuracies (>80%). Interestingly, deep learning showed potential to advance informal settlement identification. Multi-city comparison studies demonstrated need for texture features to be locally specific in order to allow transferability. Thus, integration of remote sensing data and field survey statistics could be crucial in enhancing understanding of morphological variations for improved informal settlement mapping.

Keywords: Remote sensing; informal settlements; modelling; image texture

2.1. Introduction

'Slums', herein defined as informal settlements (ISs) (Gibson et al., 2021) have become a growing concern, globally. They are home to about 1.6 billion dwellers, worldwide (UNDP, 2018), and the figure is projected to increase to three billion by 2050 (United-Nations, 2019). In Africa, 62% of the city residents dwells in ISs, in Asia; 30%; and in Latin America and the Caribbean; 24% (UN-Habitat, 2015). Urban poverty, lack of cities' capacity to meet an increasing housing demand, inability of states or the market to provide affordable housing for the urban poor, combined with the inability to provide basic services are some of the main drivers of the growth and persistence of informal settlements in the global south (Samper et al, (2020, Tellman et al., 2022). In accordance with the 2030 Agenda for Sustainable Development (Fallatah et al., 2020b), countries have a mandate to transform all ISs into serviced and formal neighbourhoods (Brelsford et al., 2018). However, data on their location, extent and dynamics is often not available, outdated, or inconsistent (Persello and Stein, 2017, Prabhu and Parvathavarthini, 2021, Verma et al., 2019, Wang et al., 2019c). Accurate mapping of the distribution, size and patterns of ISs potentially allows effective implementation of policies and urban growth management (Samper et al., 2020).

Texture analysis approaches have the potential to capture morphological variations in ISs (Kohli et al., 2016b, Mboga et al., 2017). In that regard, various studies have explored texture feature techniques such as grey level co-occurrence matrix (GLCM) (Girija and Nikhila, 2018, Kohli et al., 2016b, Prabhu and Alagu Raja, 2018, Shabat and Tapamo, 2017), contourlets (Ansari et al., 2019b), curvelets (Ansari and Buddhiraju, 2019a), lacunarity (Fallatah et al., 2018b, Kit and Lüdeke, 2013, Kit et al., 2012a, Owen and Wong, 2013a), local Binary Patterns (LBPs) and Line Support Regions (LSRs) (Graesser et al., 2012). While some studies integrated texture analysis with object based image analysis (Kohli et al., 2016b, Kohli et al., 2013), others fused texture analysis with machine learning approaches (Leonita et al., 2018, Mboga et al., 2017).

Even though diverse texture analysis approaches have been exploited, there is lack of consensus on the most suitable approach yet (Kuffer et al., 2016b). Diversity of morphologies of informal settlements across locales presents uncertainties and challenges that compromise effective delineation of ISs using remote sensing (Kuffer et al., 2017). Furthermore, dissimilarities in feature sets (Wang et al., 2019c), data gaps due to high cost of VHR imagery (Duque et al., 2017, Taubenböck et al., 2018), sensor characteristics (Schmitt et al., 2018,

Wurm et al., 2017a), as well as scale issues have an impact in the accurate mapping of ISs. Therefore, it is crucial to synthesize the collective knowledge of all factors influencing texture-based classification.

Recently, some researchers have conducted reviews stressing the role of remote sensing in IS identification (Hofmann et al., 2015, Kuffer et al., 2016a, Mahabir et al., 2018). Kuffer et al. (2016a) gave a systematic review of different approaches and methods that used high/ very high resolution (H/VHR) imagery to study slums over the last 15 years. The main purpose was to assess the methodological advances in IS detection that are crucial for a global slum inventory. Available reviews (Hofmann et al., 2015, Mahabir et al., 2018b) only provide a brief review of texture analysis. An in-depth analysis of the application of texture analysis for IS identification is still lacking. Rather, the texture analysis approaches are scantily discussed without a comprehensible guidance on the relative performance of different texture analysis approaches for IS mapping. This work therefore provides a detailed synthesis of peer-reviewed studies on the role of texture analysis in IS mapping.

The main objective of this work is to systematically review the results of existing studies on texture based IS mapping in order to:

- 1) document various factors that are important in texture analysis such as sensors, geographical regions, algorithms and accuracy assessment methods.
- 2) identify and briefly summarise the scientific advances in texture-based algorithms for IS extraction
- 3) provide scientific guidance regarding the use of texture analysis for IS mapping

2.1.1. Conceptualizing informal settlements

2.1.1.1. Definitions

The definition of the term ‘slum’ remains a contentious construct (Patel et al., 2019). In fact there is absence of an internationally agreed definition of what informality is (Mahabir et al., 2016). The definition of what constitutes a slum varies by country, within countries or even cities (Kuffer et al., 2017). Samper et al. (2020) suggested a number of variables that define informal settlements, which include lack of basic needs such as safe water, sanitation, infrastructure and services, overcrowding, fragile structures, non-secure tenure, among others, all of which are embedded in UN-Habitat (2003)’s definition that described slums (also referred to as ISs) as overcrowded, insecure areas that are characterised by poor structural

quality housing and lacking adequate access to safe water, sanitation and other infrastructure. Samper et al. (2020) emphasized the need for an IS to be captured in any of its unique definitions. One reason is that, what one country may consider as a “slum” may be regarded as perfectly acceptable accommodation in another (Gilbert, 2007). Moreover, with time, slums may improve and become respectable low-income homes (Mahabir et al., 2018). This means that slum definition can change any time. For that reason, slums cannot be defined in any universally acceptable way (Taubenböck et al., 2018). It is also vital to note that, while United Nations seems to suggest that ISs are synonymous with ‘slums’ (Fallatah et al., 2018), in some countries, for example, South Africa, the two terms are not synonymous (Hoffman et al., 2015). The term ‘slum’ is not used in South Africa because of associated negative connotations. In fact, Gilbert (2007) described the term ‘slum’ as pejorative and emotive. Hence, Taubenböck et al. (2018) based their study on the term ‘Arrival City’ in order to avoid the conceptual restrictions. For the same reason, the term ‘informal settlement’ will be used in the current review.

2.1.1.2. Morphology of informal settlement landscape

Morphology of ISs shares unique characteristic patterns across settlements (Samper et al., 2020). These characteristics include shape, size, scale and distribution (Kuffer et al., 2017). From a remote sensing perspective, morphology refers to observable and detectable spatial and spectral characteristics that can help distinguish ISs from formal settlements (Hoffmann et al 2008, Graesser et al., 2012). Those spatial characteristics that vary across countries, across cities, or even across IS areas within the same city (Kuffer et al., 2016b) characterize informality. To enhance understanding of the concept of ‘morphology’ in the context of informal settlements, Kuffer et al. (2017) conceptualized the determinants that drive variations in ISs morphology, many of which are anchored in three key types of typologies; object type, land and site characteristics, and the area's temporal dynamics and history. These typologies vary from settlement to settlement and can be quite dynamic. For example, Suhartini and Jones (2020) observed that, in Indonesia housing units in ISs result from unplanned adaptations of domestic space, reflected in their differential organic and haphazard forms, as well as various structural layouts. In Cairo, whilst some ISs are constructed on deteriorated historic core, for example, Medieval Cairo, some occupy either abandoned agricultural land or desert land (Kuffer et al., 2017). In Mumbai, IS landscape is characterized by (1) rehabilitated ISs adjacent to high-rise apartment buildings, (2) long-established ISs, which may have regular small-scale

shops and building patterns along the main roads, and (3) very densely packed areas with only small lanes inside the area (Kuffer et al., 2016a). In Latin America, informal settlements may take variations that include occupation of public communal land as well as unlicensed subdivision of land (Fernandes, 2011). Similar to spatial layout in South Africa, ISs in Recife, are clustered in open spaces in the city and near highways (Duque et al., 2017). Remote sensing is anchored on the premise that ISs share explicit morphological features that can be recognized in an image (Taubenböck et al., 2018). According to Graesser et al. (2012) such diverse morphological characteristics can be captured in VHR imagery, and incorporating textural information would effectively characterize local IS neighbourhoods. For instance, Kuffer et al. (2016a) used GLCM variance to distinguish ISs types from formal areas. Likewise, Kuffer et al. (2017) successfully investigated the capacity of VHR imagery to map locally specific types of ISs.

2.2. Satellite image texture analysis and informal settlement identification

Texture analysis involves use of a class of mathematical procedures and models that exploit spatial variability of intensity values in image classification (Armi and Fekri-Ershad, 2019). It has been widely used in high resolution image processing. There are various texture extraction approaches that are categorised into statistical, structural, transform based and model-based techniques. The commonly used statistical approaches include GLCM and LBP (Ramola et al., 2020). GLCM is a matrix which specifies the spatial relationship between two neighbouring pixels separated at distance (d) and direction (θ), referred to as orientation angle (0^0 , 45^0 , 90^0 , and 135^0) (Ramola et al., 2020, Shabat and Tapamo, 2017). Selection of appropriate angle (θ) is important in the extraction of textural information from images containing highly directional characteristics. Most importantly, orientation of urban structures influences extraction of features that are based on a certain direction (Wurm et al., 2017a). Given the unstructured arrangement of buildings in ISs, a rotation invariant GLCM is used in some studies (Khumalo et al., 2011). During texture feature extraction, usually all the four directions are considered and from them, the mean of features are calculated (Haralick et al., 1973). However, the calculation of mean directional textural information is characterised by loss of textural information that results in low classification accuracy (Singh and Srivastava, 2017). Texture analysis techniques have since disseminated into several fields. There is a significant body of texture analysis related work in fields such as vegetation mapping, forest mapping, species diversity mapping and urban built-up area extraction, among others. The application of GLCM

has been successful in the mapping of uprooted orchard trees (Ciriza et al., 2017), desert vegetation mapping (Zhou et al., 2021), and mangroves species classification (Wang et al., 2016b). According to the aforementioned studies, the addition of GLCM texture can improve image classification. The use of LBP features has also been associated with high accuracies, particularly in classification of areas with complex textural characteristics such as bark texture (Figure 2.1a-e). However, basic local binary patterns (LBP) do not adequately discriminate features, and have been criticized for their sensitivity to noise (Fekri-Ershad, 2020). Thus, some studies have utilised modified approaches of LBP in texture analysis. For example, Fekri-Ershad (2020) used improved local ternary patterns for bark texture classification. Researchers in urban remote sensing have successfully applied texture analysis in classifying complex built up areas (Giannini and Merola, 2012, Mhangara and Odindi, 2013, Zhang et al., 2014). Most importantly, investigators have developed tools and techniques that explore texture-based classification for IS detection (Fallatah et al., 2020, Kit et al., 2012a, Kohli et al., 2016b, Kuffer et al., 2016b). GLCM has been broadly accepted in IS identification (Girija and Nikhila, 2018, Kohli et al., 2016b, Kuffer et al., 2016b, Wurm et al., 2017b). According to Haralick et al. (1973), the advantage of using GLCM in texture analysis has been its ability to capture the spatial variation of neighbouring pixel values. The results of most studies that employed GLCM showed robustness of the approach in IS identification. Interestingly, Owen and Wong (2013a) revealed representative values expected of ISs (Table 2.1).

Table 2.1. Commonly used GLCM texture metrics and expected values for informal settlement areas

Features	Description	Formulae	Expected values for slum areas
Homogeneity	It measures image homogeneity as it assumes larger values for smaller gray tone differences in pair elements	$\sum_{i=1}^N \sum_{j=1}^N \frac{P(i,j)}{(1+(i-j)^2)}$	Lower than buildings
Energy	Provides the sum of squared elements in the GLCM. High values of energy occur when the window is very orderly	$\sum_{i=1}^{N-1} \sum_{j=1}^{N-1} (P(i,j))^2$	Higher than buildings
Correlation	Returns a measure of how correlated a pixel is to its neighbor over the whole image range = [- 1 1]. Correlation is 1/- 1 for a perfectly positively or negatively correlated image. Correlation is NaN for a constant image	$\frac{\sum_{i=1}^{N-1} \sum_{j=1}^{N-1} (ij)P(i,j) - \mu_x \mu_y}{\sigma_x \sigma_y}$	Lower than buildings
Entropy	Entropy is a statistical measure of randomness that can be used to characterize the texture of the input image	$\sum_{i,j=0}^{N-1} P_{i,j} (-\ln P_{i,j})$	Higher than buildings
Contrast	Returns a measure of the intensity contrast between a pixel and its neighbor over the whole. Measures the local variations in the gray-level co-occurrence matrix	$\sum_{i=0}^{N-1} \sum_{j=0}^{N-1} P_{i,j} (i-j)^2$	Lower than buildings

Adopted from (Prabhu and Alagu Raja, 2018)

Apart from orientation angle, window size is also an important parameter in texture analysis (Engstrom et al., 2017, Ghaffarian and Emtihani, 2021). The previous studies in classifying

ISs (Kuffer et al., 2016b, Schmitt et al., 2018, Wurm et al., 2017a) have addressed the issue of multi scales by varying window sizes. Figure 2.1 is an illustration of the possible impact of a particular size of window on classification. If a small window size is chosen (red boxes in 2.1e), then there will be inadequate statistical information to define the texture (Baykal, 2019), causing misclassification. When the window size is too large, overlapping with other land cover classes may occur, introducing inaccurate spatial information (Kabir et al., 2010).

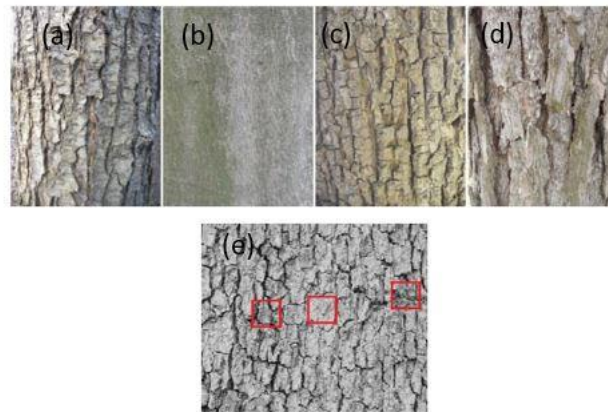


Figure 2.1a-e. Some examples of tree bark different textures. *Sources: (Fekri-Ershad, 2020); (Baykal, 2019)*

However, taking cognisance of implications of too small and too large window sizes, there is need to establish an optimum window size in texture analysis (Lan and Liu, 2018). Lan and Liu (2018) argued that, obtaining an optimum window size would create a link between scale and real object sizes. The issue of various scales has been addressed by some researchers through use of multi-resolution analysis (MRA) based approaches such as contourlets (Ansari and Buddhiraju, 2019c), wavelets and curvelets (Ansari and Buddhiraju, 2019b). Table 2.1 shows advantages and disadvantages of various approaches used in texture based informal settlement identification.

2.3. Literature search methods

A systematic literature search was conducted in four databases; Google Scholar, Scopus, ScienceDirect and Web of Science. The search for literature focused on articles that investigated application of image texture in the mapping of ISs. Published articles within the last 21 years, that is from 2000-2021 were considered. This selection of the period was important to guarantee that recent literature on the subject area was incorporated in the study to keep track with advances in methodologies and approaches. The databases were searched

using the search rule ("Texture analysis" OR "Image texture" OR "Texture features") AND "Remote Sensing" AND ("informal settlements " OR "slums" OR "Unplanned settlements") AND ("Classification" OR "Mapping"). Refinement of articles was done by date, article type, subject areas, title, and abstract. Double records were removed from the databases to further refine the search. Only the literature published between 2000 and 2021 was considered. Conference proceedings and two theses were also considered in this review. There was no limitation regarding the spatial scope of research but articles were limited to those written in English. For the paper to be included in this analysis, the papers needed to meet the following criteria: Each study should: 1) utilize remotely sensed data; 2) incorporate image texture in IS mapping. Following the above process, a database was created with fields containing the following information: authors, title, year published, imagery type, texture analysis algorithm used, location of study (city, country and continent), classifier used, accuracy assessment information. All cities listed in the paper were included in order to determine the geographic coverage of the studies

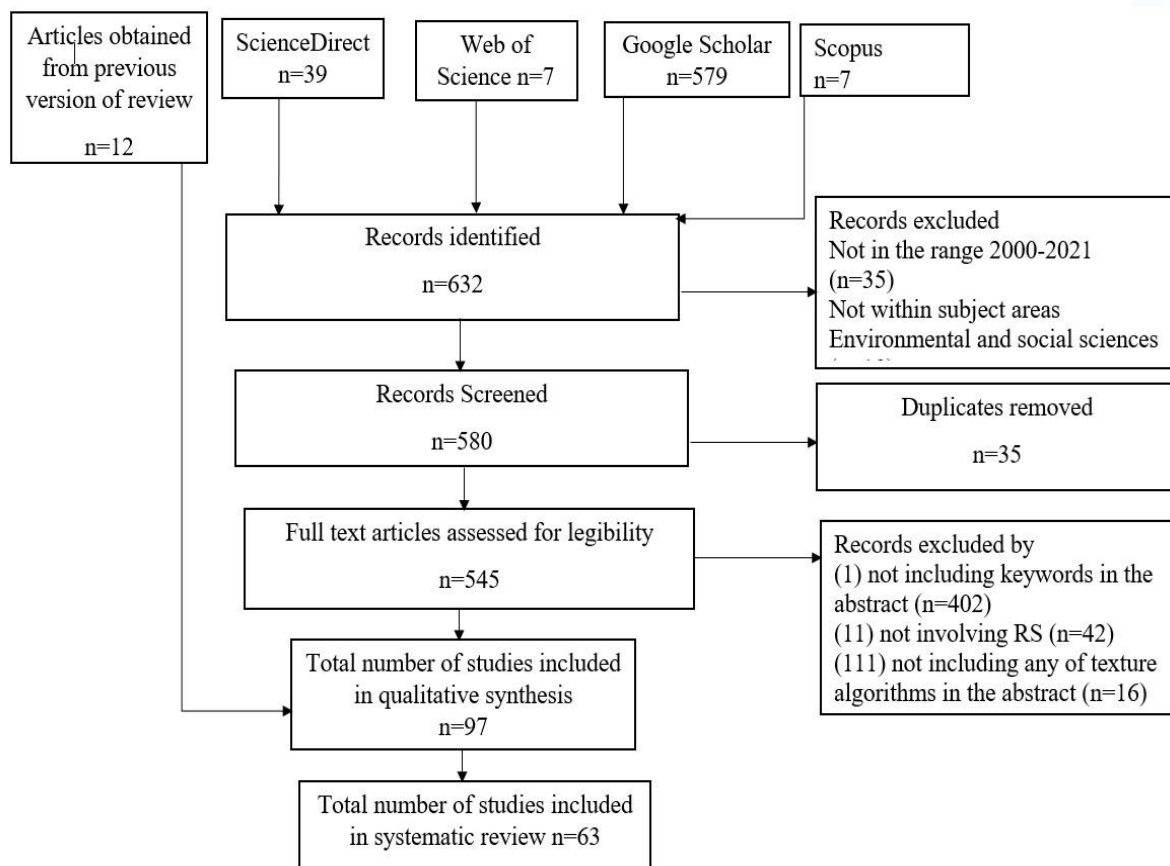


Figure 2.2. The number of published articles for informal settlement mapping

2.4. Meta-Data analysis

The study focused on quantifying the studies and investigating several features of image texture-based classification, that include sensors, window size, classifiers, classification accuracy, texture features extracted, and texture analysis algorithm. Measures of overall accuracy were also analysed from individual case studies. Statistics were also collected on the frequency of use of algorithms, sensors and classifiers. However, during the analysis of the influence of each uncertainty, it was observed that some case studies failed to clearly provide information for all fields. Therefore, in accordance with the specific objectives of the research, only relevant case studies that clearly expounded the corresponding uncertainties were considered during the quantitative analyses.

2.5. Results

The number of articles retained by the initial literature search was 632. The articles were then refined considering those that fell within the range 2000-2021, within subject areas of environmental and social sciences, and which were either research articles or proceedings. The refinement returned 580 articles. After further searches, 97 articles were retained for qualitative analysis after removing duplicates, those that did not directly exploit application of image texture in IS modelling. Sixty- three articles finally remained for quantitative analysis. Figure 2.2 illustrates the process of literature determination including inclusion and exclusion criteria.

2.5.1. Geographic location of texture analysis studies

This review considered texture analysis studies carried out from across the world (Figure 2.3). All publications under review came from 23 countries. Figure 2.3 shows the spatial distribution of studies that applied texture analysis approaches for IS modelling. From the spatial point of view, most of the articles on image texture based IS identification are mainly located in Asia (49.4%), with the largest percentage of case studies (35%) focusing on India. The three next studied countries include South Africa (10.4%), Brazil (9.1%) and Rwanda (7.8%). In India, the 27 studies were distributed across six cities, distributed in four states of India, which are Maharashtra, Telangana, Gujarat and Tamil Nadu. It is important to note that Mumbai city had the largest proportion of studies (15.6%), followed by Madurai city (7.8%), both in India. Other cities with fair numbers of studies included Johannesburg (7.8%) and Kigali (7.8%), both in sub-Saharan Africa.

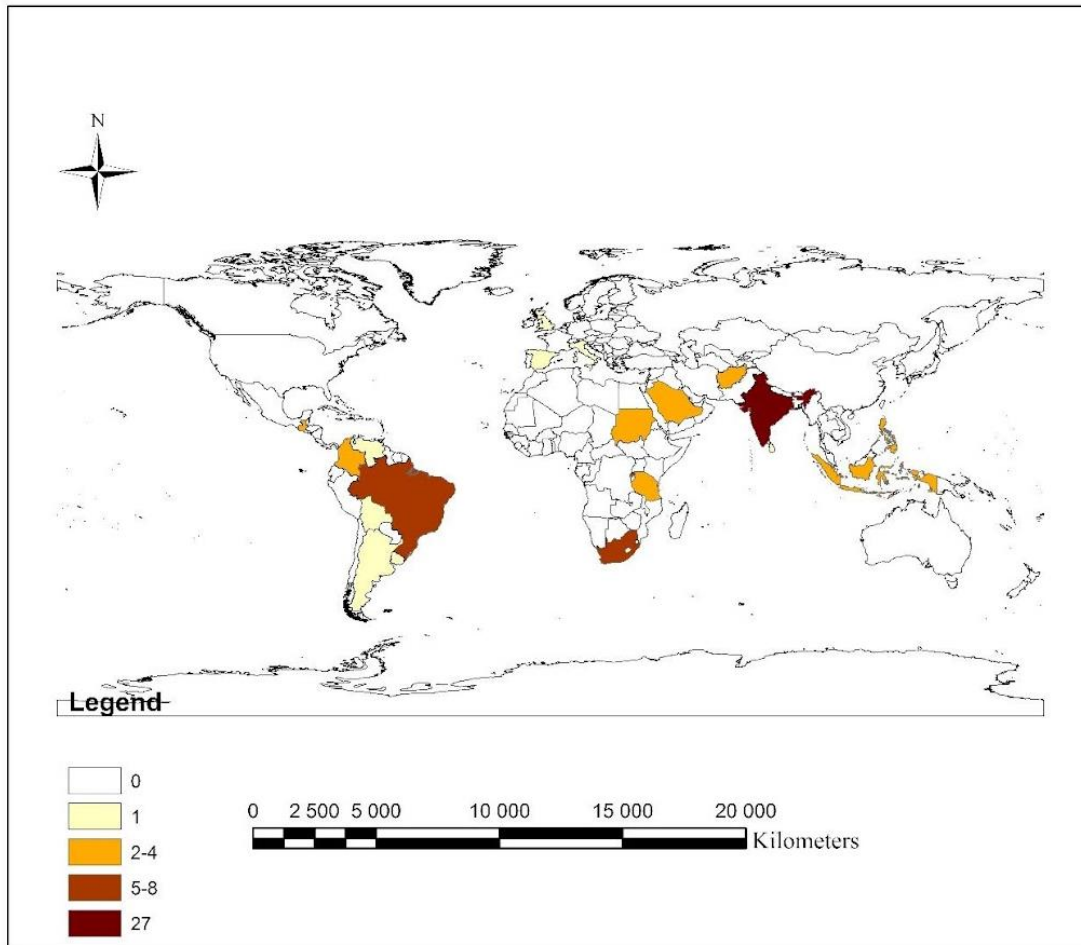


Figure 2.3. Country level distribution of texture analysis studies for informal settlement identification (studies published from 2005-2021).

2.5.2. Trends in texture analysis based on published articles

The numbers and the trend of publications from 2005 to 2021 are presented in Figure 2.4. From the literature search, the first texture analysis paper for IS extraction dates back to 2005 (Barros Filho and Sobreira, 2005). Prior to 2011, the number of related publications did not noticeably increase. However, from 2011 onwards, research on texture-based IS identification began to increase gradually as shown by the increase in publications. From the year 2005 to 2013 (eight years), there were six publications using texture analysis algorithms for IS mapping. There was a notable sharp increase from 2014 to 2017. The year 2017 witnessed the highest number (12) of publications while the year 2018 had five articles. The literature review showed that a significant number of studies employing texture analysis for IS identification (47.6%) were

published between 2014 and 2018. Generally, the trend of publication is increasing (Figure 2.4)

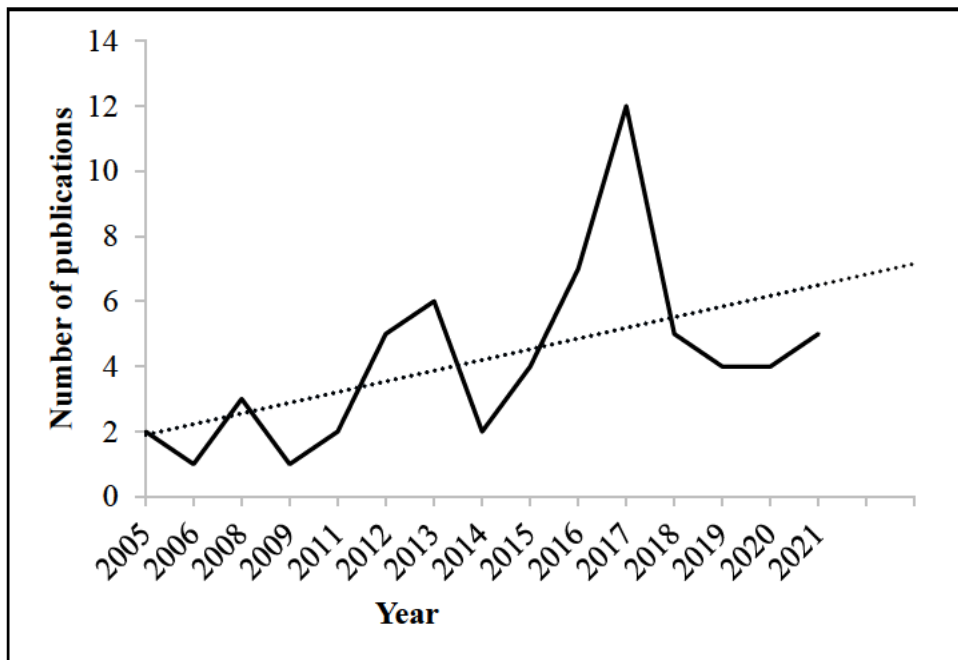


Figure 2.4. Number of published articles from 2005 to 2021 (The dotted line indicates the trend line)

2.5.3. Satellite data types and texture analysis

In this analysis, sensors that were used more than once were considered as frequently used sensors and those that were used once were grouped in the class of ‘others’. Figure 2.5 illustrates nine frequently used sensors and their frequencies. Those in the class of others included Landsat 8-OLI, Ikonos, Orbview, Resourcesat, ALOS Palsar, and others. Quickbird was the most commonly used sensor, followed by Worldview. Out of 63 publications, 31.7% and 25.4% of the published articles made use of Quickbird and Worldview sensor, respectively. Considering eight studies that employed a combination of two or more sensors, for example, Kit and Lüdeke (2013) and Kuffer et al. (2016b), $\frac{3}{4}$ of the studies included either Quickbird or worldview sensors. Interestingly, most combinations of satellite data were used mostly in India (Ansari et al., 2019b, Kit and Lüdeke, 2013). Only five studies from our sample used active remote sensing like RADAR data.

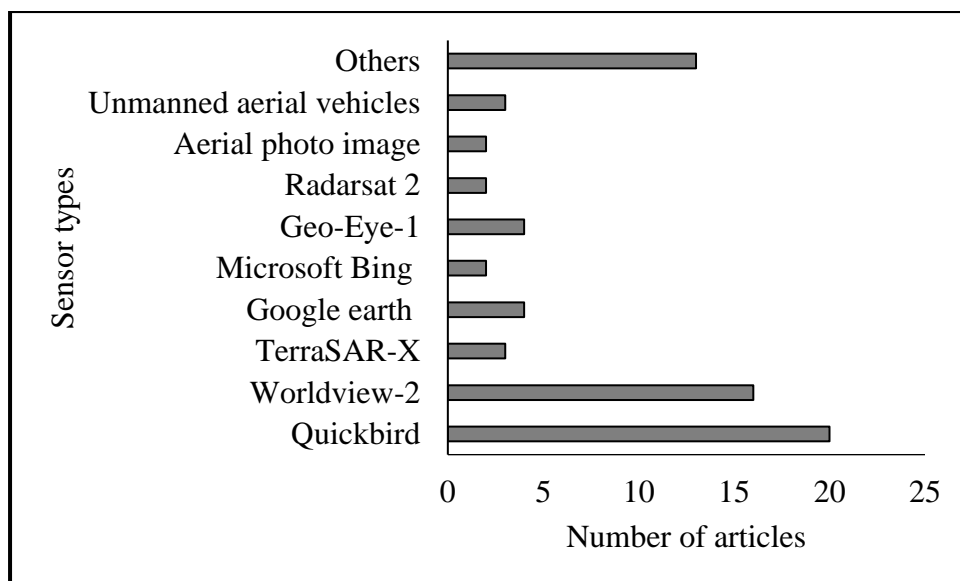


Figure 2.5. Satellite data used for texture based informal settlement modelling from year 2005 to 2021

2.5.4. Texture analysis approaches for the identification of informal settlements

Several texture analysis approaches were employed in various publications under review. The current review synthesized the types of algorithms that were most frequently used. The selection was based on the availability of information such as texture algorithm, classifier and well stated accuracy. Again, only approaches that were used in more than one study were incorporated in quantitative analysis. These approaches are represented in Figure 2.6.

Table 2.2. Studies with well documented classifiers and accuracy levels.

Study	Texture algorithm	Classifier	Classification accuracy (%)
(Ansari and Buddhiraju, 2019c)	GLCM, MRA based contourlet, MRA based wavelet, Crisp contourlet	MDM	93-96
(Ansari and Buddhiraju, 2019b)	Curvelet transforms, Contourlet transforms, MRA based wavelet, GLCM	SVM, MDM	91.4-95.4
(Wurm et al., 2017b)	GLCM, DMP	RF	81.65
(Mboga et al., 2017)	GLCM, LBP	CNN, SVM	91.71
(Stasolla and Gamba, 2008)	GLCM	Fuzzy ARTMAP Neural Network	90
(Fallatah et al., 2020)	GLCM	RF	91
(Wurm et al., 2017a)	GLCM, DMP	RF, LDA	88.58
(Kuffer et al., 2017)	GLCM	RF, LR	98.9

(Kuffer et al., 2016b)	GLCM	RF	90
(Leonita et al., 2018)	GLCM Pantex, LBP, Morphological features	RF, SVM	88.5
(Mugiraneza et al., 2019)	GLCM	SVM	85.36
(Duque et al., 2017)	GLCM, Histogram of pixel values	RF, SVM, LR	F2 scores 0.81
(Bürgmann, 2015)	GLCM	LDA, SVM, RF	91
(Khumalo et al., 2011)	GLCM, Gabor filters	I-Nearest neighbour	92.45
(Lai and Yang, 2020)	GLCM	SVM	90.7
(Praptono and Sirait, 2013)	Gabor Filters, Gaussian weighted grey level co-occurrence probabilities	Decision trees	74.15
(Gevaert et al., 2017)	LBP	SVM	91.6-95.2
(Prabhu and Alagu Raja, 2018)	GLCM, Tamura, Wavelet transform	Rule based, Fuzzy C means	68.5-73.5
(Prabhu and Parvathavarthini, 2021)	MSh-MSi-MP, GLCM, wavelet frame transform, MP, Morphological attribute profile, Modified MP	SVM	89.99-96.25
(Prabhu et al., 2021b)	MShMSiMP-GF	SVM	91.37-99.36
(Gevaert et al., 2016)	LBP	MKL- SVMs	90.29
(Weigand, 2017)	GLCM, DMP	RF, LDA	88.58
(Fallatah et al., 2018)	GLCM	CART	92.9

Accuracies were reported across algorithms basing on overall accuracy. In Table 1. RF refers to random forest, MDM is minimum distance to mean classifier, SVM is support vector machine, ANN refers to the Artificial Neural Network, LDA is linear discriminant analysis and CART is classification and regression tree.

Statistics of the current review (Figure 2.6) indicate that GLCM was the most commonly used texture analysis algorithm, followed by local binary patterns, both of which are statistical approaches. The results indicated that 73% of the research papers used GLCM texture metrics, whilst 14.3 % of the published papers used LBP. It is important to note that the trend of use of GLCM has been increasing (Figure 2.7) as shown by the number of publications that continue to increase over years. The search results revealed that, of the published articles, 13% utilised lacunarity approach. Structural based IS mapping approaches in the form of mathematical morphologies (MM) were exploited in 8% of the studies. These are studies that explored conventional mathematical morphologies. There were also few studies that successfully used transform based multi resolution approaches such as contourlets (Ansari et al., 2019a), curvelets (Ansari et al., 2019b), wavelets (Ansari and Buddhiraju, 2019b, Ansari et al., 2019b) and Gabor filters (Khumalo et al., 2011, Praptono and Sirait, 2013). The most commonly used transform-based approaches were contourlets (5%) and Gabor filters (5%). Table 2.3 shows advantages and disadvantages of the commonly used approaches in IS mapping.

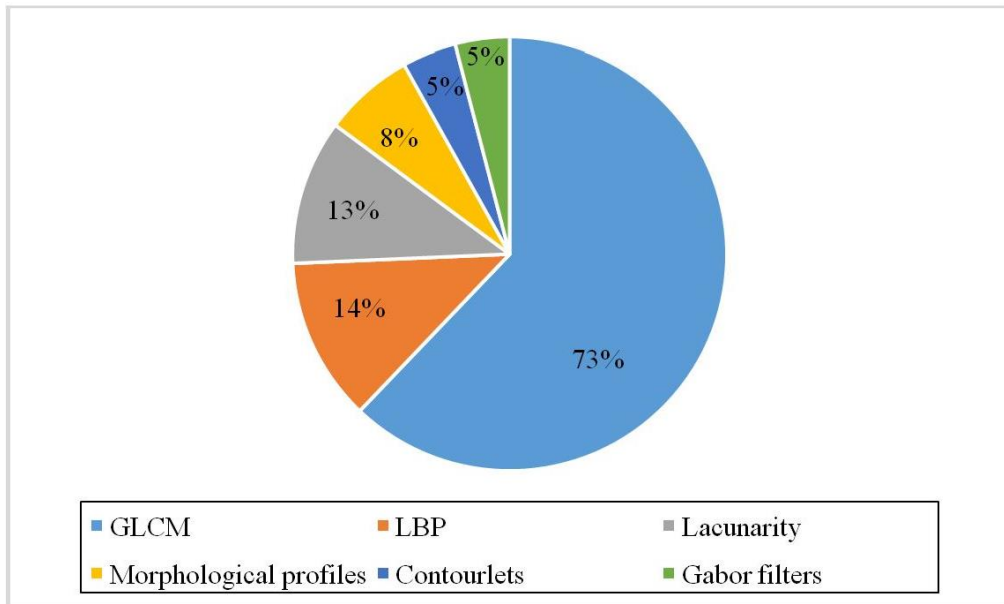


Figure 2.6. Studies that have used texture analysis approaches for the mapping of informal settlements from year 2005 to 2021

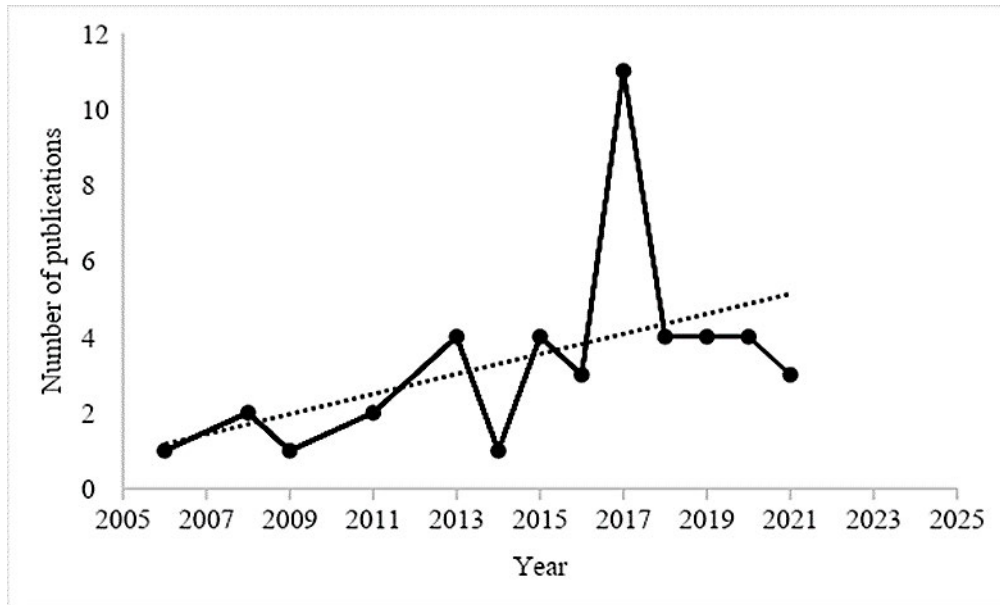


Figure 2.7. Literature review results for the number of publications (per year) using the grey level co-occurrence matrix analysis approach for mapping informal settlements from year 2005 to 2021

Table 2.3. Strengths and limitations of various texture analysis methods for informal settlement identification

Algorithm	Properties
GLCM	<p>Description</p> <p>It defines texture in terms of local grey level statistics based on the spatial distribution of reflectance values</p>
	<p>Sample studies</p> <p>Prabhu et al. (2021a) Wurm et al. (2017a) Kuffer et al. (2016b)</p>
	<p>Advantages</p> <ol style="list-style-type: none"> 1. GLCM addresses a large spatial neighborhood of the pixels 2. Characterize the detailed and complex urban structure at a reliable level
	<p>Limitations</p> <ol style="list-style-type: none"> 1. GLCM features can be obtained for a single orientation as well as combining all the orientation together making GLCM direction independent. 2. The GLCM is originally designed for texture analysis of two-dimensional (2D) images but today its scope is extended as scientists are using GLCM features to extract texture information from three-dimensional (3D) surfaces 3. Incapability of describing texture information at multiple scales which is overcome by extending GLCM to multiple scales. 4. GLCM computation requires long processing time 5. High dimensionality of the matrix 6. High correlation of Haralick features

	texture features such as GLCM and LBP are sensitive to viewing and illumination geometry differences
Local Binary Patterns	<p style="text-align: center;">Description</p> <ol style="list-style-type: none"> 1. LBP combines structural methods and statistical methods through analysis of local structures and occurrences, respectively 2. Through LBP one can easily define the image texture by two complementary measures, that is, “local spatial patterns” and “grayscale contrast.
	<p style="text-align: center;">Sample studies</p> <p>van den Bergh (2011) Luus et al. (2014) Fekri-Ershad (2020)</p>
	<p style="text-align: center;">Advantages</p> <ol style="list-style-type: none"> 1. Can define the local spatial structure and the local contrast of the image or part of the image 2. It is simple to implement and extraction of proper features with high classification accuracy 3.LBP are sensitive to viewing and illumination geometry differences 4. It is invariant to grayscale changes
	<p style="text-align: center;">Limitations</p> <ol style="list-style-type: none"> 1. Under certain circumstances, they miss the local structure as they don't consider the effect of the center pixel 2. They are often characterized by high dimensionality histograms 3. Some versions of local binary patterns are sensitive to noise. 4.They are not invariant to rotations. 5. High computational complexity
Lacunarity	<p style="text-align: center;">Description</p> <p>Distinguishes spatial patterns through the analysis of their gap distribution in different scales</p>
	<p style="text-align: center;">Sample studies</p> <p>Kit et al. (2012a) Kit and Lüdeke (2013) Owen and Wong (2013a)</p>
	<p style="text-align: center;">Advantages</p> <ol style="list-style-type: none"> 1. Properties of objects at different scales aid in better discrimination. 2. Provide information on intra and inter diversity. 3. Can provide valuable information to study the structural changes of a feature over time
	<p style="text-align: center;">Limitations</p> <ol style="list-style-type: none"> 1.Has the potential to misplace or misidentify ISs covering areas smaller than the grid sizes used to collect information. 2.Lacunarity values from one IS may be non-transferable to another IS due to specific qualities of the imagery being used such as its spatial and radiometric resolution. 3.Research on lacunarity mainly focus on the use binarized imagery, which leads to the loss of valuable image properties of ISs compared to the use of grayscale or color imagery.
Mathematical morphology	<p style="text-align: center;">Description</p> <p>Powerful tools used to extract spatial, structural information through opening and closing profiles with increasing sizes of structuring elements</p>
	<p style="text-align: center;">Sample studies</p> <p>Prabhu and Parvathavarthini (2021) Wurm et al. (2017b) Prabhu et al. (2021a)</p>
	<p style="text-align: center;">Advantages</p> <ol style="list-style-type: none"> 1.Discriminate urban ISs for different sizes and shapes 2.Allows the utility of implementing different shapes and sizes of opening, closing profiles in an image that yields spatially regular and homogeneous land
	<p style="text-align: center;">Limitations</p>

	MM uses scene specific rules which may not be transferrable to other image scenes.
Contourlets	Description
	Composed of basis images oriented at varying directions in multiple scales, with flexible nonlinear aspect ratios.
	Sample studies
	Ansari and Buddhiraju (2019b) Ansari et al. (2019b)
Contourlets	Advantages
	1. Exhibit a strong ability to capture intrinsic geometrical details and directional selectivity 2. Efficiently capture the curvilinear details and represents the structures having various orientation and anisotropic characteristics.
	Limitations
	They have a problem in effectively capturing the geometry of image edges
Gabor filters	Description
	A gabor filter is a linear local filter
	Sample studies
	Engstrom et al. (2017) Khumalo et al. (2011) Praptono and Sirait (2013)
	Advantages
	1. Ability to be adjusted in the areas of the place and in the frequency domain 2. The multiresolutional aspect of the approach allows the extraction of frequency and orientation information.
Limitations	
	1.It is characterized by high redundancy of features 2.The dimension of feature vector is too long

2.5.5. Spatial analysis of informal settlement mapping studies

Tables 2.4 and 2.5 compare peer reviewed published texture analysis studies in the most studied areas of India and South Africa. In the case of India, the most popularly used approaches, starting with the most frequent approach, were: (A) GLCM (B) LBP (C) Lacunarity (D) MM (E) Contourlets (F) Gabor filters. Results of analysis have indicated that of the 27 studies done in India on texture analysis approaches, 20 studies used GLCM approach. It is also important to note that, of the 10 texture-based studies conducted in Mumbai, all of them incorporated GLCM, which is indicative of the popularity of GLCM in Mumbai city. Gabor filters have not been explored in India. Almost similarly, GLCM was incorporated in all the texture analysis studies done in South Africa. Lacunarity, mathematical morphology and contourlets have not been explored in South Africa. It is also important to note that five out of the seven studies that used GLCM approach in South Africa were carried out in Soweto suburb. Tables 2.4 and 2.5 reveal that the use of more than one texture analysis approach has not been very common in the studies reviewed here (11 studies out of 31 studies).

Table 2.4. Studies of informal settlements in India using texture-based approaches classified by texture descriptor

A) GLCM; (B) LBP; (C) Lacunarity; (D) MM; (E) Contourlets; (F) Gabor filters

Author	Approach						City	Province
	A	*B	C	D	E	*F		
(Ansari and Buddhiraju, 2019c)	x				x		Pune	Maharashtra
(Ansari and Buddhiraju, 2019b)	x				x		Mumbai	Maharashtra
(Wurm et al., 2017a)	x			x			Mumbai	Maharashtra
(Wurm et al., 2017b)	x			x			Mumbai	Maharashtra
(Kit et al., 2012a)			x				Hyderabad	Telangana
(Kit and Lüdeke, 2013)	x						Ahmedabad	Gujarat
(Kuffer et al., 2017)	x						Mumbai	Maharashtra
(Bürgmann, 2015)	x						Mumbai	Maharashtra
(Kuffer et al., 2016b)	x						Mumbai	Maharashtra
(Kuffer et al., 2016b)	x						Ahmedabad	Gujarat
(Kuffer et al., 2015)	x						Mumbai	Maharashtra
(Kohli et al., 2016a)	x						Pune	Maharashtra
(Kuffer et al., 2013)	x						Mumbai	Maharashtra
(Shekhar, 2012)	x						Pune	Maharashtra
(Kohli et al., 2016c)	x						Pune	Maharashtra
(Prabhu and Alagu Raja, 2018)	x			x			Madurai	Tamil Nadu
(Prabhu and Parvathavarthini, 2021)				x			Madurai	Tamil Nadu
(Prabhu et al., 2021a)	x			x			Madurai	Tamil Nadu
(Prabhu et al., 2021b)				x			Madurai	Tamil Nadu
(Kit and Lüdeke, 2013)			x				Hyderabad	Telangana
(Girija and Nikhila, 2018)	x						Madurai	Tamil Nadu
(Naorem et al., 2016)	x						Mumbai	Maharashtra
(Prabhu et al., 2017)	x						Madurai	Tamil Nadu
(Weigand, 2017)	x			x			Mumbai	Maharashtra
No of studies	20		2	7	2			

* No studies using this approach occurred in India

Table 2.5. Studies of informal settlements in South Africa using texture-based approaches classified by texture descriptor

A) GLCM; (B) LBP; (C) Lacunarity; (D) MM; (E) Contourlets; (F) Gabor filters

Author	Approach						City	Province
	A	B	*C	*D	*E	F		
(Khumalo et al., 2011)	x					x	Johannesburg	Gauteng
(van den Bergh, 2011)	x	x					Johannesburg	Gauteng
(Mudau and Mhangara, 2021)	x						Tshwane	Gauteng
(Ella et al., 2008)	x	x					Johannesburg	Gauteng
(Shabat and Tapamo, 2017)	x						Johannesburg	Gauteng
(Luus et al., 2014)	x	x					Johannesburg	Gauteng
(Mdakane and van den Bergh, 2012)	x	x					Johannesburg	Gauteng
Total	7	4						

* No studies using this approach occurred in South Africa

2.5.6. Texture feature selection

Analysis of reviewed articles showed that feature selection did not attract adequate attention. Of the selected studies (Table 2.2), those that explicitly employed the feature selection method only account for 15.9%. The majority of studies failed to adopt the feature selection method or explicitly state whether the feature selection method was employed. Most of the studies that performed texture feature selection chose either GLCM or GLCM texture metrics as indicators of importance (Duque et al., 2017, Graesser et al., 2012, Owen and Wong, 2013a). Results of texture feature extraction varied across studies. Some texture metrics chosen as variables of importance included contrast (Duque et al., 2017, Kohli et al., 2016b, Kohli et al., 2013b), entropy (Owen and Wong, 2013a, Praptono and Sirait, 2013), variance (Girija and Nikhila, 2018, Kuffer et al., 2016b, Lai and Yang, 2020) and homogeneity and dissimilarity (Wurm et al., 2017a).

2.6. Comparison studies

2.6.1. Comparing methodological performance

Analysis of reviewed studies revealed that few studies compared texture-based algorithms in multiple countries (Duque et al., 2017, Graesser et al., 2012, Kuffer et al., 2016b, Schmitt et

al., 2018, Stasolla and Gamba, 2008). About 13% of published articles focused on multiple countries. Most of those studies crossed continental boundaries (Graesser et al., 2012, Kuffer et al., 2016b, Stasolla and Gamba, 2008) while Prabhu et al. (2021b) discriminated ISs in two cities of the same country, Madurai and Tiruppur, India. Kuffer et al. (2016b) revealed that GLCM variance allowed clear separation of ISs from formal settlements. On the other hand, Graesser et al. (2012) revealed failure of lacunarity approach to accurately distinguish ISs from formal settlements in Kabur, Kandahar, Caracas and La Paz.

2.6.2. Comparison of used classifiers

In this analysis, only classifiers that were used in two or more publications were considered. Considering all the classifiers used in the 63 publications, 36.5% employed conventional machine learning classifiers. Frequencies of most commonly used classifiers based on the above-mentioned criteria were listed in Table 2.2, and the classifiers include MDM, SVM, RF, LDA, CNN and LR. Figure 2.8 shows the frequency of the commonly used classifiers, as represented in Table 2.2. Random Forest was the most commonly used classifier, followed by SVM. Results showed that 28.6% of the 63 publications used RF whilst 20.6% used SVM. In terms of classification accuracy, the results also indicate that machine learning classifiers yielded higher accuracies than conventional classifiers with most of the classification accuracies achieved being above 80%. Comparing accuracies for the two commonly used classifiers, SVM demonstrated superiority in terms of classification accuracy (Figure 2.9). SVM, on average performed better than RF with mean accuracy (~90%) and (~ 89%), respectively.

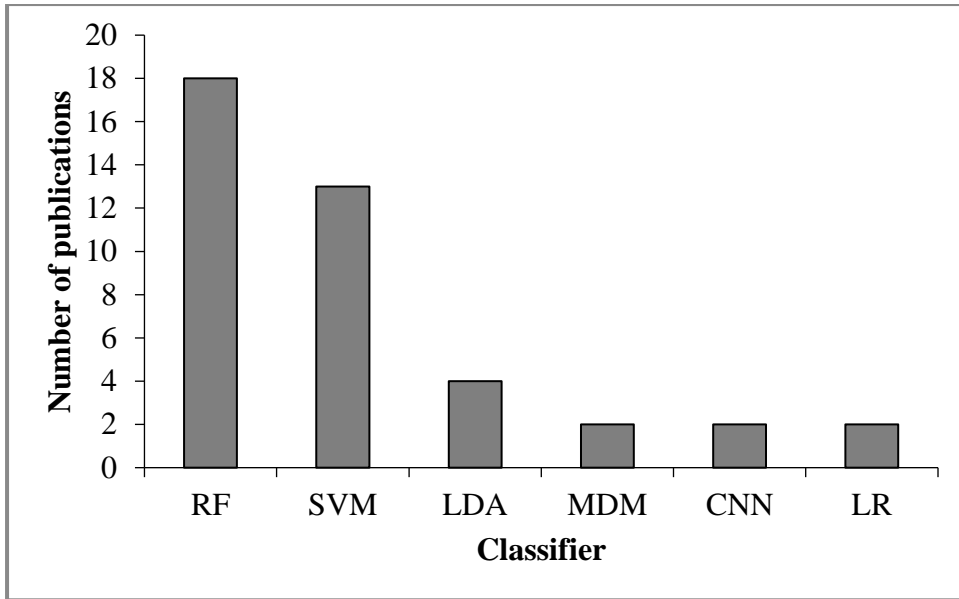


Figure 2.8. Frequency of classifiers used for the mapping of informal settlements using texture analysis approaches from year 2005 to 2021

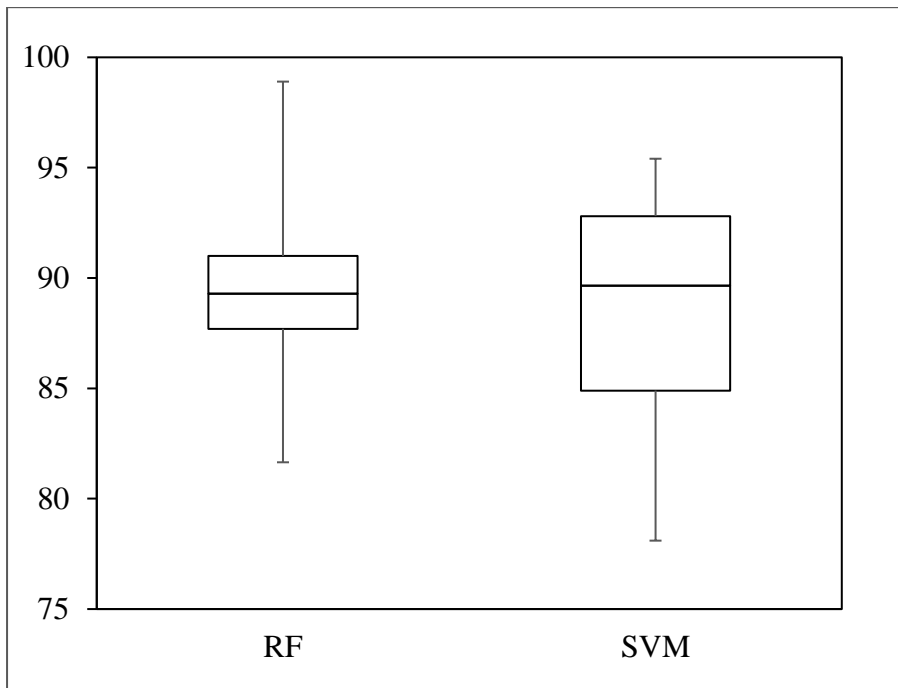


Figure 2.9. Overall accuracy of Random Forest vs Support Vector Machine algorithms in the mapping of informal settlements using texture analysis approaches from year 2005 to 2021

Deep learning, on the other hand, has also shown an emerging trend in texture based IS identification with 3 out of 63 studies having used deep learning algorithms.

2.7. Effect of window size in informal settlement extraction

The importance of scale in texture analysis for IS detection was emphasised in numerous studies (Ansari and Buddhiraju, 2019b, Graesser et al., 2012, Wurm et al., 2017a). To take cognizance of scale dependent nature of image texture, some studies investigated the discriminative power of multi-resolution analysis (MRA) based feature descriptors such as wavelets, contourlets and curvelets (Ansari and Buddhiraju, 2019b, Ansari and Buddhiraju, 2019c). MRA approach showed some popularity with 10% of the studies having exploited wavelets, curvelets, and contourlets. Whilst 17% of the studies varied window sizes and established optimum window sizes, some just varied window sizes and were not conclusive of the optimum window size (Ansari and Buddhiraju, 2019b, Ansari and Buddhiraju, 2019c). Of the studies that determined optimum window sizes, most of them ranged from 19 x 19 to 200 x 200. However, some studies used small window size of 3x3 (Lai and Yang, 2020, Owen and Wong, 2013a).

3. Discussion of results, gaps in knowledge and future directions

3.1. Geographic distribution of case studies

The results of the current analysis highlighted a number of knowledge gaps. The major gaps are found in the spatial locations for which texture analysis techniques are employed for IS identification. Most notably, the approaches are only found in a few countries, with studies focusing largely on India, followed by South Africa. This result is consistent with Mahabir et al. (2018) who also revealed highest concentrations of informal settlement studies in India and South Africa. According to Tellman et al. (2022), high resolution (<10 m) satellite data is a requirement when mapping informal settlements. In their assessment of spatial distribution of H/VHR imagery for the study of informal settlements, Mahabir et al. (2018) discovered that India and South Africa were among the major regions with the highest usage of H/VHR imagery. The authors' results also indicated that the application of analysis methods including, among others, image texture analysis, follow the similar trend. One could then explain higher prevalence of texture analysis approaches in India and South Africa in terms of higher utilization of H/ VHR in the regions. The underutilization in other regions could be due to unavailability or cost-prohibitive nature of commercial satellites, for example Quickbird, WorldView and GeoEye especially in resource constrained countries, which leaves many regions understudied. For example, cities with records of dynamic IS population, for example, Nairobi (60%) and Cairo (65%) (Satterthwaite et al., 2020) have not been studied. Given

projections for significant growth of IS dwellers, worldwide, especially in sub-Saharan Africa over the next 20 years (Girija and Nikhila, 2018, United-Nations, 2015), there is need for case studies that stretch across the range of all urban frameworks for better understanding of IS characterization.

The results of analysis also showed that case studies are sparsely distributed within few cities in a country. For example, in India, the 27 studies were distributed across six cities, distributed in four states of India, which are Maharashtra, Telangana, Gujarat and Tamil Nadu. Prabhu et al. (2021a) submitted that there are huge IS populations in other Indian states such as Andhra Pradesh, West Bengal, Madhya Pradesh, and Uttar Pradesh for which published studies have not been found. The case study distribution is also skewed towards large cities, with small and medium sized urban areas remaining significantly less studied. Leao and Leao (2011) explained this distribution in terms of well distinguishable morphological differences between formal and informal urban development in large cities. For instance, in India, studies are more concentrated in Mumbai (11 studies out of the 27 studies), followed by Madurai city (6). Apart from being home to one of the largest ISs in Asia (Dharavi), Mumbai's characteristic high IS population (42% of Mumbai's dwellers) occupying 13–15% of the city (Wurm et al., 2017a) could attract IS research. Moreover, heterogeneity of IS size relating to the characteristic morphology of Indian ISs (Kuffer et al., 2017) make Mumbai well-suited to develop and test IS mapping techniques (Taubenböck and Wiesner, 2015). Most importantly, Kuffer et al. (2017) argued that morphologic characteristics of Mumbai ISs can be easily extracted by texture based methods.

For South Africa, the eight studies identified in literature are spread in only three cities, which are Johannesburg, Tshwane and Capetown. Interestingly, seven out of the eight studies are found in Gauteng province. The large gaps in the spatial coverage of studies could be explained in terms of restrictive data costs that limit usage of high resolution commercial satellites, especially in cities of the global south (Taubenböck et al., 2018). Arribas-Bel et al. (2017) submitted that globally, many researchers or research institutions lack the financial capacity to purchase full satellite imagery, thus limiting research. Those financial constraints make many researchers to prefer focusing on methodological advances and not exploring new study areas. Although other sensors for example MODIS (250 m) and Landsat (30 m) are free for research use, Tellman et al. (2022) argued that their resolution is not sufficient to capture informal

settlement patterns. Again, one would argue that availability of freely available sensors, for example Sentinel imagery, should fill the gap and improve image availability. Even though, image availability may still remain problematic due to frequent cloud cover in tropical cities, such as Kenya, Tanzania and Uganda (Kuffer et al., 2016a). In that regard SAR sensors such as TerraSAR-X are available and can penetrate clouds. However, such sensors have been scarcely used in texture analysis (Wurm et al., 2017a).

Across all geographical scales, selective coverage of case study areas may hinder comprehensive understanding of informality globally (Mahabir et al., 2018). The unbalanced spatial coverage of studies would mean that the global IS inventory that Kuffer et al. (2016a) initiated could still be far from being achieved. There is, therefore, need for more studies in smaller and medium sized cities in order to improve understanding of morphological variations across all spatial scales (Wang et al., 2019c). Clearly though, lack of studies in some areas presents potential opportunities to deliver science, especially in the small towns and cities where science-informed policy guidance is crucial for sustainable urban development (Reba and Seto, 2020).

Sensors

Very High-Resolution sensors such as QuickBird, WorldView and SPOT have been major sources of data for IS extraction using texture analysis (Kuffer et al. 2016a). The advantage of VHR earth observation satellites is that they allow extraction of detailed information, allowing characterization of IS landscapes based on their morphological characteristics (Gevaert et al. 2017, Graesser et al., 2012). The analysis of the employed methods shows that most studies used commercial and rather expensive imagery (QuickBird, WorldView). Only very few studies used free data sources such as Google Earth (GE) (Arribas-Bel et al., 2017, Duque et al., 2017, Duque et al., 2015, Praptono and Sirait, 2013) and Sentinel-2 A (Wurm et al., 2017b). Analyzing the satellite sensors used in the reviewed studies (Figure 5), QuickBird was identified as the most frequently used sensor (33%). The QuickBird sensor provides a geometric resolution of 0.60 m in panchromatic mode and therefore basically allows for a delineation of the objects in ISs (Kuffer et al., 2016b). Although radar images (PALSAR, Terra-SAR-X) have been scantily used in texture based informal settlement mapping, there has been progress in their use (Burgmann, 2015, Wurm et al., 2017). Weigand (2017) described SAR sensors as a reliable data source for large area IS mapping because of their ability to trace potential locations of ISs (Schmitt et al., 2018). Their reliability is enhanced by their capability

to penetrate clouds and other atmospheric components, a characteristic that is lacking in optical remote sensing (Burgmann, 2015). Radar data presents opportunities for studies in developing countries that lie in the tropical regions (Weigand, 2017).

3.2. Application of texture analysis approaches for informal settlement modelling

3.2.1. Performance of texture analysis approaches in informal settlement mapping

Several methods have been exploited to identify IS areas. Information extracted from reviewed case studies indicated that GLCM was the most commonly used approach (73%). Comparing an algorithm to another allows assessment of effectiveness of that algorithm as well as establishment of its strengths and weaknesses (Ma et al., 2017). Analysis of studies that compared algorithms (Ansari and Buddhiraju, 2019b, Ansari et al., 2019a, Leonita et al., 2018, Prabhu and Alagu Raja, 2018, Wurm et al., 2017a) revealed that most comparisons involved GLCM. While some of those studies compared two algorithms (Ella et al., 2008, Shabat and Tapamo, 2017, Wurm et al., 2017a), others investigated more than two algorithms (Ansari and Buddhiraju, 2019b, Ansari and Buddhiraju, 2019c). The results of comparing GLCM and LBP (Ella et al., 2008, Mboga et al., 2017) indicated that LBP outperformed GLCM. Findings from Ella et al. (2008)'s research revealed that LBP outperformed GLCM with accuracy levels of 98% and 94%, respectively. In a similar manner, Mboga et al. (2017) also observed superiority of LBP against GLCM with accuracy levels of 90.48% and 86.65%, respectively. Almost similarly, Shabat and Tapamo (2017) compared local directional patterns (LDP) and GLCM. Results indicated that LDP outperformed GLCM but the results were not conclusive with regard to the final accuracy level. GLCM, lacunarity, histogram gradients, linear feature distribution, line support regions, vegetation indices, and textons were also compared in Graesser et al. (2012)'s study. This study utilised a large dataset to develop consistent predictors for formal built up areas and IS areas. The robustness of textons was revealed in all included cities with the features achieving maximum accuracy of 92%. Other works (Ansari and Buddhiraju, 2019c), compared GLCM with 3 transform based approaches, which are, MRA based contourlets and wavelets, as well as CRISP contourlets. The results indicated that contourlets performed better than GLCM and wavelets with overall classification accuracy ranging from 93-96%. The wavelets were criticized for their inability to show directional information besides horizontal, vertical and diagonal directions. Similar works (Ansari and Buddhiraju, 2019b) compared GLCM with contourlets, curvelets and wavelet transforms. Results of their study indicated that curvelet based statistical feature descriptors yielded the

best discriminative power than all the other approaches. Ansari et al. (2019a) attributed the performance of curvelets and contourlets to their ability to extract textural information at multiple scales and in varied directions.

The GLCM's compromised performance in most of the comparison studies is largely due to its incapability to extract and characterise ISs at different scales (deSiqueira et al., 2013, Prabhu and Alagu Raja, 2018, Ramola et al., 2020). Ansari and Buddhiraju (2019c) iterated that those methods which do not employ multi resolution strategy in texture analysis cannot exploit the scale dependency nature of texture. The issue of scale was, thus, a concerning factor in the studies.

3.2.2. Multi-scale analysis

To deal with the multi-scale complexity of IS landscapes (Wurm et al., 2017a), several researchers have employed multi-scale based approaches in discriminating ISs. Some researchers extended GLCM to multiple scales through varying window sizes (Graesser et al., 2012, Luus et al., 2014, Owen and Wong, 2013a, Wurm et al., 2017a). Even though Graesser et al. (2012) used a discrete window size, the authors acknowledged that accuracies would improve if statistics were computed with a moving window, instead. Wurm et al. (2017a) observed that the effect of window size on accuracy is dependent on the size of target objects. In this regard, several studies (Kuffer et al., 2016b, Weigand, 2017, Wurm et al., 2017a) agreed that for large IS areas, large window sizes improve IS identification accuracy. On the other hand, small window sizes are needed for small IS patches (Lai and Yang, 2020, Owen and Wong, 2013a). Whilst Owen and Wong (2013a) criticised the larger window sizes because of their resultant smoothing effect. Wurm et al. (2017b) regarded the smoothing effect of large window size as beneficial to IS mapping. However, large window sizes are associated with long processing times and the process of varying them is computationally expensive (Graesser et al., 2012).

In order to incorporate variability of scale in an image, some studies that exploited GLCM algorithm also integrated the approach with different conventional mathematical morphologies (Leonita et al., 2018, Prabhu et al., 2021a, Wurm et al., 2017a). According to Ramola et al. (2020), integrating GLCM and MM have the capability to enhance classification accuracy for texture images. GLCM and MM complement each other in that, while morphological features

possess the capability to capture geometric information and dissimilar structures in an image, determining their shape and size (Prabhu and Alagu Raja, 2018), GLCM texture features determine the built up densities (Leonita et al., 2018). Wurm et al. (2017b) applied MM on SAR to distinguish formal and ISs in Italy and Sudan. Wurm et al. (2017a) utilised GLCM together with morphological profiles (MP), obtained from polarimetric SAR, to characterise ISs in Mumbai city. They revealed the capability of GLCM to detect large IS patches with higher accuracies than smaller patches. The authors observed that GLCM performed better than MP. The authors cited that the performance of MP was compromised by the strip map data used (6 m) which could not allow meaningful extraction of IS dwellings. Moreover, the sensor is hugely affected by the orientation of buildings thus affecting image classification (Wurm et al., 2017a). In another study, Wurm et al. (2017b) explored the use of GLCM and differential morphological profiles using Sentinel-2A data for IS mapping in Mumbai city. Their results revealed that neither GLCM nor DMP alone could accurately depict the presence of ISs. However, the integration of the two approaches produced increased accuracy. Similarly, when Tamura features and wavelets could not distinguish ISs of different shapes and sizes, Prabhu and Alagu Raja (2018) successfully integrated them with MM to incorporate shape and size. These studies that combined approaches supported Graesser et al. (2012)'s findings who argued that integration of texture metrics may be necessary for discrimination of complex urban settlement patterns.

Lacunarity is also a multiscale approach whose discriminating power was investigated in several studies (Amorim et al., 2014, Kit and Lüdeke, 2013, Kit et al., 2012a, Owen and Wong, 2013a). However, conflicting results were reported in the reviewed literature with regard to its strength in capturing the presence of ISs. While some studies (Graesser et al., 2012, Kit et al., 2012a) reported higher lacunarity values to be indicators of IS presence, others reported lower lacunarity values as indicators (Amorim et al., 2014, Barros Filho and Sobreira, 2008). Such differences could emanate from variations in defining the term IS. Describing ISs as comprising "less gathered buildings" (Prabhu et al., 2021a) would imply higher gappiness and hence higher lacunarity values. On the other hand describing them as "densely built up areas" (Persello and Stein, 2017) would lead to adoption of lower permeability and lower gappiness (Amorim et al., 2014, Barros Filho and Sobreira, 2008), implying lower lacunarity. While lacunarity was effective in discriminating ISs (Kit et al., 2012a), its effectiveness was questioned in Kit and Lüdeke (2013) and Owen and Wong (2013a)'s studies. Kit and Lüdeke (2013) observed that lacunarity could not identify small IS pockets. The authors argued that

the approach requires a large window so complex residential boundaries may lead to potential misclassification or misidentification of ISs where small areas are concerned. Owen and Wong (2013a) explained differences in results as they indicated that lacunarity values calculated for ISs in one area may not be applicable to another location. One can conclude that, because of morphological variations between study areas, it may be difficult to derive generalised research results.

3.2.3. Application of machine learning in texture based informal settlement detection.

In the current review, studies exploited machine learning algorithms either to learn features directly from the data (Mboga et al., 2017) or as classification algorithms. Those that employed machine learning for classification purposes used conventional algorithms such as RF, SVM, LR, DTs, and others (Duque et al., 2017, Fallatah et al., 2020, Kuffer et al., 2017, Leonita et al., 2018, Wurm et al., 2017b). Results have shown superiority of SVM in terms of mean accuracy of ~ 90% whilst RF obtained mean accuracy of ~ 89%. However, there are inconsistent results as to which one performs better. Some studies suggested that RF produces the best IS accuracy (Arribas-Bel et al., 2017, Bürgmann, 2015, Fallatah et al., 2020, Wurm et al., 2017b). Random Forest algorithm is advantageous in that it can handle wide spectrum of training areas (Wurm et al., 2017a). Wurm et al. (2017a), however, observed that training random forests using large quantities of training pixels is extremely time consuming. On the other hand, studies that utilised SVM observed that it performed better in differentiating IS areas from non-IS areas (Duque et al., 2017, Leonita et al., 2018, Prabhu and Parvathavarthini, 2021). Duque et al. (2017) put forward that SVM algorithm works well even with few training samples. Ma et al. (2017) submitted that performances of various classifiers may be inconsistent due to influences of other uncertain factors, notably, scale and texture feature selection (Ma et al., 2015). The DTs and RF classifiers perform better at processing redundant features, while other classifiers benefit more from feature selection (Ma et al., 2017). Another advantage of DT is that it can perform feature selection on its own, a characteristic that most classifiers do not have (Graesser et al., 2012).

Recently, deep learning has gained attention in IS analysis (Mboga et al., 2017, Persello and Stein, 2017, Prabhu et al., 2021b). Mboga et al. (2017) utilised CNN to detect ISs in Dar es Salaam, Tanzania. While Persello and Stein (2017) successfully distinguished ISs using deep fully convolutional networks (FCNs), Prabhu et al. (2021b) explored the potential of kernel

based deep convolutional neural network (DK-DCNN). The main advantage of machine learning is the capacity to incorporate any number of variables without being concerned about multicollinearity as well as to capture non-linear relationships (Wurm et al., 2017a).

3.2.4. Spatial analysis of texture analysis algorithms

There are also gaps in the geographies for which texture analysis techniques are exploited in different countries. The spread of the most used algorithms in literature was analysed considering the most commonly used approaches in the highly studied countries of India and South Africa. Results of analysis revealed that GLCM approach is the most commonly used approach in both India and South Africa (Table 2.4 and 2.5). More specifically, the approach is most concentrated in Mumbai where out of 11 texture analysis studies exploited in Mumbai, 10 utilised GLCM (Table 2.4). Studies have shown that locally specific ISs in Mumbai can be easily mapped using GLCM texture measures, particularly, GLCM variance (Kuffer et al., 2016b, Kuffer et al., 2017, Wurm et al., 2017a). The 7 studies carried out in South Africa using GLCM are found in 2 cities, Johannesburg and Tshwane. All the studies performed in Johannesburg were biased towards Soweto. Gabor filters were never explored in India. Similarly, there were no studies that exploited mathematical morphology and contourlets in South Africa. From a spatial point of view, Kuffer et al. (2016a) submitted that, such discriminative use of analytical approaches, and in the same areas raises the concern of probable biases in the analysis as well as in the comprehension of ISs (as derived from these studies). However, underutilised approaches and understudied areas present potential opportunities in terms of research avenues for the exploration of those texture analysis approaches in other areas.

3.2.5. Effect of feature selection on classification

The reviewed studies indicated that there is uncertainty as to whether feature selection could improve the process of texture based IS identification or not. Graesser et al. (2012) demonstrated that, using a full set of image features may cause the inclusion of redundant or highly correlated features which, apart from being computationally expensive, may degrade performance of classifiers. In the current review, there are studies that performed well using single texture feature, for example, variance (Kuffer et al., 2016b). Lai and Yang (2020) put forward that variance resolves the confusion between formal built up land and informal structures and allows extraction of ISs in complex urban morphologies. Duque et al. (2017),

however, put forward that, although feature selection may reduce classification complexity and improve classification accuracies, not all studies guarantee that feature selection improves classification accuracy. This observation was consistent with Wurm et al. (2017b) who combined morphological profiles and GLCM when each of the texture features had failed to characterise structure of IS settlements alone. In agreement Graesser et al. (2012) argued that one feature may not be sufficient to characterise ISs. Ma et al. (2015) put forward that feature selection may be associated with several uncertainties introduced by performance of classifiers that influence classification performance. Duque et al. (2017) 's study demonstrated that selected texture features performed better with the use of SVM as a classifier than RF. The author argued that low classification scores provided by RF could be due to existence of peculiarities within cities that may complicate the identification of ISs using the model. The results presented by Duque et al. (2017) showed that SVM classification accuracy improved with decreased number of dimensions. Graesser et al. (2012) assessed and tested the capability of 230 variables, using DTs and selected 10 variables which resulted in improved overall accuracies, 91%, 89%, 92% and 85% for the cities of Caracas, Venezuela, Kabul and Kandahar, respectively. According to the authors, DTs are advantageous in that it is a classification scheme that performs texture feature selection on its own, a property that other classifiers do not have. However, although feature selection is an important step to ensure working with the best and achieving high accuracies, it is computationally costly.

3.2.6. Comparisons between countries

To demonstrate methodological reproducibility, some researchers performed cross city comparisons (Duque et al., 2017, Graesser et al., 2012, Kuffer et al., 2016b, Owen and Wong, 2013a, Schmitt et al., 2018). Some studies were carried out in cities within the same country (Owen and Wong, 2013a), cities of different countries within the same continent (Duque et al., 2017), cities of different countries across continents (Graesser et al., 2012) and some across continents, but including a city in sub-Saharan Africa (Ansari and Buddhiraju, 2019c, Gevaert et al., 2017, Kuffer et al., 2016b, Schmitt et al., 2018, Stasolla and Gamba, 2008). Duque et al. (2017) tested the ability of LR, SVM and RF to depict presence of ISs in Buenos Aires (Argentina), Medellin (Colombia) and Recife (Brazil). SVM algorithm accurately identified ISs in all the three countries. Almost similarly, Schmitt et al. (2018) used schmittlets to identify ISs in Cape town, Manilla and Mumbai with accuracy levels reaching 87%, 60% and 54%, respectively. Both studies focused on similarity of ISs. Schmitt et al. (2018) put forward that,

although ISs can be mapped with similarity in all the three cities, the way in which each IS's morphology varies in relation to the surrounding urban morphology differs. Both studies acknowledged the importance of considering local patterns or specific characteristics of each city instead of using a unified model. Even in the same continent, Duque et al. (2017) established that it is impossible to fit one method for IS identification. This is because morphological variations are better captured using locally specific feature sets (Wang et al., 2019c). The method may seem applicable basing on overall accuracy values but the respective class accuracy is highly dependent on the specific city structure (Schmitt et al., 2018).

Although statistics are robust in capturing IS diversity, there were inconsistencies in results where methodologies were tested in two different localities. Owen and Wong (2013b)'s study revealed that indicator significance may differ depending on weather, climatic conditions as well as altitude. If mapping IS areas in cities within the same country (Coban and Guatemala) would be impacted by environmental conditions (Owen and Wong, 2013b), one would question how feature sets could be transferred across continents. Kuffer et al. (2016b)'s study depicted that low GLCM variance values represented ISs whilst high values represented formal settlements. The results indicated that, whilst methodology could be successfully applied to Kigali, transferring to Ahmedabad required variation of window sizes, making it difficult to generalise results. Structural differences, attributed to high socio-economic gradient between the two countries, could help explain the inconsistencies in the results (Owen and Wong, 2013b). Transferability issues could also arise from capturing settlements at different stages of development. Detecting ISs that are at infancy stage and those at maturity stage using the same model may be challenging and misleading (Owen and Wong, 2013b), since newly established ones may not be evident in the image, whilst the mature ones would be captured well.

Schmitt et al. (2018) also suggested that the impact of sensors in the detection of ISs should be taken into consideration especially in areas of differing altitudes. From the reviewed studies on comparisons, it could be observed that the studies only focused on transferability and robustness of approaches and ignored the impact of sensors, which in most comparison cases were of different resolutions. Schmitt et al. (2018), in agreement with Wurm et al. (2017a) also put forward that although texture and structural information could distinguish between informality and formal built up areas, the impact of orientation on the class accuracy is high. The authors pointed out that, sensors, for example Space –borne SAR sensors that only provide a narrow range of image geometries would not be able to picture multiple geometries, thus

compromising accuracy. This means that sensor requirements should suit the morphological variations in order to enhance replicability. Schmitt et al. (2018) recommended more research into appropriate sensors that would suit specific IS typologies.

Due to complexity of IS morphology, RS still leads to incomparable datasets across studies (Taubenböck et al., 2018). Kuffer et al. (2017) suggested that an inventory of morphological types be carried out for each locality as conceptual foundation. An interplay of earth observation data with field surveys is imperative in the process, since there is proven correlation of image features with socio-economic parameters of an area (Duque et al., 2015). Schmitt et al. (2018) also pointed out that IS locations may be detected, but whether it is inhabited or not cannot be taken automatically. The authors recommended human interaction to be integrated with texture based remote sensing methods.

3.3. Integrating texture analysis and socio-economic data

Fusion of textural information and other ancillary datasets are important for improvement of IS identification and accuracy. Some researchers have attempted to integrate spatial features with other complimentary socio-economic information such as employment status, educational status, population figures and population density, to avoid representation of ISs as one-dimensional phenomena, that is, physical characteristics (Baud et al., 2010). Weeks et al. (2007) integrated satellite information, from Quickbird imagery, with cultural and socioeconomic characteristics, obtained from the census, to locate ISs in Ghana. In this study texture was used as an additional metric. Sandborn and Engstrom (2016) extracted five spatial features, from imagery, which include line support regions, Pantex, histograms of oriented gradients, local binary patterns, and fourier transform and then correlated them to census variables. The results obtained from this analysis suggested that socio-economic characteristics can be mapped from spatial features derived from satellite imagery and can help detect deprived areas. Such indirect extraction of socio-economic data from remotely sensed imagery to characterise ISs is important, especially in countries in the global south where census data is either non-existent, outdated or of low temporal resolution (Mahabir et al., 2018). According to Baud et al. (2010), the success of such integrative studies shows the importance of combining socio economic information and RS. However, Mahabir et al. (2016) postulated that one major limitation of integrating RS derived socio-economic information with existing socio-economic data from traditional sources, for example, census, are differences in temporal and spatial

resolutions of these data. However, in cases where socioeconomic data from surveys exists, their accessibility for research purposes may be hampered due to protection of privacy and confidentiality. This limits the use of census surveys, alone, in acquiring information for the mapping of deprived areas and hence promotes the fusion with remote sensing datasets.

3.4. Limitations of texture analysis in informal settlement identification

Whilst texture analysis has capability to improve informal settlement identification, it does not offer total solution to heterogeneity problem in urban areas (Zhang et al., 2003). A major limitation in the use of image texture for classification emanates from failure to identify suitable textures and the computation costs associated with texture feature selection (Mhangara and Odindi, 2013). Moreso, Mahabir et al. (2018) revealed that there is little guidance in literature on the selection of the most effective texture metrics to use in IS identification, often leading to the process of trial and error. A scrutiny of literature revealed that texture varies with the characteristics of the landscape under investigation and the image data used. Because of morphological variations, the texture measures extracted vary within the same slum or across different locations (Schmitt et al., 2018). The unique properties of individual slums and the imagery used makes it difficult to transfer textures at specific window sizes and at a particular shape found significant for one slum to another slum (Wurm et al., 2017a). While varying window sizes and averaging the textures over all directions are acknowledged in texture analysis (Engstrom et al., 2017), a thorough understanding of their relevance is limited since they are usually performed through simple trial-and-error (Wang et al., 2019a). Moreso, averaging directions is computationally expensive and often lead to loss of textural information (Singh and Srivastava, 2017).

3.5. Conclusion

This study aimed at understanding the contribution of texture analysis in IS modelling. The current research has shown that there is huge progress in the use of texture analysis for IS detection. However, analysis of results pointed to significant gaps in knowledge, especially in the spatial coverage of studies and methods. Results revealed that the geographical coverage of texture analysis approaches is scarce across the world. Many studies focus on Indian cities. Many cities, especially in sub-Saharan Africa, are being understudied. Even within well studied countries, there is concentration of studies in particular cities, and limited work in other cities. This suggests the need for a wider geographic coverage in order to better understand and

characterize ISs across the globe. GLCM proved to be the most popularly used approach. Interestingly, analyses showed that there are gaps in the geographical coverage of approaches where some approaches are concentrated in certain geographical areas and are sparse in others. With regard to datasets, Quickbird was the most employed sensor. Freely available satellites Sentinel-2A have not been largely exploited. Results have also shown that not all studies could safely regard feature selection as contributing to enhanced classification accuracy because of uncertainties introduced in the process of texture-based classification. Hence, feature selection requires substantial further research.

The use of machine learning classifiers, particularly, RF and SVM has proved to have a great potential of improving texture based IS identification. Although RF and SVM classifiers have also attracted great attention owing to their excellent classification performance, deep learning is showing immense potential to enhance classification accuracy. Studies revealed that, not all unified models could cater for morphologic characteristics of IS areas in different geographic settings. Where applicability of algorithms in different localities is investigated region specific feature sets should be developed. Studies recommended integration of RS data and socio-economic parameters derived from field surveys in order to have a comprehensive understanding of region-specific morphologies. Future review studies should explore the integration of texture analysis and field surveys in locally specific contexts in order to enhance understanding of the techniques in relation to particular IS typologies.

3.6. Summary

This chapter provided an investigation of application of texture analysis algorithms for informal settlement identification. Investigations revealed that GLCM was the most popularly used texture feature extraction algorithm. Whilst all studies that were carried out in South Africa utilized GLCM, they were mainly concentrated in Johannesburg. Only one of seven studies that utilized GLCM algorithm was done in Tshwane. This presented a research gap for a study in Durban which equally grapples with proliferation of these low-income housing settlements. The study also revealed that Quickbird was the most utilized sensor for informal settlement identification. Sentinel-2A, which is freely downloadable was scantily exploited. Sentinel-2A, having high spectral resolution, coupled with its characteristic 10 m bands presents potential to exploit pan sharpening technique for informal settlement mapping. Thus,

the next chapter will exploit possibility of pan sharpening Sentinel-2A for precise informal settlement mapping in Durban.

CHAPTER THREE:

Performance evaluation of pan sharpening Sentinel 2A imagery for informal settlement identification by spectral-textural features

This chapter is based on:

Matarira, D., Mutanga, O., & Naidu, M. (2022). Performance evaluation of pansharpening Sentinel 2A imagery for informal settlement identification by spectral-textural features. *Transactions of the Royal Society of South Africa*, 1-14. doi:10.1080/0035919x.2022.2144538

Abstract:

The diversity of informal settlement morphologies across locales makes their mapping inherently challenging in heterogeneous urban landscapes. This study sought to evaluate the potential of pan sharpening techniques on Sentinel-2A data, and textural features in enhancing informal settlement identification accuracy, in a fragmented urban environment. Brovey transform, Intensity, Hue and Saturation transform, ESRI, Simple mean, and Gram-Schmidt techniques were employed to pan sharpen multispectral bands of Sentinel-2A, bands 5, 6, and 7 in the first group, and bands 8A, 11 and 12 in another, using an average of bands 4 and 8 as the panchromatic band. The main objective was to investigate the efficacy of pan sharpening Sentinel-2A imagery and texture analysis in automated mapping of morphologically varied informal settlements. An evaluation of the quality of fused images was undertaken through computation of the correlation between the spectral values of the original multispectral and pan sharpened image. Grey-level-co-occurrence matrix texture features were extracted from the pan sharpened images, and subsequently incorporated in the classification process, using a support vector machine classifier. Our results confirm that Gram Schmidt fusion technique yielded the highest performance (F-score 95.2%; Overall accuracy 91.8%). The experimental results demonstrated the potential of pan sharpening Sentinel-2A, and the added value of image texture for a more nuanced characterization of informal settlements.

Keywords: Pan sharpening, sentinel 2A, informal settlement mapping, remote sensing, image texture

3.1. Introduction

Informal settlements have become a major constituent of urban development, worldwide. Having, approximately, 1 billion informal settlement dwellers globally (UN-Habitat, 2016), projections reveal that, as the population in urban areas of sub-Saharan Africa grows by 10 million yearly, 7 million people are likely to occupy informal settlements (United-Nations, 2015, Mahabir et al., 2018). Often described as a physical expression of poverty and inequalities (Mahabir et al., 2018, Müller et al., 2020), informal settlements are characterized by overcrowding, insecurity of tenure, low quality housing structures and lack of access to adequate basic amenities (Hofmann et al., 2015). Taking cognizance of informal settlements' deprivations, the United Nations mandated governments to address the growing urban poverty through Goal 11 of 2030 Sustainable Development Goals (Fallatah et al., 2022, Mugiraneza et al., 2019) that prioritized the urban poor. However, in order to support improvements in informal settlements, up-to date information on their morphology, in terms of location, extent and dynamics is a prerequisite. Such information is often either unavailable, outdated or inconsistent (Wang et al., 2019b). Characteristic diversity of informal settlement morphologies renders their automatic detection inherently complex (Hofmann et al., 2015), making it difficult to map and model their extent and distribution (Mahabir et al., 2018, Patel and Baptist, 2012). Accurately capturing their variability provides baseline information for tackling issues to do with urban development, poverty reduction, environmental protection and urban risk management (Tellman et al., 2022).

Remote sensing provides potential data for capturing of the diversity of informal settlement morphologies as well as their spatial dynamics (Kraff et al., 2020). Technological advancements, particularly in terms of enhanced spatial and spectral resolutions of sensors have allowed detailed characterization of these urban deprived areas (Fallatah et al., 2022, Prabhu and Parvathavarthini, 2021). Various high resolution earth observation (EO) data have been tested to map informal settlements, which include commercial satellites such as Quickbird imagery (Kohli et al., 2016a, Mboga et al., 2017, Persello and Stein, 2017), World view (Ansari and Buddhiraju, 2019b, Kuffer et al., 2016b), GeoEye (Fallatah et al., 2020, Fallatah et al., 2019, Fallatah et al., 2022). However, selection of the proper remote sensing data for a particular application is controlled by factors such as the cost and resolutions (Mahmoud, 2021). For instance, the unavailability and cost prohibitive nature of high resolution imagery makes extraction of urban deprived areas challenging (Taubenböck et al., 2018). Some studies

have thus exploited freely available Sentinel-2A data for the mapping of informal settlements (Gram-Hansen et al., 2019, Wurm et al., 2017b). However, the relatively coarse spatial resolution of Sentinel-2A multispectral (MS) bands may pose challenges for more precise localization of informal settlement morphological features, limiting mapping accuracy. Mechanical and technological restraints in the design of satellite sensors makes it impractical for a single sensor to provide images with high resolution in both spectral and spatial domains (Hashim et al., 2022). Remotely sensed data acquired by sensors such as Quickbird, Worldview and GeoEye have the panchromatic band (PAN) which has higher spatial resolution than that in the multispectral bands (MS) of the same sensor (Pereira et al., 2017, Zhang, 2004). On the other hand, sensors, for example Sentinel-2, and Rapid-Eye only capture images in a multispectral mode (Mahmoud, 2021). According to Kumar et al. (2014), the availability of high spectral and spatial resolution images is crucial when mapping areas with complex morphologic structures such as urban environment. The fusion (pan sharpening) of MS and PAN bands has become a promising tool to obtain images with high spatial and spectral resolution simultaneously (Hashim et al., 2022, Mallick et al., 2021, Park et al., 2017).

Pan sharpening improves the MS bands by exploiting a high resolution PAN image to produce spatially enhanced MS image (Ge et al., 2020), which, potentially, improves classification accuracy (Gašparović and Jogun, 2017, Hashim et al., 2022, Zheng et al., 2017). The enhanced images provide an opportunity to capitalize on the advantages of each of the images, particularly for mapping complex environments (Kumar et al., 2014). Overviews and comparisons of various pan sharpening algorithms have been provided (Alparone et al., 2007, Kösesoy et al., 2012, Pushparaj and Hegde, 2016, Vivone et al., 2015). These pan sharpening approaches can be grouped into two classes which are, component substitution (CS) and multi-resolution analysis (MRA) (Pandit and Bhiwani, 2015, Park et al., 2017, Selva et al., 2015). Whilst numerous researchers have indicated superiority of CS over MRA approaches in achieving high resolution image fusion (Mahmoud, 2021, Mallick et al., 2021, Mhangara et al., 2020), Zheng et al. (2017) propounded that the MRA-based pan sharpening algorithms can potentially attain finer spectral and spatial quality than those based on CS. However, other investigators articulated that a fusion method can only be better for as long as it could preserve the spectral characteristics and the spatial information of the multispectral and the panchromatic data, respectively (Kaplan, 2018, Park et al., 2017, Zheng et al., 2017). Pan sharpening has been reported for numerous image types and sensors, including, for example, Landsat ETM+ (Lwin and Murayama, 2013), synthetic aperture radar (Quan et al., 2020),

China–Brazil Earth Resources Satellite (CBERS-4) (Pereira et al., 2017), and GeoEye-1 imagery (Johnson et al., 2012). More specifically, pan sharpening Sentinel-2A imagery has received widespread attention owing to the availability of 10m bands which provide an opportunity to enhance the resolution of other 20m bands (Park et al., 2017, Phiri et al., 2020, Zhang, 2004). The approach has been exploited for various remote sensing applications ranging from water bodies mapping (Du et al., 2016, Che et al., 2015, Feng et al., 2012, Wu and Liu, 2015), mineral mapping (Ge et al., 2020), retrieving leaf area index and chlorophyll content (Zhang et al., 2019b), and for land use/land cover (LULC) classification (Gašparović and Jogun, 2017, Zheng et al., 2017) leveraging the high resolution 10 m bands as the PAN bands. Interestingly, pan sharpening has also been reported for informal settlement mapping (Kohli et al., 2016a, Mugiraneza et al., 2019, Owen and Wong, 2013b). For instance, pan sharpened Quickbird image (Kohli et al., 2016a) and pan sharpened Worldview image (Kuffer et al., 2016b) have been used to map informal settlements in Pune (India) and Kigali, Mumbai and Ahmedabad, respectively. In another study Owen and Wong (2013b) pan sharpened Quickbird MS imagery using 0.6 m PAN band, employing the rational polynomial coefficients approach in Guatemala.

Although pan sharpening has potential to enhance mapping applications through increased spatial resolution, several investigators have argued that it is associated with spectral and spatial distortions (Grochala and Kedzierski, 2017, Jawak and Luis, 2013, Pandit and Bhiwani, 2015, Park et al., 2017), depending largely on the pan sharpening approach used. To compensate for the loss in spatial information, some researchers recommended the use of image texture and contextual information to exploit full benefits of pan sharpening, and ensure a more comprehensive evaluation (Zheng et al., 2017, Du et al., 2016, Palsson et al., 2012). Most importantly, in spatially heterogeneous urban landscapes, it is nontrivial to accurately capture spatial morphology of deprivation pockets using spectral information alone (Prabhu et al., 2021b). In earlier research undertakings using Sentinel-2A, Wurm et al. (2017b) extracted textural features using only Sentinel-2A 10 m bands in order to capture morphological variations in Mumbai. Mumbai's informal settlement landscape is characterized by varied typologies ranging from rehabilitated informal settlements in proximity to double storey buildings, age-old informal settlements, characterized by small-sized business enterprises and regular housing units lining major roads, and very compactly packed areas with only small lanes inside the area (Kuffer et al., 2016b). Wurm et al. (2017b) results indicated that, whilst large informal settlement patches would be captured more accurately, smaller patches were

compromised. Although methods for mapping urban deprivation using EO data have advanced in recent times, the detection of discrete pockets of deprivation, the location of many smaller and lesser-known informal settlements remains compromised (Stark et al., 2020). Exploiting the high spatial and spectral resolution of Sentinel-2A data could help in extracting highly variable morphological informal settlement features in complex urban built up landscapes. To the best of found knowledge, there has been no systematic exploration of capabilities of pan sharpening Sentinel-2A for capturing the distribution of morphologic informal settlements.

Owing to this background, the current study sought to investigate the potential to enhance capturing of spatial morphology of deprivation pockets in the diverse Durban landscape through pan sharpening freely available Sentinel-2A data. Further, the study exploits the value added in combining pan sharpening with texture analysis in mapping the diversity of informal settlement morphologies.

The specific objectives of this work are to:

- (1) To merge the spatial details of Sentinel-2A 10 m bands into its 20 m bands and produce a composite image constituted by all ten multispectral bands at a 10 m spatial resolution
- (2) Compare the performance of various popular pan sharpening algorithms in producing an enhanced Sentinel-2A that captures fine grained heterogeneity existing in informal settlement landscape
- (3) Investigate the value of increased spectral information and texture metrics for more precise capturing of diversity of morphological informal settlements in Durban landscape.

3.2. Methods and Materials

3.2.1. Data and pre-processing

The research work was based on Sentinel-2A multispectral imagery. This study used a radiometrically and geometrically corrected Sentinel-2 level 1C image product. The Level-1C processed data were georeferenced in the WGS 84 UTM 36S coordinate system and resampled using nearest neighbour algorithm. Sentinel-2A image covers 13 bands in the visible, near-infrared and shortwave infrared (SWIR) wavelengths and consists of four bands at 10 m, six bands at 20 m and three bands at 60 m (Lanaras et al., 2018, Phiri et al., 2020). Sentinel-2A does not offer a panchromatic band with high resolution. The satellite was launched on June 23, 2015 (Kaplan and Avdan, 2018). The image, depicting parts of the city of Durban, South Africa, was captured on 11 August 2020 and was downloaded from Sentinel Hub

(<https://scihub.copernicus.eu/>). The sentinel image was clipped to a subset of 339 x 364 pixels and the whole study area is over the coverage of one tile. The characteristics of Sentinel-2A bands are shown in Table 3.1.

Table 3.1. Specifications of the Sentinel-2A satellite imagery

Band number	Spatial resolution (m)	Central wavelength (nm)	Bandwidth (nm)	
MS₁	60	443	20	
MS₂	10	490	65	
MS₃	10	560	35	
MS₄	10	665	30	
VNIR	MS₅	20	705	15
	MS₆	20	740	15
	MS₇	20	783	20
	MS₈	10	842	115
	MS_{8a}	20	865	20
	MS₉	60	945	20
	MS₁₀	60	1375	30
SWIR	MS₁₁	20	1610	90
	MS₁₂	20	2190	180

Adapted from (Park et al., 2017a)

3.3. Methods

The methodological approach of this study is shown in Figure 3.1. In the first stage, the Sentinel-2A, 20 m bands were pan sharpened using five pan sharpening algorithms. Next, the 20 m bands were resampled to create a reference image before evaluation of the performance of image sharpening methods, followed by a separability analysis. Image classification was performed on the pan sharpened images. The classification scheme consisted of six classes, which include formal settlements, informal settlements, vegetation, water, road and bare land. Last, classification accuracies were compared and an informal settlement map was produced.

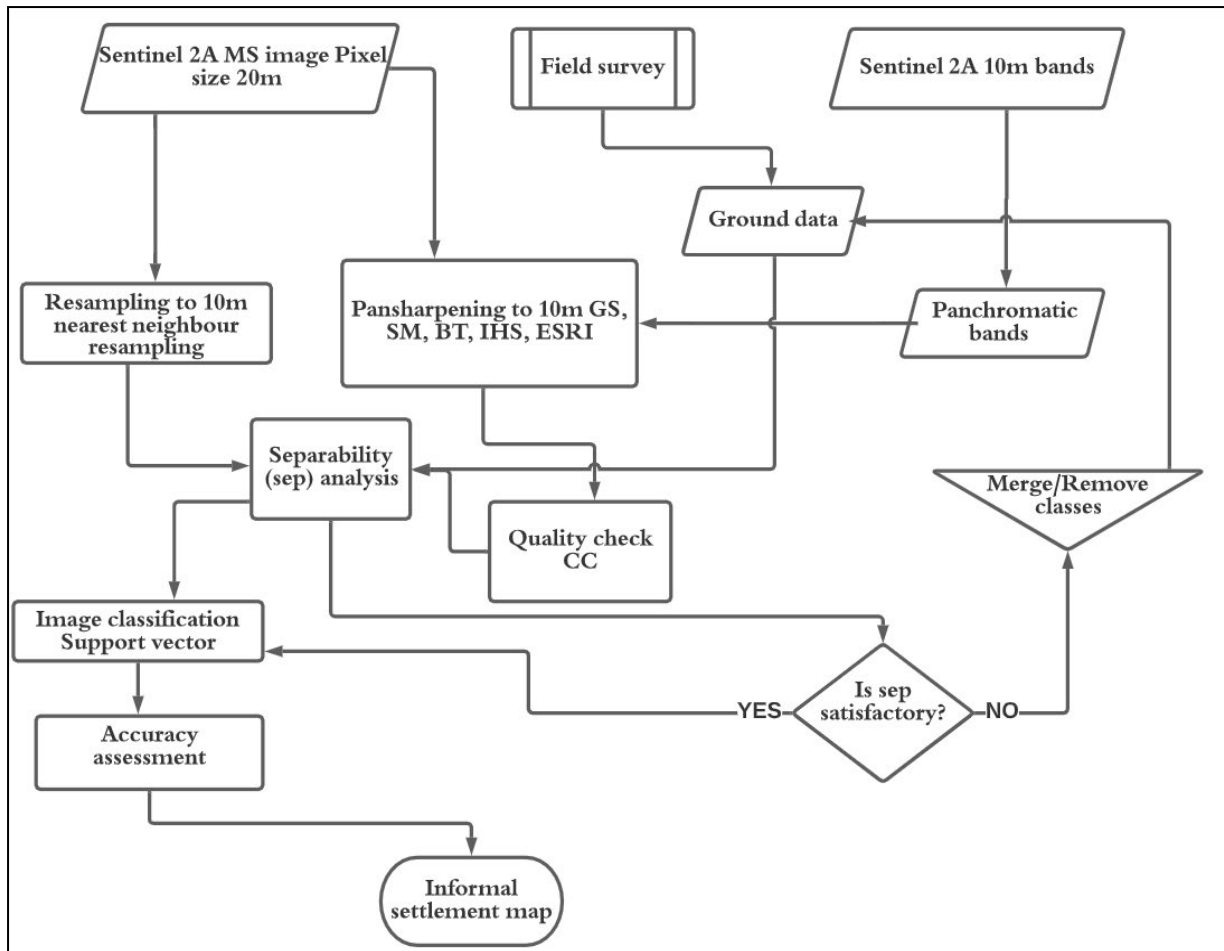


Figure 3.1. Technical flow chart.

3.3.1. Pan sharpening methods

For pan sharpening, five algorithms that have been previously used in published articles were used in this study. These include Brovey transform (BT), Intensity, hue and saturation (IHS), ESRI, Gram Schmidt (GS), and Simple Mean (SM), all of which belong to component substitution category. These approaches have been described by Nikolakopoulos (2008), as producing good quality fused images.

Brovey transform : Brovey is described as a simple method (Palsson et al., 2012, Pandit and Bhiwani, 2015) that uses a mathematical combination of the MS bands and PAN band for pan sharpening (Pandit and Bhiwani, 2015). Equation 1 defines the Brovey transform. The approach involves use of an algebraic expression to inject the overall brightness of the PAN image into each pixel of the MS image (Pushparaj and Hegde, 2016). According to Pandit and Bhiwani (2015), it sometimes causes distortion of radiometric characteristics of the bands.

$$DN_{fusedMSi} = \frac{DN_{bi}}{DN_{b1} + DN_{b2} + \dots + DN_{bn}} DN_{PAN} \text{ (Equation 1)}$$

Where DN is the digital number of that particular band and b_i is the particular band of the MS image.

Intensity, Hue and Saturation is regarded as the most widely used pan sharpening technique (Niazi et al., 2015, Sarp, 2014), with fast computing capabilities (Pandit and Bhiwani, 2015). This approach is based on colour space transformation (Grochala and Kedzierski, 2017). The technique entails that a composite of red-green-blue (RGB) bands is converted into an IHS colour space (Sanli et al., 2016, Zhang, 2004). The transformation separates the intensity from the two colour components (Du et al., 2007). During the fusion process, a high resolution PAN image replaces the intensity (I) band (Borana et al., 2019, Zhang, 2004). Simultaneously, an interpolation technique is used to resample the hue and saturation bands to the higher resolution pixel size (Nikolakopoulos, 2008). To obtain a pan sharpened image, a reverse IHS transformation is executed on the PAN band, as well as on the hue (H) and saturation (S) bands (Zhang, 2004). Although IHS may cause large spectral distortion (Choi, 2006), the approach is regarded as simple and efficient (Niazi et al., 2015).

Gram Schmidt: GS uses averaging of the multi- spectral bands (Sarp, 2014). Like IHS method, this method requires forward and backward transformation of multispectral image, and pan sharpened multispectral bands are created from an inverse GS transform (Pandit and Bhiwani, 2015). Although it is regarded as the best pan-sharpening method in terms of minimizing spectral distortion, it is more complex and computationally expensive than most other methods (Maurer, 2013). Despite its shortfalls, Borana et al. (2019) described GS as a successfully accurate technique

Simple Mean: According to <https://desktop.arcgis.com/en/arcmap/latest/extensions/spatial-analyst/mapalgebra/what-is-map-algebra.htm> cited in (Alcaras et al., 2021), SM method uses a simple mean-averaging equation for each merger of PAN with one multispectral image. Consequently, the pan sharpened image is supplied by the formula:

$$MS_k^f = \frac{PAN}{\mu_{PAN}} \cdot MS_k \text{ (Equation 2)}$$

Where MS_k is the original MS image and MS_k^f is the pan sharpened image.

ESRI: The ESRI method initially exploits the MS bands to produce a weighted image. Further, the reflectance values of the weighted image from the original PAN image are subtracted in order to construct an adjustment image. Ultimately, the adjustment image is joined to each of the discrete MS bands, proportionately, to come up with individual pan sharpened MS bands.

In this study, BT, IHS, ESRI and SM algorithms were implemented in ArcMap 10.4 whilst GS was implemented using ENVI 5.3 software. Because pan sharpening depends on the availability of fine spatial resolution PAN band (Du et al., 2016), the properties of Sentinel-2A dataset were considered in the selection of input bands for the establishment of that band, as well as selection of the input lower resolution bands. Zheng et al. (2017) stipulated that the center wavelength proximity determines criterion for selecting optimal PAN-like band. In this study, bands 1, 9 and 10, whose resolution is 60 m, were not considered for pan sharpening process. This is because those bands were not intended for land cover classification (Gašparović and Jogun, 2017). Since Sentinel-2A provides six bands at 20 m resolution, and most pan sharpening algorithms, for example, IHS and Brovey are restricted to a maximum of 3 bands at a time (Borana et al., 2019, Gašparović and Jogun, 2017), two groups of bands were created from the 6, Sentinel-2A 20 m bands. The grouping was done following Gašparović and Jogun (2017) and Vaiopoulos and Karantzalos (2016). The aforementioned researchers put bands 5, 6, and 7 in the first group and bands 8A, 11 and 12 in the second group, considering their spectral ranges. The establishment of panchromatic band relied on the supposition that for each relevant portion of the spectrum, only one high resolution band (the panchromatic one) exists, overlapping, at least partly, with the lower resolution bands to be sharpened (Lanaras et al., 2018, Zheng et al., 2017). Following that notion, Gašparović and Jogun (2017) put forward that, although band 4 and 8 are the spectrally closest higher resolution bands for the first group, neither of the two bands completely overlaps the spectral range of the first group bands. For that reason, Selva et al. (2015) suggested a combination of the bands 4 and 8, through calculation of their mean (Equation 3) to be used as a panchromatic image for band 5, 6 and 7. Following the suggestion, this study utilized the average of bands 4 and 8, which was also utilised by Gašparović and Jogun (2017) and Vaiopoulos and Karantzalos (2016), as PAN band for the case of bands 5, 6 and 7.

$$S = \frac{B4+B8}{2} \text{ where } S \text{ represents synthesized band.} \quad (\text{Equation 3})$$

For the case of bands 8A, 11 and 12, the band 8 was considered directly as the PAN band, as suggested by Gašparović and Jogun (2017) described band 8 as the only probable higher resolution band at 10 m spatial resolution spectrally closest to all the bands in the second group. Figure 3.2 illustrates the pan sharpening framework implemented in this study.

Pan sharpening framework

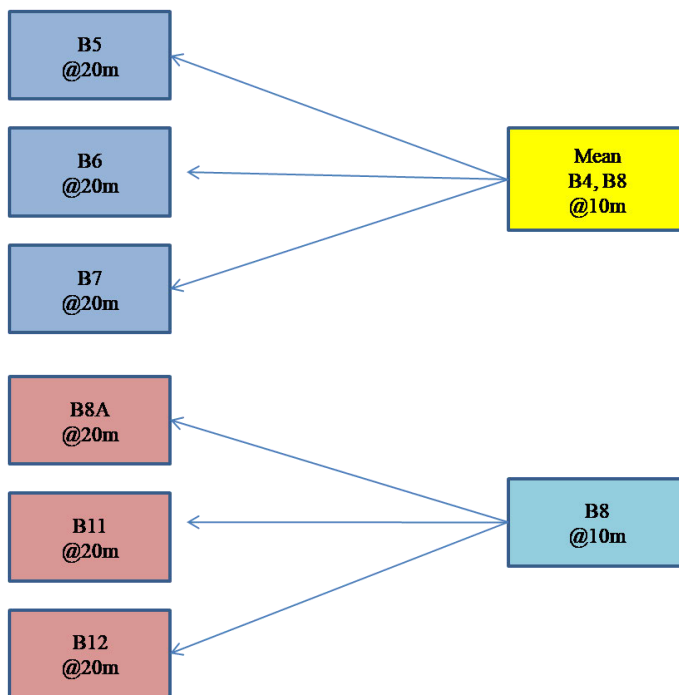


Figure 3.2. The structure of pan sharpening procedure

3.3.2. Performance evaluation of the pan-sharpened images

After the application of five pan sharpening algorithms, pan sharpened Sentinel-2A images were quantitatively evaluated. The process of evaluation of the performance of the algorithms required a reference image, which, according to Amro et al. (2011), is the MS image at the resolution of the PAN image. Gangkofner et al. (2007) pointed out that resampling the original MS image to the size of the PAN image may help create a reference image. Following studies by Gašparović and Jogun (2017), as well as Park et al. (2017), this study utilised resampling in order to obtain the reference image. The 20 m bands were resampled to 10 m bands using nearest neighbour algorithm, and a composite image was established. According to Liu et al.

(2020), the existing pan sharpening methods may produce spectral distortions, making quality assessments imperative. This study used the correlation coefficient to compare the spectral performances of the pan sharpening algorithms. Correlation coefficient quantifies how much the algorithm preserves spectral information (Palsson et al., 2012), or how close the enhanced image and the original image/reference image are, in terms of spectral quality (Nikolakopoulos, 2008). Each band of the original MS image was correlated with the respective pan sharpened bands in excel.

3.3.3. Separability analysis

A class pair separability analysis was conducted on pan sharpened images and resampled image for each algorithm. The analysis was done using ENVI software version 5.3. Separability analysis was done to determine which algorithm best discriminates informal settlements. The performance of each algorithm was examined and compared with other algorithms.

3.3.4. Texture feature extraction and analysis

According to Kavitha and Suruliandi (2018), selection of image texture features that can distinguish classes well is an important aspect in texture analysis. In the current study, 8 texture metrics were statistically extracted from sentinel-2A imagery using the GLCM texture analysis method. These included mean, variance, homogeneity, contrast, dissimilarity, entropy, angular second moment, and correlation (Table 3.2). The selection of the textural features was elicited by their potency in studies that utilized high resolution data to detect informal settlements using high resolution data (Kabir et al., 2010). In this study, the red (band 4), green (band 3), and blue (band 2) bands were used as input bands in the computation of GLCM textures. GLCM texture measures were measured based on the average of all directions (0, 45, 90, and 135), the same co-occurrence shift (1,1), quantization level of 64, and 7x7 window size. According to Giannini and Merola (2012), a quantization level of 64 preserves information and has an acceptable computing time. In an attempt to determine the optimum window size for informal settlement extraction, the current study applied the methodology implemented by (Kabir et al., 2010). The method involves calculation of coefficient of variation. Based on the visual inspection of texture images, mean texture feature seemed to provide the most useful information on informal settlements. Therefore, the mean texture feature was used for the determination of optimum window size. The process involved computation of class statistics for mean texture feature. The class statistics included minimum, maximum, mean and standard

deviation. These statistics were calculated for the red, blue and green bands and for the window sizes 3x3, 5x5, 7x7, 9x9, 11x11, 13x13, 15x15. Coefficients of variation were calculated in Excel, using the formula $CV = \frac{\sigma}{\mu}$, where

CV= coefficient of variation

σ = standard deviation

μ = mean

A graph showing coefficient of variation against window size was presented for each band.

Table 3.2. Image texture measures derived from Sentinel-2A imagery for informal settlement extraction

Second order statistic	Statistic description of behaviour	Statistic formula
Angular second moment	High when GLCM is locally homogeneous	$\sum_i \sum_j \{p(i,j)\}^2$
Contrast	A measure of the amount of local variation in pixel values among neighbouring pixels. It is opposite of homogeneity	$\sum_{n=0}^{n=1} n^2 \left\{ \sum_{i=1}^N \sum_{j=1}^N p(i,j) \right\}$
Correlation	Linear dependency of pixel values on those of neighbouring pixels	$\frac{\sum_i \sum_j (ij)p(i,j) - \mu_x \mu_y}{\sigma_x \sigma_y}$
Dissimilarity	Similar to contrast and inversely related to homogeneity	$\sum_{n=0}^{N=1} n \left\{ \sum_{i=1}^N \sum_{j=1}^N p(i,j) \right\}$
Entropy	High when the pixel values of GLCM have varying values. Opposite of angular second moment.	$\sum_i \sum_j p(i,j) \log(p(i,j))$
Homogeneity	A measure of homogeneous pixel values across an image	$\sum_i \sum_j \frac{1}{1 + (i-j)^2} p(i,j)$
Mean	Grey level average in the GLCM window	$\mu_i = \sum_{i,j=0}^{N-1} i(p_{i,j})$ $\mu_j = \sum_{i,j=0}^{N-1} j(p_{i,j})$
Variance	Grey level variance in the GLCM window	$\sigma_i^2 = \sum_{i,j=0}^{N-1} p_{i,j} (i - \mu)^2$ $\sigma_j^2 = \sum_{i,j=0}^{N-1} p_{i,j} (i - \mu_j)^2$

3.3.5. Image classification

Performance evaluation of various unification schemes on LULC classification was achieved through comparison of the classification accuracies of images generated by five pan sharpening approaches and the one generated by nearest neighbour interpolation technique. The classification was applied for each of the following 4 datasets: the pan sharpened bands only (Pan), pan sharpened bands + rgbnir (Pan + rgbnir), pan sharpened bands in addition to image texture (Pan + mean), and pan sharpened bands in addition to the original 10m bands and image texture (Pan+rgbnir+mean). The acronym rgbnir refers to Sentinel-2A original 10 m bands: red (r), green (g), blue (b) and near-infrared (nir) bands. The first experiment was to classify the pan sharpened MS image. The second experiment was to classify a composite of pan sharpened multispectral image + 4 Sentinel-2A 10 m resolution bands. The third experiment involved classification of the pan sharpened texture image. With respect to the third experiment, mean texture was extracted from the pan sharpened images and classification was done on texture images. In the fourth experiment, mean texture image extracted from a composite image of pan sharpened MS image plus original 10m resolution bands was classified.

To guide the processes of classification and accuracy assessments the training and testing samples were collected. All the training sites comprised the corresponding group of the regions of interest. The classification scheme contained six classes, which include formal settlement, water, vegetation, bare land, informal settlement and road. Table 3.3 shows a description of LULC classes used in the classification. The training polygons were digitized from RGB band of Sentinel-2A imagery. The same training polygons were used for all the feature sets. Image classification involved use of support vector machine algorithm basing on the default parameters that included use of a radial basis function as a kernel type. The image classification steps were performed using ENVI 5.3.

Table 3.3. Land use/Land cover classes used in the study

Class	Description
Formal settlement	Housing units, with regular layout pattern, and with well-structured road layouts
Water	Water bodies like dams, rivers, ponds and swamps
Vegetation	Area covered by grasslands, forests, croplands, small shrubs, sparse and dense trees
Bare land	Exposed soil with neither grass, trees nor built up structures
Informal settlement	Densely built housing units that are contiguous
Road	Paved road, freeways, interstates, highways, and tertiary local roads.

3.3.6. Accuracy assessment

In the current study, evaluation of all classification was done using the confusion matrix. The initial step in accuracy assessment involved determination of reference polygons from google earth Pro. Ground truth data for the six classes (formal settlements, informal settlements, water, vegetation, road, bare land) was obtained. All classification accuracies were calculated using ENVI version 5.3 and were presented using the overall accuracy (OA), producer accuracy (PA), user accuracy (UA), and F-score. The F-score was used in the comparison analysis since it is class specific. According to Zurqani et al. (2019), the F-score reflects the goodness of the classifier in the context of both producer's and user's accuracies by weighting their mean.

$$\text{F-score} = 2 * \frac{(PA * UA)}{(PA + UA)} \quad (\text{Equation 4})$$

3.4. Experimental Results

3.4.1. Establishing optimum window size

The window size was computed from mean texture images. After calculating coefficients of variation for each mean texture image using the 3x3, 5x5, 9x9, 11x11, 13x13, 15x15 window sizes (Matarira et al., 2022a), the window size of 7x7 was considered as the optimum window size. Following Kabir et al. (2010), the coefficients of variation began to stabilize at the 7x7 pixel window size for the informal settlement class.

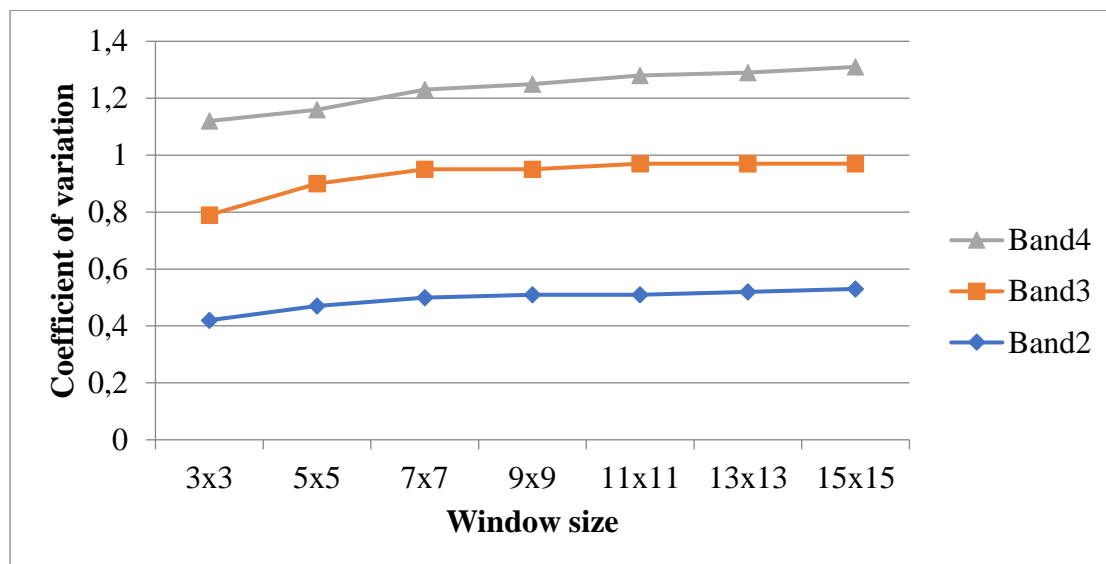


Figure 3.3. Coefficient of variation curve using the mean feature for informal settlement classes

In an attempt to exploit the full spatial potential of pan sharpened bands (Palsson et al., 2012), mean textural information was extracted from a composite of pan sharpened bands to be used in the subsequent classification. The mean texture was computed with an inter-pixel distance of 1, a window size of 7×7 and quantization level of 64 (Matarira et al., 2022a) .

3.4.2. Spectral quality

In this study, the correlation coefficient was used for the quantitative assessment of the quality of pan sharpened images. This was done through comparison of pan sharpened images and the resampling image. The correlation coefficients were calculated for all the employed algorithms and results were listed in Table 3.4. Correlation coefficient showed levels of quantitative agreement between the spectral quality of resampled image and pan sharpened images for all the pan sharpening methods.

Generally, results of pan sharpening indicated low spectral quality of the sharpened images. The assessment of values of correlation coefficients showed that the best results obtained were for the SM method, where the value was highest (0.85). The results indicated that, while SM had the highest correlation, the lowest value was obtained for BT method. These results showed that SM algorithm preserved more perfectly the spectral integrity of the original image. The second-best result was produced by ESRI method. While results indicated statistically significant differences ($p < 0.05$) between results from SM and each of the methods (BT, GS and IHS), from the chi squared proportional tests, it was not true for ESRI.

Table 3.4. Quantitative assessment of performance of pan sharpening methods

Pan sharpening method	Correlation coefficient
BT	0.62
ESRI	0.81
GS	0.72
IHS	0.68
SM	0.85

3.4.3. Pan sharpening and interclass separability

The effects of pan sharpening on class separability were evaluated. Class pair separability analysis was conducted on each pan sharpened image in order to establish the best pan sharpening algorithm, in terms of separating different classes, for informal settlement

extraction. Transformed Divergence Separability Index (TDSI) values were obtained from class separability test conducted using ENVI software. Figure 3.4 presents TDSI values for class pairs involving informal settlements, calculated for each pan sharpening method. The TDSI values ranged from 0.5 to 2. Analysis of class pairs (Figure 3.4) revealed that pan sharpening produced significant improvement of informal settlement separability. For all the algorithms, most classes displayed separability ranging from 1 to 2, with the exception of IS vs formal settlement, which ranged from 0.55 to 1.5. For all images, informal vs vegetation, as well as informal vs water seemed to be the most separable as shown by their highest TDSI values, approximately equal to 2 for all pan sharpening algorithms. According to Mushore et al. (2022), the TDSI varies from 0 to 2 with values near 0 implying that the classes cannot be easily distinguished, while values close to 2 indicating that two LULC classes are easily distinguishable. The least separable class was IS and formal settlement (TDSI < 1.5). Figure 3.5 presents average separability indices for the pan sharpening algorithms. From the results presented, pan sharpened data had higher separability values than resampled/reference data (Figure 3.5). The average TDSI for the resampled image was 1.63, the lowest value, compared to pan sharpened images. From the spearman's rank correlation test, the differences between TDSI for resampled image and that for BR, ESR, IHS and simple mean were statistically significant ($p < 0.05$). However, for GS the difference between the average separability index and that of the resampled image was not statistically significant ($p > 0.05$).

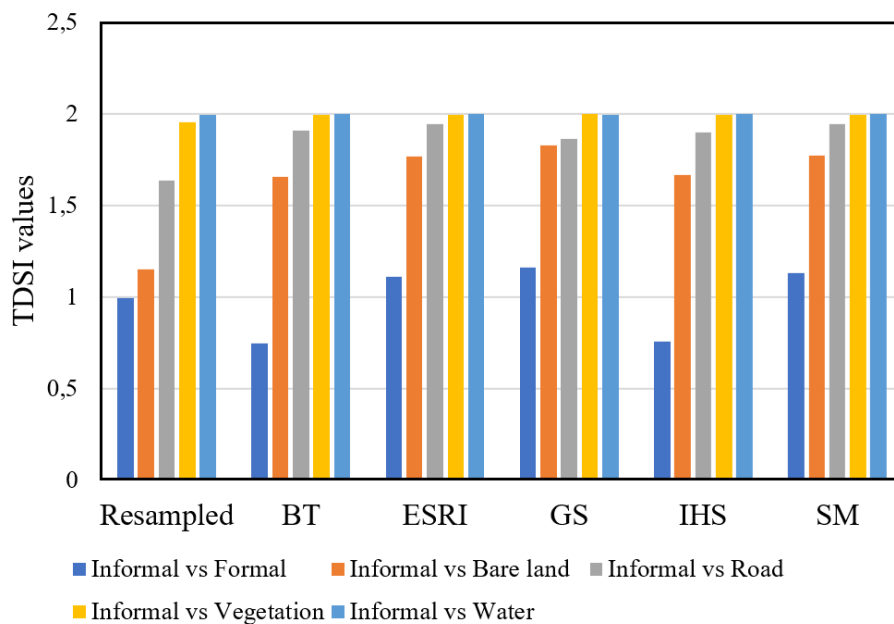


Figure 3.4. TDSI values for class pairs involving informal settlements

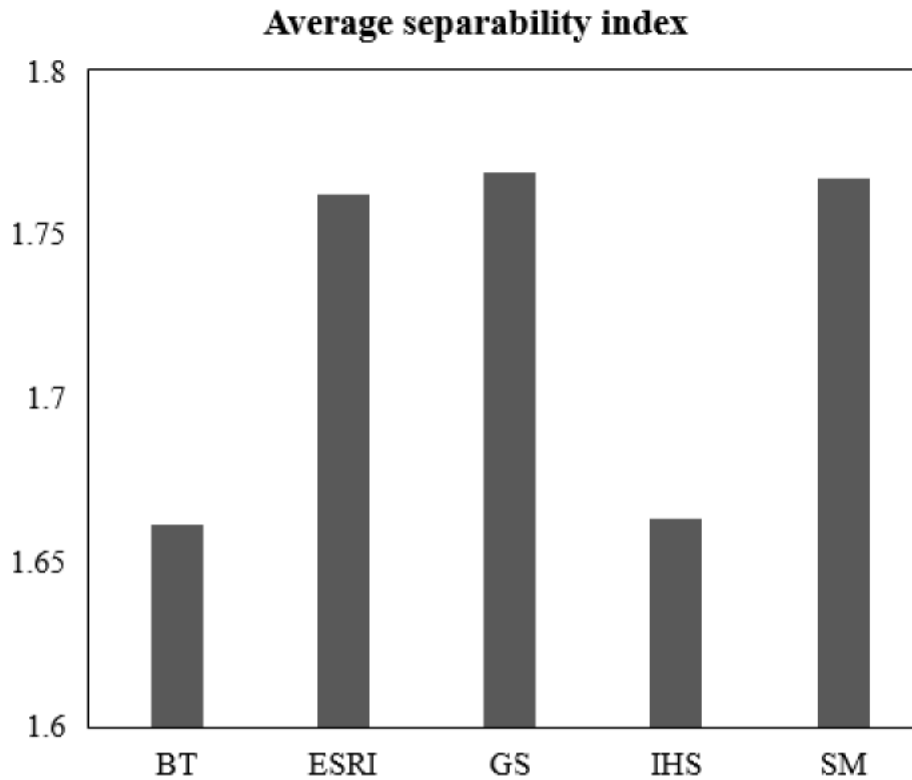


Figure 3.5. Average separability indices for the pan sharpening algorithms

3.4.4. Image classification results

Based on Table 3.5, Figure 3.6 was plotted to show the distinct classification performances obtained by different classification scenarios more fundamentally. Figure 3.7 summarizes the results obtained from the four experiments carried out using different classification scenarios, performed using ENVI 5.3 software. In the illustration of results for this study, the F-score was the accuracy metric used. Generally, distinct results were obtained from the four classification scenarios. The results clearly showed that, based on spectral bands, the increase in accuracy was negligible.

The results for the four classification scenarios were presented below:

- (1) **Pan sharpened multispectral image:** Figure 3.6 shows variation in classification accuracy obtained by different pan sharpening algorithms. The results presented in Table 3.5 indicate that, although pan sharpening outperformed the reference image for all algorithms, the difference was small. BT method, which yielded the best accuracy of 62.9% differed from the reference image by 1.7%. The IHS results had the worst accuracy at 61.6%. For this experiment, average accuracy produced by pan sharpening

algorithms was 62.3%. Subtracting the worst accuracy from the best accuracy gave a difference of 1.3%.

Table 3.5. Classification results (in percentage) for the resampled and pan sharpened images

Accuracy	Resampled	BT	ESRI	GS	IHS	SM
OA	66.7	66.5	66	66.9	64.7	64.8
PA	65.6	68.9	68.7	68.1	66.9	69.5
UA	57.3	57.9	57.8	58.7	57	56.5
F-score	61.2	62.9	62.8	62.1	61.6	62.3

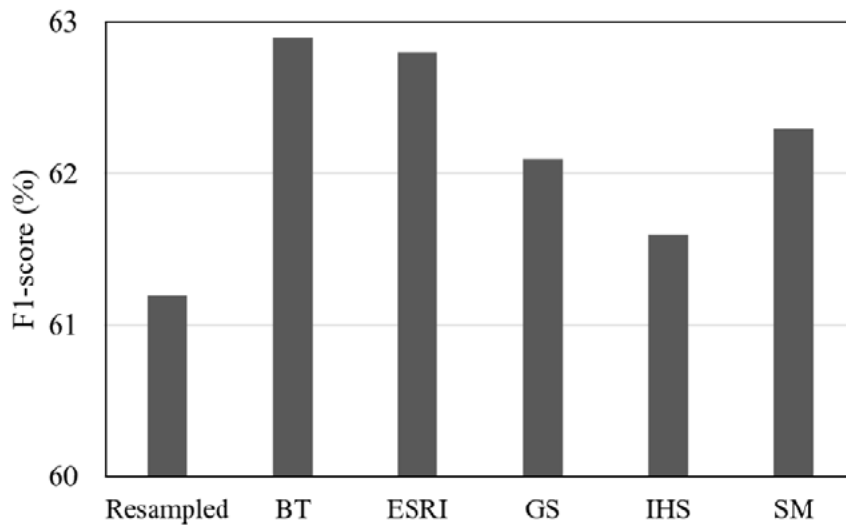


Figure 3.6. Classification results for the pan sharpened images

Pan sharpened MS image + rgbnir: The effect of additional spectral information to the pan sharpened bands was evaluated. The benefit of adding the four high resolution bands to the pan sharpened images was clear. Based on Table 3.6, it can be deduced that the addition of high-resolution spectral bands to pan sharpened images generally led to an improvement in informal settlement identification accuracy, with BT yielding the best accuracy at 73%. The average accuracy was 72.3%.

Table 3.6. Classification results (in percentage) for the 4 classification scenarios

Feature	Accuracy	BT	ESRI	GS	IHS	SM
Pan	OA	66.5	66	66.9	64.7	64.8
	PA	68.9	68.7	68.1	66.9	69.5
	UA	57.9	57.8	58.7	57	56.5
	F-score	62.9	62.8	62.1	61.6	62.3
Pan + rgbnir	OA	72.9	71	70.3	71.3	71.1
	PA	78.5	80.4	76.4	78	81
	UA	68.2	65.7	67.4	67	66
	F-score	73	72.3	71.6	72	72.7
Pan + mean	OA	72.8	72.2	74.6	78	70.2
	PA	72.1	70.3	73.5	68.5	67.8
	UA	62	61	65	77.3	57.4
	F-score	66.7	65.3	69	72.6	62.2
Pan + rgbnir + mean	OA	86.9	87.9	91.8	87.6	87.2
	PA	88.2	89.5	92	87.9	88.2
	UA	98.5	98.7	98.7	99.3	98.3
	F-score	93.1	93.9	95.2	93.3	93

Pan sharpened MS image + mean: When mean texture was added to the classification of pan sharpened images, there was marginal increase in classification accuracy as compared to the scenario where the high-resolution bands were added to the enhanced image. When image texture was integrated, IHS showed the highest accuracy of 72.6%. When compared with only pan sharpened images, IHS also showed the greatest difference between accuracy levels. The difference was 11%. SM, with the most spectrally consistent results, had the lowest accuracy of 62.2% in this experiment.

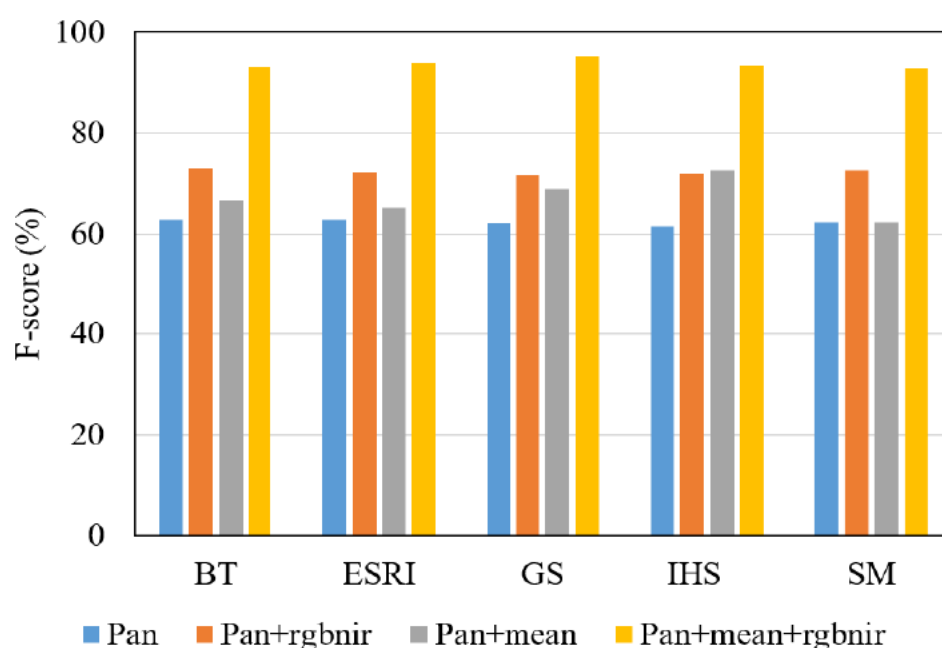


Figure 3.7. Classification results for the four classification scenarios

(4) **Pan sharpened MS image + rgbnir + mean:** The inclusion of image texture to composites of pan sharpened images and rgbnir caused significant increases ($p < 0.05$) in classification accuracy for all algorithms, compared to results of pan sharpening alone (Table 3.6). Gram Schmidt had the highest accuracy of 95.2%. The average accuracy was 93.7% for this experiment. From the results, it can be inferred that a combination of pan sharpened image, additional 4 high resolution bands and image texture produced pronounced results for all the methods.

Considering all scenarios, GS produced the highest F-score when mean texture image of a combination of pan sharpened image and the four high resolution bands were classified. An IS map was therefore produced using results for scenario four produced by GS method. Figure 3.8 shows the informal settlement map of part of Durban Metro.

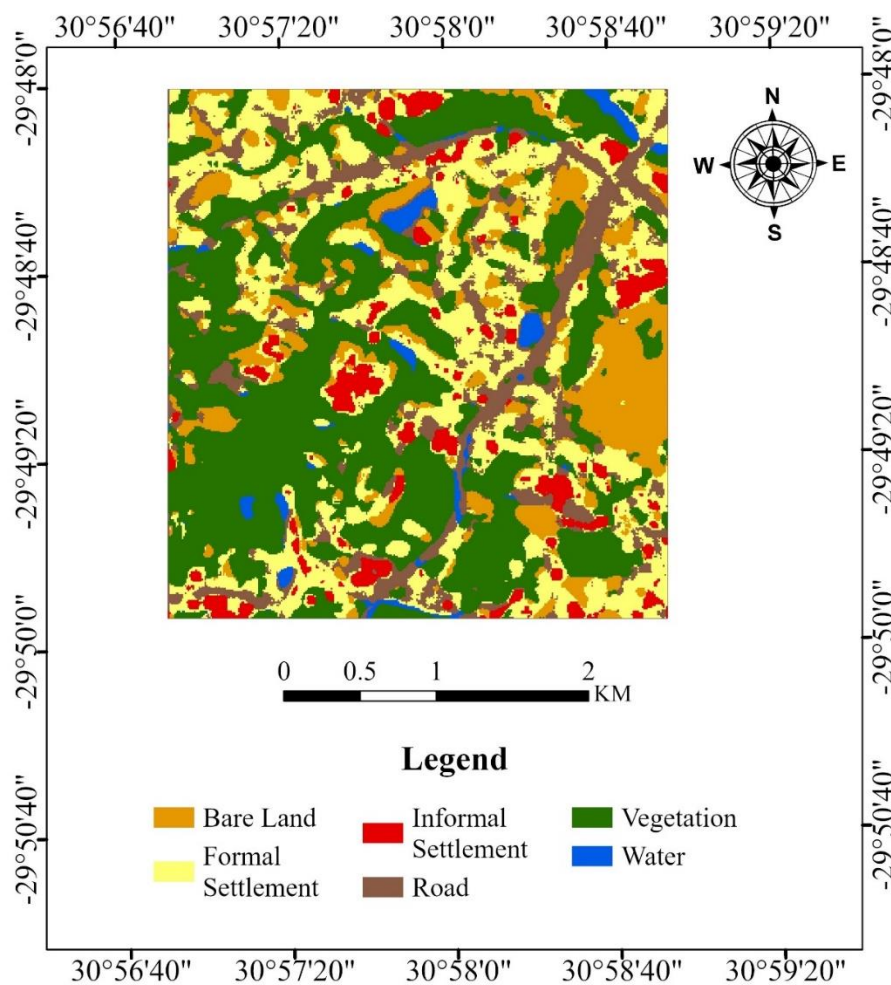


Figure 3.8. Land use/Land cover map showing informal settlements for part of Durban Metro

3.5. Discussion

The current study sought to investigate the potential of pan sharpening Sentinel-2A for capturing diverse morphological informal settlements in the complex urban built up landscape of Durban. Sentinel-2A 20 m bands were pan sharpened using the 10 m bands. Brovey, Gram Schmidt, ESRI, Intensity-Hue and Saturation as well as Simple Mean algorithms were the pan sharpening approaches used. A correlation between spectral values of resampled MS images and pan sharpened images was done to examine the quality of pan sharpened images.

The results of the study demonstrated that pan sharpening Sentinel-2A has potential to increase mapping precision of informal settlements. Because of complexity of urban environments, informal settlements are usually poorly characterized and comprehended. Although Brovey performed poorly in spectral preservation (Table 3.4), results of spectral classification of pan sharpened images indicated its superiority in capturing the diversity of informal settlements, as indicated by the highest mapping accuracy compared to other algorithms. This result is consistent with more similar mapping applications involving raw pan sharpened images (Mallick et al., 2021, Wang et al., 2018) that yielded the most accurate classification results using Brovey algorithm. However, comparing classification accuracy levels for all pan sharpened images produced by the various algorithms, subtle differences were recorded as compared with the yardstick image downsampled by nearest neighbour resampling. Results of pan sharpening indicated an average accuracy of 62.3%, against 61.2% for the reference image and an average difference of 1.14%. In agreement, results from Vaiopoulos and Karantzas (2016)'s review of 21 pan sharpening algorithms on the Sentinel 2, 20 m bands also indicated that none of the pan sharpening methods significantly outperformed standard bicubic interpolation on the original low resolution bands. Also, the results were consistent with Zheng et al. (2017)'s study that showed classification accuracies that were almost the same as that of the reference image. Such results agree with the assertion that during pan sharpening spatial resolution is enhanced at the expense of some spectral detail (Kaplan, 2018, Park et al., 2017). This finding is, however, inconsistent with Gilbertson et al. (2017) who, from a pan sharpened Landsat 8 data, demonstrated improved classification accuracy by ~15% using Pixel Based Image Analysis (PBIA) and Object Based Image Analysis (OBIA) approaches in Western Cape, South Africa. Gilbertson et al. (2017) 's increase in accuracy of about 5% could be due to less complexity of their study area, which was agricultural whereas the current study is in an urban setting characterized by a complex landscape. To explain these inconsistencies Zheng et

al. (2017) iterated that numerous factors could be at play in influencing the classification accuracy, and not only dependant on spectral fidelity of these pan sharpening algorithms. These factors include the classification system as well as the data inputs.

Considering pixel-based classification of raw pan sharpened images, informal settlement identification accuracies were <70% for all algorithms (62.3%, on average) (Table 3.5). The accuracy levels could not satisfy the lowest precision requirements proposed by (Lu and Weng, 2007). Apart from the impacts of loss of spectral information resulting from pan sharpening (Zheng et al., 2017), the results demonstrate that, utilizing only spectral information, pan sharpening failed to adequately provide much more detailed information for semantic abstraction of morphologic informal settlements in Durban. Inherent within class variability in heterogeneous urban environments could help explain low classification outputs, post pansharpening (Irons et al., 2007). More specifically, complexities in capturing boundaries and similarity in morphological features with formal built-up structures (Stark et al., 2020) potentially result in complex affiliation of formal settlements with informal settlement category. The classification results support the class separability tests conducted in the current study, where, in comparison with other class pairs, the lowest TDSI values were between informal and formal settlement class (Figure 3.4) for all the pan sharpening algorithms. These results confirm the non-triviality of separating informal from formal settlement class. Müller et al. (2020) explained that, due to potential similarity in morphological layouts, the spectrum of morphological settlement structures tends to be the same in heterogeneous urban built up landscapes, making distinction between formal and formal structures complex. However, combining pan sharpened images with the original 10m bands restored the loss in spectral quality through increased spectral resolution, and yielded much more enhanced accuracy (Table 3.6). Compared with pan sharpened images alone, the results of increasing spectral information led to an increase in average accuracy from 62.3% to 72.3%. This result agrees with Palsson et al. (2012)'s result where accuracy improved significantly when spectral information was added through combining the original high resolution (PAN) bands with the fused image.

In order to capitalize on the increased spatial details from image sharpening, and to fully exploit the efficacy of image sharpening for informal settlement identification using Sentinel-2A (Zheng et al., 2017), GLCM texture was extracted from pan sharpened images. The results revealed that, all algorithms showed remarkable improvements in accuracy, especially, when the classification scenario involved texture images generated from composites of pan

sharpened images and the original 10 m bands. The F-scores for all the algorithms ranged from 93% - 95.2% for the classification scenario Pan + rgbnir + mean. These results confirm Mallick et al. (2021) 's assertion, that in order to generate reliable accuracy maps from pan sharpening there should be incorporation of the spatial domain in the form of image texture. In addition, the results concur Zheng et al. (2017) 's assertion that, for LULC classification using Sentinel-2 data, from the viewpoint of feature sets , the more features are used as inputs, the higher the accuracy. The results also demonstrated the added advantage of increased spectral information. Overall, Gram Schmidt fusion technique, that also attained the highest average separability index, provided higher overall accuracies with a combination of enhanced spectral resolution and contextual information. Image texture extracted from a combination of pan sharpening and 10 m bands, showed potential to extract unique informal settlement typologies in Durban. The result produced by the GS in this last experiment was, overall, the best performance of all classifications and was utilized to generate the informal settlement map for the study area.

In a nutshell, results of the study demonstrated the advantages of the four 10 m bands and six 20 m bands of sentinel-2A in providing the richest spatial and spectral information for more precise extraction of deprived urban areas. However, the applied methodology could be tested with locally specific feature sets to find the most appropriate fusion technique for detection of morphologic informal settlements in Durban, and to better understand the role morphological informal settlement landscapes play in determining the suitability of pan sharpening methods.

3.6. Conclusion

This paper assessed the contribution of pan sharpening Sentinel-2A to informal settlement detection. Spatial features in the form of image texture were added to compensate for the shortfalls of image sharpening in terms of spatial information loss. Results indicated that the pan sharpened Sentinel-2A imagery has the potential for enhanced capturing of informal settlement diversity. The following conclusions were drawn:

- Considering the four classification scenarios, the results demonstrated that different image sharpening algorithms had distinct effects on classification, since no specific method constantly outperformed the other.
- Although pan sharpening led to increased separability of informal settlements from the other classes, solely based on the pan sharpened spectral bands, image sharpening has been observed to be of limited benefit in terms of informal settlement identification.

- Robust discrimination of informal settlements can be achieved by a combination of texture analysis and increased spectral resolution generated through combination of pan sharpened bands and the original four, 10 m resolution bands.

Overall, the results point out that fused images can be better classified, but the quality depends on the method used for pan sharpening. Gram Schmidt sharpened image provided the best result with a combination of pan sharpened image, four original 10 m bands, and image texture. This study did not aim to determine the best method for image pan sharpening, but it focused on how full benefits of pan sharpening can be exploited through addition of spectral information and spatial features, in order to enhance informal settlement discriminability.

3.7. Summary

This chapter presented pan sharpening technique for informal settlement mapping. The research was a comparison analysis involving four classification scenarios. The scenario that produced the highest accuracies for all the pan sharpening algorithms involved composite image of four, Sentinel-2A, raw 10 m bands, pansharpened image and image texture. Gram-Schmidt technique outperformed all the other techniques including Brovey and Simple mean. However, pan sharpening in its own sense produced relatively low accuracy levels owing to high spectral distortion associated with component substitution methods. The low classification outputs for pan sharpened images could also be attributed to use of mean as the only texture variable. Prior research has indicated that extraction of a large number of feature sets from satellite imagery could enhance mapping accuracy. However, extraction of a number of texture features as well as calculation of their window sizes would require fast computer processing. In addition, previous research has advocated for various spectral indices as vital in enhancing mapping accuracy. Data preparation, feature extraction, and classification of various combinations of input features has been reported as weighty, computationally expensive, tedious and time consuming when using classical image processing softwares. Recent advances in cloud computing present potential for solutions to these challenges through built-in time saving aspects. Some researchers put forward that GEE is a considerably efficient approach for operational mapping in complex urban environments. Thus, the next chapter leverages GEE' cloud computing capabilities, through their inbuilt machine learning algorithms for accurate capturing of informal settlements' morphologic variations.

CHAPTER FOUR:

Google Earth Engine for Informal Settlement Mapping: A Random Forest Classification Using Spectral and Textural Information

This chapter is based on:

Matarira, D., Mutanga, O., & Naidu, M. (2022). Google Earth Engine for Informal Settlement Mapping: A Random Forest Classification Using Spectral and Textural Information. *Remote Sensing*, 14(20). doi:10.3390/rs14205130

The screenshot shows the MDPI journal website interface. At the top, there is a navigation bar with links for Journals, Topics, Information, Author Services, Initiatives, and About, along with a Sign In / Sign Up button. Below the navigation bar is a search bar with the text 'Search for Articles:' and several input fields: 'Title / Keyword', 'Author / Affiliation', 'Remote Sensing' (with a dropdown arrow), and 'All Article Types' (with a dropdown arrow). A 'Search' button is located to the right of these fields. Below the search bar, the breadcrumb trail reads 'Journals / Remote Sensing / Volume 14 / Issue 20 / 10.3390/rs14205130'. The main content area is divided into two columns. The left column features the 'remote sensing' logo, a 'Submit to this Journal' button, a 'Review for this Journal' button, an 'Edit a Special Issue' button, and an 'Article Menu' section with 'Academic Editors' listed below. The right column displays the article title 'Google Earth Engine for Informal Settlement Mapping: A Random Forest Classification Using Spectral and Textural Information' in a large, bold font. Below the title, the authors are listed: 'by Dairai Matarira^{1*}, Onesimo Mutanga² and Maheshvari Naidu³'. To the right of the title is an 'Order Article Reprints' button with a gear icon. Below the authors, three footnotes are provided: ¹ School of Agriculture, Earth and Environmental Science, University of KwaZulu-Natal, P. Bag X01 Scottsville, Pietermaritzburg 3209, South Africa; ² Department of Geography, University of KwaZulu-Natal, P. Bag X01 Scottsville, Pietermaritzburg 3209, South Africa; ³ Department of Humanities, School of Social Sciences, University of KwaZulu-Natal, Durban 4041, South Africa.

Abstract:

Accurate and reliable informal settlement maps are fundamental decision-making tools for planning, and for expediting informed management of cities. However, extraction of spatial information for informal settlements has remained a mammoth task due to the spatial heterogeneity of urban landscape components, requiring complex analytical processes. To date, the use of Google Earth Engine platform (GEE) with cloud computing prowess, provides unique opportunities to map informal settlements with precision and enhanced accuracy. This paper leverages cloud-based computing techniques within GEE to integrate spectral and textural features for accurate extraction of the location and spatial extent of informal settlements in Durban, South Africa. The paper aims to investigate the potential and advantages of GEE's innovative image processing techniques to precisely depict morphologically varied informal settlements. Seven data input models derived from Sentinel-2A bands, band-derived texture metrics, and spectral indices were investigated through a random forest supervised protocol. The main objective was to explore the value of different data input combinations in

accurately mapping informal settlements. The results revealed that the classification based on spectral bands + textural information yielded the highest informal settlement identification accuracy (94% F-score). The addition of spectral indices decreased mapping accuracy. Our results confirm that the highest spatial accuracy is achieved with the ‘textural features’ model, which yielded the lowest root-mean-square log error (0.51) and mean absolute percent error (0.36). Our approach highlights the capability of GEE’s complex integrative data processing capabilities in extracting morphological variations of informal settlements in rugged and heterogeneous urban landscapes, with reliable accuracy.

Keywords: cloud computing; heterogeneous urban landscapes; Sentinel 2A; textural features; data input combinations

4.1. Introduction

Informal settlements are a growing concern in urban landscapes, worldwide. According to Samper et al. (2020), informal settlements are described as overcrowded housing units that are constituted by fragile structures, often deprived of basic amenities such as safe water, sanitation, infrastructure and services, and lacking secure tenure. Recent statistics have indicated that, of the four billion people who are currently residing in urban areas (UNDP, 2018), 1.6 billion live in informal areas (United-Nations, 2019), a figure that is estimated to rise to 3 billion by the mid-21st century (Samper et al., 2020). According to the 2030 Agenda for Sustainable Development (Fallatah et al., 2022), countries are expected to increase efforts in upgrading and improving the quality of life of their residents. To support that vision, and guide upgrading processes (Mboga et al., 2017, Persello and Stein, 2017), city planners and policy makers need information on their location and extent (Wang et al., 2019a), which is often scanty, not up-to-date, or inaccurate (Persello and Stein, 2017, Prabhu and Parvathavarthini, 2021). Furthermore, as informal settlements, particularly in Durban, South Africa, continue to be flood vulnerability hotspots (Membele et al., 2022b), occupying precarious sites (Satterthwaite et al., 2020), determining their locations and extents provides baseline information for planning integrated management in the event of floods. Therefore, a realistic approach which allows production of consistent, reliable and comprehensive informal settlement morphologies is critical for disaster preparedness, and also as baseline data for supporting mitigation measures in the event of foreseen or unforeseen climate scenarios.

The formation, location and expansion of informal settlements are a result of multifaceted and inter-related factors including, but not limited to, poor urban planning and management, uncontrolled population growth, rural-urban migration, inadequate housing provision (Fox, 2014, Winter et al., 2020) and the fact that in some sub-Saharan African countries, they are a manifestation of segregationist past (Loggia and Govender, 2020, Patel et al., 2019). Whilst economic globalization is associated with the spread of growth and greater opportunities (Balsa-Barreiro et al., 2019, Parnell and Crankshaw, 2009), city authorities in developing countries fail to keep pace with increased urbanization in terms of provision of housing. Being characterized by erratic urban morphology (Quesada-Román, 2022), the emergence of informal settlements is reflective of increased inequalities and socio-economic disparities (Balsa-Barreiro et al., 2019). In the global north, some countries, such as the United Nations Economic Commission for Europe (UNECE) (18) countries, have also experienced these radical transformations.

To date, the increasing availability of remote sensing data has made whole city studies possible. Geospatial techniques have emerged as reliable tools for the capture of more detailed, accurate, up-to-date, and objective spatial information on informal settlements, their dynamics and their morphologic characteristics at high temporal frequency (Kuffer et al., 2016b, Mboga et al., 2017). Traditionally, the measurement of informal settlements' extents was usually based on census data. However, because of the fluidity of informal settlements (Mudau and Mhangara, 2022), survey-based information is often outdated (Kohli et al., 2013b), characterized by huge temporal gaps (Mudau and Mhangara, 2021) and masks demographic and socio-economic differences in informal settlements (Membele et al., 2022a). Utilization of high-resolution imagery enables both spatial analytics and spectral analysis of informal settlements, (Farda, 2017), and are more efficient when compared with terrestrial surveys. However, obtaining reliable and accurate data on informal settlements continues to be hindered by (1) heterogeneity and complex spectral characteristics of urban land (Chen et al., 2015), (2) fragmented spatial configuration (Mugiraneza et al., 2019) and (3) diversity of morphologies of informal settlements (Stark et al., 2020). These characteristics vary extensively between countries, cities, within cities, and socio-economic contexts, making the characterization of spatial resolution and data input combinations difficult (Mananze et al., 2020, Wekesa et al., 2011). Given the fragmentation of urban landscapes, high spatial resolution often leads to high spectral mixing especially when spectral information is the sole data input (Persello and Stein, 2017). For that reason, spatial contextual information in the form of image texture can be exploited in capturing their morphological variations (Kohli et al., 2013a, Kuffer et al., 2017, Kuffer et al., 2018, Mboga et al., 2017).

Scientific research has been carried out in exploiting texture analysis to clearly identify and capture informal settlements (Kuffer et al., 2016b, Leonita et al., 2018, Prabhu et al., 2021b). In particular, several studies have explored texture feature algorithms such as grey level co-occurrence matrix (GLCM) (Girija and Nikhila, 2018, Kohli et al., 2016b, Prabhu and Alagu Raja, 2018, Shabat and Tapamo, 2017), contourlets (Ansari et al., 2019b), curvelets (Ansari and Buddhiraju, 2019a), lacunarity (Fallatah et al., 2019, Kit and Lüdeke, 2013, Kit et al., 2012a, Owen and Wong, 2013a), local Binary Patterns (LBPs) and Line Support Regions (LSRs) (Graesser et al., 2012). In other studies (Graesser et al., 2012, Kuffer et al., 2016b, Owen and Wong, 2013b), spectral information, spectral indices and textural information have been integrated for improved accuracy, with NDVI being the widely used spectral index. For instance, Kuffer et al. (2016b) achieved accuracy levels of between 84% and 88% when grey

level co-occurrence matrix (GLCM) variance was combined with NDVI, and an accuracy level of 90% when spectral information was combined with GLCM variance. However, such studies used limited numbers of input variables. Integration of image texture with spectral indices such as normalized difference water index (NDWI), the soil-adjusted vegetation index (SAVI) and the normalized difference building index (NDBI) for informal settlement detection to date, has rarely been exploited. Since urban areas are constituted by varied feature classes such as water bodies, built-up areas and vegetation (Fallatah et al., 2019), incorporation of the aforementioned spectral indices can help enhance class separability, thus contributing to increased informal settlement identification. Although the combination of the band-derived features has the potential to enhance image classification accuracy, their computation is accomplished through the application of numerous, tedious and sometimes time-consuming functions. For example, the extraction of texture features, particularly grey level co-occurrence matrix (GLCM) texture features, is carried out through the application of numerous functions to the image bands at varied window sizes. This often results in huge volumes of input data (Rodriguez-Galiano et al., 2012). There are also computation costs involved in averaging directions, as well as in texture feature selection. Apart from being time consuming (Graesser et al., 2012), the handling of large datasets with many features usually results in computational limitations, especially for a personal computer, where classical image-processing software is concerned (Stromann et al., 2019). In addition, the integration of the various input parameters would generate high dimensional feature sets, resulting in a sheer volume of data processing that traditional image processing platforms may fail to handle, thus causing classification complexity (Chen* et al., 2010, Shafizadeh-Moghadam et al., 2021).

Google Earth Engine (GEE), with its advancements in data processing and analytic tools, high computational power, and huge storage capacities (Dong et al., 2016), presents the potential to help overcome the limitations associated with handling voluminous data, in terms of storage, integration, processing, and analysis (Gorelick et al., 2017, Mananze et al., 2020). GEE's abundant imagery archives and data products (Zhang et al., 2019), for example Landsat-8, Sentinel-1 and -2, and MODIS (Amani et al., 2019c) mean that users do not need to download large datasets to local directories. Its integrative ability through effective script writing (Tassi and Vizzari, 2020), and parallelized processing of a stack of images have offered opportunities for integrating different feature sets at great speed, making timely outputs a reality (Patel et al., 2015). Furthermore, its provision of a complete package in terms of a plethora of remotely sensed images and cloud resources that warrant fast processing and analysis of images makes

traditional software and desktop-based image analysis obsolete (Liang et al., 2020). Given that background, several investigators have thus taken advantage of GEE cloud-computing for mapping purposes at diversified scales, ranging from global (Liu et al., 2018), continental (Liu et al., 2020, Xiong et al., 2017), to country scale (Mananze et al., 2020, Phan et al., 2020).

The application of GEE has been investigated in urban environments (Goldblatt et al., 2018, Rudiastuti et al., 2021, Tassi and Vizzari, 2020). For instance, Shafizadeh-Moghadam et al. (2021) integrated spectral, textural and topographical features in LULC in the Tigris–Euphrates basin. In another study, Tassi and Vizzari (2020) utilized spectral indices and GLCM textural indices for object based LULC classification in Trasimeno Lake, in Umbria, Central Italy. In Mananze et al. (2020) Landsat 7 and Landsat 8 bands, vegetation indices, and GLCM textural features were used to obtain a land cover map in Mozambique. The researchers took advantage of an environment in GEE that allows building of composite images from integrated feature sets (Teluguntla et al., 2018), summoning, processing, and stacking of image input data, running all analyses in parallel (Kelley et al., 2018). In one of the first studies on the application of GEE in informal settlement mapping, Tingzon et al. (2020) took advantage of the aforementioned cloud computing capabilities of GEE to map informal settlements in Colombia, through integration of spectral bands and spectral band-derived indices. In Colombia, informal settlements mainly occupy steep escarpments and are along urban fringes (Kamalipour and Dovey, 2019). The study did not explore the impact of adding image texture for informal settlement extraction. According to Duque et al. (2015), texture features have the capability to quantitatively differentiate informal settlement morphological characteristics such as high densities, organic morphology and disarranged spatial patterns, from planned, organized and well-structured urban layouts.

The paper seeks to extend the work of Tingzon et al. (2020) through integration of spectral bands, spectral indices and textural features for the precise mapping of informal settlements using the GEE software, in a South African context. On the other hand, Matarira et al. (2022b) discovered that studies on informal settlements in South Africa (Ella et al., 2008, Khumalo et al., 2011, Mudau and Mhangara, 2021, Shabat and Tapamo, 2017, van den Bergh, 2011) have mainly concentrated in Johannesburg city (Ella et al., 2008, Khumalo et al., 2011, Shabat and Tapamo, 2017, van den Bergh, 2011), Soweto township, and mostly used Quickbird imagery. Durban lacks coverage on application of image texture for the mapping of informal settlements. Durban is characterized by varied morphological patterns, ranging from lining traffic arteries, steep terrain (e.g., Bester's Camp (Inanda), open spaces, to being in proximity to river

networks, for example, Palmiet River (e.g., Quarry Road West). Texture analysis allows extraction of the diverse and explicit morphological features (Graesser et al., 2012, Kuffer et al., 2017).

Owing to this background, the study seeks to test performance of various data input combinations for precise characterization of informal settlements through exploitation of GEE cloud computing capabilities in the heterogeneous landscape of Durban, South Africa. The paper presents an approach for the creation of a reproducible classification framework, which would allow for the production of consistent data on a regular basis.

Specifically, the objectives were to:

- 1) Present an operational framework based on various Sentinel 2A band-derived spectral and texture feature combinations for capturing informal settlements in Durban, South Africa.
- 2) Determine the extent to which GEE's data analysis capabilities can precisely depict morphologically diverse informal settlements in the Durban landscape.
- 3) Statistically assess the deviations in informal settlement spatial extents derived from comparison analysis between modelled outputs and reference area estimates.

The results exhibit a paradigm shift from classical image processing software and approaches for detection of informal settlements towards advanced cloud computing resources that simplify access to datasets and processing of large feature sets.

4.2. Materials and Methods

4.2.1. Datasets

Sentinel 2A image collection (COPERNICUS/S2_SR surface reflectance dataset) was used in the analysis. The Sentinel 2A image covers 13 bands in the visible, near-infrared, and shortwave infrared (SWIR) wavelengths and consists of four bands at 10 m, six bands at 20 m, and three bands at 60 m (Lanaras et al., 2018, Phiri et al., 2020). To select data from the GEE archive, the filtered collection by date function was used. Multiple images covering a period from 1 August 2020 to 30 August 2020 in the study area were combined in a GEE collection. After filtering by date, three images were obtained that were used to form a composite, and a median value was assigned to each pixel. The resulting single image object represents the median value in each band of all the images in the filtered collection. Because clouds appear in different positions in the images, collections of several images acquired over a period of

time and over the same study area are a powerful way to removing many of the cloud-contaminated pixels (Patel et al., 2015, Tassi and Vizzari, 2020). Sentinel-2A image with less than 10% cloud coverage was employed.

4.2.2. Methods

Figure 4.1 illustrates the full approach adopted in this study. Our analysis consists of 7 methodological steps, which include: loading image collection and pre-processing, spectral feature extraction, texture feature calculation, feature input integration, feature importance evaluation, image classification, and accuracy assessment. GEE was the tool used to perform the bulk of the processing and analysis of Sentinel-2A imagery.

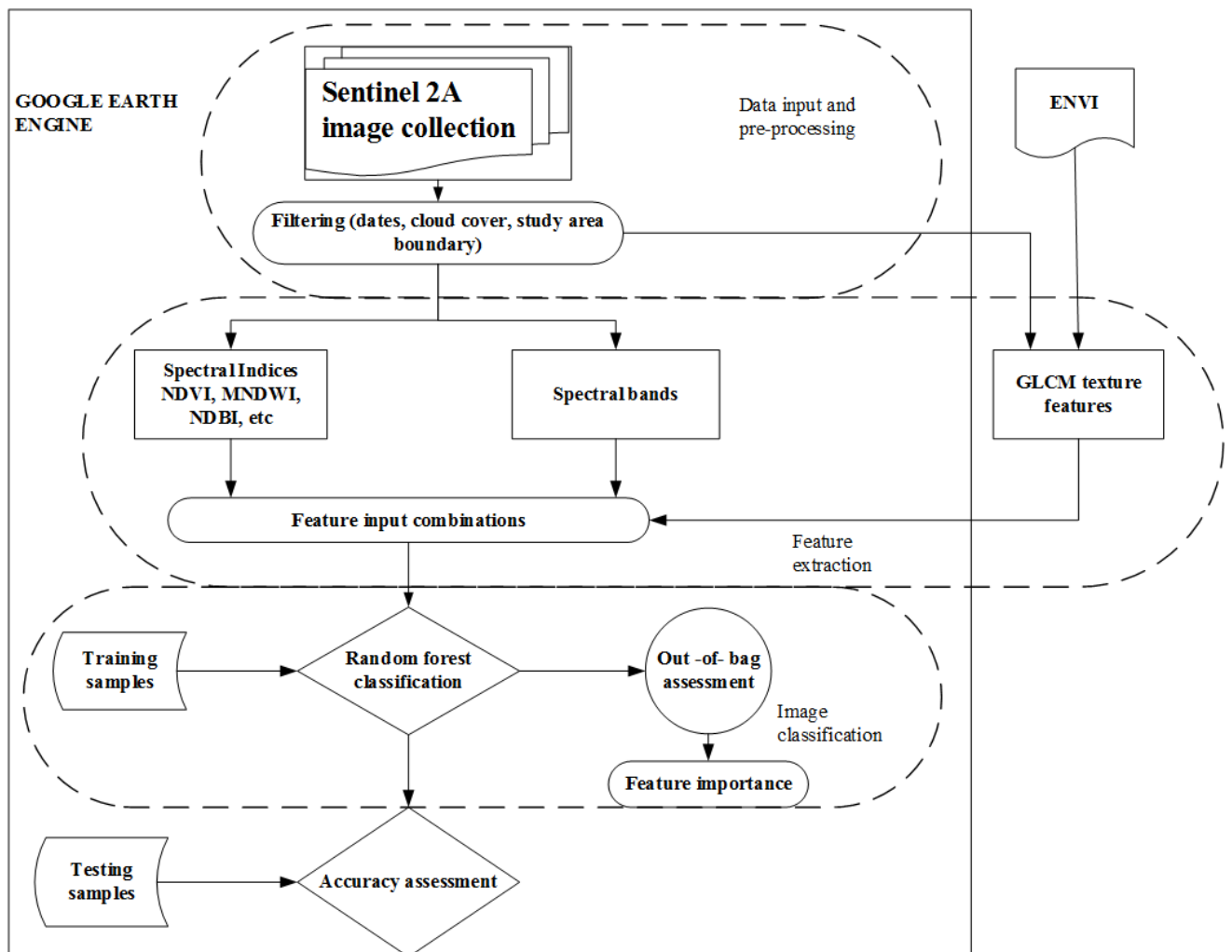


Figure 4.1. Research workflow chart.

4.2.3. Feature Extraction

In this study, both spectral and texture features were used as classification inputs. The extracted features included 10 spectral bands, eight spectral indices, and 24 texture features, as shown in Table 4.1.

Table 4.1. Image feature sets that were extracted from Sentinel 2A imagery.

Image features	Names	Number of features
Spectral bands (SBs)	Band (B2, B3, B4, B5, B6, B7, B8, B8A, B11, B12)	10
Spectral indices (SIs)	NDVI, NDWI, SAVI, NDBI, UI, NBI, BRBA, MNDWI	8
Texture metrics (Txs)	B2, B3, B4, (mean, variance, homogeneity, correlation, entropy, dissimilarity, contrast, angular second moment)	24

4.2.3.1. Spectral Features

Following the reviewed literature (Firozjaei et al., 2019, Tingzon et al., 2020), 10 spectral bands were selected as input features, which are B2, B3, B4, B5, B6, B7, B8, B8A, B11, B12 of Sentinel-2A imagery. Bands 1, 9, and 10 were not included because, according to Wang et al. (2016a), the three bands are not useful in LULC classification. In addition to the spectral bands, eight spectral indices were calculated from Sentinel-2A band combinations. These spectral indices were selected based on familiarity with the present land cover classes, such as urban, vegetation, and water (Li et al., 2020). Computed on the GEE cloud computing platform, these indices included two frequently used vegetation indices, namely NDVI and SAVI (Mananze et al., 2020). NDVI, being the widely used index in texture-based informal settlement detection (Graesser et al., 2012, Mudau and Mhangara, 2021, Owen and Wong, 2013b), quantifies vegetation cover and better discriminates LULC classes. Calculation of SAVI involved the multiplication of the pixel values by a scale factor of 0.0001 to convert them to reflectance values, as recommended by Gandhi (2021).

Among the several spectral indices, water indices, namely, NDWI and the modified normalized difference water index (MNDWI) were included. Built-up area indices that were used in the current study included normalized difference building index (NDBI), urban index (UI), new built-up index (NBI), and the band ratio for built-up areas (BRBA). These indices have been previously incorporated for the extraction of built-up areas (Kaimaris and Patias, 2016) and LULC mapping (Adepoju and Adelabu, 2019). According to Firozjaei et al. (2019), the NDBI and UI provide fast detection of built-up areas or bare land. The mathematical equations used for the calculation of the aforementioned indices are presented in Table 4.2.

Table 4.2. Spectral indices used for the mapping of informal settlements in the study.

Spectral Index	Equation	Main Reference
NDVI	$\frac{B8 - B4}{B8 + B4}$	(Rudiasuti et al., 2021, Shafizadeh-Moghadam et al., 2021, Zurqani et al., 2019)
SAVI	$1.5 \times ((B8 - B4)/(B8 + B4 + 0.5))$	(Gandhi, 2021)
NDWI	$\frac{B3 - B8}{B3 + B8}$	(Shafizadeh-Moghadam et al., 2021, Zurqani et al., 2019)
MNDWI	$\frac{B3 - B11}{B3 + B11}$	(Rudiasuti et al , 2021, Tingzon et al., 2020)
BRBA	$\frac{B4}{B11}$	(Tingzon et al., 2020)
NDBI	$\frac{B11 - B8}{B11 + B8}$	(Rudiasuti et al , 2021, Tingzon et al., 2020)
NBI	$\frac{B4 * B11}{B8A}$	(Rudiasuti et al , 2021, Tingzon et al., 2020)
UI	$\frac{B7 - B5}{B7 + B5}$	(Tingzon et al., 2020)

4.2.3.2. GLCM Textural Features

To derive textural information, the GLCM algorithm was used. GLCM describes the probability of relationships between the reflectance values of neighbouring pixels at a distance and orientation invariant within the image (Haralick et al., 1973). The resultant raster layer that is made up of derived texture measurements may be input into the further analysis (Hall-Beyer, 2017). The metrics involved in the current study included angular second moment, contrast, correlation, variance, entropy, dissimilarity, mean, and homogeneity, computed from Sentinel 2A visible bands. According to Ruiz Hernandez and Shi (2017), texture measurements can provide additional contextual information that enhances discrimination of diverse classes. The texture feature extraction was carried out using the GLCM implementation that is provided within the ENVI 5.3 software. In total, 24 texture features were obtained from the three visible

bands. In their study on leaf area index estimation using textural features, Zhou et al. (2017) carried out the sensitivity analysis of the GLCM parameters and discovered that the most important parameters to be considered in image processing included orientation, displacement, and moving window size. Adopting that notion, GLCM texture measures were measured based on the average of all directions (0°, 45°, 90°, and 135°), the same co-occurrence shift (1,1), quantization level of 64, and 7 × 7 window size. According to Giannini and Merola (2012), a quantization level of 64 preserves information and has an acceptable computing time. As pointed out in the literature (Kabir et al., 2010, Lan and Liu, 2018, Roberti de Siqueira et al., 2013), the window size is an important variable that has the potential to influence the discrimination capacity of extracted texture features. Selection of the optimal window size was performed using the method of coefficient of variation. The method of coefficient of variation was adopted from Kabir et al. (2010)'s study in their analysis of urban LULC classification. The process involved computation of class statistics for mean texture feature, which, through visual analysis, showed the most discriminative capability for informal settlements. The class statistics included minimum, maximum, mean and standard deviation. These statistics were calculated for the red, blue and green bands and for the window sizes 3 × 3, 5 × 5, 7 × 7, 9 × 9, 11 × 11, 13 × 13, 15 × 15. Coefficients of variation were calculated in Excel, using the formula $CV = \frac{\hat{\sigma}}{\mu}$, where

CV = coefficient of variation

$\hat{\sigma}$ = standard deviation

μ = mean

After texture feature extraction, the texture features were imported into GEE, exploiting the capability of the cloud computing platform to import and upload data on its public data catalog (Kumar and Mutanga, 2018).

4.2.4. Feature Combinations

After the extraction of spectral and texture features from Sentinel-2A bands, combinations of various feature types were established. In that respect, 42 features were used to develop feature combinations that were incorporated in differentiating informal areas and other land uses. The input feature sets were composed of spectral bands (SBs), spectral indices (SIs), spectral bands plus spectral indices (SBS + SIs), texture features (TxTs), spectral bands plus texture features

(SBs + Txts), texture features plus spectral indices (SIs + Txts), and spectral bands + spectral indices + texture features (SBs + SIs + Txts) derived from Sentinel-2A imagery. Based on the extracted features, three feature sets and four feature combinations were constructed to assess the influence of feature sets in distinguishing informal settlements.

4.2.5. Random Forest Classification

A pixel-based supervised RF machine learning algorithm was used for classification. RF classifiers applied to Sentinel 2A imagery in GEE have successfully mapped built-up areas (Rudiastuti et al., 2021), human settlements (Trianni et al., 2014), and, specifically, informal settlements (Tingzon et al., 2020). The choice of classifier for the current study was made owing to its capability to handle urban area classification where high-dimensional feature spaces are concerned and its robustness for informal settlement mapping in complex environments (Wurm et al., 2017a). Random Forest classifiers also measure each variable's contribution to the classification output, which is critical in assessing the value of each variable (Teluguntla et al., 2018). The entire classification process was performed in GEE where the building and tuning of the classification model were all based on the code “ee. Classifier package”. The seven constructed feature sets were used as inputs in the classification models. Following (Rudiastuti et al., 2021), an RF model with 100 trees was created, and the number of variables per split was set to the square root of the number of variables (Mananze et al., 2020, Phan et al., 2020). Following Phan et al. (2020), training samples were selected as small polygons to ensure that a polygon contains homogeneous pixels of a given land cover. In addition, small training polygons minimize the effect of spatial correlation (Phan et al., 2020). The classification was completed using 782 training samples and 309 testing samples. The model was designed to perform a random sampling strategy to create approximately 70% of the training samples from the original dataset and generating a decision tree for each training sample separately, with the remaining 30% of the training samples being used as validation data for internal cross validation to evaluate the classification accuracy of the random forest (Zhao et al., 2022). Furthermore, five land cover classes that characterise the study area landscape were proposed in the land classification scheme. These included informal settlement, vegetation, water, formal buildings and bare land.

To obtain an accurate representation of the performance of the classifier (Shetty et al., 2021), achieve better classifier stability (Jin et al., 2018), and consider potential variation in accuracy levels resulting from a random sampling of training samples (Belgiu and Drăguț, 2016), 20

replications of bootstrap sampling were performed and the same number of iterative classification trials performed for each model. Random Forest algorithms apply a bagging approach involving randomly resampling training data subsets to allow iterative construction of numerous, comparatively unbiased models which would then be averaged (Belgiu and Drăguț, 2016). This means 20 classification results were obtained for each input feature set.

4.2.6. Variable Importance

In the current study, the RF algorithm was used for variable importance evaluation. In the evaluation of variable importance score, the value of a feature parameter is turned into a random number and the impact on the accuracy of the model calculated (Zhao et al., 2022). The importance of the parameter was calculated from the out-of-bag error of each decision tree, calculated from the OOB data, following Jin et al. (2018). Feature importance evaluation was performed on feature combinations that consisted of more than 10 variables (Txts, SBs + SIs, SBs + Txts, SIs + Txts, and SBs + SIs + Txts) in order to obtain the 10 most significant variables, following (Bessinger et al., 2022, Hao et al., 2015). Five new feature subsets, made up of the important variables from each evaluated model were used to train the classifier. After repetition of the classification process 20 times, average values of the 20 F-scores were calculated for each feature subset model. Performance evaluation of feature subsets was carried out through a comparison of classification results of different feature subsets against the original feature set from which they were derived. The assessment was completed in order to establish if feature reduction would significantly improve informal settlement identification or not.

4.2.7. Accuracy Assessment, Classification Comparison, and Statistical Testing

According to Teluguntla et al. (2018), accuracy assessment is critical in map production using remote sensing data. Establishing the relative comparative performances of different feature sets, against the SBs (benchmark experiment) was an important focus of this paper.

4.2.7.1 Pixel-Based Accuracy Assessment

Classification performances of all seven classification models; SBs, SIs, Txts, SBs + SIs, SBs + Txts, SIs + Txts, and SBs + SIs + Txts were assessed. The confusion matrix implemented in GEE was used for the accuracy assessment of LULC classifications. User's accuracy (UA) and producer's accuracy (PA), calculated from the confusion matrix, were used to determine F-

scores that were used as the accuracy metric for informal settlement identification. The calculated F-scores were representative of classification accuracies for the informal settlement class. F-scores were used to quantify variations in the results for all feature-based models and the feature subset-based models. According to Zurqani et al. (2019), the F-score shows how good the classifier is in the context of both producer's and user's accuracies by weighting their average. The percentage deviations of F-score were calculated to assess the precision of the model vis-à-vis its accuracy.

$$\text{F-score} = 2 \times \frac{(UA)(PA)}{UA+PA} \quad (1)$$

F-score was calculated for each of the 20 classification iterations run for each feature set.

After performing 20 iterative classifications for a particular classification model, the 20 results of each experiment were tested for normality of distribution using the Shapiro test. Subsequently, the relative comparison between performances of pairs of different feature set combinations were performed using either the Welch Two-sample *t*-test or Wilcoxon Rank Sum test, depending on whether pairs of data were normally distributed or not. Where both datasets attained normal distribution, the Welch Two sample *t*-test was used to test if a significant difference existed between the means, with a corresponding calculation of *p*-values. Given the null hypothesis, $H_0: \mu_1 - \mu_2 = 0$ or $H_0: \mu_1 = \mu_2$ and alternative hypothesis $H_1: \mu_1 - \mu_2 \neq 0$ or $H_0: \mu_1 \neq \mu_2$, μ_1 and μ_2 represented means for the classification results for models 1 and 2, respectively. The *p*-value was calculated for a 95% confidence level and the null hypothesis of equal means was rejected at $p < 0.05$. Where one dataset was normally distributed and the other one was not, the Wilcoxon Rank Sum test was carried out. Given the null hypothesis, $H_0: \eta_A = \eta_B$ and alternative hypothesis $H_1: \eta_A \neq \eta_B$, η_A , and η_B represented medians for the classification results for models A and B respectively. Similarly, the *p*-value was calculated at a 95% confidence level, and the null hypothesis of equal medians was rejected at $p < 0.05$. Particularly, the main aim of this analysis was to determine whether statistically significant differences existed between classification results of different feature input combinations. Statistical significance tests were also executed for each pair of predictions made by feature subset-based and all feature-based models.

4.2.7.2. Patch-Based Accuracy Assessment

For the patch-based accuracy assessment, seven informal settlements (labelled A-G) (Figure 4.2) were considered as independently derived reference data for spatial estimation of informal

settlement areas. Boundaries for the respective informal settlements were digitized from Google Earth Pro and are shown in Figure 4.2. The polygons were used to compute areal estimates of informal settlements on the ground that were compared to the areal estimates on classified maps. The areas for the corresponding patches on classified maps were calculated using spatial analyst tools in ArcMap.

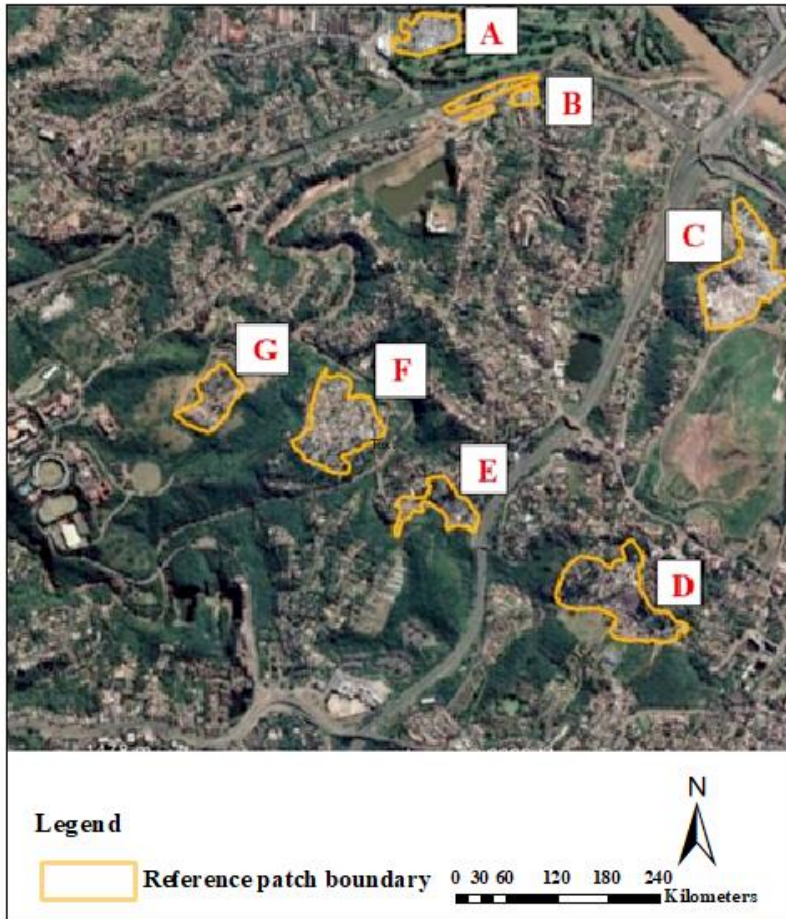


Figure 4.2. Ground truth samples of informal settlements (A-G (red)) in the study area.

4.2.7.3. Regression between Extracted Informal Settlement Areas and Ground Truth Data

Regression analysis was carried out to analyse the spatial variations in the relationship between ground truth area data and estimated areas. The focus of this analysis was to quantify the discrimination power of different feature input combinations through the measurement of the magnitude of error between predicted and observed spatial extents. In their research on spatial accuracy assessment of object boundaries, Albretch et al. (2010) suggested that validation concepts need to be extended to a spatial accuracy assessment of the objects' boundaries. In

this regard, this paper presented two different spatial error assessment methods, which included root-mean-square log error (RMSLE) and mean absolute percent error (MAPE). These error metrics, calculated in R statistical software, were used to compare the predictive ability of each input feature combination, in terms of deviation between boundaries of classification outputs and a reference dataset.

4. 3. Results

4.3.1. Evaluation and Comparative Analysis of Classification Results

4.3.1.1. Visual Analysis of Different Feature Input Models

The study tested seven different feature set options (1) spectral bands (SBs), (2) spectral indices (SIs), (3) texture features (Ttxts), (4) spectral bands and spectral indices (SBs + SIs), (5) spectral bands and texture features (SBs + Ttxts), (6) spectral indices and texture features (SIs + Ttxts), and a combination of spectral bands, spectral indices and texture features (SBs + SIs + Ttxts). Through visual comparison, differences were noted in the classification outputs, paying particular attention to the degree of misclassification between the informal built-up land and other land uses. From a visual inspection, the drawback of “salt and pepper” effects could be evident in the models SIs, SBs + SIs, and SBs. Misclassifications were noticed, especially between informal areas and bare land. Some informal settlement patches could be seen in areas that, on the ground, were represented as bare land. Examples of misclassified areas are shown in black squares (Figure 4b,e,f). The black squares mark out areas with evident misclassifications of bare land and informal settlements. The distinct separation of informal settlements from other LULC classes could be identified in Ttxts, SBs + Ttxts, SBs + SIs + Ttxts, and SBs + Ttxts models where large and well-defined patches of informal settlements were labelled as informal built-up land.

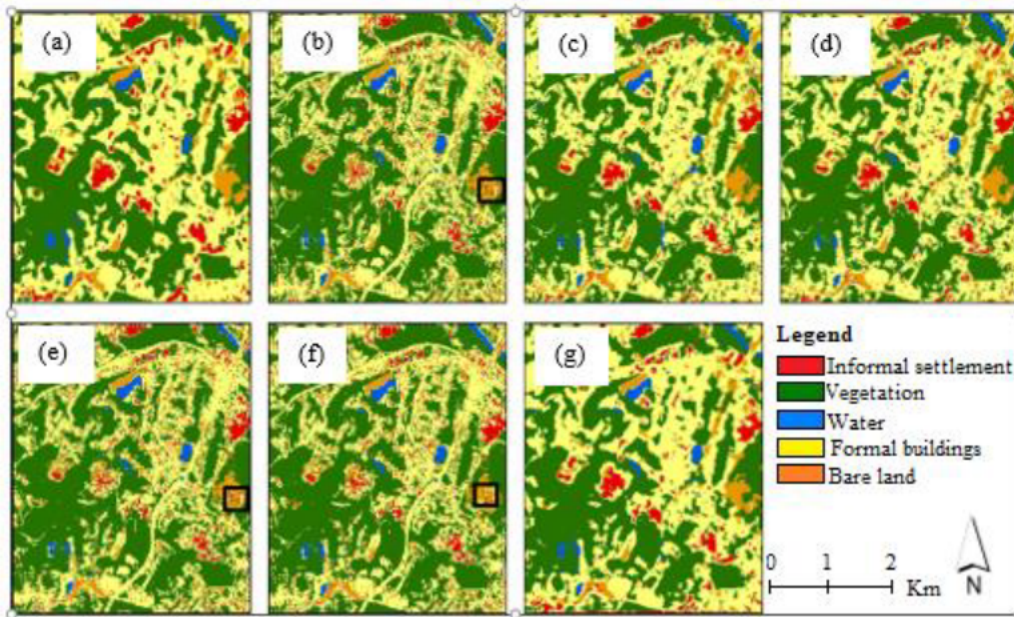


Figure 4.3. Land use/Land cover maps obtained using different feature combinations from (a) Texture features, (b) Spectral indices, (c) Spectral indices + texture features, (d) Spectral bands + spectral indices + texture features (e) Spectral bands + spectral indices, (f) Spectral bands, (g) Spectral bands + texture features

4.3.1.2. Accuracy Assessment and Analysis

To assess the performance of the models, F-score, percentage deviation, and statistical tests were calculated for the various feature sets. Table 4.3 shows average F-scores, standard deviations, and statistical significance obtained by using SBs as a benchmark, and different types of features. The best accuracy results are displayed in bold.

Table 4.3. Producer accuracy (%), user accuracy (%), average F-scores and standard deviation for different feature input models.

Model	PA	UA	F-score
SBs	83	89	86 ± 1.98
SIs	73	80	76 ± 2.06
Txts	86	94	90 ± 1.19
SBs + SIs	79	86	82 ± 1.43
SBs + Txts	91	97	94 ± 1.27
SIs + Txts	91	94	92 ± 0.91
SBs + SIs + Txts	91	96	93 ± 1.08

Generally, accuracy was high for all feature-based models, averaging beyond 80%. The average F-scores ranged from $94 \pm 1.27\%$ (SBs + Txts) to $76 \pm 2.06\%$ (SIs). In fact, the descending order of IS identification accuracy was 94% (SBs + Txts), 93% (SBs + SIs + Txts), 92% (SIs + Txts), 90% (Txts), 86% (SBs), 82% (SBs + SIs), and 76% (SIs). Generally, the results suggested that the inclusion of image texture significantly boosted classification accuracy, since classification performances were enhanced in all the models that incorporated textural features. More specifically, the addition of textural features to spectral bands yielded the highest accuracy improvement when spectral bands alone were used as a benchmark experiment. On the other hand, combining spectral bands and spectral indices decreased the F-score by 4%. The results also show that the sole use of spectral bands resulted in relatively higher performance than “spectral bands + spectral indices”. Considering models that incorporated textural features, the descending order of importance was SBs + Txts (94%), SBs + SIs + Txts (93%), SIs + Txts (92%), and Txts (90%). It is also important to note that, whilst the addition of textural information to spectral bands (SBs + Txts) yielded the highest accuracy levels, results declined when spectral indices were added to the feature set. Almost similarly, compared with Txts alone, the composite of spectral indices and texture metric (SIs + Txts) yielded decreased accuracy. Result analysis also demonstrated that combining multispectral bands with texture features performed better (94%) than using each type of feature solely (SBs-86%, Txts-90%). Furthermore, a composite of all three feature sets (SBs + SIs + Txts) did not provide superior results. Most importantly, all six experiments that were compared against the performance of only spectral bands showed significant differences between classification performances ($p < 0.05$) (Table 4.4).

Whilst the accuracy deviations, as represented by standard deviations, were not very large, there was no consistency in terms of precision. For instance, considering the 20 test runs for the SBs + Txts models, its accuracy was the best, but its precision, as measured by standard deviation, was not. Although SIs + Txts model yielded lower accuracy than SBs + Txts, the result showed more precision as indicated by the low standard deviation. The percentage deviations of average F1-scores were 1.98%, 2.06%, 1.19%, 1.43%, 1.27%, 0.91%, 1.08% (Table 4.4). These standard deviations were for SBs, SIs, Txts, SBs + SIs, SBs + Txts, SIs + Txts, and SBs + SIs + Txts, respectively.

Table 4.4. Two sample *t*-tests for the mapping of informal settlements and their *p* values.

First model	Second model	Mean of first model	Mean of second model	P-value
SBs vs	SIs	86	76	< 0.05
SBs vs	Txts	86	90	< 0.05
SBs vs	SBs + SIs	86	82	< 0.05
SBs vs	SBs + Txts	86	94	< 0.05
SBs vs	SIs + Txts	86	92	< 0.05
SBs vs	SBs + SIs + Txts	86	93	< 0.05

4.3.1.3. Importance of Features for Informal Settlement Mapping

Figure 4.4 shows the 10 most important variables of the models Txts, SBs + SIs, SBs + Txts, SIs + Txts, and SBs + SIs + Txts. The results demonstrated that there was no consistency in terms of performance of feature subset-based models. Whilst some feature–subset models FS (SBs + Txts), FS (SIs + Txts), and FS (SBs + SIs + Txts) achieved significant decreases in classification accuracy (Table 4.5), feature reduction did not yield any changes in classification accuracy for models such as Txts and SBs + SIs. In addition, features with high importance scores changed with changes in feature combinations. For instance, variable importance scores indicated that $B2_{\text{mean}}$, $B3_{\text{mean}}$, $B4_{\text{mean}}$, and $B4_{\text{variance}}$ were the four most important variables in the Txts model. For the SBs + Txts model, $B2_{\text{mean}}$, $B3_{\text{mean}}$, $B4_{\text{mean}}$, and B8A were the most important. In the SIs + Txts model, $B2_{\text{mean}}$, $B3_{\text{mean}}$, $B4_{\text{mean}}$, and *ui* contributed the most information to the model. Similarly, $B2_{\text{mean}}$, $B3_{\text{mean}}$, $B4_{\text{mean}}$, and *ui* were the most important variables in the SBs + SIs + Txts model. Considering SBs + SIs model, B2, B12, *ui*, and ndwi had the most influence in the classification.

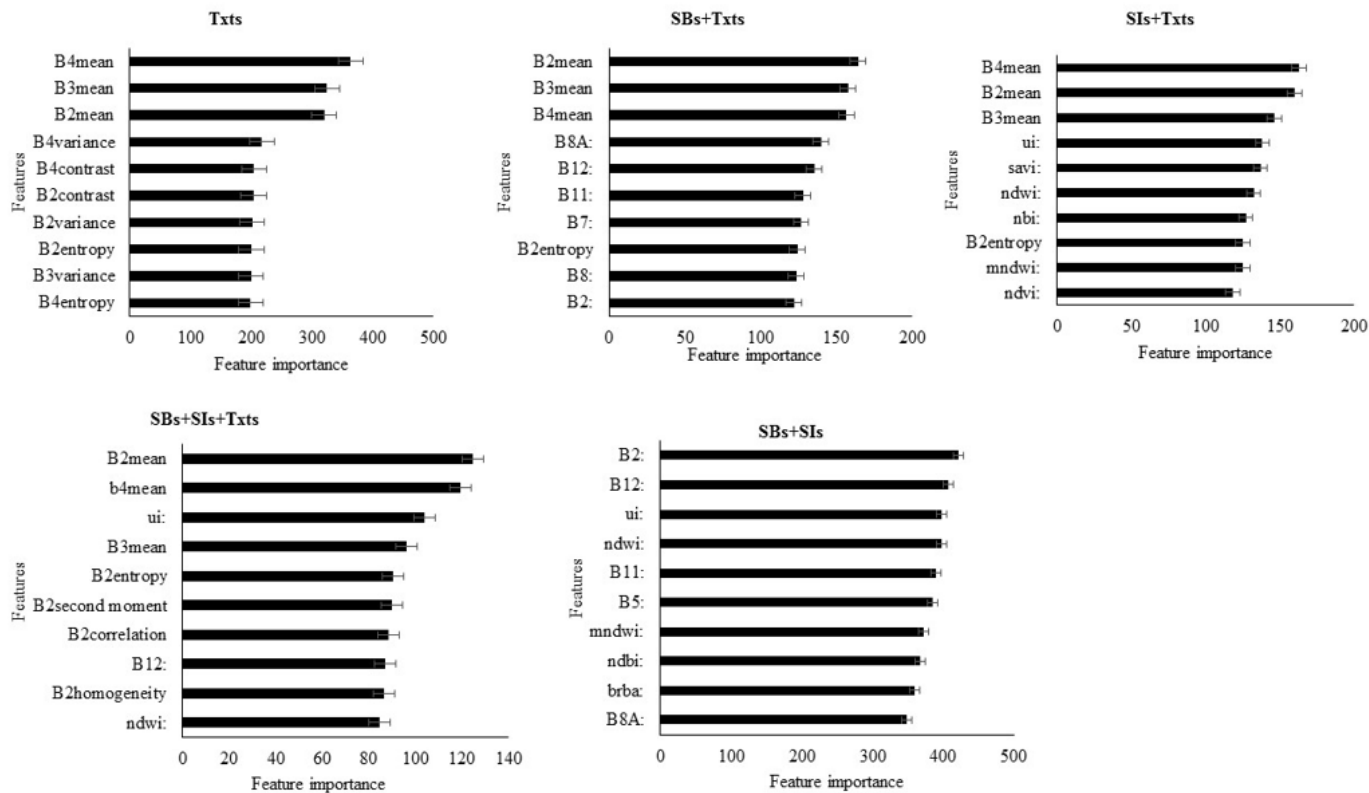


Figure 4.4. Feature importance scores of the 10 most important features for the image combinations.

In the feature combinations where spectral indices were incorporated, *ui* obtained the highest importance score and would feature in the top four variables. When textural features were incorporated, *B2_{mean}*, *B3_{mean}*, and *B4_{mean}* attained the highest importance score, indicating the relevance of mean texture in the classification process. There was no consistency with regard to the most important spectral band, with *B8A* contributing most in the model SBs + Txts and *B2* contributing most in the SBs+ SIs model. From Figure 4.4, it could be observed that the variable importance score also decreased when the number of features used to build the RF model increased. For example, considering the Txts model, *B2_{mean}*, *B3_{mean}*, and *B4_{mean}* attained feature scores ranging between 300–400. When Txts were combined with either SBs or SIs, importance scores were reduced to between 150 and 200. The feature importance score was reduced further to between 100 and 140 when Txts was combined with both SBs and SIs.

4.3.1.4. Feature Subset Evaluation

From the two-sample *t*-tests that were carried out, three models showed significant differences between the performance of feature models and feature subset-based models. Classification

results for feature subsets extracted from SBs + Txts, SBs + Txts + SIs, and Txts + SIs models were significantly lower than that for their corresponding all feature models. This suggests that feature reduction caused a decline in classification results. The average decrease in classification was 6%. On the other hand, there were no observed differences in informal settlement identification accuracy for the subsets derived from Txts and SBs + SIs. Table 4.5 shows the performance of feature subsets against the feature sets from which the subsets were selected. The same trends of accuracy measures were observed for the feature-subset-based models as for the feature-based models, where the descending order of F1-scores was FS (SBs + Txts), FS (SBs + SIs + Txts), and FS (SIs + Txts).

Table 4.5. Two sample *t*-tests for all variables vs feature subsets for feature input models.

Feature input model	F-score		P-value
	All variables	Feature subset	
Txts	90	90	
SBs + SIs	82	82	
SBs + Txts	94	90	p < 0.05
SBs + SIs + Txts	93	88	p < 0.05
SIs + Txts	92	84	p < 0.05

4.3.1.5. Patch-Based Accuracy Assessment

The results demonstrated the underestimation of informal settlement extents by all the models. Figure 4.5 shows informal settlement patches overlaid on digitized polygons for the same settlement. The results indicate that the informal settlement patches on classified maps covered smaller areas than the real areas on the ground. Calculations of relative spatial errors demonstrated high RMSE values for all the models ranging from 0.51 to 1.2 and MAPE values ranging from 0.36 to 0.61. For both RMSLE and MAPE, the results indicate that the Txts model yielded the best spatial accuracy (RMSLE = 0.51; MAPE = 0.36) (Table 4.6).

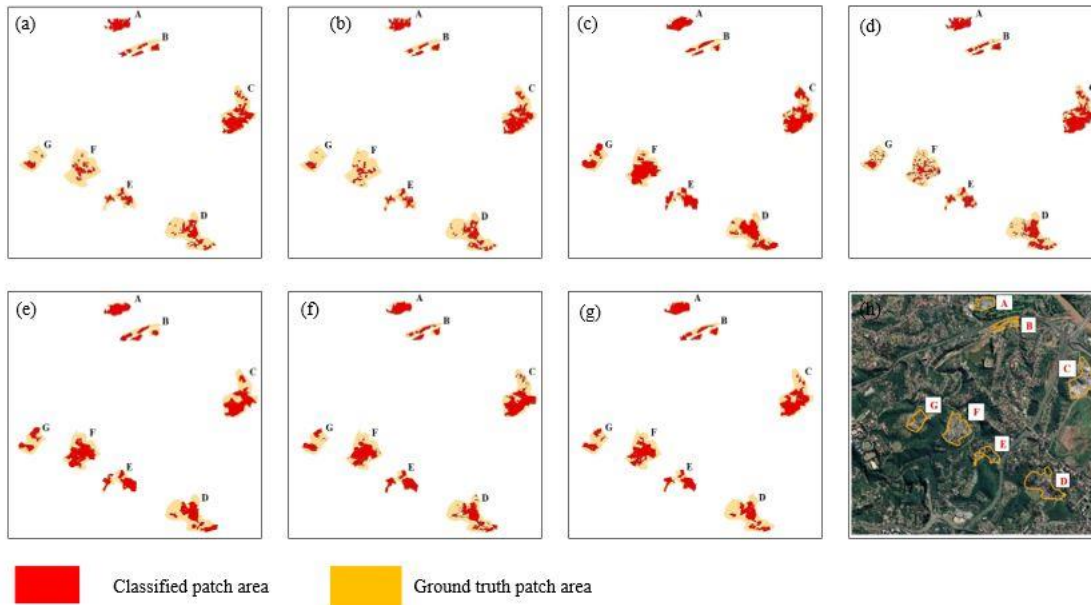


Figure 4.5. Classified informal settlement patch areas (A-G (black)) for models (a) Spectral bands, (b) Spectral indices, (c) Texture features, (d) Spectral bands + spectral indices, (e) Spectral bands + texture features, (f) Spectral indices + texture features, (g) Spectral bands + spectral indices + texture features, and corresponding ground truth polygons (A-G (red)).

Table 4.6. Spatial accuracy assessment results for area-based classification.

Classification Model	Patch	Classified	Reference	Difference	Difference (%)	RMSLE	MAPE
		Patch Area (ha)	Patch Area (ha)				
SBs	A	2.97	3.94	0.97	24.62	1.13	0.57
	B	1.89	1.86	-0.03	-1.61		
	C	6.96	12.43	5.47	44.01		
	D	3.89	13.55	9.66	71.29		
	E	1.83	4.49	2.66	59.24		
	F	1.97	11.22	9.25	82.44		
	G	0.95	5.09	4.14	81.34		
SIs	A	2.72	3.94	1.22	30.96	1.2	0.61
	B	1.50	1.86	0.36	19.35		
	C	6.76	12.43	5.67	45.62		
	D	3.80	13.55	9.75	71.96		

	E	1.88	4.49	2.61	58.13		
	F	1.82	11.22	9.4	83.78		
	G	0.83	5.09	4.26	83.69		
	A	3.25	3.94	0.69	17.51		
	B	1.73	1.86	0.13	6.99		
	C	7.83	12.43	4.6	37.01		
Txts	D	6.47	13.55	7.08	52.25	0.51	0.36
	E	3.85	4.49	0.64	14.25		
	F	6.70	11.22	4.52	40.29		
	G	2.62	5.09	2.47	48.53		
	A	3.11	3.94	0.83	21.07		
	B	1.80	1.86	0.06	3.23		
	C	7.83	12.43	4.6	37.01		
SBs + SIs	D	4.97	13.55	8.58	63.32	0.88	0.50
	E	2.61	4.49	1.88	41.87		
	F	3.04	11.22	8.18	72.91		
	G	1.28	5.09	3.81	74.85		
	A	3.88	3.94	0.06	1.52		
	B	1.42	1.86	0.44	23.66		
	C	8.31	12.43	4.12	33.15		
SBs + Txts	D	5.28	13.55	8.27	61.03	0.63	0.38
	E	3.63	4.49	0.86	19.15		
	F	6.44	11.22	4.78	42.60		
	G	2.12	5.09	2.97	58.35		
	A	2.93	3.94	1.01	25.63		
	B	1.85	1.86	0.01	0.54		
	C	7.04	12.43	5.39	43.36		
SIs + Txts	D	5.04	13.55	8.51	62.80	0.68	0.44
	E	3.53	4.49	0.96	21.38		
	F	5.71	11.22	5.51	49.11		
	G	1.82	5.09	3.27	64.24		
SBs + SIs + Txts	A	3.11	3.94	0.83	21.07	0.73	0.46
	B	1.70	1.86	0.16	8.60		

C	6.75	12.43	5.68	45.70
D	4.45	13.55	9.1	67.16
E	3.19	4.49	1.3	28.95
F	5.50	11.22	5.72	50.98
G	1.83	5.09	3.26	64.05

4.4. Discussion

The study sought to investigate performance of different feature input combinations in accurately depicting morphologically varied informal settlements as well as their spatial extents within the GEE platform. Variable results were obtained depending on the input datasets. Average accuracy of >80% suggests the success of RF in extracting informal built-up areas in the study area. Results demonstrated that classification of spectral bands alone yielded relatively low model performance (86%), whilst models that incorporated texture features performed better, ranging from 90% to 94%. In agreement with the current study results, Kuffer et al. (2016b) achieved an increase in accuracy from 62% to 65% when image texture was integrated with spectral bands. Both results are supported by Shafizadeh-Moghadam et al. (2021), who alluded that spectral bands alone are insufficient in discriminating different LULC types, and that similar morphological characteristics, in the form of constructional materials, paint or roof colours (Gevaert et al., 2016, Myint et al., 2011) can help explain confusion within urban landscapes. GLCM texture-based analysis can capture urban morphological characteristics such as built up densities (Leonita et al., 2018), shape, size, orientation and roof colours (Kuffer et al., 2017). However comparing the classification performances, RF classification using the GEE platform, performed in the current study, yielded significantly higher accuracies than RF classification implemented by Kuffer et al. (2016b) in the eCognition software. Given some similarities in morphological characteristics of informal settlements in Mumbai and Durban (high densities, organic morphology, iron and asbestos roofing sheets), higher accuracy in the current study can largely be explained in terms of GEE's integrative ability through effective script writing (Tassi and Vizzari, 2020), and parallelized processing of a stack of input features, that offers opportunities for integrating different feature sets for enhanced mapping accuracy. Whilst 24 texture variables were integrated in the current study, Kuffer et al. (2016b) only used variance. In Kuffer et al. (2016b), it is argued that combining a number of texture descriptors is crucial in discriminating complex urban settlement patterns.

Mirroring these findings, RF models within the GEE were able to capture the morphological characteristics of informal settlements better than studies that used classical software.

Results also indicate that, while the addition of spectral indices to the “spectral bands + texture features” model reduced the accuracy level from 94% to 93% in the current study, the addition of NDVI to the “spectral bands + texture” model increased informal settlement identification accuracy in Kuffer et al. (2016b)’s study, from 65% to 90%. The results from Kuffer et al. (2016b) showed the relevance of NDVI in distinguishing informal settlements in Mumbai. Conversely, considering combinations that incorporated spectral indices, variable importance analyses indicated that NDVI only featured in 1 out of 3 feature subsets (Figure 4.4), where it assumed the lowest rank. The low performance of NDVI in the current study could also help explain the reduced accuracies when spectral indices were incorporated into other feature sets. Nonetheless, the current results appear consistent with (Graesser et al., 2012)’s findings, where NDVI resulted in consistently low accuracies. This result is potentially explained by the lack of variance in urban vegetation in many cities (Amani et al., 2019c, Graesser et al., 2012). In addition, the significant fall in classification accuracy in the current results when spectral indices were added to the “spectral bands + texture features” model is in agreement with other studies in spatially heterogeneous complex landscapes (Li et al., 2016, Lin et al., 2021). In their mapping of complex surface-mined and agricultural landscapes, Li et al. (2016) attributed reduced accuracy to the importation of redundant information, since spectral indices are derived from the linear computation of spectral bands (Chen et al., 2017). Furthermore, Dolean et al. (2020) argued that the main problem with spectral indices being used for urban area mapping is that they cause spectral mixing between built-up areas and bare surfaces due to their similarity in spectral response patterns, especially in spatially heterogeneous environments. These explanations conform with the current results where misclassifications of bare land as informal settlements were evident (see the black rectangles in Figure 4.3b, e) in models that incorporated spectral indices (Figure 4.3). In their study, Firozjahi et al. (2019) also observed similar spectral behaviours between built-up and bare lands. Most importantly, the current results mean that, although informal settlement mapping can be performed better through the RF algorithm, some problems of spectral confusion, especially between bare surfaces and built-up areas, remain unsolved.

Examination of the performance of feature subset-based models revealed that feature subsets either yielded significantly reduced classification accuracies ($p < 0.05$) at a 95% confidence interval, with an average value of 6%, or yielded no change in classification results. This

finding agrees with Graesser et al. (2012)'s findings in which feature reduction caused decreased accuracy, and no feature subsets were as powerful as the full combination. The current findings are, however, inconsistent with Maxwell et al. (2014), who in their mapping of a complex mining environment, reported significant improvement in accuracy from the utilization of the top 10% of variables selected using variable importance measures. The fact that combinations of different input features yielded higher results than single feature sets suggest that, although adding additional features such as textural variables to the original spectral bands increases the dimensionality of feature space Graesser et al. (2012), more input variables could enhance informal settlement discriminability. This observation is consistent with Amani et al. (2019b), who alluded that extraction of many features from satellite data is one way of increasing image classification accuracy. Current findings contribute to revealing the strength of the RF classifier in dealing with high-dimensional feature sets (Ruiz Hernandez and Shi, 2017).

Estimated Informal Settlement Areas

From the analysis of modelled slum patches and ground truth samples of slum patches, the results indicate that, although distinct informal settlement patches and clear boundaries could be identified from RF classification, there were inconsistencies in the mapping. Results demonstrated evidence of underestimation of informal settlement spatial extents (Figure 4.5). Generally, high RMSLE values were evident ranging from 0.51 to 1.2. Whilst mapping results suggest the effectiveness of RF classification in capturing informal settlement locations, underestimation indicates lack of robustness in the capturing of their diversity. The inconsistencies could be attributed to the complexity of informal settlement morphologies (Taubenböck et al., 2018). Challenges exist in capturing informal settlements characterized by varied typologies within the area. For instance, remote sensing data fail to reveal the dynamics in factors that shape the apparent morphologies of the informal settlements, for example, culture, socio-political and economic status. Capturing informal settlements at varied stages of development could be challenging (Owen and Wong, 2013b). Whilst remotely sensed data and socio-economic parameters of an area may correlate (Duque et al., 2015), structural variations emanating from a high socio-economic gradient between two informal settlement areas could compromise the reliability of results. In Kuffer et al. (2017), it is suggested that integrating remotely sensed data with survey-derived socio-economic information such as employment status, educational status, population figures and population density would avoid representation of informal settlements as one-dimensional.

In the current study, there were also some limitations. Firstly, the near-infra-red band which was not used in the extraction of image texture could be exploited, since according to Ruiz Hernandez and Shi (2017), it provides greater contrast and thus carries the most significant data spikes. Secondly, our method utilized Sentinel-2A images with relatively low spatial resolution, which could explain some false identification that was evident in the results. The definition of adequate spatial resolution has been regarded as a key issue in the mapping of complex environments (Mananze et al., 2020, Räsänen and Virtanen, 2019). For instance, the potential of PlanetScope data for precise mapping of heterogeneous landscapes, for example, in identifying crop types and extents in small holder environments, has been emphasized (Kpienbaareh et al., 2021, Rufin et al., 2022). In addition, the application of object-oriented analysis techniques, particularly within GEE, is constantly evolving (Tassi and Vizzari, 2020). In Vizzari (2022), land cover was mapped using object-based image classification and PlanetScope imagery within GEE and increased accuracy was achieved. Further, the author integrated PlanetScope with Sentinel-1 and Sentinel-2 data using the object-based oriented approach and achieved improved geometric and thematic accuracy. These findings present an opportunity to explore the capabilities of high resolution PlanetScope and object-oriented analysis in overcoming challenges of inaccurate identification of dynamic, spatially and morphologically complex informal settlements. Accurate and consistent characterization of informal settlements would provide insights into their historical and contemporary dynamics, as well as in simulating future land changes.

4.5. Conclusions

GEE cloud computing was successfully applied for informal settlement mapping in part of Durban Metro, South Africa. GEE showed considerable versatility and adaptability due to its integrative capabilities and its efficient platform for script writing. Within the GEE environment, this work developed and tested pixel-based classification of various input combinations. The best performing input variables for the random forest ensemble classifier were identified through systematic testing of different feature input combinations.

The following conclusions were drawn:

- The RF model performed well in distinguishing informal settlements, yielding an average accuracy above 80%.
- The addition of texture features yielded statistically significant accuracy levels

- The addition of spectral indices generated significantly reduced accuracy levels.
- Considering the accuracy level of the informal settlement class, the spectral bands + texture features model achieved the best performance (94%).
- The texture features model yielded the lowest spatial error, enabling it to most accurately depict informal settlement boundaries.

The results demonstrate how the GEE framework, by simplifying access and processing of a large amount of satellite data, is shifting the paradigm in built-up area mapping from a static, product-based approach into a more dynamic and application-specific one with reasonable accuracy and in no time.

4.6. Summary

This chapter mapped informal settlement diversities using a combination of spectral bands, spectral indices and GLCM textural variables. Innovative image processing techniques available within the GEE were exploited. Among the seven data input combinations that were tested, a combination of spectral bands and textural variables yielded the highest accuracy. Although the value of inbuilt RF algorithm was shown through high accuracy levels, fuzziness still existed in classification, either between informal settlements and bare land, or between informal settlements and formal buildings. One explanation for this could be pixel-based classification used in the study. These uncertainties call for the need for a more improved classification framework that would accurately capture informal settlement heterogeneities. An object-based algorithm can possibly ease the challenges of misclassification as it takes into account the contextual information within a given imaging neighbourhood. The availability of a segmentation algorithm within GEE, as well as GLCM texture feature extraction algorithm allows exploration of GEOBIA for a more accurate classification. The next chapter will implement GEOBIA within the GEE, exploring the efficacy of integration of data from diverse range of multiple datasets.

CHAPTER FIVE:

Object-Based informal settlement mapping in Google Earth Engine using the integration of Sentinel-1, Sentinel-2, and PlanetScope Satellite Data

This chapter is based on:

Matarira, D., Mutanga, O., Naidu, M., & Vizzari, M. (2022). Object-Based Informal Settlement Mapping in Google Earth Engine Using the Integration of Sentinel-1, Sentinel-2, and PlanetScope Satellite Data. *Land*, 12(1). doi:10.3390/land12010099

Abstract:

Mapping informal settlements' diverse morphological patterns remains intricate due to unavailability and huge costs of high-resolution data, as well as spatial heterogeneity of urban environments. Accessibility to high-spatial resolution PlanetScope imagery, coupled with the convenience of simple non-iterative clustering (SNIC) algorithm within the Google Earth Engine present potential for geographic object-based image analysis (GEOBIA) to map spatial morphology of deprivation pockets in a complex built up environment of Durban. Such advances in multi-sensor satellite image inventories on GEE also afford possibility to integrate data from sensors with different spectral characteristics and spatial resolutions for effective abstraction of informal settlement diversity. The main objective is to exploit Sentinel-1(S1) radar data, Sentinel-2 (S2) and PlanetScope (PL) optical data fusion for more accurate and precise localization of informal settlements using GEOBIA, within GEE. The findings reveal that the random forest classification model achieved informal settlement identification accuracy of 87% (F-score) and overall accuracy of 96%. An assessment of agreement between observed informal settlement extents and ground truth dimensions was conducted through regression analysis, yielding root mean square log error (RMSLE) = 0.69 and mean absolute percent error (MAPE) = 0.28. The results demonstrate reliability of the classification model in capturing variability of spatial characteristics of informal settlements. The research findings confirm efficacy of combined advantages of OBIA within GEE, and integrated datasets for more precise capturing of characteristic morphologic informal settlement features in a heterogeneous urban landscape. The outcomes demonstrate a transition from informal settlement mapping using conventional static approaches towards more dynamic cloud computing platform that simplifies processing of voluminous data. The study has important implications for the identification of the most effective ways to map informal settlements in a

complex urban landscape, thus providing a yardstick for other regions that are characterized by large landscape multiformity.

Keywords: Google Earth Engine, simple non iterative clustering, object-based image analysis, informal settlements, texture features, mapping.

5.1. Introduction

Unprecedented processes of urbanization, especially in developing countries, result in highly dynamic urban patterns, characterised by dominance of informal urban development (Wurm et al., 2019). Being inexorably a reflection of “urbanization of poverty” (Hofmann et al., 2015), informal settlements are characterized by dense housing, made up of sub-standard, heterogeneous constructional materials, which, when coupled with their characteristic location on flood vulnerable areas, exacerbate residents’ risk and vulnerability to natural hazards such as flood events (Kuffer et al., 2020). Housing approximately 1 billion dwellers globally (UN-Habitat, 2016), the United Nations has prioritized informal settlement improvements in the 2030 Sustainable development goals (Fallatah et al., 2022, Pratomo et al., 2017). Despite their stipulated targets, informal settlements continue to grow (Pratomo et al., 2017). Ameliorating the conditions of deprivation in informal settlements requires up-to date base maps with comprehensive information on their spatial locations and dimensions (Kuffer et al., 2020), which is mostly inconsistent, generalized or simply non-existent (Taubenböck et al., 2018). Given the dynamic nature of these deprived areas (Kraff et al., 2020), there is exigency for techniques that can provide rapid and reliable information on their morphological layouts. Furthermore, the understanding of informal settlements’ level of marginalization as it relates to natural hazards and climate change risk requires precise and comprehensive identification of their spatiality.

Remote sensing provides ease in spatial analytics (Farda, 2017), and its synoptic and repetitive capabilities afford updated, consistent and comprehensive geospatial information with great thematic detail, especially in complex urban environments (Wang et al., 2019b). Exploiting the convenience of high-resolution sensors, such as GeoEye, IKONOS, QuickBird, and WorldView, concerted research efforts have been made to map informal settlements (Kuffer et al., 2016b, Mboga et al., 2017a, Mudau and Mhangara, 2021, Prabhu and Parvathavarthini, 2021). However, the intricacy of semantic abstraction of informal settlements has been emphasized (Fallatah et al., 2020, Kohli et al., 2016a, Mugiraneza et al., 2019). Firstly, the cost prohibitive and sometimes unavailable high resolution earth observation (EO) data (Taubenböck et al., 2018) is a major drawback in efforts for accurate delineation of urban deprived areas. Secondly, the inherent variations in informal settlement morphological appearances either within or across geographical locations (Stark et al., 2020) confound the task. Also, fragmented urban landscapes are difficult to represent using a pixel-based

classification approach where only spectral values are concerned (Fallatah et al., 2020), making characterization of informal settlement morphologic differences complex (Leonita et al., 2018, Mboga et al., 2017).

Recently, object-based image analysis (OBIA or geographic object based image analysis (GEOBIA) has been applied more frequently in capturing heterogeneity in fragmented urban landscapes for informal settlement identification (Fallatah et al., 2020, Fallatah et al., 2022, Kohli et al., 2016a, Pratomo et al., 2017, Mugiraneza et al., 2019). The strength of object oriented approaches (OOA) for informal settlement analysis is in its capability to incorporate spectral, spatial and contextual characteristics of an image, which intensify potential to capture informal settlement morphological diversities (Kohli et al., 2016a, Kohli et al., 2013a). Kohli et al. (2016a) used OBIA to map informal settlements in Pune, India, using Quickbird imagery, and yielding overall accuracy of 80.8%. In another study, Fallatah et al. (2019) mapped informal settlements in Jeddah, Saudi Arabia, and distinguished informal and formal areas with an overall accuracy of 83%. Fallatah et al. (2020) advanced Fallatah et al. (2019) 's work and took advantage of machine learning, synergistically combined with OBIA to improve informal settlement mapping in Saudi Arabia, achieving enhanced overall accuracy of 91% from GeoEye-1 imagery. An attempt to integrate data from 2 sensors for OBIA was presented by Fallatah et al. (2022), combining GeoEye-1 and Landsat data in the Middle Eastern environment achieving overall random forest (RF) classification accuracy of 95%. These past efforts focused on the ontological framework suggested by Kohli et al. (2012) using a range of informal settlement indicators for segmentation at different scale levels. In that regard, Fallatah et al. (2019) reported the need for expert knowledge in transferring informal settlement indicators into local knowledge. In addition, the popularly used eCognition software, for segmentation, requires high level of image analysis skill in translating such indicators into informal settlement identification (Fallatah et al., 2019). Also, the framework involves different levels of rigorous segmentation as well as numerous processing steps for the classification refinement, at different spatial levels (Mugiraneza et al., 2019). Sometimes, segmentation and classification are performed in two different softwares (Fallatah et al., 2020). Fallatah et al. (2020) described the whole process as time consuming and cumbersome. In fact, numerous processing steps enforce a weighty computational and storage burden on local computation platforms.

Google Earth Engine (GEE), with its engrained segmentation algorithms, has presented potential solutions to long proven challenges of complex segmentation and classification steps encountered when using classical image processing softwares. GEE's open access and accessibility of advanced classification algorithms, coupled with its parallelized framework throughscripting (Phan et al., 2020) presents ease of analysis, classification as well as visualization of outputs (Shafizadeh-Moghadam et al., 2021). Besides being a powerful platform for image collection and organisation (Teluguntla et al., 2018), GEE provides an application program interface for summoning, processing, and stacking image input data, running all analyses in parallel (Kelley et al., 2018). Within GEE, 3 segmentation algorithms can be implemented, which include, K-means, G-means, and Simple Non-Iterative Clustering (SNIC) (Yang et al., 2021). According to Achanta and Susstrunk (2017), SNIC is computationally cheaper and uses lesser memory than the K-means and G-means. The feasibility of SNIC algorithm for object based mapping applications has been investigated (Luo et al., 2021, Qu et al., 2021, Shafizadeh-Moghadam et al., 2021, Vizzari, 2022). SNIC has been successfully employed for LULC mapping using PlanetScope, Sentinel -2, and Sentinel -1 data for central Brazil (Vizzari, 2022), for winter wheat mapping, using Sentinel- 2 in China (Yang et al., 2021) and for crop mapping in China, using Sentinel 1 data (Luo et al., 2021). Significant improvements in mapping accuracy have also been reported when OBIA approach was integrated with Grey Level Co-occurrence Matrix (GLCM) texture features within GEE (Shafizadeh-Moghadam et al., 2021, Tassi et al., 2021, Tassi and Vizzari, 2020, Vizzari, 2022). GLCM algorithm permits the calculation of image textural indices based on second-order statistics for image texture analysis (Mugiraneza et al., 2020). According to Kohli et al. (2013a), a texture analysis approach is critical in discriminating between, sometimes difficult to distinguish, formal and informal areas using the OBIA technique.

The advent of Google Earth Engine has also increased data accessibility through the engrained abundant imagery archives, for example Sentinel-1 and -2 (S1 and S2), Landsat and MODIS (Zhang et al., 2019a). Of late, the accessibilty of high resolution PlanetScope (PL) data within GEE has made OBIA implementable in the mapping of heterogeneous terrestrial environments (Vizzari, 2022). To take advantage of variations in spectral or spatial domains of sensors available within the GEE platform, GEE presents opportunities for data fusion (Li et al., 2022). Whilst optical sensors, for example S2, are sensitive to reflectivities of ground targets (Mahdianpari et al., 2018c), SAR sensors (e.g S1) are reactive to their structural, textural, and dielectric characteristics (Mahdianpari et al., 2017). Amani et al. (2019a) added that SAR data

can provide more differentiable land cover information than multi-spectral data. The synergistic use of different sensors such as S1, S2 and PL EO data has offered opportunities for different mapping applications, especially in highly dynamic fragmented landscapes. For instance, Mahdianpari et al. (2018b) integrated S2 and S1 for wetland mapping. Almost similarly, Tavares et al. (2019) combined S2 and S1 for urban land use/land cover (LULC) mapping in Brazil. Vizzari (2022) and Rao et al. (2021) compared the performances of PlanetScope, Sentinel-2 and Sentinel-1 for LULC and crop mapping, respectively. The authors demonstrated the benefits of integrating data from all three sensors, yielding accuracy levels of 91% and 85%, respectively. Research endeavours that incorporated PL imagery reported improved classification of subtle features (Rao et al., 2021, Tassi and Vizzari, 2020, Vizzari, 2022), presenting opportunities for semantic abstraction of small deprivation pockets, whose identification is inherently difficult (Fallatah et al., 2022). According to Bwangoy et al. (2010), classification of multi-source satellite data yields more accurate classification results than that achieved by a single source data.

Owing to this background, the study sought to integrate data from PL, S2 and S1 and perform GEOBIA, within GEE, to map spatial heterogeneity of morphological informal settlements in a geographically diverse Durban landscape, South Africa. To the extent of the authors' knowledge, there has not been any study that has exploited OBIA on PlanetScope imagery for capturing structural heterogeneity of informal settlements. Most importantly, GEOBIA, comprising integration of object segmentation and object textural analysis, has not been exploited for informal settlement analysis within the GEE environment.

The main objectives of the study are to:

- 1) develop an improved, reliable and reproducible object-based classification workflow, using GEE, for capturing high morphological variability in an informal settlement landscape
- 2) investigate SNIC based OBIA, within GEE, in accurately capturing subtle deprivation pockets in a heterogeneous landscape
- 3) exploit the potential of multiple datasets to synergistically enhance semantic abstraction of morphologically diverse areas of deprivation in fragmented built up area of Durban

5.2. Methodology

The workflow of this approach mainly included image acquisition, pre-processing, and composition, image segmentation and texture feature extraction, random forest classification, and accuracy assessment (Figure 5.1). Firstly, PlanetScope, Sentinel-2 and Sentinel-1 images were collected for the chosen period and study area. Secondly, segmentation of the image into clusters was performed using SNIC algorithm. Thirdly, GLCM algorithm was computed for the calculation of texture metrics. Fourth, object-based classification was performed using Random Forest protocol. The confusion matrix was finally computed for accuracy assessment. The GEE platform was utilized for implementation of all the mentioned procedures.

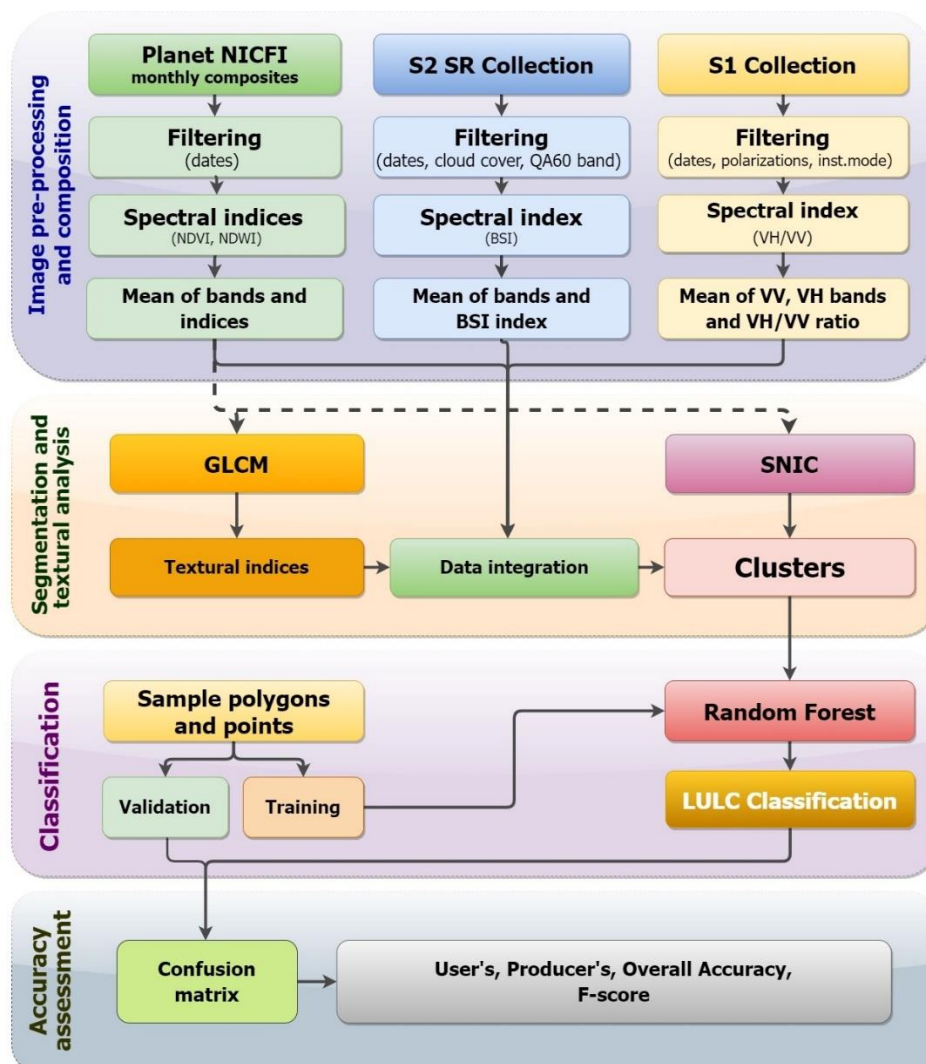


Figure 5.1. Flowchart showing summary of procedures used in this study

5.2.1. Data collection, pre-processing, and image composition

According to Tassi et al. (2021), an important step in LULC classification within GEE is the generation of the base composite dataset. The study utilized data from two optical sensors, PlanetScope and Sentinel-2, and one radar sensor, Sentinel-1, that fell within the study period (1 June 2021 to 31 December 2021). PL imagery are acquired by 120 CubeSat 3U satellites measuring 10 x 10 x 30 cm, referred to as a dove (Marfai et al., 2018). Its sensors can detect four spectral bands (RGB and NIR) with a spatial resolution of between 3–5 m. The high-resolution composite base maps for PL have lately become accessible in GEE for the tropical regions, appreciations to the alliance between Google and the NICFI (Norway's International Climate and Forest Initiative). In the study period, PL images are available in GEE as cloud-free monthly composite. S2 data, already available in GEE as orthorectified and radio-corrected to provide surface reflectance values, was utilized in the analysis (Vizzari, 2022, Carrasco et al., 2019). S2 images were filtered considering the cloud coverage of less than 10%. In this step, the study leveraged band QA60 of S2 that signifies the opaque and cirrus clouds to mask cloud cover for S2.

Normalized difference vegetation index (NDVI), and normalized difference water index (NDWI) were computed from PL data, while bare soil index (BSI) was calculated using S2 data. Being the widely used index in texture-based informal settlement detection (Kuffer et al., 2016b, Mudau and Mhangara, 2021), NDVI quantifies vegetation cover and better discriminates LULC classes. According to Bouzekri et al. (2015), NDWI is the best index for distinguishing road networks, for example tarred roads in formal areas against a mixture of sand, gravel and mud which is characteristic of informal settlements. In addition to capturing brightness of roads, thus, detecting tarred roads with low brightness (Fallatah et al., 2020), NDWI also identifies water bodies (Carrasco et al., 2019). The NDVI layer was calculated from the red (B3) and near-infrared (B4) bands of the PL image, whilst NDWI was computed from the green (B2) and near-infrared (B4) bands of the same satellite. BSI is an index constructed from a combination of the NDVI and the normalized difference built-up index (NDBI) (Diek et al., 2017). The index effectively distinguishes bare land from built up land, land cover classes with relatively similar spectral characteristics (Nguyen et al., 2020).

S1 carries a single C-band synthetic aperture radar instrument that supports operation in single polarization (HH or VV) and dual polarization (HH+HV or VV+VH). Following Tassi et al.

(2021), the study utilized two diverse polarisation modes which include single co-polarisation with vertical transmit/receive (VV) and dual-band co-polarization with vertical transmit and horizontal receive (VH). Following Vizzari (2022), the ratio between two polarization modes was used to create an additional band, VH_VV. The ratio feature partially compensates for the radiometric instability of the sensor and shows higher stability than the single polarization (Vergni et al., 2021). The ratio has been proven promising for identifying non-forested wetlands (Amani et al., 2019a). The mean values were obtained in GEE with a simple “reduce” step for all the PL, S2, and S1 bands and derived indices, thus creating 6-month composite images.

5.2.2. Image segmentation with SNIC

Segmentation involves splitting an image into objects by clustering neighbouring pixels with common values (Hu et al., 2018). The current study implemented image segmentation within the GEE environment, using the SNIC algorithm. SNIC is an enhanced version of Simple Linear Iterative Clustering algorithm (SLIC) (Achanta et al., 2012) which uses super pixel segmentation to simplify image into discrete clusters of image connected pixels (Achanta and Susstrunk, 2017). In the current research, SNIC analysis was executed on the visible and NIR (4) bands of PL datasets, segmenting the image into a set of super pixels. Within the GEE platform, SNIC categorizes the objects (clusters) with regard to the set input parameters, visits pixels only once and clusters pixels without iterations (Achanta and Susstrunk, 2017). The input parameters include: “image”, “size”, “compactness”, “connectivity”, “neighbourhood size” and “seeds” (Luo et al., 2021) (see (Shafizadeh-Moghadam et al., 2021) for definitions). Of these parameters, Shafizadeh-Moghadam et al. (2021) iterated that the main ones are “compactness factor”, the “connectivity”, and a “neighborhoodSize”. Accordingly, after consideration of landscape characteristics in the area of study, these parameters were experimentally set as follows: “compactness” = 1, “connectivity” = 8, “neighbourhood Size” = 128. The selection of parameters and parameter values are based on repeated iterations as well as visual evaluation of the outputs (Tassi et al., 2021, Qu et al., 2021). SNIC is performed using a regular grid of seeds as input generated by the “Image.Segmentation.seedGrid” function (Tassi and Vizzari, 2020) which requires a super pixel seed location spacing (in pixels) for the generation of seed grid. After consideration of the textural characteristics of the landscape patches in the study areas, seed spacing values (5, 10, 15, 20) were also tested iteratively and was then set at 10 for PlanetScope. To create the dataset for classification, the

mean value of bands contained in the multispectral-textural datasets were computed on an object basis using a “reduce connected component” step. In order to allow visualization of the actual size of the objects, a suitable output scale of clusters was fixed using the “reproject” function (scale = 5) (Tassi and Vizzari, 2020). Finally, the algorithm was used to compress the dataset and generate a combined raster made up of clusters and added data layers encompassing the mean values of the input features.

5.2.3. Texture analysis

In order to improve the image classification and avoid fuzziness (Chen et al., 2018, Luo et al., 2021), additional contextual information in the form of textural information was computed in GEE using the GLCM algorithm. The textural information was extracted only from PL imagery. Following prior studies that have incorporated image texture in OBIA for informal settlement detection (Fallatah et al., 2020, Fallatah et al., 2019, Fallatah et al., 2022, Prabhu and Alagu Raja, 2018), contrast, entropy, variance, homogeneity, mean and angular second moment were the texture indices employed in the mapping. The descriptions of the texture metrics are shown in Table 5.1. GLCM application in GEE requires establishment of a grey level 8-bit image as the input image (Tassi and Vizzari, 2020). In the current study, the grey level image was generated from PL data using the following formula:

$$\text{Grey} = (0.3 \times \text{NIR}) + (0.59 \times \text{RED}) + (0.11 \times \text{GREEN}) \quad (\text{Equation 1}).$$

Prior application of GLCM, the gray level image was rescaled in the 0–255 range, using the 2nd and the 98th percentile as lower and upper limits (Vizzari, 2022), in order to improve the results. The window size used in the current study for GLCM was 5 x 5, that was established after various testing operations.

Table 5.1. Texture metrics computed using grey level co-occurrence matrix

Texture features	Textural index description
Angular second moment	Describes how uniform the distribution of grey levels is in the image
Contrast	Measures variations in intensity of neighbouring pixel pairs
Mean	Measures the mean of the grey level sum distribution of the image
Entropy	quantifies the randomness of the grey-level intensity distribution
Variance	Measures how spread out the distribution of grey-levels is in the image
Homogeneity	Measures the homogeneity of the image

5.2.4. Object based Image Classification

Table 5.2 shows the spectral bands, spectral indices and texture metrics used for the object-based RF classification. The table also presents the sensors from which the variables were derived.

Table 5.2. The optical, synthetic aperture radar, spectral and textural features applied to the classifications in this study

Satellite		Features
PL	Main channels	B1 (blue), B3 (red), B4 (NIR)
	Spectral indices	$NDVI = \frac{B4 - B3}{B4 + B3}$, $NDWI = \frac{B2 - B4}{B2 + B4}$
	Textural features	Angular second moment, Contrast, variance, homogeneity, mean, entropy
S2	Main channels	B8, B11, B12
	Spectral index	$BSI = \frac{(B12 + B4) - (B8 + B2)}{(B12 + B4) + (B8 + B2)}$
S1	Main channels	VV, VH
	Ratio features	VH-VV

Following Vizzari (2022), prior proceeding to the final band fusion, a bicubic interpolation was used to resample S2- and S1-derived layers to a resolution of 5 m. A “reduce connected components” step was performed to calculate average values of all available bands based on PL-derived SNIC objects. A RF protocol involving 200 trees was implemented on PL, S2, S1 composite dataset. The RF approach uses bootstrap sampling technology that selects, at random, a specific number of samples from the original set of training samples to create a new training data set (Luo et al., 2021). The choice of the classifier was made owing to its capability to handle urban area classification where dimensional feature spaces are concerned, as well as its robustness for informal settlement detection in complex urban environments (Wurm et al., 2017a). Numerous mapping applications using OBIA within GEE (Qu et al., 2021, Shafizadeh-Moghadam et al., 2021, Tavares et al., 2019) have shown superiority of RF in object based LULC classification. RF method has the strength of easy parameterization, robustness against high-dimensional data and overfitting (Qu et al., 2021), as well as ability to compute the relative importance of all elements in the classification model (Teluguntla et al., 2018). Five land cover types, (i) Informal settlement, (ii) Bare land, (iii) Water, (iv) Other urban, and (v) Vegetation were used as the classification scheme. Table 5.3 shows the definitions of the land cover classes. One thousand seven hundred fifty random sample points were collected and classified using high spatial resolution imagery. These points were used to train the RF classifier (70%) and validate the final LULC classification results (30%).

Table 5.3. The definitions of Land use/ Land cover classes used in the study

Class	Description
Informal settlement	Densely, irregularly built housing units that are contiguous
Bare land	Unused land, including barren land, exposed soil with neither grass, trees nor built up structures
Water	Water bodies like dams, rivers, ponds and swamps
Other Urban	High and low density formal residential buildings, commercial and industrial buildings, transportation networks
Vegetation	Area covered by grasslands, forests, croplands, small shrubs, sparse and dense trees, plantations

5.2.5. Accuracy assessment

To allow assessment of classification performance of the RF classifier, the model was designed to perform a random sampling strategy to create approximately 70% of the training samples from the original polygon dataset, with the remaining 30% of the samples (525 points) being used for cross validation. According to Hu et al. (2018), an assessment of the quality of a classified map is crucial for verification of its aptness for the intended purpose and for the understanding of the corresponding map errors. Quantitative analysis of accuracy of classification involved use of a confusion matrix, and its derived accuracy indices, which are, overall accuracy (OA) (Equation 2), producer accuracy (PA) (Equation 3), user accuracy (UA) (Equation 4), and F- score measure, all computed within GEE. According to Zurqani et al. (2019), the F-score shows how good the classifier is in the context of both PA and UA, by weighting their average. F-score is computed as a harmonic mean of PA and UA (Equation 5).

$$OA = \frac{\text{Number of correct predictions}}{\text{Total number of predictions}} \quad (\text{Equation 2})$$

$$PA = \frac{\text{Number correctly identified in a given map class}}{\text{Number actually in that reference class}} \quad (\text{Equation 3})$$

$$UA = \frac{\text{Number correctly identified in a given map}}{\text{Number claimed to be in that map class}} \quad (\text{Equation 4})$$

$$F\text{- score} = 2 * \frac{(PA * UA)}{(PA + UA)} \quad (\text{Equation 5})$$

Further, the study also assessed spatial agreement of the classified outputs with ground truth samples, with regard to the extent of informal settlements. Seven reference informal settlement samples were identified from the VHR Google Earth Pro image. Malambo and Heatwole

(2020) demonstrated the reliability of VHR image depiction as an independent source for validation data collection. For the area assessment, polygons for these ground truth samples were digitized and their areas measured. Corresponding areas for the classified patches for the same identified samples were also calculated. The statistical evaluation of correct depiction of spatial extents was carried out using regression analysis in R statistical software, using root mean square log error (RMSLE) and mean absolute percent error (MAPE) accuracy metrics.

5.2.6. Feature Importance Assessment

The current research utilized RF algorithm for variable importance evaluation. According to Zhao et al. (2022), the evaluation of variable importance score entails turning into a number, the contribution of a feature parameter in terms of impact on the accuracy. A variable importance graph was drawn in GEE to show the relevance of all the features used in the classification. This graph supported an iterative selection of the most relevant features in the classification.

5.3. Results

5.3.1. Accuracy assessment of the LULC map

The LULC object-based classification map using PL, S2, and S1 combined data is presented in Figure 5.2. The Google Earth Pro imagery and a confusion matrix were jointly used for the visual and statistical analysis of LULC map, respectively. For effective demonstration of classification details, some informal settlement areas were selected from the classified map and compared with their corresponding Google Earth Pro images. Visually, when compared with high-resolution satellite imagery, results of LULC classification indicates that SNIC based object-based classification using integrated data inputs from PL, S2 and S1 accurately captured informal settlements.

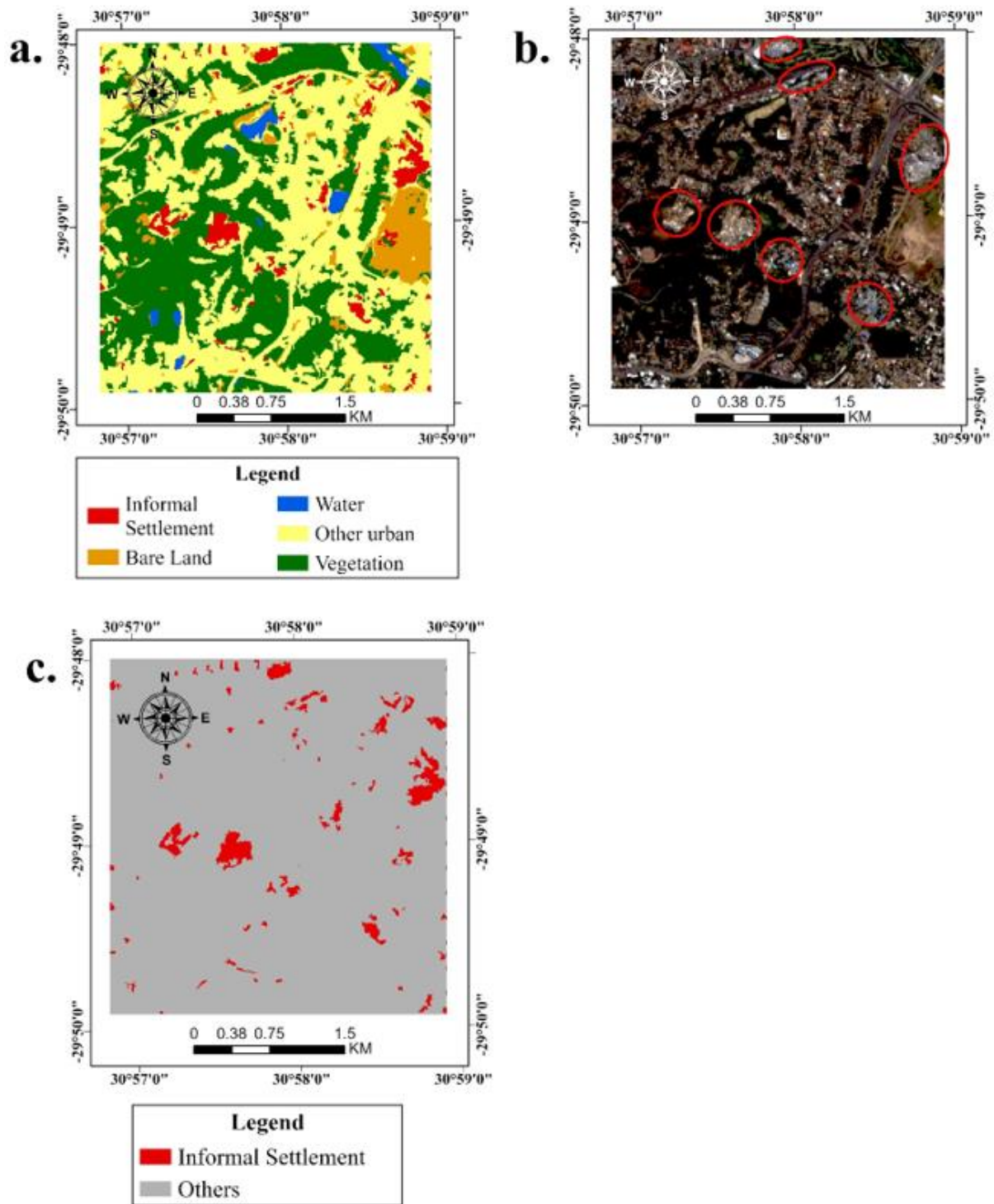


Figure 5.2. Comparison of results of informal settlements and LULC classification (a) and (c), and visual appearance of sample informal settlements on an RGB image (b) (circled in red)

Table 5.4 provides the classification performances obtained from the confusion matrix. The overall accuracy from this experiment is 96%, exceeding 85%, which, according to (Kpienbaareh et al., 2021) is the threshold for a good classification. The class-based performance evaluation revealed that all LULC classes had high F-score values (>85%), indicating that all the classes were overall, clearly identifiable using this approach. Informal settlement class yielded F-score of 87%. However, the informal settlement class registered the lowest F-score considering results for other LULC classes.

Table 5.4. Confusion matrix derived from LULC classification

	Informal settlement	Bare land	Water	Other urban	Vegetation	PA
Informal settlement	44	0	0	10	0	81%
Bare land	1	39	0	1	1	93%
Water	0	0	26	0	0	100%
Other urban	0	0	0	115	0	100%
Vegetation	2	1	0	3	282	98%
UA	94%	98%	100%	89%	100%	96%
F-score	87%	95%	100%	94%	99%	

Figure 5.3 shows informal settlement patches overlaid on digitized polygons for the same settlement. Calculations of relative spatial errors demonstrated RMSLE of 0.69 and MAPE of 0.28. These results reflect existing discrepancy between the areas from classified outputs and that from ground truth samples, visible in Figure 5.3. Assuming object-based classification results to be correct, spatial accuracy assessment results suggest underestimation of spatial extent in the classified maps, revealing disagreement in spatial extents.

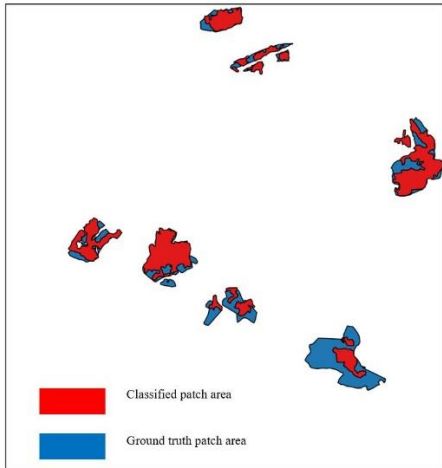


Figure 5.3. Classified informal settlement patch areas against ground truth patch extents

5.3.2. Relative contribution of input variables in RF classification

Figure 5.4 shows the relative importance of the different input features in the classification model, and the sensors from which the features are derived. The results indicate that band 8, blue band, NDWI, BSI, T5 (homogeneity), and T4 (variance) were the six most important input variables in the classification. Homogeneity was the most important texture variable.

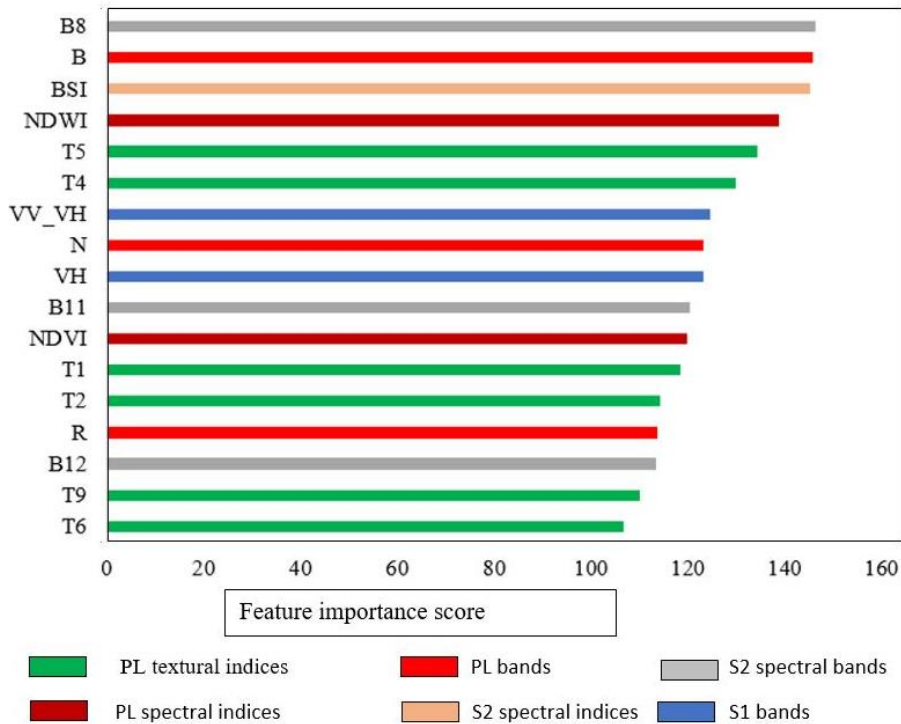


Figure 5.4. Importance assessment of LULC classification features

5.4. Discussion

The current study sought to assess the capability of object-based image classification, performed within GEE' cloud computing environment, for improved mapping of complex informal settlement morphologies. The study capitalized on the embedded SNIC segmentation algorithm, the GLCM algorithm, as well as availability of high-resolution PL imagery within GEE to precisely capture informal settlement diversities in a heterogeneous built-up landscape. Versatility of the coding platform available within GEE (Hamud et al., 2021) and good reliability of GEE integrative packages for feature construction and ease of classification process have been explored to allow reproducibility of reliable maps. This study is the first to introduce OBIA in GEE for informal settlement identification.

Generally, the results of the analysis demonstrated that performing OBIA on a three-sensor dataset, within the GEE was successful in accurately depicting all LULC classes in the study area, yielding overall accuracy of 96%. This accuracy value is way above 85% which, according to Kpienbaareh et al. (2021), is a threshold for good classification. Class specific accuracy results also indicated that all classes were accurately captured with F-score values ranging from 87% to 100%. Such high classification results demonstrate the proficiency of OBIA classification within GEE. Informal settlement identification accuracy of 87% demonstrates how an improved workflow within the GEE can generate high quality informal settlement map in an area with high morphological variability. The results confirm proficiency of experimental design and code writing (Luo et al., 2021) in allowing accurate informal settlement identification. Taking advantage of enfolded SNIC segmentation algorithm, and integrated data from PL, S2, and S1, the results confirm the potency of the approach in capturing variability of spatial characteristics of informal settlements in a heterogeneous urban environment of Durban. Mirroring the findings, both overall and at class level, the RF model was also able to capture the inner structural heterogeneity in the informal settlement landscape. The importance of RF in mapping complex environments using GEE is emphasized (Qu et al., 2021, Shafizadeh-Moghadam et al., 2021, Tavares et al., 2019, Vizzari, 2022). The current findings concur with previous studies that integrated sensors using GEE in mapping complex environments, for example, crop types (Kpienbaareh et al., 2021, Rao et al., 2021), and LULC in the complex agri-natural space (Vizzari, 2022). Their studies suggested the importance of including all the sensors in the classification. Agreeing with Bwangoy et al. (2010)'s assertion that classification of multi-source satellite data yields higher classification performances in comparison with the performance of a single source data, Vizzari (2022) observed that the more

accurate textural analysis on image objects computed from PL data, integrated with the spectral information derived from S2 and S1 boosted the efficacy of the three-sensor dataset combination.

The high accuracy levels shown from integrating various datasets are also in agreement with earlier efforts by Fallatah et al. (2022), who through the integration of GeoEye data with time-series Landsat data confirmed relevance of integrating data from different sensors in informal settlement mapping. Their study was advancing works by Fallatah et al. (2019) and by Fallatah et al. (2022) in their object based mapping of informal settlements in Jeddah, Saudi Arabia. The integrated efforts by Fallatah et al. (2022) yielded overall accuracy levels of 95%, compared to 83% for OBIA alone (Fallatah et al., 2019), and 91% for integrated machine learning and OBIA (Fallatah et al., 2020).

The suitability of texture parameters in clearly distinguishing built up area from other complex classes especially bare land has been emphasized (Duque et al., 2015, Kohli et al., 2016a, Kohli et al., 2013a). Through the use of GLCM algorithm engrained within the GEE, contextual information for LULC mapping was added (Fallatah et al., 2019). However, compared with previous works on OBIA, there are inconsistencies in terms of the most contributing texture metrics in the classifications. For instance, the current study revealed that, homogeneity attained the highest importance score of all the texture features. The result is not in agreement with other studies (Fallatah et al., 2020, Fallatah et al., 2022) who, after investigating contrast, entropy, homogeneity, correlation, and mean, found contrast and entropy to be the most significant texture parameter at settlement level. Also, in an earlier study, Duque et al. (2015) utilized entropy to map informal settlements layout and other land cover classes. In another study, Lai and Yang (2020) found variance to be of high merit in the separation of built up areas. In a more comprehensive manner, Lai and Yang (2020) explained that the relevance of particular textural measures in capturing heterogeneity is reliant upon myriad of influencing factors that range from image spatial resolution, convoluted landscape, complexity of relationships among multifarious land cover categories, as well as the choice of suitable textural features. For instance, in the context of variability in landscape components, Fallatah et al. (2019) revealed that informal settlements in Jeddah differ in typology with informal settlements in other cities in Asia, and others in Africa, in that both formal and informal settlement types are made up of similar building materials, causing textural complexities. On the other hand, in Pune, slums generally have diverse appearances that differ with planned residential complexes (Shekhar, 2012, Kohli et al., 2016a), whilst in Durban, they are usually

made up of corrugated iron, plastics and wood, with some upgraded areas showing similarity with formal areas. Pratomo et al. (2017) also indicated that such variability in morphology renders textural features' contribution context specific and, sometimes, data dependant.

Although high classification accuracies have been attained using OBIA methods within GEE platform, there have been some uncertainties in the identification of informal settlements. From the confusion matrix (Table 5.4), there is evident misclassification between informal settlements and “other urban” class. Whilst OBIA could accurately capture the spatial patterns of urban morphology, varying interurban morphological informal settlement features could explain the confusion (Stark et al., 2020). In confirmation, Fallatah et al. (2019) alluded to the complexity of urban areas because of their characteristic intermix of diverse man-made and natural features, which may engender confusion between the object and its spectral reflectivity. According to Taubenböck et al. (2018), a vital requirement in the delineation of informal settlements is capability to identify small pockets of deprivation for informed decision making. Although all LULC classes could be accurately captured in the current study, the approach failed to capture some discrete informal settlement patches. Figure 5.5 shows an informal settlement that is evident on high resolution RGB imagery (Figure 5.5 (d), red rectangle), but missing on a classified image (Figure 5.5 (c), red rectangle).

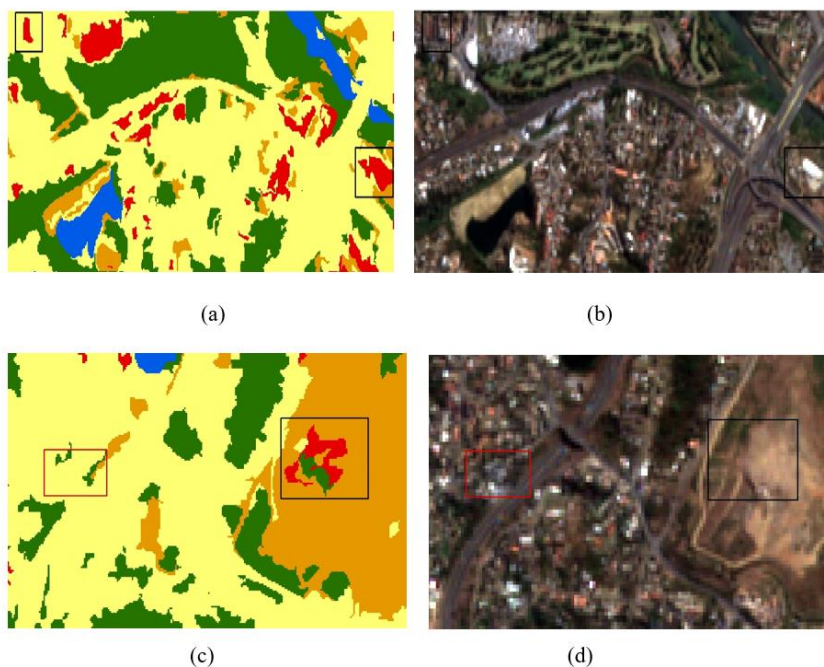


Figure 5.5. (a) shows misclassified informal settlement patches that on the ground (b) are commercial buildings. The black rectangles, (c) and (d), indicate misclassification of bare land (d) as informal settlement (c) (red patch). The red rectangle indicates missed informal settlement (c) that exists on the ground (d)

Such uncertainties can be explained in terms of complexity in defining the term informal settlement (Pratomo et al., 2017). For instance, the same characteristic of density may differ locally depending on developmental stages of informal settlements, presenting inner-structural heterogeneity of these areas of deprivation (Kohli et al., 2012). Imprecisions may also be explained in terms of similarity in some morphological characteristics with formal built up structures (Mugiraneza et al., 2019). There is also evidence of other built-up areas, for example, commercial buildings being misrepresented as informal settlements (Figure 5.5a, black rectangle). The misclassification can be explained in terms of similarity of roofing materials, causing textural complexity. Evidently, confusion was also displayed between bare land and informal settlements. An informal settlement patch exists (Figure 5.5c, black rectangle) on an area that is predominantly bare (Figure 5.5d, black rectangle), which is evidence of potential similarity in spectrum (Kohli et al., 2016a). According to Gevaert et al. (2016) rusted iron sheets, that is common roofing material in informal settlements, tend to be reflect similarly to bare soils which are usually reddish in colour.

Conceptual imprecision in OBIA within the GEE platform may also be compounded by complexity in application of segmentation algorithms in particular areas (Qu et al., 2021). Myint et al. (2011) observed that, because of landscape heterogeneity, unvarying segmentation parameters may not yield the best results for all LULC types. Qu et al. (2021) added that segmentation results may be compromised due to similarity in spectral characteristics among different land cover classes, as well as complexity in delineating the boundaries between the objects, especially, between formal and informal areas. Some researchers (Amani et al., 2019a, Hay Chung et al., 2021) also noted that misclassifications could result from the quality of training samples that largely affects performance of classifiers, resulting in failure to capture the dynamics. In that regard, Pratomo et al. (2017) propounded that it is critical to explicitly clarify these uncertainties' influence on classification results when aiming at remote sensing based informal settlement mapping.

However, notwithstanding the limitations, the present study exhibited the value of classifying informal settlements utilizing OBIA and multi-source data within GEE.

5.5. Conclusion

This study presented an object-based approach for informal settlement identification within the GEE, using integrated datasets from PL, S2 and S1. GEE cloud computing was successfully applied for informal settlement mapping in Durban, South Africa. The GEE provided a powerful analysis platform for classification, allowing image segmentation and texture feature extraction using inbuilt SNIC and GLCM algorithms, respectively.

The main conclusions were:

- The produced informal settlement map yielded high overall accuracy and informal settlement identification accuracy of 98% and 94%, respectively.
- Spatial accuracy assessment yielded RMSLE of 0.69 and MAPE of 0.28
- The derived error metrics presented reasonable agreement between the classified output with the ground truth statistics from Google earth Pro.

The results indicated that the proposed object-based approach satisfactorily captured the morphological variations within the informal settlement of Durban and could form the basis for derivation of subsequent on demand products.

5.6. Summary

GEOBIA was successfully implemented within GEE yielding high overall and class specific accuracy levels. It is important to note that informal settlement mapping has implications for policy. The LULC map provides valuable information about the location and extent of informal settlements which can also contribute to understanding of the amount of loss and gain in informal settlement areas over time. The next chapter presents an approach that analyzes inter categorical transitions that are as a result of informal settlement expansion. Intensity analysis will be implemented to provide a systematic analysis of growth patterns of informal settlements linking pattern to process. The understanding of informal settlement dynamics would assist in planning and fundamental decision making for expediting informed management of cities.

CHAPTER SIX:

Characterizing informal settlement dynamics using GEE and intensity analysis in Durban Metropolitan area, South Africa: Linking pattern to process

This chapter is based on:

Matarira, D., Mutanga, O., Naidu, M., Mushore, T. D., & Vizzari, M. (2023). Characterizing Informal Settlement Dynamics Using Google Earth Engine and Intensity Analysis in Durban Metropolitan Area, South Africa: Linking Pattern to Process. *Sustainability*, 15(3). doi:10.3390/su15032724

Abstract:

The growing population in informal settlements expedites alterations in land use and land cover over time. Understanding the patterns, processes of landscape transitions associated with informal settlement dynamics in rapidly urbanizing cities is critical for better understanding of consequences, especially in environmentally vulnerable areas. The study sought to map and systematically analyze informal settlement growth patterns, dynamics and processes and associated land use and land cover transitions in Durban Metropolitan area, from 2015 to 2021. The study applied an object-based image classification on PlanetScope imagery within the Google Earth Engine platform. Further, intensity analysis approach was utilized to quantitatively investigate inter category transitions, at category, and transition levels. Thus far, no study of land conversion to and from informal settlement areas in South Africa has been exploited using both Google Earth Engine and intensity analysis approaches. The results suggest spatial growth of informal settlements with a total net gain of 3%. Intensity analysis results at category level revealed that informal settlements were actively losing and gaining land area within the period, with yearly gain and loss intensity of 72% and 54%, respectively, compared to the uniform intensity of 26%. Whilst the growth of informal settlements avoided water bodies over the studied period, there was an observed systematic process of transition between informal settlements and other urban land. Government policy initiatives in upgrading informal housing could be attributed to the transitions between informal settlement and other urban. This study illustrates the efficacy of intensity analysis in enhancing comprehension of the patterns and processes in land changes, which aids decision-making for suitable urban land upgrading plans in the Durban Metropolitan area.

Keywords: Intensity analysis; informal settlements; land-use transition; systematic transition

6.1. Introduction

Globalization, typifying advancements in the economic and social dimensions (Rodriguez Lopez et al., 2017) has stirred urban population dynamics, with subsequent emergence of social inequalities in most cities of the global south (Balsa-Barreiro et al., 2019). Informal settlements are growing at unprecedented rates in response to disjointed urbanization (Jones, 2017), instigating major land use/land cover (LULC) changes, with implications on functioning of urban landscape components and disaster risk (Samper et al., 2020, Tellman et al., 2022). Systematic empirical analysis of their growth patterns and comprehension of associated LULC transitions are critical in addressing questions that deal with how much, what kind of land is consumed and the process at play (Solecki et al., 2013). Subsequent findings would be key in the modelling of future rates of change, with potential to reveal insights on better matched solutions, whether in the form of informal settlement management policies or adaptive strategies (Mwangi et al., 2017, Samper et al., 2020).

With its characteristic repeat coverage, remote sensing is an important data source for producing consistent and easily updateable land use maps that allow detection of relationships between different classes of LULC changes (Msofe et al., 2019). In recent times, increasing availability of high-resolution time series data within the Google Earth Engine (GEE) data archives have brought forth robustness in mapping urban area LULC changes. Since the advent of GEE, scores of studies have harnessed GEE's powerful image processing capabilities in accessing multi temporal data (Li et al., 2020), as well as its estimation tools for change detection analyses in broader urban areas (Hamud et al., 2021, Mugiraneza et al., 2020, Rudiastuti et al., 2021). For instance, Celik (2018) investigated the possibilities of identifying changed areas in Ankara, Turkey, using Sentinel-1 and Sentinel-2 within GEE. In one study, Mugiraneza et al. (2020) used Landsat data for continuous monitoring of urban land cover change trajectories in Kigali Rwanda. In another study, Zurqani et al. (2019) mapped urban growth trends in a forested landscape in South-eastern United States. These analyses were able to identify the patterns, magnitude, as well as rates of LULC changes (Mwangi et al., 2017). Even though, several studies (Fuchs et al., 2015, Manandhar et al., 2010, Xie et al., 2020) have discounted net change analyses due to failure to account for all area gains and losses, and incapacity to offer in-depth signals concerning land changes, as well as insight into the underlying processes (Huang et al., 2018, Xie et al., 2020, Yuan et al., 2015). In as much as zero net change may ordinarily mean absence of change, there could be a probability of location

changes or swapping among categories (Mwangi et al., 2017). A comprehensive understanding of observed change patterns and their link with processes responsible for the changes is insightful as it allows integration of remote sensing and social science in developing sustainable urban management policies (Badmos et al., 2018).

Intensity analysis framework analyzes land cover changes by considering categorical transitions with regard to gains, losses, net change and swapping (Aldwaik and Pontius Jr, 2013). Apart from being designed to gain in-depth understanding of factors and processes driving LULC changes, the mathematical approach allows visualization of both the size and intensity of land transitions, and evaluates the consistency and irregularity of the LULC patterns (Akinyemi et al., 2016, Zhou et al., 2014). Intensity analysis is designed to explore changes among land categories at three levels: interval, category and transition, quantifying the deviation between observed change intensity and hypothesized uniform change intensity (Yang et al., 2017). In addition to consideration of the sizes of categories in the calculation of change intensities (Hasani et al., 2017, Quan et al., 2019), the approach allows detection of systematic and random processes of landscape transitions (Mwangi et al., 2017, Teixeira et al., 2014). Identifying the processes at play would aid in relating the observed change patterns to possible causes and potential pressures on environmental sustainability (Pontius et al., 2004, Teixeira et al., 2014).

A plethora of studies have successfully employed intensity analysis in various applications (Huang et al., 2012, Mushore et al., 2022, Nyamekye et al., 2020, Quan et al., 2019, Tong et al., 2020, Yang et al., 2017). In an earlier study, Gandharum et al. (2022) used Landsat data to produce LULC maps within GEE and incorporated intensity analysis, simultaneously, to explore the influence of urban growth on agricultural land in the north coastal region of West Java Province. In another study, Tong et al. (2020) employed intensity analysis and barycenter migration models to investigate land use dynamics from 1990 to 2015 in four municipalities of China (Beijing, Tianjin, Shanghai, and Chongqing). Results of intensity analysis revealed that transitions were mainly between arable land and construction land. Also, Nyamekye et al. (2020) utilized a combined approach of machine learning and intensity analysis to investigate the changes among the major LULC categories in New Juaben Municipality, Ghana. Their results indicated that transitions between built-up and agricultural land were the most prominent. Mushore et al. (2022) used local climate zones (LCZs) and intensity analysis to assess the influence of long-term urban growth on surface urban heat islands. Results of

transition level intensity demonstrated that growth of built LCZs was rampant in areas designated as water, low plants and dense forest LCZ in the two analysed intervals (2005-2020). Results of transition-level analysis proved that the expansion of built-up areas strongly targeted agricultural land. Notably, majority of the afore mentioned studies focused on the broader LULC changes involving built up areas, a broad class including all impervious surfaces in a locality. In one of the first attempts, Badmos et al. (2018) applied intensity analysis for the quantification of yearly change intensities at categorical and transitional levels, relating patterns and processes of informal settlement expansion in Lagos city. Their results revealed that, at category level slums gained and lost in land area, simultaneously. One of the explanations for the gain was encroachment onto bodies of water and vacant space. Most importantly, the loss was explained in terms of gentrification and demolition processes.

Durban is a city with rapidly expanding informal settlement landscape. The city's spatial structure is neither shaped by planned growth nor is it a vision of urban form, but a result of legacy of past Apartheid based planning (Loggia and Govender, 2019). The legacy has caused inequalities in access to decent housing causing spread of lower income settlements, that are usually located on precarious land (Jagarnath et al., 2019). Reflecting on the morphology of informal settlements in Durban, the informal settlements locate close to road networks, on vacant land, steep slopes, sometimes characterized by fragile soils, and follow natural features such as rivers or ravines (Marx and Charlton, 2003a). Such locations make the residents vulnerable to landslides and flood hazards, during extreme climatic conditions. Since the inception of the South African Constitution (1996), the South African government has developed proactive urban policies aimed at transforming spatial visions for the country's cities, restructuring its urban spaces as well as emphasizing sustainable urban development and land use management (Berrisford, 2011, Ogunrobi, 2014). To underscore the national urban agenda, policy frameworks that have been developed include the National Spatial development Framework (NSDF), Spatial Planning and Land Use Management Act, as well as Integrated Urban Development Framework, 2016 (IUDF) (Ogunrobi, 2014). The policies' priorities are to ensure effective and improved management of urban spaces and achieve cities and human settlements that are inclusive, safe, resilient and sustainable, as informed by Sustainable development Goal 11 (Van der Berg, 2017).

Of late, Durban has been experiencing worst climate scenarios in terms of flood hazard, with informal settlement dwellers being the worst affected. For instance, Quarry Road settlement had on several occasions been badly affected by the impacts of floods, with the huge impacts being attributed to their location on a road reserve and flood plain (Membele et al., 2022b, Williams et al., 2018, Williams et al., 2019). Despite the flood impacts, Quarry Road West has also undergone several periods of rapid expansion with most of these occurring just after significant flood (Williams et al., 2018). Such developments create evidence that, whilst, the mapping of perimeter extensions serves as a tool to confirm the challenges and resilience of informal settlements (Samper et al., 2020), in depth analysis is required to link the pattern and the process, and subsequently establish the possible driving forces. In support, Manzoor et al. (2022) iterated that intensity analysis can support evidence for a hypothesized change process and, sometimes, potential for development of new hypotheses. According to Solecki et al. (2013), lack of intrinsic analysis of the fundamentals involved in land use change makes interpretations fragmented, lacking scientific consensus on which to build evidence based policies. Therefore, there is need for in-depth analysis such as authored by intensity analysis in order to improve interpretation of land use changes especially in complex settings of informal settlements.

Owing to this background, the current study sought to exploit intensity analysis approach to quantitatively measure the spatiotemporal changes of LULC and understand the dynamics of informal settlements in Durban over a period of six years. Currently, there are limited land change studies in South Africa (Jagarnath et al., 2019). Moreso, most previous land cover change studies in Durban focused on general land changes with focus on the transitions between vegetation and broader built up land but little focus on informal settlements (Jagarnath et al., 2019, Mazeka et al., 2021, Otunga et al., 2014). The aforementioned studies largely used the “from-to” change detection approach which is not as revealing of the change process as with intensity analysis. Besides the usual “from-to” analysis, intensity analysis also calculates important information such as which transitions are targeted or avoided by specific classes during a period. Intensity analysis will not only show changes in coverage of informal settlements but also has potential to depict and quantify the land use and land cover types that were affected by their dynamics. Interestingly though, Jewitt et al. (2015) earlier attempted to apply intensity analysis to systematically analyze land cover changes in Kwa-Zulu Natal Province, South Africa but with focus on impacts of the changes on biodiversity loss.

The current study expands on work done by Gandharum et al. (2022) in the combined use of GEE and intensity analysis. Whilst Gandharum et al. (2022) successfully combined the two approaches, their focus was on agricultural land, and without emphasis on other important applications of intensity approach that links patterns to causes of change. In the study in Lagos, Badmos et al. (2018) characterized informal settlement growth over one time period using RapidEye data, but without exploiting GEE provisions. The SNIC algorithm embedded within the GEE afford solutions to complexities associated with tuning parameters for segmentation, which is cumbersome when classical image processing software, for example ENVI and ERDAS software, are involved. Object based classification would allow comprehensive empirical analysis of informal settlement dynamics using intensity analysis. Given the irregular nature and perceived expansion of informal settlements globally, it is crucial to understand area specific patterns in order to inform policies and strategies to ensure sustainable growth of cities.

Badmos et al. (2018) conducted an in-depth analysis of informal settlement patterns in Lagos where spatial structures, temporal trends and government policies differ to those in South Africa. The current study provides an analysis specific to Durban, which is important for regional and international comparison, as well as for guidance of formulation of government and local policies and strategies towards sustainable and smart cities in South Africa.

The specific objectives of the study are thus:

- 1) To determine and examine spatiotemporal changes in LULC from 2015 to 2021 in Durban informal settlement landscape.
- 2) Measure the intensity of land cover alterations involved during informal settlement expansion process.
- 3) To link the informal settlement growth patterns with processes in land transitions, together with related national policy factors.

6.2. Materials and methods

6.2.1 Study area

The area of study encompasses part of Durban metropolitan region, which includes the central city area of Durban. It is located in the province of KwaZulu-Natal, South Africa (Figure 1a) and stretches from 30°55'00" E to 31°00'30" E and from 29°50'30" N to 29°47'30" N, occupying an area of 7410 ha. Durban is characterized by an estimated population of 3.6 million (Williams et al., 2018). The topography of the area is steep and highly undulating,

ranging from about 30 m to 120 m above sea level. The humid subtropical climate, with mean annual precipitation exceeding 1000 mm per annum describes the climate of Durban (Williams et al., 2018). In addition, warm, wet summers and mild, dry winters form part of the climate of the city. The morphological informal settlements in Durban follow a steep topography and often lead down to Umgeni River, making the residents vulnerable to flood hazards during extreme climatic conditions. Their location on vacant land, low land areas, steep slopes, sometimes characterized by fragile soils (Marx and Charlton, 2003a) often contribute to their exposure to landslides and flood hazards. For instance, the Havelock informal settlement is located on privately owned land and a portion within the Durban Metro Open Space System (Parikh et al., 2020), whilst the Quarry Road settlement is partly in close proximity to road network and in a flood plain. Durban’s landscape is described as complex, in terms of both physical and biological diversity perpetuated by varied use and ownership of the landscape (Jewitt et al., 2015).

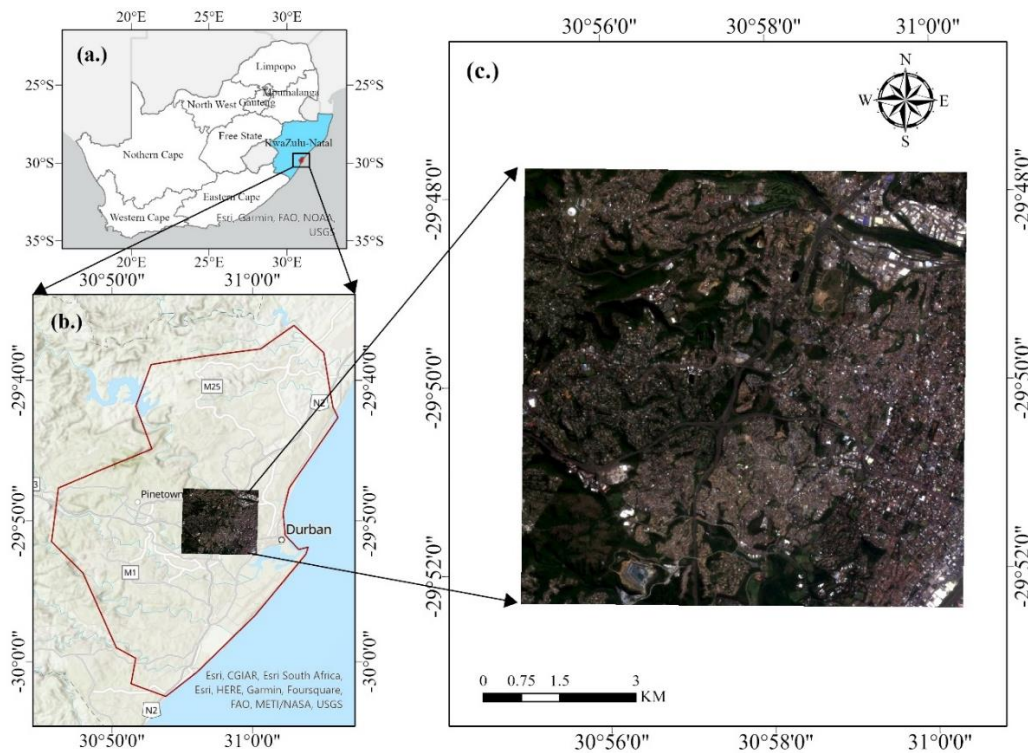


Figure 6.1. Study area selected in KwaZulu-Natal province (a), within Durban Metropolis (b), South Africa. (c) is the overview of the area obtained with an RGB PlanetScope imagery, in UTM/WGS84 plane coordinate

The workflow of this approach mainly included (1) image collection, pre-processing, and composition (2) image segmentation and texture feature extraction, (3) object-based image

classification and accuracy assessment, (4) LULC change and intensity analysis (Figure 6.2). The first step involved the collection of PlanetScope and Sentinel-1 images for the chosen period and study area. Secondly, segmentation of the image into clusters was performed using SNIC algorithm and GLCM algorithm was computed for the calculation of texture metrics using PlanetScope data. Thirdly, object-based classification was performed using Random Forest protocol with subsequent accuracy assessment done using confusion matrix. Fourth, cross tabulation matrix was produced in ARGIS Pro. Finally, intensity analysis was performed using Pontius excel file.

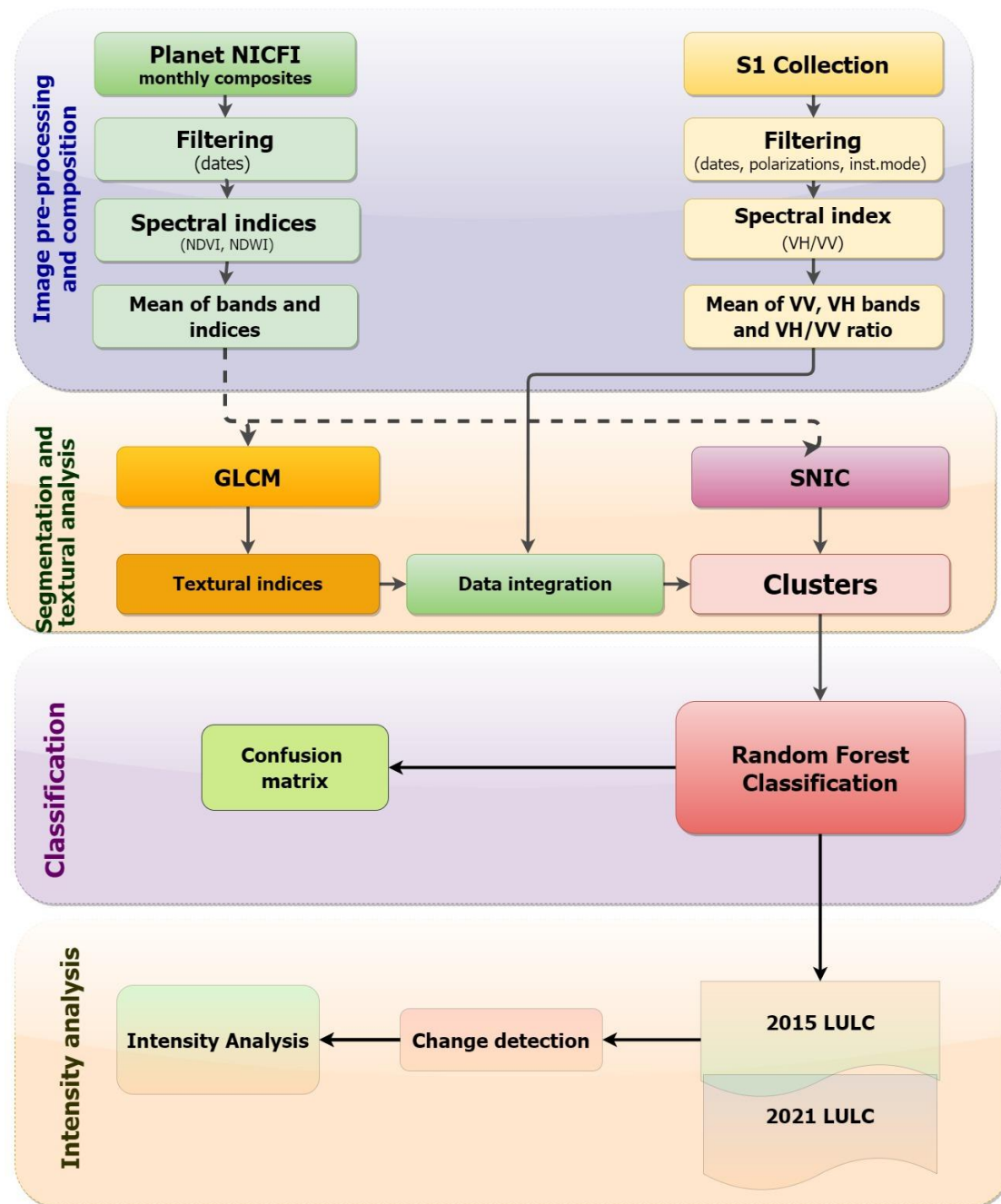


Figure 6.2. Work flow of the study

6.2.2. Data collection and pre processing

The study utilized data from optical and SAR (Synthetic Aperture Radar), PL and S1 that fell within the study period (1 June 2021 to 31 December 2021). PL imagery are acquired by 120 CubeSat 3U satellites measuring 10 x 10 x 30 cm, referred to as a dove (Marfai et al., 2018). Its sensors can detect four spectral bands (RGB and NIR) with a spatial resolution of between 3–5 m. PL high-resolution composite base maps have recently become accessible in GEE for the tropical regions, thanks to the partnership between Google and the NICFI (Norway's International Climate and Forest Initiative). In the study period, PL images are available in GEE as cloud-free monthly composite. Normalized difference vegetation index (NDVI), and normalized difference water index (NDWI) were calculated from PL data. NDVI and NDWI have been extensively used to improve the accuracy of classification in complex environments (Amani et al., 2019b, Mahdianpari et al., 2018a). The NDVI layer was calculated from the red (B3) and near-infrared (B4) bands of the PL image, whilst NDWI was calculated from the green (B2) and near-infrared (B4) bands of the same satellite. S1 carries a single C-band synthetic aperture radar instrument that supports operation in single polarization (HH or VV) and dual polarization (HH+HV or VV+VH). The study utilized two diverse polarization modes which include single co-polarization with vertical transmit/receive (VV) and dual-band co-polarization with vertical transmit and horizontal receive (VH). Following Vizzari (2022), the ratio between two polarization modes was used to create an additional band, VH_VV. The ratio feature partially compensates for the radiometric instability of the sensor and shows higher stability than the single polarization (Vergni et al., 2021). The mean values were obtained in GEE with a simple “reduce” step for all the PL, and S1 bands and derived indices, thus creating 6-month composite images.

6.2.3. Object based image classification

Object-based image analysis (OBIA) was utilized in the preparation of LULC maps for the 2015 and 2021 time points, within the GEE. OBIA involves segmentation of images, that is splitting an image into homogeneous clusters of pixels called segments (Ye et al., 2018). According to Mui et al. (2015) the packaging of pixels into discrete objects minimizes the variance experienced by high spatial resolution images, allowing the objects, rather than individual pixels to be classified. In the current study, image segmentation was performed using SNIC algorithm within the GEE environment. SNIC categorizes the objects (clusters) according to the set input parameters, visits pixels only once and clusters pixels without

iterations (Achanta and Susstrunk, 2017). SNIC analysis was executed on the visible and NIR (4) bands of PL datasets, segmenting the image into a set of super pixels. Contextual information in the form of textural information was also extracted from the segments using GLCM algorithm within the GEE (Vizzari, 2022). Following prior studies that have incorporated image texture in OBIA for informal settlement detection (Fallatah et al., 2020, Fallatah et al., 2019, Fallatah et al., 2022, Prabhu and Alagu Raja, 2018), contrast, entropy, variance, homogeneity, mean and angular second moment were the texture indices employed in the mapping. Object based classification was carried out on the composite image made out of mean bands of PL and S1. The LULC classification scheme included informal settlement, bare land, other urban, water, and vegetation (see Table 5.3 for LULC class descriptions). One thousand seven hundred fifty random sample points were collected and classified using high spatial resolution imagery. These points were used to train the RF classifier (70%) and for validation of the final LULC classification results (30%).

6.2.4. Land-Cover Transition Matrix

A post-classification technique was utilized for detection of transitions in the land use maps over the study period. The post classification was explored because of its provision of change matrix for different categories (Hasani et al., 2017). The superimposition of the LULC maps generated a transition matrix for 2015 and 2021. The matrix shows areas that transition from the initial category to the subsequent category (Huang et al., 2012). The study exploited the thematic change workflow in the ArcGIS Pro software package for the detection of the spatial changes in absolute terms, as well as through consideration of inter category transitions to and from informal settlements. The transition matrix/cross-tabulation matrix became the input for intensity analysis for the time period. The intensity analysis approach was carried out on category, and transition levels.

6.2.5. Intensity Analysis

Intensity analysis is a mathematical approach that examines LULC dynamics through calculation of categorical changes in relation to the sizes of the categories and the intensities of change (Nyamekye et al., 2020, Pontius et al., 2013). The approach depends on accessibility of maps for disparate time points, for the same area and consisting of the similar land cover categories. Because of limited availability of temporal data at high resolution, the current study's focus was on one-time period (2015–2021). In this study, intensity analysis was carried out

using a PontiusMatrix41.xlsx available for free from www.clarku.edu/~rpontius and developed by Aldwaik and Pontius Jr (2013).

6.2.5.1 Category level analysis

The category level of analysis focuses on intensity of gain or loss of each land use type in the time interval (Pontius et al., 2013). Category analysis entailed examination of the degree and magnitude of gross gains and gross losses in five LULC classes and among different categories during time interval t (where t represents the time interval period 2015 to 2021), producing change trends for each individual LULC category. According to Quan et al. (2019), there is a common hypothesis with regard to the category level that suggests that for each interval, all categories undergo gross loss and gross gain with the same yearly intensity. The intensity of a uniform change during interval t is S_t . Equation (1) calculates the uniform intensity by dividing size of the transition by length of the time interval resulting in a percentage of spatial extent. Using Equation (2) a category's annual gross gain intensity (G_{tj}) in an interval is determined by the size of the category's annual gross gain divided by the size of the category at the final stage of each time interval (Quan et al., 2019). On the other hand, a category's yearly gross loss intensity (L_{ti}) in an interval is attained using Equation (3) by dividing the size of the category's yearly gross loss by the size of the category at the starting point of each interval.

The annual percentage of the study area that changed during the time interval, S_t , is calculated by

$$S_t = \frac{\text{Change during } [Y_t, Y_{t+1}]}{(\text{Duration of } [Y_t, Y_{t+1}])(\text{Extent Size})} \times 100\% = \frac{\sum_{j=1}^J (\sum_{i=1}^J C_{tij}) - C_{tij}}{(Y_{t+1} - Y_t) (\sum_{j=1}^J \sum_{i=1}^J C_{tij})} \times 100\% \quad (1)$$

The gross gain intensities, G_{tj} , were calculated by:

$$G_{tj} = \frac{\text{Annual gain of } j \text{ during } [Y_t, Y_{t+1}]}{\text{Size of } j \text{ at } Y_{t+1}} \times 100\% = \frac{[(\sum_{i=1}^J C_{tij}) - C_{tij}]/(Y_{t+1} - Y_t)}{\sum_{i=1}^J C_{tij}} \times 100\% \quad (2)$$

The gross loss intensities, L_{ti} , were calculated by:

$$L_{ti} = \frac{\text{Annual loss of } i \text{ during } [Y_t, Y_{t+1}]}{\text{Size of } i \text{ at } Y_t} \times 100\% = \frac{[(\sum_{i=1}^J C_{tij}) - C_{tij}]/(Y_{t+1} - Y_t)}{\sum_{i=1}^J C_{tij}} \times 100\% \quad (3)$$

Category level also provides information on all the dormant and active categories during that time period (Badmos et al., 2018). If $L_{ti} < S_t$, or $G_{tj} < S_t$ then we say the respective loss from category i or gain to category j during interval t is dormant. On the other hand, if $L_{ti} > S_t$, or $G_{tj} > S_t$, then the respective loss from category i or gain to category j is considered active within the time interval t .

Table 6.1. Mathematical notations used in the study

Symbol	Description
T	number of time points
Y_t	year at time point t
t	index for the initial time point of an interval [$Y_t - Y_{t+1}$], where t ranges from 1 to $T - 1$
J	number of categories
i	index for a category at the initial time point of an interval
j	index for a category at the latter time point of an interval
n	index of the gaining category for the selected transition
C_{tij}	size of transition from category i to category j during interval [$Y_t - Y_{t+1}$]
S_t	annual change during interval [$Y_t - Y_{t+1}$]
G_{tj}	intensity of annual gain of category j during interval [$Y_t - Y_{t+1}$] relative to size of category j at time $t + 1$
L_{ti}	intensity of annual loss of category i during interval [$Y_t - Y_{t+1}$] relative to size of category i at time t
R_{tin}	intensity of annual transition from category i to category n during interval [$Y_t - Y_{t+1}$] relative to size of category i at time t
W_{tn}	uniform intensity of annual transition from all non- n categories to category n during interval [$Y_t - Y_{t+1}$] relative to size of all non- n categories at time t

Adopted from (Kourosh Niya et al., 2019)

6.2.5.2 Transition level analysis

Intensity analysis at transition level evaluates which land-cover categories transition to which other land-cover categories in a process expressed as either “targeting” or “avoidance” (Manzoor et al., 2022). At this level, the size and intensity of transitions as a category gains

from other categories are calculated (Gandharum et al., 2022). In this study, the transition level focuses on informal settlement areas. Equation 4 and Equation 5 represent the transition level equations. Equation (4) calculates observed intensity R_{tin} of annual transition from category i to category n for a given time period relative to the size of category i at the start of the interval (Mwangi et al., 2017). It is the transition intensity from category i to category n where $i \neq n$. The observed intensity R_{tin} is compared with uniform intensity W_{tn} calculated using Equation (5) which assumes that category n gains uniformly across the landscape. If $R_{tin} > W_{tn}$, the gain of category n is considered to target category i at time t . In the event that $R_{tin} < W_{tn}$, the gain of category n is seen as avoiding the category i at time t .

$$R_{tin} = \frac{\text{size of annual transition from } i \text{ to } n \text{ during } [Y_t, Y_{t+1}]}{\text{size of } i \text{ at } t} = \frac{C_{tin}/(Y_{t+1}-Y_t)}{\sum_{j=1}^J C_{tij}} \times 100\% \quad (4)$$

The uniform intensity for category n , W_{tn} , which distributes the intensity of annual transition gains to category n uniformly across the study area, is calculated by:

$$W_{tn} = \frac{\text{size of annual gain of } n \text{ during } [Y_t, Y_{t+1}]}{\text{size of not } n \text{ at } t} = \frac{[(\sum_{i=1}^J C_{tin}) - C_{tnn}]/(Y_{t+1}-Y_t)}{\sum_{j=1}^J [(\sum_{i=1}^J C_{tij}) - C_{tnj}]} \times 100\% \quad (5)$$

The transition level intensity allows the identification of which land use categories are targeted or avoided during the process of informal settlement expansion.

6.3. Results

6.3.1. Observed Patterns of LULC Change Dynamics

Figure 6.3 shows the LULC maps produced for the years 2015 and 2021 as well as the proportions of all the categories at the time points. The accuracies of LULC classification for 2015 and 2021 are illustrated in Table 6.2. The accuracy assessment matrices used were overall accuracy (OA), user accuracy (UA), producer accuracy (PA), and F1-score. The year 2015 yielded overall accuracy and F-score for informal settlement class of 96% and 67%, respectively. On the other hand, year 2021 yielded higher overall accuracy of 97% and F-score value of 92% for informal settlement class. Figure 6.3 presents maps showing amount of

modifications of different categories during the time interval. The maps for the two time points appear similar indicating small areal changes between consecutive time points. At the initial time the results reveal that urban is the dominant land, covering 47% of the study area. The second largest category was vegetation. Between the two time points, results indicate increase in area for informal settlements, other urban and bare land areas, while it decreased for vegetated areas and water. As shown in Figure 6.3, informal settlement had a net increase of 3%, an increase from 5% to 8% of the total study area. Other urban class increased by 8% (47% to 55%). Vegetated land experienced the major decline, considering all the other land cover classes, with a net decrease of 10% (41% to 31%).

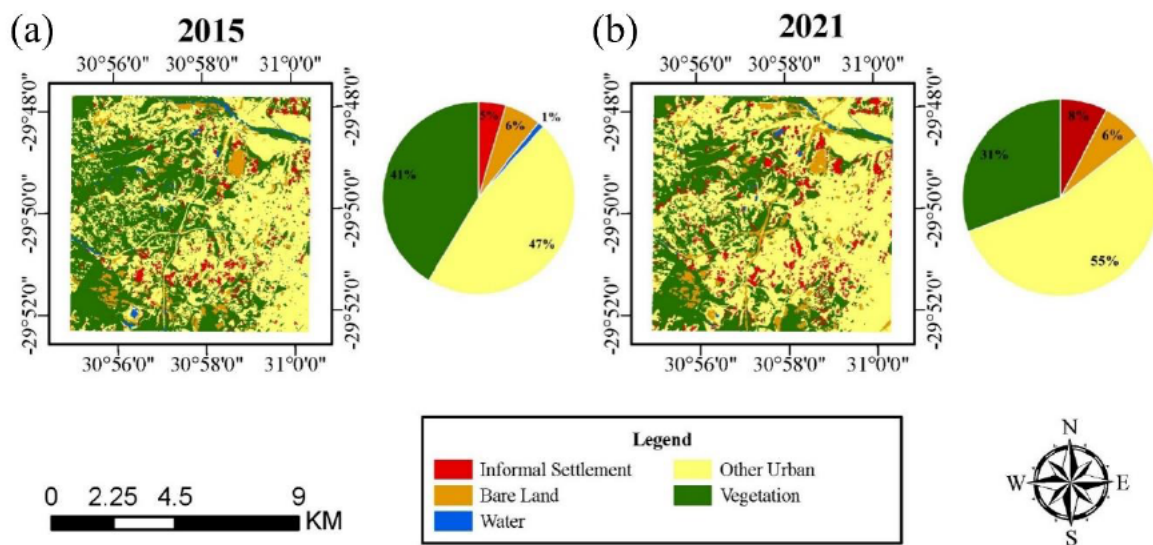


Figure 6.3. (a) LULC map for 2015; and (b) LULC map for 2021.

Table 6.2. Summary of LULC map accuracies (%) for 2015 and 2021

Land use	2015			2021		
	User's accuracy (%)	Producer's accuracy (%)	F-score	User's accuracy (%)	Producer's accuracy (%)	F-score
Informal settlement	75	60	67	96	88	92
Bare land	100	92	96	100	81	90
Water	100	100	100	100	100	100
Other urban	95	98	96	95	99	97
Vegetation	99	100	100	100	100	100
Overall accuracy (%)	96			97		

Figure 6.4 clearly shows the areal changes over the time period.

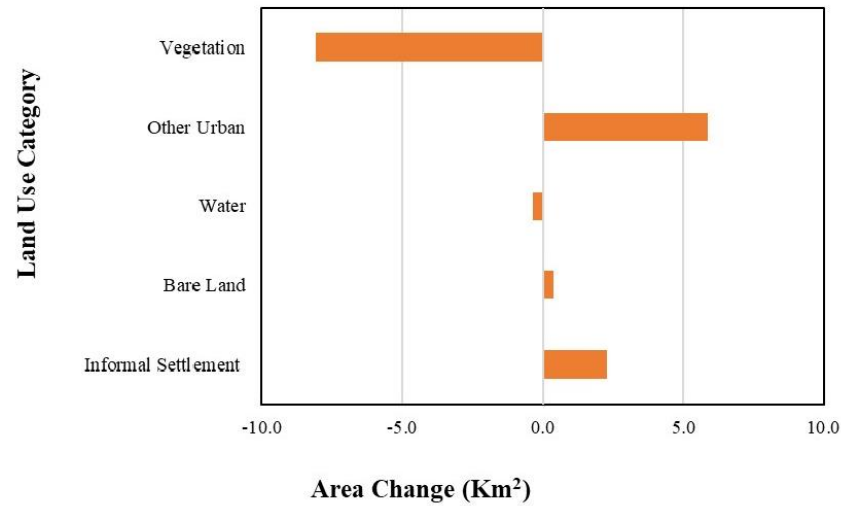


Figure 6.4. Areal changes of land use categories in the study area from 2015 to 2021

Figure 6.5 represents the maps of category losses and gains distinguished from persistence (no change) during the interval. Grey indicates areas of no change and any other colour represents either corresponding loss or gain of the category. The results indicate that vegetation is the category with the largest losses (Figure 6.5a), whilst the largest gaining category is other urban (Figure 6.5b).

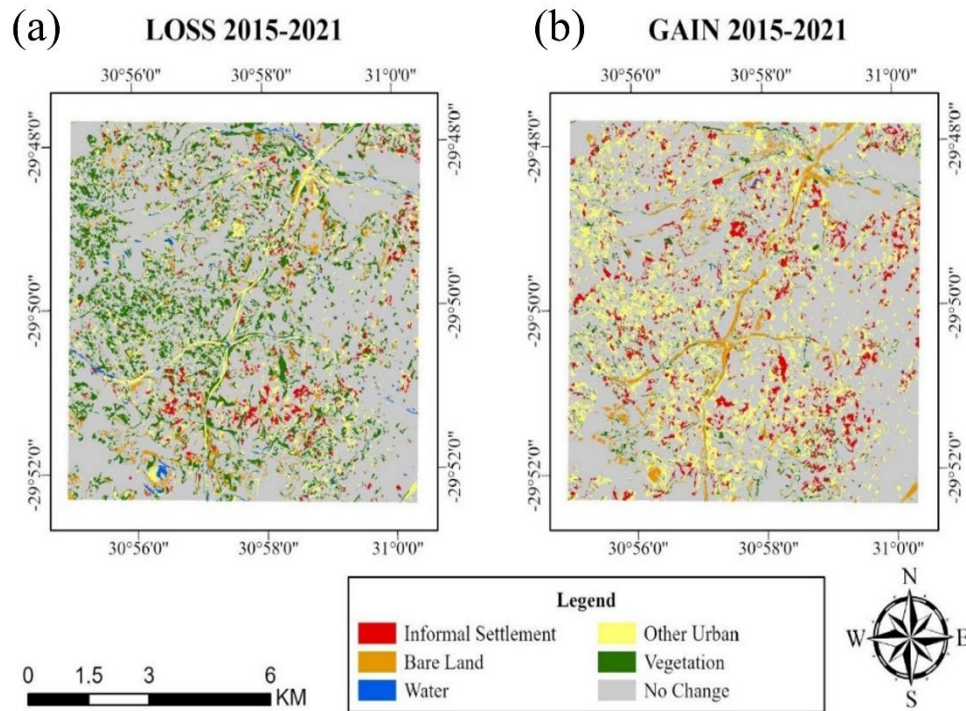


Figure 6.5. (a) The category loss map; and (b) the category gain map for the time interval 2015 to 2021.

6.3.2. Intensity analysis

6.3.2.1. Category level

Figure 6.6 shows graphical representation of the loss and gain intensities for different classes at the category level. Each category has pair of bars which show the intensity of the changes. The main focus in the current study is on the informal settlement class losses or gains. The results revealed that the informal settlements were both actively gaining and actively losing during the period since the intensities passed the uniform intensity line. However, the gain intensity was greater than the loss intensity. Although “other urban” class experienced gross gains, the gain was dormant. In fact, the other urban class is dormant for both gain and loss during the interval. Results also reveal that bare land and informal settlements were both actively gaining and losing, rendering them the most active of all land use categories (Badmos et al., 2018). However, for both categories the gain was more intensive than the loss.

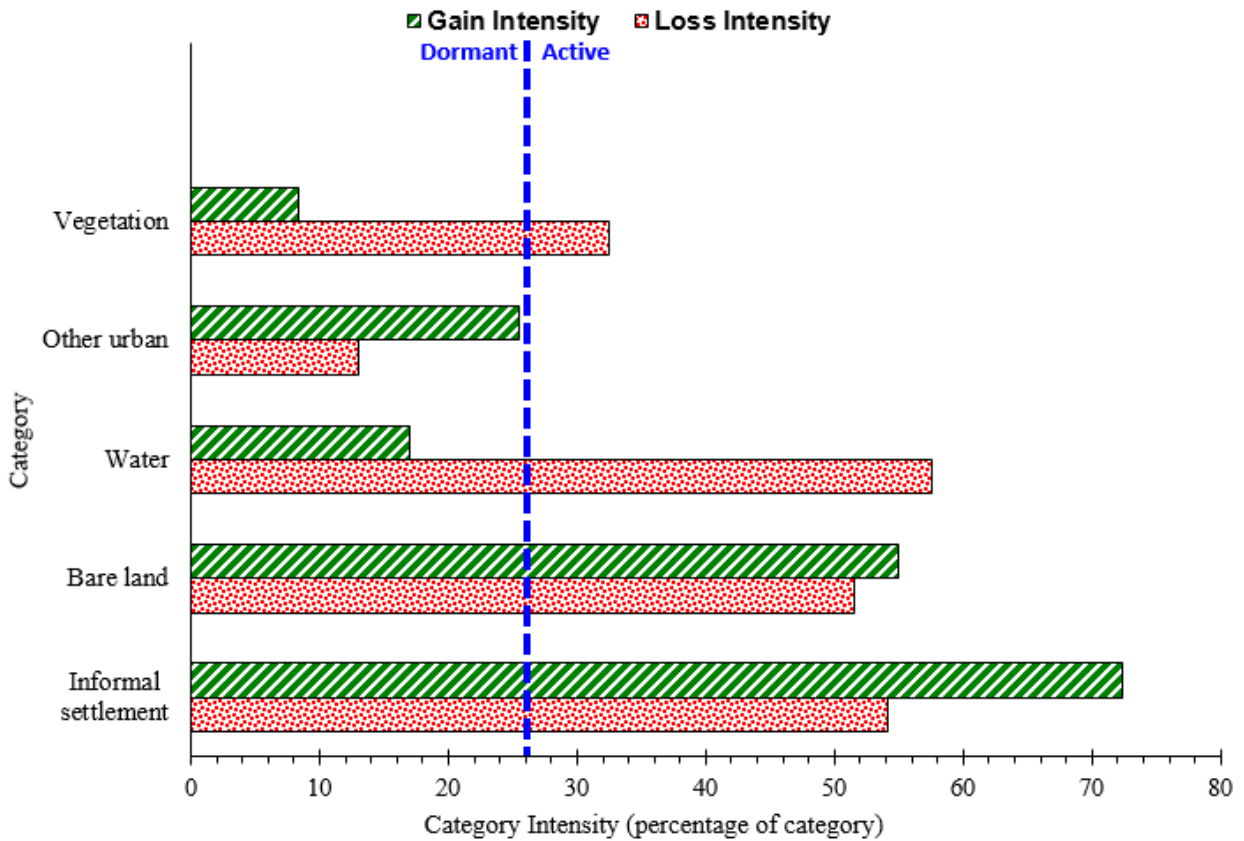


Figure 6.6. Intensity Analysis for category-level changes for each land category during the time interval 2015-2021

6.3.2.2. Transition level

The category level analysis revealed that informal settlements are actively losing and gaining. Of importance is the determination of which land use categories the informal settlements are either gaining from or losing to. Figure 6.7 presents the map of the transitions between informal settlements and other categories. Figure 6.7a shows transition of other categories to informal settlement, whilst Figure 6.7b shows transition from informal settlement to other categories. Throughout the time period, other urban, bare land and vegetation were transforming into informal settlements (Figure 6.7a), so informal settlements experienced high rates of increase from those classes. Similarly, informal settlements also lost to other urban and vegetated lands (Figure 6.7b).

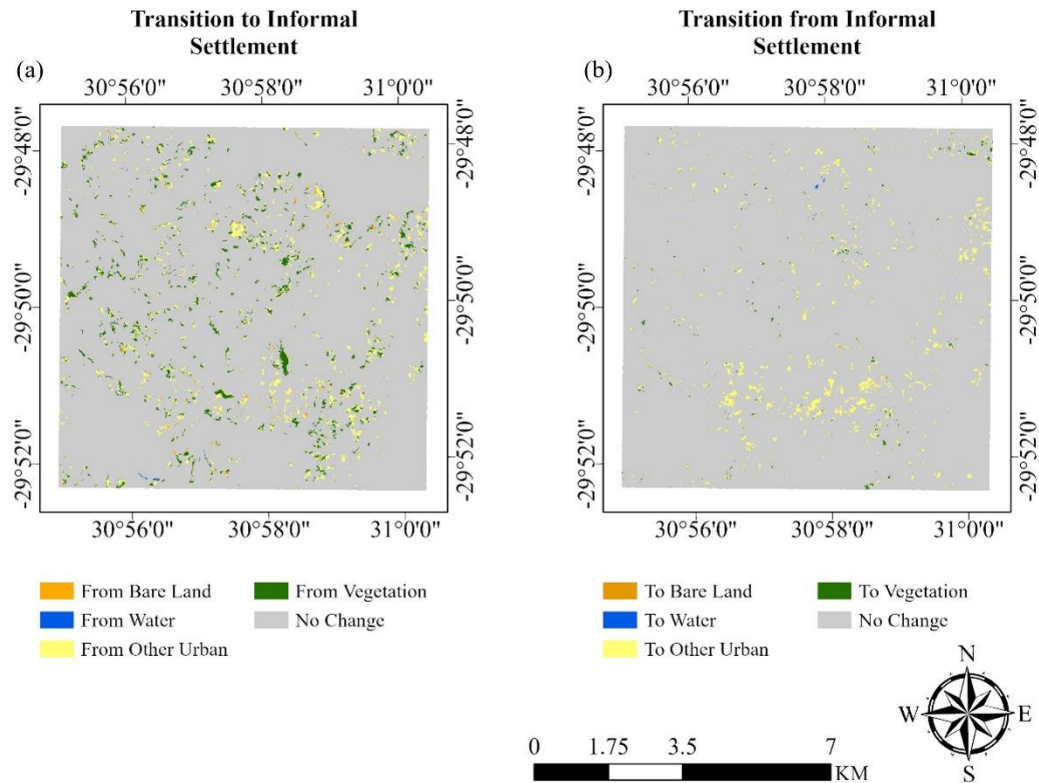


Figure 6.7. (a) Maps of land transitions to informal settlements, and (b) transitions from informal settlement for the 2015-2021 time period

Figure 6.8a presents the graphical representation of intensities of observed transitions given the gain of informal settlement, gain of other urban, gain of bare land, and gain of vegetation. The transition of water class to informal settlement lies to the left of the transition intensity line indicating avoidance of the water category. The bar for other urban stretches beyond the uniform line. This suggests that the informal settlement class most intensively targeted other urban. It is also crucial to note that during the same time interval other urban areas were also systematically targeting informal settlements (Figure 6.8b), so informal settlements experienced high conversion rates into other urban category in the area of study. Figure 6.8b confirms the targeting of informal settlement class by the other urban class. The scenario where on one hand informal settlements target other urban areas and , simultaneously, urban area targets informal settlements represents a systematic process of transition (Aldwaik and Pontius, 2012).

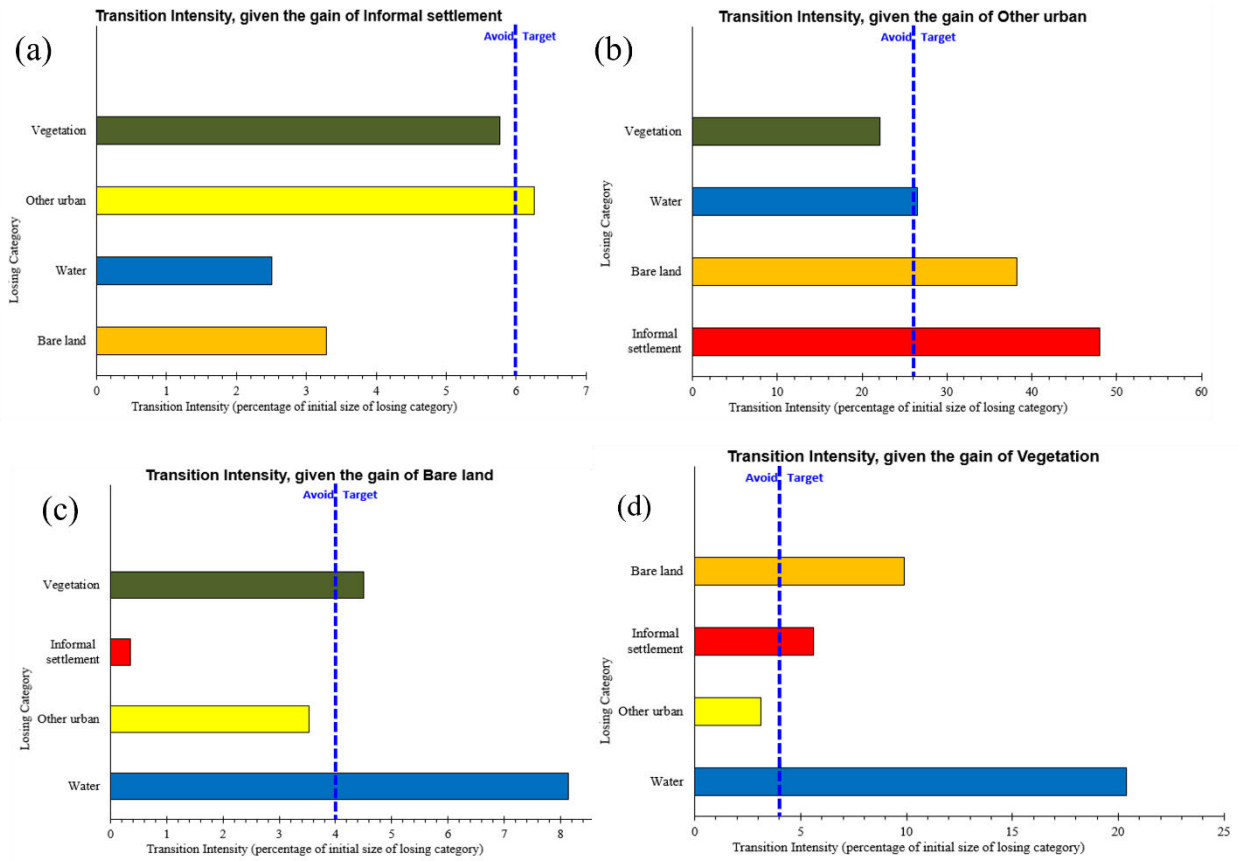


Figure 6.8. Intensity of the observed transitions (a) given the gross gain of informal settlement, (b) gross gain of other urban, (c) gross gain of bare land, and (d) gross gain of vegetation

Interestingly, the rate at which other categories were changing into the informal settlement class are higher than the rate at which informal settlements were changing to other classes, as shown in Figure 8.9 Considering all the transitions between informal settlements and other categories over the time period, about 68.9% of the transitions involved changes from other categories to informal settlements. This shows that informal settlement expansion was greater than their decline during the period.

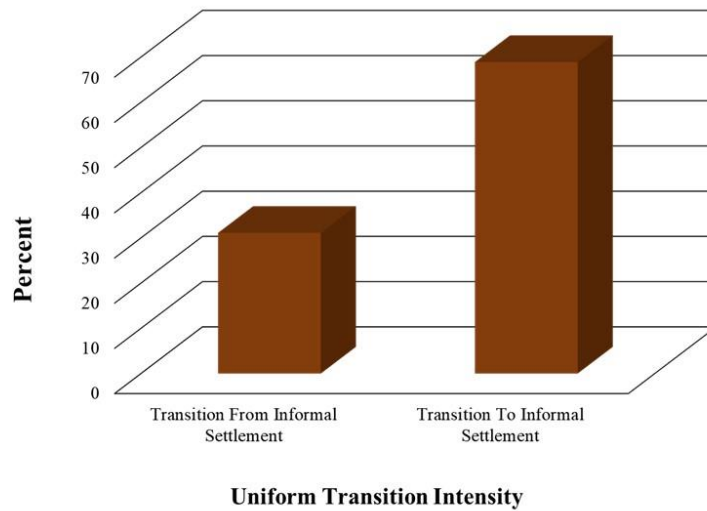


Figure 6.9. A representation of variation of uniform transition intensity of informal settlement during the 2015–2021 time interval.

6.4. Discussion

The study sought to investigate informal settlement dynamics in the context of subsequent LULC transitions for an area in Durban Metropolis, South Africa. In this study, GEE, with its geospatial analysis tools and parallel processing capabilities allowed effective implementation of OBIA for LULC classification. Classification results revealed a much lower F-score value of 67% for informal settlement class for 2015 than 2021, which yielded F-score of 92%. The 2015 classification result potentially demonstrates substantial confusion between informal settlements and other classes in the LULC map. Following Amani et al. (2019c), in their mapping of complex wetland environment, a trade off was considered between the efficiency of the model and level of accuracy. Due to fragmentation of the landscape, the lower classification result is potentially explained by the informal settlement class being less spectrally distinguishable during that year. Visual analysis of informal settlement layouts indicates sparsely laid out informal settlements in 2015 which, hypothetically, would be complex to distinguish from formal built up residential areas, due to similarity of the spectrum. Because of the dynamic nature of informal settlements (Kraff et al., 2020), they changed significantly over time and assumed morphological layout of contiguity, typical of informal

settlements, making 2021 class level more reasonable. Also, unclear and fuzzy boundaries between formal and informal housing units could have caused uncertainties in boundary delineation. Some informal settlements are found adjacent to high density formal buildings without clear cut borders, making them hardly distinguishable. According to Amani et al. (2019c), boundaries should be conservatively determined in order to avoid transitional areas.

Generally, the results of intensity analysis showed a net increase in area coverage of informal settlements. Category level analysis revealed informal settlements as actively gaining and losing within the period. However, the intensity of gain was higher than the loss. Whilst rural urban migration has been regarded as the major cause of rapid expansion of informal settlements, for example Quarry Road West informal settlement in Durban (Williams et al., 2019), South Africa also grapples with influx of illegal migrants from the neighbouring countries. The influx of these migrants potentially explains the gain as they increasingly settle into these spontaneous, low-income settlements. These results compare favourably with Badmos et al. (2018) who also observed a net increase in area covered by informal settlements within the study period. It was also observed that areas that were initially covered by informal settlements in 2015 had been changed to other land use categories in 2021 (bare land, other urban area, and vegetation). Such conversions potentially explain the intense loss of informal settlements within the period. The observed transitions of informal settlements to other land cover classes in this interval could be attributed to some catastrophic events that happened between 2015 and 2021. For example, a fire engulfed Havelock informal settlement in December 2019 and engulfed the whole settlement (Georgiadou et al., 2021). Devastating climate events for example floods that have hit Durban in 2016 and 2019 can also help explain transitions from informal settlements to other classes. For instance, in May 2016 and April 2019 informal settlements experienced some of the worst and most devastating floods in the Quarry road west informal settlement, as they caused washing away of houses and massive displacements (Membele, 2022). Despite these disaster events, Williams et al. (2018) put forward that the settlement encountered numerous periods of rapid expansion, with most of these occurring just after significant flood and fire events.

Government responses to such catastrophic events help explain transitions from informal settlements to urban class. For instance, in response to Havelock fire incident, Project Preparation Trust, a local non-profit organization has embarked on reconstruction programme where new typologies, for instance, double-storey shacks are tested together with introduction

of climate-proof dwelling design in ten informal settlements in Durban, including Havelock (Georgiadou et al., 2021). Thus, the conversion of informal settlements to other urban land use category in the area of study could be a result of these disaster events or upgrading programmes.

The current result showing evidence of transitions from informal settlement to other categories is also consistent with Badmos et al. (2018)'s results, where there were also observed transitions from informal settlements to other land use categories. However, whilst the causes of the transitions in Durban are naturally induced, through disasters, Badmos et al. (2018) pointed out that demolitions were the causes in Lagos. This reveals differences in government policies between the nations, with South Africa aiming at protecting the right of each individual to the city.

The findings of the current study revealed an increase in area covered by other urban within the time interval. One explanation for the expansion is potentially due to South Africa's spatial development policies (Du Plessis, 2015) aimed at restructuring and redressing imbalances created by apartheid spatial planning, through and upgrading programmes, as well as associated physical infrastructural development. Before 1994, South Africa's highly regulated urban growth was shaped by the restrictive Prevention of Illegal Squatters Act of 1951 (Odindi et al., 2012). Today, the South African constitution enforces citizens' 'right to the city' (Parikh et al., 2020). Notwithstanding, the post-apartheid continues to define human settlements. Even though, the South African Constitution (1996) maintains a progressive legal and policy framework that guarantees the right of the individual to access adequate housing (Parikh et al., 2020). Thus, in an effort to redress the imbalances, state-subsidized housing programmes are ongoing, where eligible beneficiaries are granted a variety of state subsidized housing options.

Transition level analysis results indicated that informal settlements actively targeted other urban class. Theoretically, the transition from other urban to informal settlement could also be large for two reasons. First, other urban's start size is larger than most categories. Second, informal settlement's gain targets other urban. If all transition intensities were equal, then informal settlement would take more from other urban than any other category. A question would be asked "What processes drive informal settlement dwellers to target other urban and to avoid vegetation?" Figure 8.8b shows also that less than half of other urban's intensity bar is to the right of the uniform line, which means that informal settlement's targeting of other urban explains less of the transition from other urban to informal settlement. Instead, more than

half of other urban's intensity bar is to the left of the uniform line meaning that other urban's size explains most of the transition from other urban to Informal settlement. The fact that other urban targets informal settlements and informal settlements targets other urban imply systematic process of transition (Badmos et al., 2018). Accentuating the argument, Teixeira et al. (2014) alluded that a given systematic transition over a period corroborates potential link of that specific transition to some management policy prevailing during that period of time. The targeting of informal settlement class by other urban class (Figure 8b) can, thus, be attributed to the in-situ upgrading programmes that involve the formalization of informal settlements in their original location, preserving social and economic networks (Del Mistro and Hensher, 2009).

There was also an indication of decline in vegetated area as well as area designated as water between 2015 and 2021 (Figure 6.4). According to Badmos et al. (2018), vegetation loss is a common feature in urban areas, where encroachment of vegetated land forms part of urban expansion. In their investigation of LULC in the context of green spaces, earlier study by also revealed a decline in green urban spaces owing to transformation of the landscape in eThekweni municipality through government's Reconstruction and Development Programme aiming to address housing challenges. It is important to note that, although there was evident decline in vegetation over time, results of intensity analysis stipulated that informal settlement class avoided vegetation. This is partially expounded by the fact that most vegetated land in South Africa is protected. Even so, previous study by Odindi et al. (2012) submitted that once green areas are cleared for establishment of physical structures, the informal dwellers may contribute to further exploitation of the greenery through wood extraction for fuel. Ordinarily, an increase in population is usually associated with increased demand for fuel firewood which makes logging prevalent in areas near human settlements. In agreement with results of the current study, Badmos et al. (2018), in their study in Lagos, also identified a decline in vegetated areas. Similarly, the authors revealed that informal settlements in Lagos were not targeting vegetation. However, the authors acknowledged that as migrants flocked Lagos the inflow was accommodated in already established informal settlement communities. Thus, their expansion cannot be explained in terms clearance of forest for establishment of new settlements but expansion of existing informal settlements. However, despite the fact that informal settlement's gain avoids vegetation, the change from vegetation to informal settlement is large (Figure 6.7a), theoretically, because of vegetation's large start size.

Satterthwaite et al. (2020) asserted that informal settlements experience the worst climate change effects because of their ill preparedness as well as poor construction materials and lack of preventative infrastructure that makes them highly vulnerable to high risks of floods and landslides. They tend to be located in flood prone areas such as flood plains or in proximity to water bodies (Abunyewah et al., 2018, De Risi et al., 2013). Although the findings for transition level of intensity analysis demonstrated avoidance of water bodies by informal settlements during the 2015–2021 time interval, the loss in area of coverage is indicative of encroachment. Since other urban class has shown that it targets water, and similarly informal settlements target urban, the systematic process of transition could be indicative of encroachment of water bodies even by the informal settlements.

Overall, the main two targeting transitions from other urban to informal settlement and vice versa are in line with policy. However, if land change patterns are not adequately linked to processes, sustainability issues persist. Given the complexity of Kwazulu-Natal landscape, it is vital to understand the drivers, patterns and processes of LULC change for different urban management and policy implications. To help in developing the best land use strategies, a further validation on social factors is imperative.

6.5. Conclusion

This study contributes to assessment of informal settlement dynamics in Durban and implications for sustainable urban management. The study successfully utilized OBIA, leveraging the SNIC algorithm for segmentation, and the GLCM algorithm within the GEE. The resultant maps were useful in providing input data for intensity analysis.

The main conclusions were:

- Informal settlement dimensions, as well as their spatial extent increased with a net percentage increase of 3%. This could be attributed to in migration from rural area and neighbouring countries.
- Results from category level analysis demonstrated an active gain of informal settlement class with gain intensity of 72%.
- Transition level of intensity analysis showed a systematic process of transition between informal settlements and other urban areas.
- The systematic transitions were influenced by government policy through its development programmes.

- Informal settlement growth was faster than its decline in the interval studied.
- Disaster events for example fires and flood events were major contributory factors contributing to informal settlements losing land to other categories.
- Poor maintenance of existing building structures such as industries could also help explain the transition of other urban areas to informal settlements.

The results reveal the potential for spatial challenges to continue to marginalize the poor, with impact on South Africa's long-term development. More specifically, such dynamics pose potential planning challenges for disaster risk protection and municipal service provision. On the other hand, transition level intensity analysis showed a systematic process of transition between informal settlements and other urban areas, potentially influenced by government policy, through its development programs. Although the Durban municipality strives to improve the livelihoods of informal settlement dwellers through in situ upgrading, under the National Housing Code, the findings read as a tale of caution to policy makers within South Africa, as well as countries within the developing world as a whole. The results suggest that city authorities should respond to the detailed urban space and planning requirements for sustainable urban area management policies, design of effective intervention strategies in order to minimize disaster risk, as well as legislative decisions toward curbing settling on precarious areas.

CHAPTER SEVEN:

Integrating texture analysis and innovative modelling approaches for capturing morphological diversities and dynamics of informal settlements in Durban metropolitan area, South Africa: A Synthesis

7.1. Introduction

The urban fabric in most developing countries faces the challenge of burgeoning informal settlements. The alarming growth of the informal settlements has resulted in a slew of disasters including poverty, and exposure to natural disasters, such as floods, induced by their location on flood vulnerable areas. Urbanization's complexities, such as, uncontrolled population growth, rural-urban migration, under and unemployment, discrimination and marginalization, as well as segregation policies, in some cases, are perpetuating the ongoing growth of informal settlements (Fox, 2014, UN-Habitat, 2015). These factors pose challenges for sustainable urbanization policies and strategies (Jones, 2017). Furthermore, the lack of accurate base maps and spatial information, complex morphological layouts, inherent spatial heterogeneity, and the dynamic nature of these deprived areas (i.e. informal settlements) impede accurate prediction of their geographies and thus complicates efforts to achieve goals aimed at improving their deplorable living conditions (Hofmann et al., 2015, Taubenböck et al., 2018, Wang et al., 2019a). Consequently, there is a need for techniques that provide more refined characterization of informal settlements in a timelier and reliable manner, in order to guide sustainable policy decisions and monitor their progression (Pratomo et al., 2017). With increased availability of high-resolution data, there has been progress in the use of, particularly image texture, in enhancing and capturing the morphological features of informal settlements (Kohli et al., 2016c, Mboga et al., 2017, Prabhu and Parvathavarthini, 2021). However, unavailability or high costs of appropriate earth observation (EO) data (for example, QuickBird, WorldView, and Orbview) (Taubenböck et al., 2018) has also been a hindrance to precise characterization of their varied forms in resource constrained countries. Freely downloadable Sentinel-2A has however presented a solution. Taking advantage of Sentinel-2A's high spatial and spectral resolution with strategically positioned bands including red-edge can enhance the mapping of complex morphologies of urban built-up areas. Similarly, the availability of high resolution PlanetScope imagery in Google Earth Engine Platform has complemented efforts to enhance mapping precision in complex urban environments (Kelley

et al., 2018, Mananze et al., 2020, Teluguntla et al., 2018). Its inbuilt simple non-iterative clustering (SNIC) and grey-level co-occurrence matrix (GLCM) for segmentation and texture feature extraction, respectively, has allowed more nuanced approaches such as GEOBIA for improving the mapping of informal settlements. In addition, given the constantly changing urban form (Kraff et al., 2020), there is a need for quantitative characterization of informal settlements and their dynamics in relation to LULC transitions. Intensity analysis allows an in-depth monitoring of LULC changes, providing linkages between patterns and processes, thus bridging the gap from static to multi-temporal measurement (Mwangi et al., 2017, Teixeira et al., 2014). In general, cutting-edge classification methods, particularly through the GEE embedded machine learning RF algorithm, have enabled quantitative characterization of informal settlements for evaluation of dynamic morphologic informal settlements. Therefore, this study explored the integration of texture analysis and innovative modeling approaches for capturing the morphological diversities and dynamics of informal settlements in the Durban metropolitan area in South Africa.

7.2. Conclusions

The thesis sought to explore the integration of image texture features with cutting edge approaches in characterization of spatial heterogeneity and dynamics of morphological informal settlements in a fragmented landscape of Durban. Findings reported in the current study demonstrated the efficacy of incorporating image texture in varied approaches that ranged from fusion of data, exploitation of varied feature sets, an object-based image classification framework and most importantly, within the cloud computing environment of GEE in capturing characteristic morphologic informal settlement features. The main conclusions were as follows:

- 1) Progress on the use of texture analysis in mapping informal settlements was well documented. However, gaps existed in the use of texture-based approaches in sub-Saharan African cities, particularly in South Africa where studies were concentrated in Johannesburg with no coverage for Durban. An investigation of the applicability of various texture analysis algorithms also revealed transferability issues in different geographical settings owing to varied morphological and typological characteristics. From the few studies that exploited texture feature selection, it could be inferred that there were uncertainties as to whether reduction of feature dimensional space would

enhance informal settlement accuracy or not, presenting research gap in the South African landscape context. Also, whilst high data costs and, sometimes unavailability of high-resolution data were cited as a hindrance for precision mapping of informal settlements, freely downloadable Sentinel-2A was scarcely exploited.

- 2) Capitalizing on the 10 m bands of Sentinel-2A, the 20 m bands were successfully pan sharpened using five algorithms in the component substitution category. Pan sharpening Sentinel-2A showed potential to increase the mapping accuracy of the areas of deprivation. Integration of pan sharpened images with image texture revealed the best result when the full range of the Sentinel spectrum was exploited, using Gram Schmidt algorithm. The findings revealed the potency of integrating pansharpening, image texture as well as high spectral resolution in the capturing of characteristic morphology of informal settlements in the Durban landscape.
- 3) GEE's Sentinel-2 archive, its advanced data processing functionality, and integrative potential through scripting allowed combination of a variety of data input features ranging from spectral data, spectral indices, and textural features for informal settlement mapping. Feature reduction reduced accuracy levels. The highest classification accuracies were achieved using a combination of textural features and spectral bands, with spectral indices reducing accuracy levels. The study demonstrated the efficacy of inbuilt RF model in extracting semantic land cover information for informal settlement identification.
- 4) Leveraging the computational power of the Google Earth Engine, the availability of high spatial resolution PlanetScope imagery, SNIC segmentation algorithm, and GLCM, OBIA was successfully explored for precise mapping of morphological informal settlements in Durban. Although there were some compromises in terms of accuracy, potentially due to heterogeneity of the landscape, and different typologies in terms of age, layout and size, results demonstrated potency of the approach.
- 5) Exploiting GEE and intensity analysis for mapping and assessment of informal settlement dynamics and associated LULC transitions delivered dependable results. Through determining the patterns of change, potential causes of nature of transitions involving informal settlements were established. In absolute terms, there was a net increase in area covered by informal settlements. Intensity

analysis at category level revealed an active gain of informal settlements between 2015 and 2021. The intensity analysis results indicated that informal settlements and other urban land dominated the dynamics of LULC change, with each of the two categories targeting each other, a representation of systematic process of transition. Efforts of the South African government to redress imbalances in terms of housing, through restructuring programmes, for example in situ upgrading programmes could potentially explain the systematic process. Intensity analysis approach effectually allowed analysis of linkages between patterns and processes.

7.3. Challenges and Recommendations for the future

The findings of this study accentuated the importance of synthesizing texture analysis with cutting edge approaches for enhanced characterisation of heterogenous morphological layouts of informal settlements. The requirement for high resolution imagery for texture analysis presents potential for exploration of pan sharpening approaches using Sentinel-2A imagery. Also, the availability of high resolution PlanetScope, allowed data fusion with Sentinel-2A imagery as well as leveraging of its computational power for object-based image classification. However, accurate capturing of the informal settlements' heterogeneity relies on the ability of the approach to capture accurately their morphological and typological diversities. Accurate capturing of their dynamic forms would also allow accurate monitoring of their spatial expansion with regard to subsequent LULC transitions. In this regard, the following recommendations should be considered for future research:

- Transferability of texture analysis approaches remains a challenge owing to diversities of morphological characteristics as well as absence of unified models to characterize informal settlements. The uniqueness of informal settlements' characteristic morphologies implies variations in applicability of approaches from place to place. Remote sensing fails to capture socio-political, economic, and cultural dynamics that shape the heterogeneous urban landscapes. Approaches that investigate the integration of earth observation data and field survey data should be investigated to promote comprehensive understanding of applicability of texture-based approaches in unique geographical settings.
- The study utilized Component substitution approaches such as Brovey transform and Gram-Schmidt approaches to pan sharpen Sentinel-2A for informal settlement

mapping. However, these approaches are characterised by high spectral distortion that compromises accuracy of mapping. The recommendation is thus to exploit multi-resolution analysis approaches such as PanNet which have competitive ability in addressing the pan sharpening issues both quantitatively and visually. Also, the spatial resolution of the PAN image was just two times better than that of the MS. Investigation of pan sharpening methods with scale ratio of at least 4 would be recommended.

- Cloud computing capabilities of GEE, as well as integrative potential through script writing, enabled successful classification of large feature sets using inbuilt machine learning RF algorithm for enhanced informal settlement mapping. However, intricate relations with other classes such as formal buildings and bare land was evident. To eliminate the noise, the current study recommends incorporation of topographic variables to augment input data, in order to capture the influence of aspect given that informal settlements locate on steep slopes.
- Despite the integration of PL, S2, and S1 for more comprehensive capturing of dynamic, morphologic informal settlements using GEOBIA, within GEE, uncertainties still remained, affecting class accuracy. Because of fragmentation of the landscape, there is need for careful segmentation during object-based classification in order to produce objects with appropriate size for classification. During the study, textural features were extracted from PlanetScope data. Given complementary advantages of SAR data, extraction of texture features from S1 could offer a potential avenue for further research in future studies.
- Leveraging the opportunities offered by cloud-computing resources for GEOBIA in the cloud, LULC maps were produced to use as input data for intensity analysis. However, informal settlement identification accuracy for 2015 was relatively too low for monitoring the changes in informal settlement areas. In addition to segmentation intricacies, the low accuracy could be related to the number of training data available for the class. In order to improve classification in future studies, it is recommended that more field data be included in order to initially improve classification result and allow subsequent operational informal settlement growth monitoring with appropriate accuracy.

References

- ABUNYEWAH, M., GAJENDRAN, T. & MAUND, K. 2018. Profiling informal settlements for disaster risks. . *Procedia engineering*, 212, 238-245.
- ACHANTA, R., SHAJI, A., SMITH, K., LUCCHI, A., FUA, P. & SÜSSTRUNK, S. 2012. SLIC superpixels compared to state-of-the-art superpixel methods. . *IEEE transactions on pattern analysis and machine intelligence* 34, 2274-2282.
- ACHANTA, R. & SUSSTRUNK, S. 2017. Superpixels and polygons using simple non-iterative clustering. . *In Proceedings of the IEEE Conference on Computer Vision and Pattern Recognition.*, 4651-4660.
- ADEPOJU, K. A. & ADELABU, S. A. 2019. Improving accuracy of Landsat-8 OLI classification using image composite and multisource data with Google Earth Engine. *Remote Sensing Letters*, 11, 107-116.
- AKINYEMI, F. O., PONTIUS, R. G. & BRAIMOH, A. K. 2016. Land change dynamics: insights from Intensity Analysis applied to an African emerging city. *Journal of Spatial Science*, 1-15.
- ALBRETCH, F., LANG, S. & HOLBLING, D. 2010. Spatial accuracy assessment of object boundaries for object-based image analysis. *ISPRS - International Archives of the Photogrammetry Remote Sensing and Spatial Information Sciences*
- ALCARAS, E., PARENTE, C. & VALLARIO, A. 2021. Automation of Pan-Sharpener Methods for Pléiades Images Using GIS Basic Functions. *Remote Sensing*, 13, 1550.
- ALDWAIK, S. Z. & PONTIUS JR, R. G. 2013. Map errors that could account for deviations from a uniform intensity of land change. *International Journal of Geographical Information Science*, 27, 1717-1739.
- ALDWAIK, S. Z. & PONTIUS, R. G. 2012. Intensity analysis to unify measurements of size and stationarity of land changes by interval, category, and transition. *Landscape and Urban Planning*, 106, 103-114.
- ALPARONE, L., WALD, L., CHANUSSOT, J., THOMAS, C., GAMBA, P. & BRUCE, L. M. 2007. Comparison of Pansharpening Algorithms: Outcome of the 2006 GRS-S Data-Fusion Contest. *IEEE Transactions on Geoscience and Remote Sensing*, 45, 3012-3021.
- AMANI, M., BRISCO, B., AFSHAR, M., MIRMAZLOUMI, S. M., MAHDAVI, S., MIRZADEH, S. M. J., HUANG, W. & GRANGER, J. 2019a. A generalized supervised classification scheme to produce provincial wetland inventory maps: an application of Google Earth Engine for big geo data processing. *Big Earth Data*, 3, 378-394.
- AMANI, M., MAHDAVI, S., AFSHAR, M., BRISCO, B., HUANG, W., MOHAMMAD JAVAD MIRZADEH, S., WHITE, L., BANKS, S., MONTGOMERY, J. & HOPKINSON, C. 2019c. Canadian Wetland Inventory using Google Earth Engine: The First Map and Preliminary Results. *Remote Sensing*, 11, 842.
- AMANI, M., SALEHI, B., MAHDAVI, S., GRANGER, J. E., BRISCO, B. & HANSON, A. 2017. Wetland Classification Using Multi-Source and Multi-Temporal Optical Remote Sensing Data in Newfoundland and Labrador, Canada. *Canadian Journal of Remote Sensing*, 43, 360-373.
- AMORIM, L. M. D. E., BARROS FILHO, M. N. M. & CRUZ, D. 2014. Urban texture and space configuration: An essay on integrating socio-spatial analytical techniques. *Cities*, 39, 58-67.
- AMRO, I., MATEOS, J., VEGA, M., MOLINA, R. & KATSAGGELOS, A. K. 2011. A survey of classical methods and new trends in pansharpening of multispectral images. *EURASIP Journal on Advances in Signal Processing.*, 1-22.

- ANSARI, R. A. & BUDDHIRAJU, K. M. 2019a. Textural segmentation of remotely sensed images using multiresolution analysis for slum area identification. *European Journal of Remote Sensing*, 52, 74-88.
- ANSARI, R. A., BUDDHIRAJU, K. M. & BHATTACHARYA, A. 2019a. Textural classification of remotely sensed images using multiresolution techniques. *Geocarto International*, 35, 1580-1602.
- ANSARI, R. A., MALHOTRA, R. & BUDDHIRAJU, K. M. Texture Based Identification of Informal Settlements in Contourlet Feature Space. Proceedings - 2019 IEEE International Symposium on Multimedia, ISM 2019, 2019b. 267-270.
- ARIMAH, B. C. 2010. SLUMS AS EXPRESSIONS OF SOCIAL EXCLUSION: EXPLAINING THE PREVALENCE OF SLUMS IN AFRICAN COUNTRIES*. *United Nations Human Settlements Programme (UN-HABITAT) Nairobi, Kenya*.
- ARMI, L. S. & FEKRI-ERSHAD, S. 2019. Texture Image Analysis and Texture Classification Methods - A Review. *International Online Journal of Image Processing and Pattern Recognition*, 2, 1-29.
- ARRIBAS-BEL, D., PATINO, J. E. & DUQUE, J. C. 2017. Remote sensing-based measurement of Living Environment Deprivation: Improving classical approaches with machine learning. *PLoS ONE*, 12.
- BADMOS, O., RIENOW, A., CALLO-CONCHA, D., GREVE, K. & JÜRGENS, C. 2018. Urban Development in West Africa—Monitoring and Intensity Analysis of Slum Growth in Lagos: Linking Pattern and Process. *Remote Sensing*, 10, 1044.
- BALSA-BARREIRO, J., LI, Y., MORALES, A. & PENTLAND, A. S. 2019. Globalization and the shifting centers of gravity of world's human dynamics: Implications for sustainability. *Journal of Cleaner Production*, 239, 117923.
- BARROS FILHO, M. & SOBREIRA, F. 2005. Assessing Texture Pattern in Slum Across Scales An Unsupervised Approach. *Centre for Advanced Spatial Analysis, University College London, Torrington Place, Gower St London, WC1E 7HB*.
- BARROS FILHO, M. N. & SOBREIRA, F. J. A. 2008. Accuracy of Lacunarity Algorithms InTexture Classification Of High Spatial Resolution Images From Urban areas *The International Archives of the Photogrammetry, Remote Sensing and Spatial Information Sciences*, XXXVII.
- BAUD, I., KUFFER, M., PFEFFER, K., SLIUZAS, R. & KARUPPANNAN, S. 2010. Understanding heterogeneity in metropolitan India: The added value of remote sensing data for analyzing sub-standard residential areas. *International Journal of Applied Earth Observation and Geoinformation*, 12, 359-374.
- BAYKAL, I. C. 2019. Performance Comparison of Texture Classifiers on Small Windows. *International Artificial Intelligence and Data Processing Symposium (IDAP). IEEE*.
- BELGIU, M. & DRĂGUȚ, L. 2016. Random forest in remote sensing: A review of applications and future directions. *ISPRS Journal of Photogrammetry and Remote Sensing*, 114, 24-31.
- BERRISFORD, S., 2011, September. Unravelling apartheid spatial planning legislation in South Africa: A case study. In *Urban forum*. Dordrecht: Springer Netherlands, 22, 3, 247-263.
- BESSINGER, M., LÜCK-VOGEL, M., SKOWNO, A. & CONRAD, F. 2022. Landsat-8 based coastal ecosystem mapping in South Africa using random forest classification in Google Earth Engine. *South African Journal of Botany*, 150, 928-939.
- BORANA, S. L., YADAV, S. K., PARIHAR, S. K. & KAPLAN, G. 2019. Pan-Sharpening of Landsat-8 Using Synthetic Sentinel-2 PAN Data. *Esri India User Conference, August 28-29, 2019*.

- BOUZEKRI, S., LASBET, A. A. & LACHEHAB, A. 2015. A New Spectral Index for Extraction of Built-Up Area Using Landsat-8 Data. *Journal of the Indian Society of Remote Sensing*, 43, 867-873.
- BRELSFORD, C., MARTIN, T., HAND, J. & BETTENCOURT, L. M. A. 2018. Toward cities without slums: Topology and the spatial evolution of neighborhoods. *SCIENCE ADVANCES*.
- BREN D'AMOUR, C., REITSMA, F., BAIOCCHI, G., BARTHEL, S., GUNERALP, B., ERB, K. H., HABERL, H., CREUTZIG, F. & SETO, K. C. 2017. Future urban land expansion and implications for global croplands. *Proc Natl Acad Sci U S A*, 114, 8939-8944.
- BÜRGMANN, T. 2015. Investigating the Separability of Slums in Mumbai based on RADARSAT Images using Object-based Image Analysis Methods. *Bachelor Thesis: HOCHSCHULE KARLSRUHE – UNIVERSITY OF APPLIED SCIENCES Faculty of Information Management and Media*.
- BWANGOY, J.-R. B., HANSEN, M. C., ROY, D. P., GRANDI, G. D. & JUSTICE, C. O. 2010. Wetland mapping in the Congo Basin using optical and radar remotely sensed data and derived topographical indices. *Remote Sensing of Environment*, 114, 73-86.
- CARRASCO, L., O'NEIL, A., MORTON, R. & ROWLAND, C. 2019. Evaluating Combinations of Temporally Aggregated Sentinel-1, Sentinel-2 and Landsat 8 for Land Cover Mapping with Google Earth Engine. *Remote Sensing*, 11, 288.
- CELIK, N. 2018. Change detection of urban areas in Ankara through Google Earth engine. In 2018 41st International Conference on Telecommunications and Signal Processing (TSP). 1-5. IEEE.
- CHE, X., FENG, M., JIANG, H., SONG, J. & JIA, B. 2015. Downscaling MODIS Surface Reflectance to Improve Water Body Extraction. *Advances in Meteorology*, 2015, 1-13.
- CHEN, J., CHEN, J., LIAO, A., CAO, X., CHEN, L., CHEN, X., HE, C., HAN, G., PENG, S., LU, M., ZHANG, W., TONG, X. & MILLS, J. 2015. Global land cover mapping at 30m resolution: A POK-based operational approach. *ISPRS Journal of Photogrammetry and Remote Sensing*, 103, 7-27.
- CHEN, W., LI, X., HE, H. & WANG, L. 2017. Assessing Different Feature Sets' Effects on Land Cover Classification in Complex Surface-Mined Landscapes by ZiYuan-3 Satellite Imagery. *Remote Sensing*, 10.
- CHEN, Y., ZHOU, Y. N., GE, Y., AN, R. & CHEN, Y. 2018. Enhancing Land Cover Mapping through Integration of Pixel-Based and Object-Based Classifications from Remotely Sensed Imagery. *Remote Sensing*, 10, 77.
- CHEN*, D., STOW, D. A. & GONG, P. 2010. Examining the effect of spatial resolution and texture window size on classification accuracy: an urban environment case. *International Journal of Remote Sensing*, 25, 2177-2192.
- CHOI, M. 2006. A new intensity-hue-saturation fusion approach to image fusion with a tradeoff parameter. *IEEE Transactions on Geoscience and Remote Sensing*, 44, 1672-1682.
- CIRIZA, R., SOLA, I., ALBIZUA, L., ÁLVAREZ-MOZOS, J. & GONZÁLEZ-AUDÍCANA, M. 2017. Automatic detection of uprooted orchards based on orthophoto texture analysis. *Remote Sensing*, 9.
- DE RISI, R., JALAYER, F., DE PAOLA, F., IERVOLINO, I., GIUGNI, M., TOPA, M. E., MBUYA, E., KYESSI, A., MANFREDI, G. & GASPARINI, P. 2013. Flood risk assessment for informal settlements. *Natural Hazards*, 69, 1003-1032.
- DEL MISTRO, R. & HENSHER, D. A. 2009. Upgrading Informal Settlements in South Africa: Policy, Rhetoric and what Residents really Value. *Housing Studies*, 24, 333-354.

- DESIQUEIRA, F. R., W.R., S. & PEDRINI, H. 2013. Multi-scale graylevelco-occurrence matrices for texture description. *Neurocomputing*, 120, 336–345
- DIEK, S., FORNALLAZ, F. & SCHAEPMAN, M. E. 2017. Barest Pixel Composite for Agricultural Areas Using Landsat Time Series. *Remote Sensing*, 9, 1245.
- DOLEAN, B.-E., BILAȘCO, Ș., PETREA, D., MOLDOVAN, C., VESCAN, I., ROȘCA, S. & FODOREAN, I. 2020. Evaluation of the Built-Up Area Dynamics in the First Ring of Cluj-Napoca Metropolitan Area, Romania by Semi-Automatic GIS Analysis of Landsat Satellite Images. *Applied Sciences*, 10, 7722.
- DONG, J., XIAO, X., MENARGUEZ, M. A., ZHANG, G., QIN, Y., THAU, D., BIRADAR, C. & MOORE, B., 3RD 2016. Mapping paddy rice planting area in northeastern Asia with Landsat 8 images, phenology-based algorithm and Google Earth Engine. *Remote Sens Environ*, 185, 142-154.
- DU PLESSIS, D. J. 2015. Land-use mix in South African cities and the influence of spatial planning: Innovation or following the trend? *South African Geographical Journal= Suid-Afrikaanse Geografiese Tydskrif*, 97, 217-242.
- DU, Q., YOUNAN, N. H., KING, R. & SHAH, V. P. 2007. On the Performance Evaluation of Pan-Sharpener Techniques. *IEEE Geoscience and Remote Sensing Letters*, 4, 518-522.
- DU, Y., ZHANG, Y., LING, F., WANG, Q., LI, W. & LI, X. 2016. Water Bodies' Mapping from Sentinel-2 Imagery with Modified Normalized Difference Water Index at 10-m Spatial Resolution Produced by Sharpening the SWIR Band. *Remote Sensing*, 8.
- DUQUE, J., PATINO, J. & BETANCOURT, A. 2017. Exploring the Potential of Machine Learning for Automatic Slum Identification from VHR Imagery. *Remote Sensing*, 9, 895.
- DUQUE, J. C., PATINO, J. E., RUIZ, L. A. & PARDO-PASCUAL, J. E. 2015. Measuring intra-urban poverty using land cover and texture metrics derived from remote sensing data. *Landscape and Urban Planning*, 135, 11-21.
- ELLA, L. A., VAN DEN BERGH, F. & VAN WYK, B. J. 2008. A comparison of texture feature algorithms for urban settlement classification. . In *IGARSS 2008-2008 International Geoscience and Remote Sensing Symposium.IEEE.*, 3, III-1308.
- ENGSTROM, R., COPENHAVER, A., NEWHOUSE, D., HALDAVANEKAR, V. & HERSH, J. 2017. Evaluating the Relationship between Spatial and Spectral Features Derived from High Spatial Resolution Satellite Data and Urban Poverty in Colombo, Sri Lanka. *IEEE Xplore*.
- EZEH, A., OYEBODE, O., SATTERTHWAITTE, D., CHEN, Y. F., NDUGWA, R., SARTORI, J., MBERU, B., MELENDEZ-TORRES, G. J., HAREGU, T., WATSON, S. I., CAIAFFA, W., CAPON, A. & LILFORD, R. J. 2017. The history, geography, and sociology of slums and the health problems of people who live in slums. *Lancet*, 389, 547-558.
- FALLATAH, A., JONES, S. & MITCHELL, D. 2018. Mapping Informal Settlements in the Middle East 3 Environment using an Object-Based Machine- 4 Learning Approach.
- FALLATAH, A., JONES, S. & MITCHELL, D. 2020. Object-based random forest classification for informal settlements identification in the Middle East: Jeddah a case study. *International Journal of Remote Sensing*, 41, 4421-4445.
- FALLATAH, A., JONES, S., MITCHELL, D. & KOHLI, D. 2019. Mapping informal settlement indicators using object-oriented analysis in the Middle East. *International Journal of Digital Earth*, 12, 802-824.
- FALLATAH, A., JONES, S., WALLACE, L. & MITCHELL, D. 2022. Combining Object-Based Machine Learning with Long-Term Time-Series Analysis for Informal Settlement Identification. *Remote Sensing*, 14, 1226.

- FARDA, N. M. 2017. Multi-temporal Land Use Mapping of Coastal Wetlands Area using Machine Learning in Google Earth Engine. *IOP Conference Series: Earth and Environmental Science*, 98, 012042.
- FEKRI-ERSHAD, S. 2020. Bark texture classification using improved local ternary patterns and multilayer neural network. *Expert Systems with Applications*, 158.
- FENG, L., HU, C., CHEN, X., CAI, X., TIAN, L. & GAN, W. 2012. Assessment of inundation changes of Poyang Lake using MODIS observations between 2000 and 2010. *Remote Sensing of Environment*, 121, 80-92.
- FERNANDES, E. 2011. Regularization of Informal Settlements in Latin America. *Policy Focus Report • Lincoln Institute of Land Policy. Cambridge, MA, USA.*
- FIROZJAEI, SEDIGHI, KIAVARZ, QURESHI, HAASE & ALAVIPANAH 2019. Automated Built-Up Extraction Index: A New Technique for Mapping Surface Built-Up Areas Using LANDSAT 8 OLI Imagery. *Remote Sensing*, 11, 1966.
- FOX, S. 2014. The Political Economy of Slums: Theory and Evidence from Sub-Saharan Africa. *World Development*, 54, 191-203.
- FUCHS, R., HEROLD, M., VERBURG, P. H., CLEVERS, J. G. & EBERLE, J. 2015. Gross changes in reconstructions of historic land cover/use for Europe between 1900 and 2010. *Glob Chang Biol*, 21, 299-313.
- GANDHARUM, L., HARTONO, D. M., KARSIDI, A. & AHMAD, M. 2022. Monitoring Urban Expansion and Loss of Agriculture on the North Coast of West Java Province, Indonesia, Using Google Earth Engine and Intensity Analysis. *ScientificWorldJournal*, 2022, 3123788.
- GANDHI, U. 2021. End-to-End Google Earth Engine Course. Spatial Thoughts. <https://courses.spatialthoughts.com/end-to-end-gee.html>.
- GANGKOFNER, U. G., PRADHAN, P. S. & HOLCOMB, D. W. 2007. Optimizing the high-pass filter addition technique for image fusion. *Photogrammetric Engineering & Remote Sensing*, 73, 1107-1118.
- GAŠPAROVIĆ, M. & JOGUN, T. 2017. The effect of fusing Sentinel-2 bands on land-cover classification. *International Journal of Remote Sensing*, 39, 822-841.
- GE, W., CHENG, Q., JING, L., WANG, F., ZHAO, M. & DING, H. 2020. Assessment of the Capability of Sentinel-2 Imagery for Iron-Bearing Minerals Mapping: A Case Study in the Cuprite Area, Nevada. *Remote Sensing*, 12, 3028.
- GEORGIADOU, M. C., LOGGIA, C., BISAGA, I. & PARIKH, P. 2021. Towards sustainable informal settlements: a toolkit for community-led upgrading in Durban. *Proceedings of the Institution of Civil Engineers - Engineering Sustainability*, 174, 83-93.
- GEVAERT, C. M., PERSELLO, C., SLIUZAS, R. & VOSSSELMAN, G. 2016. Classification of Informal Settlements through the Integration of 2d and 3d Features Extracted from UAV Data. *ISPRS Annals of Photogrammetry, Remote Sensing and Spatial Information Sciences*, III-3, 317-324.
- GEVAERT, C. M., PERSELLO, C., SLIUZAS, R. & VOSSSELMAN, G. 2017 Informal settlement classification using point-cloud and image-based features from UAV data *ISPRS Journal of Photogrammetry and Remote Sensing* 125, 225–236.
- GHAFFARIAN, S. & EMTEHANI, S. 2021. Monitoring Urban Deprived Areas with Remote Sensing and Machine Learning in Case of Disaster Recovery. *Climate*, 9.
- GIANNINI, B. M. & MEROLA, P. 2012. Texture Analysis for Urban Areas Classification in High Resolution Satellite Imagery. *Appl Rem Sens J*, 2, 65-71.
- GIBBS, A., SIKWEYIYA, Y. & JEWKES, R. 2014. 'Men value their dignity': securing respect and identity construction in urban informal settlements in South Africa. *Glob Health Action*, 7, 23676.

- GIBSON, L., ADELEKE, A., HADDEN, R. & RUSH, D. 2021. Spatial metrics from LiDAR roof mapping for fire spread risk assessment of informal settlements in Cape Town, South Africa. *Fire Safety Journal* 120.
- GIBSON, L., ENGELBRECHT, J. & RUSH, D. 2019. Detecting historic informal settlement fires with Sentinel 1 and 2 satellite data - Two case studies in Cape Town. *Fire Safety Journal*, 108.
- GILBERT, A. 2007. The Return of the Slum: Does Language Matter? *International Journal of Urban and Regional Research*, 31, 697-713.
- GILBERTSON, J. K., KEMP, J. & VAN NIEKERK, A. 2017. Effect of pan-sharpening multi-temporal Landsat 8 imagery for crop type differentiation using different classification techniques. *Computers and Electronics in Agriculture*, 134, 151-159.
- GIRIJA, G. & NIKHILA, R. I. 2018. Slum Extraction Approaches From High Resolution Satellite Data – A Case Study Of Madurai City. *International Journal of Pure and Applied Mathematics*, 119 14509-14514.
- GOLDBLATT, R., DEININGER, K. & HANSON, G. 2018. Utilizing publicly available satellite data for urban research: Mapping built-up land cover and land use in Ho Chi Minh City, Vietnam. *Development Engineering*, 3, 83-99.
- GORELICK, N., HANCHER, M., DIXON, M., ILYUSHCHENKO, S., THAU, D. & MOORE, R. 2017. Google Earth Engine: Planetary-scale geospatial analysis for everyone. *Remote Sensing of Environment*, 202, 18-27.
- GRAESSER, J., CHERIYADAT, A., VATSAVAI, R. R., CHANDOLA, V., LONG, J. & BRIGHT, E. 2012. Image based characterization of formal and informal neighborhoods in an urban landscape. *IEEE Journal of Selected Topics in Applied Earth Observations and Remote Sensing*, 5, 1164-1176.
- GRAM-HANSEN, B. J., HELBER, P., VARATHARAJAN, I., AZAM, F., COCA-CASTRO, A., KOPACKOVA, V. & BILINSKI, P. 2019. Mapping Informal Settlements in Developing Countries using Machine Learning and Low Resolution Multi-spectral Data. 361-368.
- GROCHALA, A. & KEDZIERSKI, M. 2017. A Method of Panchromatic Image Modification for Satellite Imagery Data Fusion. *Remote Sensing*, 9.
- HALL-BEYER, M. 2017. Practical guidelines for choosing GLCM textures to use in landscape classification tasks over a range of moderate spatial scales. *International Journal of Remote Sensing*, 38, 1312-1338.
- HAMUD, A. M., SHAFRI, H. Z. M. & SHAHARUM, N. S. N. 2021. Monitoring Urban Expansion And Land Use/Land Cover Changes In Banadir, Somalia Using Google Earth Engine (GEE). *IOP Conference Series: Earth and Environmental Science*, 767, 012041.
- HAO, P., ZHAN, Y., WANG, L., NIU, Z. & SHAKIR, M. 2015. Feature Selection of Time Series MODIS Data for Early Crop Classification Using Random Forest: A Case Study in Kansas, USA. *Remote Sensing*, 7, 5347-5369.
- HARALICK, R., SHANMUGAM, K. & DINSTEN, I. 1973. Textural features for image classification. *IEEE Transactions on Systems, Man, and Cybernetics.*, 3, 610-621.
- HASANI, M., SAKIEH, Y., DEZHAKAM, S., ARDAKANI, T. & SALMANMAHINY, A. 2017. Environmental monitoring and assessment of landscape dynamics in southern coast of the Caspian Sea through intensity analysis and imprecise land-use data. *Environ Monit Assess*, 189, 163.
- HASHIM, F., DIBS, H. & SABAH JABER, H. 2022. Adopting Gram-Schmidt and Brovey Methods for Estimating Land Use and Land Cover Using Remote Sensing and Satellite Images. *Nature Environment and Pollution Technology*, 21, 867-881.

- HAY CHUNG, L. C., XIE, J. & REN, C. 2021. Improved machine-learning mapping of local climate zones in metropolitan areas using composite Earth observation data in Google Earth Engine. *Building and Environment*, 199, 107879.
- HOFMANN, P., STROBL, J., BLASCHKE, T. & KUX, H. 2008. Detecting informal settlements from QuickBird data in Rio de Janeiro using an object based approach. In: Blaschke, T., Lang, S., Hay, G.J. (Eds.), *Lecture Notes in Geoinformation and Cartography*. . Springer, Berlin, Heidelberg., 530–553
- HOFMANN, P., TAUBENBÖCK, H. & WERTHMANN, C. 2015. Monitoring and modelling of informal settlements-A review on recent developments and challenges. 2015 joint urban remote sensing event (JURSE). 1-4.
- HU, T., LIU, J., ZHENG, G., LI, Y. & XIE, B. 2018. Quantitative assessment of urban wetland dynamics using high spatial resolution satellite imagery between 2000 and 2013. *Sci Rep*, 8, 7409.
- HUANG, F., HUANG, B., HUANG, J. & LI, S. 2018. Measuring Land Change in Coastal Zone around a Rapidly Urbanized Bay. *Int J Environ Res Public Health*, 15.
- HUANG, J., PONTIUS, R. G., LI, Q. & ZHANG, Y. 2012. Use of intensity analysis to link patterns with processes of land change from 1986 to 2007 in a coastal watershed of southeast China. *Applied Geography*, 34, 371-384.
- IRONS, J. R., MARKHAM, B. L., NELSON, R. F., TOLL, D. L., WILLIAMS, D. L., LATTY, R. S. & STAUFFER, M. L. 2007. The effects of spatial resolution on the classification of Thematic Mapper data. *International Journal of Remote Sensing*, 6, 1385-1403.
- JAGARNATH, M., THAMBIRAN, T. & GEBRESLASIE, M. 2019. Modelling urban land change processes and patterns for climate change planning in the Durban metropolitan area, South Africa. *Journal of Land Use Science*, 14, 81-109.
- JAWAK, S. D. & LUIS, A. J. 2013. A Comprehensive Evaluation of PAN-Sharpening Algorithms Coupled with Resampling Methods for Image Synthesis of Very High Resolution Remotely Sensed Satellite Data. *Advances in Remote Sensing*, 02, 332-344.
- JEWITT, D., GOODMAN, P. S., ERASMUS, B. F. N., O'CONNOR, T. G. & WITKOWSKI, E. T. F. 2015. Systematic land-cover change in KwaZulu-Natal, South Africa: Implications for biodiversity. *South African Journal of Science*, 111.
- JIN, Y., LIU, X., CHEN, Y. & LIANG, X. 2018. Land-cover mapping using Random Forest classification and incorporating NDVI time-series and texture: a case study of central Shandong. *International Journal of Remote Sensing*, 39, 8703-8723.
- JOHNSON, B., TATEISHI, R. & HOAN, N. 2012. Satellite Image Pansharpening Using a Hybrid Approach for Object-Based Image Analysis. *ISPRS International Journal of Geo-Information*, 1, 228-241.
- JONES, P. 2017. Formalizing the Informal: Understanding the Position of Informal Settlements and Slums in Sustainable Urbanization Policies and Strategies in Bandung, Indonesia. *Sustainability*, 9, 1436.
- KABIR, S., HEB, D.-C., SANUSIA, M. A. & WAN HUSSINA, W. M. A. 2010. Texture analysis of IKONOS satellite imagery for urban land use and land cover classification. *The imaging Science Journal*, 58.
- KAIMARIS, D. & PATIAS, P. 2016. Identification and area measurement of the built-up area with the Built-up Index (BUI). *Int. J. Adv. Remote Sens. GIS*, 5, 1844-1858.
- KAMALIPOUR, H. & DOVEY, K. 2019. Mapping the visibility of informal settlements. *Habitat International*, 85, 63-75.
- KAPLAN, G. & AVDAN, U. 2018. Sentinel-2 Pan Sharpening—Comparative Analysis. *Proceedings of the 23rd International Conference on*, 2.

- KAVITHA, J. C. & SURULIANDI, A. 2018. Feature Extraction Using Dominant Local Texture-Color Patterns (DLTCP) and Classification of Color Images. *J Med Syst*, 42, 220.
- KELLEY, L. C., PITCHER, L. & BACON, C. 2018. Using Google Earth Engine to Map Complex Shade-Grown Coffee Landscapes in Northern Nicaragua. *Remote Sensing*, 10, 952.
- KEMPER, T., MUDAU, N., MANGARA, P. & PESARESI, M. 2015. Towards an automated monitoring of human settlements in South Africa using high resolution SPOT satellite imagery. *The International Archives of Photogrammetry, Remote Sensing and Spatial Information Sciences*, 40, 1389.
- KHUMALO, P. P., TAPAMO, J. R. & VAN DEN BERGH, F. 2011. Rotation invariant texture feature algorithms for urban settlement classification. . In *2011 IEEE International Geoscience and Remote Sensing Symposium.IEEE*.
- KIT, O. & LÜDEKE, M. 2013. Automated detection of slum area change in Hyderabad, India using multitemporal satellite imagery. *ISPRS Journal of Photogrammetry and Remote Sensing*, 83, 130-137.
- KIT, O., LÜDEKE, M. & RECKIEN, D. 2012a. Texture-based identification of urban slums in Hyderabad, India using remote sensing data. *Applied Geography*, 32, 660-667.
- KOHLI, D., SLIUZAS, R., KERLE, N. & STEIN, A. 2012. An ontology of slums for image-based classification. *Computers, Environment and Urban Systems*, 36, 154-163.
- KOHLI, D., SLIUZAS, R. & STEIN, A. 2016a. Urban slum detection using texture and spatial metrics derived from satellite imagery. *Journal of Spatial Science*, 61, 405-426.
- KOHLI, D., STEIN, A. & SLIUZAS, R. 2016c. Uncertainty analysis for image interpretations of urban slums. *Computers, Environment and Urban Systems*, 60, 37-49.
- KOHLI, D., WARWADEKAR, P., KERLE, N., SLIUZAS, R. & STEIN, A. 2013a. Transferability of Object-Oriented Image Analysis Methods for Slum Identification. *Remote Sensing*, 5, 4209-4228.
- KÖSESOY, I., TEPECİK, A. & ÇETİN, M. 2012. A COMPARATIVE ANALYSIS OF IMAGE FUSION METHODS. *IEEE 20th Signal Processing and Communications Applications conference (SIU)- Acomparative analysis of image fusion methods.*, 1-4.
- KOUROSH NIYA, A., HUANG, J., KARIMI, H., KESHTKAR, H. & NAIMI, B. 2019. Use of Intensity Analysis to Characterize Land Use/Cover Change in the Biggest Island of Persian Gulf, Qeshm Island, Iran. *Sustainability*, 11, 4396.
- KPIENBAAREH, D., SUN, X., WANG, J., LUGINAAH, I., BEZNER KERR, R., LUPAFYA, E. & DAKISHONI, L. 2021. Crop Type and Land Cover Mapping in Northern Malawi Using the Integration of Sentinel-1, Sentinel-2, and PlanetScope Satellite Data. *Remote Sensing*, 13, 700.
- KRAFF, N. J., WURM, M. & TAUBENBÖCK, H. 2020. The dynamics of poor urban areas - analyzing morphologic transformations across the globe using Earth observation data. *Cities*, 107, 102905.
- KUFFER, M., BARROS, J. & SLIUZAS, R. V. 2014. The development of a morphological unplanned settlement index using very-high-resolution (VHR) imagery. *Computers, Environment and Urban Systems*, 48, 138-152.
- KUFFER, M., PFEFFER, K., BAUD, I. & SLIUZAS, R. 2013. ANALYSING SUB-STANDARD AREAS USING HIGH RESOLUTION REMOTE (VHR) SENSING IMAGERY. *N-AERUS XIV Enschede 12 - 14th September 2013*.
- KUFFER, M., PFEFFER, K. & SLIUZAS, R. 2016a. Slums from Space—15 Years of Slum Mapping Using Remote Sensing. *Remote Sensing*, 8, 455.

- KUFFER, M., PFEFFER, K., SLIUZAS, R. & BAUD, I. 2016b. Extraction of Slum Areas From VHR Imagery Using GLCM Variance. *IEEE Journal of selected topics in Applied Earth Observations And Remote Sensing*, 9.
- KUFFER, M., PFEFFER, K., SLIUZAS, R., BAUD, I. & MAARSEVEEN, M. 2017. Capturing the Diversity of Deprived Areas with Image-Based Features: The Case of Mumbai. *Remote Sensing*, 9, 384.
- KUFFER, M., SLIUZAS, R., PFEFFER, K. & BAUD, I. 2015. The Utility of the Co-occurrence Matrix to Extract Slum Areas from VHR Imagery.
- KUFFER, M., THOMSON, D. R., BOO, G., MAHABIR, R., GRIPPA, T., VANHUYSSSE, S., ENGSTROM, R., NDUGWA, R., MAKAU, J., DARIN, E., DE ALBUQUERQUE, J. P. & KABARIA, C. 2020. The Role of Earth Observation in an Integrated Deprived Area Mapping “System” for Low-to-Middle Income Countries. *Remote Sensing*, 12, 982.
- KUFFER, M., WANG, J., NAGENBORG, M., PFEFFER, K., KOHLI, D., SLIUZAS, R. & PERSELLO, C. 2018. The Scope of Earth-Observation to Improve the Consistency of the SDG Slum Indicator. *ISPRS International Journal of Geo-Information*, 7, 428.
- KUMAR, L. & MUTANGA, O. 2018. Google Earth Engine Applications Since Inception: Usage, Trends, and Potential. *Remote Sensing*, 10, 1509.
- KUMAR, L., SINHA, P. & TAYLOR, S. 2014. Improving image classification in a complex wetland ecosystem through image fusion techniques. *Journal of Applied Remote Sensing*, 8, 083616.
- LAI, F. & YANG, X. 2020a. Integrating spectral and non-spectral data to improve urban settlement mapping in a large Latin-American city. *GIScience and Remote Sensing*, 57, 830-844.
- LAN, Z. & LIU, Y. 2018. Study on Multi-Scale Window Determination for GLCM Texture Description in High-Resolution Remote Sensing Image Geo-Analysis Supported by GIS and Domain Knowledge. *ISPRS International Journal of Geo-Information*, 7, 175.
- LANARAS, C., BIOUCAS-DIAS, J., GALLIANI, S., BALTSAVIAS, E. & SCHINDLER, K. 2018. Super-resolution of Sentinel-2 images: Learning a globally applicable deep neural network. *ISPRS Journal of Photogrammetry and Remote Sensing*, 146, 305–319.
- LEAO, S. & LEAO, D. 2011. Targeting housing problems through urban texture analysis. *In Proceedings of the 12th International Conference on Computers in Urban Planning and Urban Management, Lake Louise, AB, Canada, 5–8 July*.
- LEONITA, G., KUFFER, M., SLIUZAS, R. & PERSELLO, C. 2018. Machine Learning-Based Slum Mapping in Support of Slum Upgrading Programs: The Case of Bandung City, Indonesia. *Remote Sensing*, 10, 1522.
- LI, M., ZHANG, R., LUO, H., GU, S. & QIN, Z. 2022. Crop Mapping in the Sanjiang Plain Using an Improved Object-Oriented Method Based on Google Earth Engine and Combined Growth Period Attributes. *Remote Sensing*, 14, 273.
- LI, Q., QIU, C., MA, L., SCHMITT, M. & ZHU, X. 2020. Mapping the Land Cover of Africa at 10 m Resolution from Multi-Source Remote Sensing Data with Google Earth Engine. *Remote Sensing*, 12.
- LI, X., CHEN, W., CHENG, X. & WANG, L. 2016. A Comparison of Machine Learning Algorithms for Mapping of Complex Surface-Mined and Agricultural Landscapes Using ZiYuan-3 Stereo Satellite Imagery. *Remote Sensing*, 8.
- LIANG, J., XIE, Y., SHA, Z. & ZHOU, A. 2020. Modeling urban growth sustainability in the cloud by augmenting Google Earth Engine (GEE). *Computers, Environment and Urban Systems*, 84, 101542.

- LIN, J., JIN, X., REN, J., LIU, J., LIANG, X. & ZHOU, Y. 2021. Rapid Mapping of Large-Scale Greenhouse Based on Integrated Learning Algorithm and Google Earth Engine. *Remote Sensing*, 13.
- LIU, Q., HUANG, C. & LI, H. 2020a. Quality Assessment by Region and Land Cover of Sharpening Approaches Applied to GF-2 Imagery. *Applied Sciences*, 10, 3673.
- LIU, X., HU, G., CHEN, Y., LI, X., HU, X., LI, S., PEI, F. & WANG, S. 2018. High-resolution multi-temporal mapping of global urban land using Landsat images based on the Google Earth Engine Platform. *Remote Sensing of Environment*, 209, 227-239.
- LIU, Y., ZHANG, H., ZHANG, M., CUI, Z., LEI, K., ZHANG, J., YANG, T. & JI, P. 2022. Vietnam wetland cover map: Using hydro-periods Sentinel-2 images and Google Earth Engine to explore the mapping method of tropical wetland. *International Journal of Applied Earth Observation and Geoinformation*, 115, 103122.
- LOGGIA, C. & GOVENDER, V. 2020. A hybrid methodology to map informal settlements in Durban, South Africa. *Proceedings of the Institution of Civil Engineers - Engineering Sustainability*, 173, 257-268.
- LU, D. & WENG, Q. 2007. A survey of image classification methods and techniques for improving classification performance. *International Journal of Remote Sensing*, 28, 823-870.
- LUO, C., QI, B., LIU, H., GUO, D., LU, L., FU, Q. & SHAO, Y. 2021. Using Time Series Sentinel-1 Images for Object-Oriented Crop Classification in Google Earth Engine. *Remote Sensing*, 13, 561.
- LUUS, F. P. S., VAN DEN BERGH, F. & MAHARAJ, B. T. J. 2014. Adaptive Threshold-Based Shadow Masking for Across-Date Settlement Classification of Panchromatic QuickBird Images. *IEEE Geoscience and Remote Sensing Letters*, 11, 1153-1157.
- LWIN, K. K. & MURAYAMA, Y. 2013. Evaluation of land cover classification based on multispectral versus pansharpened landsat ETM+ imagery. *GIScience & Remote Sensing*, 50, 458-472.
- MA, L., CHENG, L., LI, M., LIU, Y. & MA, X. 2015. Training set size, scale, and features in Geographic Object-Based Image Analysis of very high resolution unmanned aerial vehicle imagery. *ISPRS Journal of Photogrammetry and Remote Sensing*, 102, 14-27.
- MA, L., LI, M., MA, X., CHENG, L., DU, P. & LIU, Y. 2017. A review of supervised object-based land-cover image classification. *ISPRS Journal of Photogrammetry and Remote Sensing*, 130, 277-293.
- MAHABIR, R., CROITORU, A., CROOKS, A., AGOURIS, P. & STEFANIDIS, A. 2018. A Critical Review of High and Very High-Resolution Remote Sensing Approaches for Detecting and Mapping Slums: Trends, Challenges and Emerging Opportunities. *Urban Science*, 2, 8.
- MAHABIR, R., CROOKS, A., CROITORU, A. & AGOURIS, P. 2016. The study of slums as social and physical constructs: challenges and emerging research opportunities. *Regional Studies, Regional Science*, 3, 399-419.
- MAHDIANPARI, M., SALEHI, B., MOHAMMADIMANESH, F. & BRISCO, B. 2017. An Assessment of Simulated Compact Polarimetric SAR Data for Wetland Classification Using Random Forest Algorithm. *Canadian Journal of Remote Sensing*, 43, 468-484.
- MAHDIANPARI, M., SALEHI, B., MOHAMMADIMANESH, F., HOMAYOUNI, S. & GILL, E. 2018b. The First Wetland Inventory Map of Newfoundland at a Spatial Resolution of 10m Using Sentinel-1 and Sentinel-2 Data on the Google Earth Engine Cloud Computing Platform. *Remote Sensing*, 11.
- MAHDIANPARI, M., SALEHI, B., REZAEI, M., MOHAMMADIMANESH, F. & ZHANG, Y. 2018c. Very Deep Convolutional Neural Networks for Complex Land Cover Mapping Using Multispectral Remote Sensing Imagery. *Remote Sensing*, 10, 1119.

- MAHMOUD, A. G. 2021. Machine Learning and Pan-Sharpening of Sentinel-2 Data for Land Use Mapping in Arid Regions: A Case Study in Fayoum, Egypt. *Journal of Soil Sciences and Agricultural Engineering*, 12, 717-723.
- MALAMBO, L. & HEATWOLE, C. D. 2020. Automated training sample definition for seasonal burned area mapping. *ISPRS Journal of Photogrammetry and Remote Sensing*, 160, 107-123.
- MALLICK, J., TALUKDAR, S., SHAHFAHAD, PAL, S. & RAHMAN, A. 2021. A novel classifier for improving wetland mapping by integrating image fusion techniques and ensemble machine learning classifiers. *Ecological Informatics*, 65, 101426.
- MANANDHAR, R., ODEH, I. O. A. & PONTIUS, R. G. 2010. Analysis of twenty years of categorical land transitions in the Lower Hunter of New South Wales, Australia. *Agriculture, Ecosystems & Environment*, 135, 336-346.
- MANANZE, S., PÔÇAS, I. & CUNHA, M. 2020. Mapping and Assessing the Dynamics of Shifting Agricultural Landscapes Using Google Earth Engine Cloud Computing, a Case Study in Mozambique. *Remote Sensing*, 12, 1279.
- MANZOOR, S. A., GRIFFITHS, G. H., ROBINSON, E., SHOYAMA, K. & LUKAC, M. 2022. Linking Pattern to Process: Intensity Analysis of Land-Change Dynamics in Ghana as Correlated to Past Socioeconomic and Policy Contexts. *Land*, 11, 1070.
- MARFAI, M. A., FARDA, N. M., KHAKHIM, N., WICAKSONO, P. & WICAKSONO, A. 2018. Tidal Correction Effects Analysis on Shoreline Mapping in Jepara Regency. *Journal of Applied Geospatial Information*, 2, 145-151.
- MARX, C. & CHARLTON, S. 2003a. Durban, South Africa. UN-HABITAT (Hg.): Global report on human settlements., 195-223.
- MARX, C. & CHARLTON, S. 2003b. UNDERSTANDING SLUMS: Case Studies for the Global Report on Human Settlements. *Urban Slums Reports: The case of Durban, South Africa*.
- MATARIRA, D., MUTANGA, O. & NAIDU, M. 2022a. Google Earth Engine for Informal Settlement Mapping: A Random Forest Classification Using Spectral and Textural Information. *Remote Sensing*, 14, 5130.
- MATARIRA, D., MUTANGA, O. & NAIDU, M. 2022b. Texture analysis approaches in modelling informal settlements: a review. *Geocarto International*, 1-28.
- MAURER, T. 2013. HOW TO PAN-SHARPEN IMAGES USING THE GRAM-SCHMIDT PAN-SHARPEN METHOD – A RECIPE. *International Archives of the Photogrammetry, Remote Sensing and Spatial Information Sciences, Volume XL-1/W1, ISPRS Hannover Workshop 2013, 21 – 24 May 2013, Hannover, Germany*.
- MAXWELL, A. E., STRAGER, M. P., WARNER, T. A., ZÉGRE, N. P. & YUILL, C. B. 2014. Comparison of NAIP orthophotography and RapidEye satellite imagery for mapping of mining and mine reclamation. *GIScience & Remote Sensing*, 51, 301-320.
- MAZEKA, B., PHINZI, K. & SUTHERLAND, C. 2021. Monitoring Changing Land Use-Land Cover Change to Reflect the Impact of Urbanisation on Environmental Assets in Durban, South Africa. *Sustainable Urban Futures in Africa*. Routledge.
- MBOGA, N., PERSELLO, C., BERGADO, J. & STEIN, A. 2017a. Detection of Informal Settlements from VHR Images Using Convolutional Neural Networks. *Remote Sensing*, 9, 1106.
- MDAKANE, L. & VAN DEN BERGH, F. 2012. Extended local binary pattern features for improving settlement type classification of QuickBird images. *In Proceedings of the Twenty-Third Annual Symposium of the Pattern Recognition Association of South Africa, PRASA (2012), pp. 68–74*.

- MEMBELE, G. M. 2022. *Integrating local, indigenous knowledge and geographical information system in mapping flood vulnerability at Quarry Road West informal settlement in Durban, KwaZulu-Natal (Doctoral dissertation).*
- MEMBELE, G. M., NAIDU, M. & MUTANGA, O. 2022a. Examining flood vulnerability mapping approaches in developing countries: A scoping review. *International Journal of Disaster Risk Reduction*, 69.
- MEMBELE, G. M., NAIDU, M. & MUTANGA, O. 2022b. Using local and indigenous knowledge in selecting indicators for mapping flood vulnerability in informal settlement contexts. *International Journal of Disaster Risk Reduction*, 71, 102836.
- MHANGARA, P., MAPURISA, W. & MUDAU, N. 2020. Comparison of Image Fusion Techniques Using Satellite Pour l'Observation de la Terre (SPOT) 6 Satellite Imagery. *Applied Sciences*, 10, 1881.
- MHANGARA, P. & ODINDI, J. 2013. Potential of texture-based classification in urban landscapes using multispectral aerial photos. *South African Journal of Science*, 109, 1-8.
- MISOFE, N., SHENG, L. & LYIMO, J. 2019. Land Use Change Trends and Their Driving Forces in the Kilombero Valley Floodplain, Southeastern Tanzania. *Sustainability*, 11, 505.
- MUDAU, N. & MHANGARA, P. 2021. Investigation of Informal Settlement Indicators in a Densely Populated Area Using Very High Spatial Resolution Satellite Imagery. *Sustainability*, 13, 4735.
- MUDAU, N. & MHANGARA, P. 2022. Towards understanding informal settlement growth patterns: Contribution to SDG reporting and spatial planning. *Remote Sensing Applications: Society and Environment*, 27, 100801.
- MUGIRANEZA, NASCETTI & BAN 2019. WorldView-2 Data for Hierarchical Object-Based Urban Land Cover Classification in Kigali: Integrating Rule-Based Approach with Urban Density and Greenness Indices. *Remote Sensing*, 11, 2128.
- MUGIRANEZA, T., NASCETTI, A. & BAN, Y. 2020. Continuous Monitoring of Urban Land Cover Change Trajectories with Landsat Time Series and LandTrendr-Google Earth Engine Cloud Computing. *Remote Sensing*, 12, 2883.
- MUI, A., HE, Y. & WENG, Q. 2015. An object-based approach to delineate wetlands across landscapes of varied disturbance with high spatial resolution satellite imagery. *ISPRS Journal of Photogrammetry and Remote Sensing*, 109, 30-46.
- MÜLLER, I., TAUBENBÖCK, H., KUFFER, M. & WURM, M. 2020. Misperceptions of Predominant Slum Locations? Spatial Analysis of Slum Locations in Terms of Topography Based on Earth Observation Data. *Remote Sensing*, 12, 2474.
- MUSHORE, T.D., MUTANGA, O., ODINDI, J., SADZA, V. & DUBE, T., 2022. Pansharpened landsat 8 thermal-infrared data for improved Land Surface Temperature characterization in a heterogeneous urban landscape. *Remote Sensing Applications: Society and Environment*, 26, 100728.
- MUSHORE, T. D., MUTANGA, O. & ODINDI, J. 2022. Determining the Influence of Long Term Urban Growth on Surface Urban Heat Islands Using Local Climate Zones and Intensity Analysis Techniques. *Remote Sensing*, 14, 2060.
- MWANGI, H., LARIU, P., JULICH, S., PATIL, S., MCDONALD, M. & FEGER, K.-H. 2017. Characterizing the Intensity and Dynamics of Land-Use Change in the Mara River Basin, East Africa. *Forests*, 9, 8.
- MYINT, S. W., GOBER, P., BRAZEL, A., GROSSMAN-CLARKE, S. & WENG, Q. 2011. Per-pixel vs. object-based classification of urban land cover extraction using high spatial resolution imagery. *Remote Sensing of Environment*, 115, 1145-1161.

- NAOREM, V., KUFFER, M., VERPLANKE, J. & KOHLI, D. 2016. ROBUSTNESS OF RULE SETS USING VHR IMAGERY TO DETECT INFORMAL SETTLEMENTS – A CASE OF MUMBAI, INDIA. *Faculty of Geo-Information Science and Earth Observation (ITC), University of Twente*.
- NGUYEN, H. T. T., DOAN, T. M., TOMPPO, E. & MCROBERTS, R. E. 2020. Land Use/Land Cover Mapping Using Multitemporal Sentinel-2 Imagery and Four Classification Methods—A Case Study from Dak Nong, Vietnam. *Remote Sensing*, 12.
- NIAZI, S., MOKHTARZADE, M. & SAEEDZADEH, F. 2015. A Novel Ihs-Ga Fusion Method Based on Enhancement Vegetated Area. *ISPRS - International Archives of the Photogrammetry, Remote Sensing and Spatial Information Sciences*, XL-1/W5, 543-548.
- NIKOLAKOPOULOS, K. G. 2008. Comparison of Nine Fusion Techniques for Very High Resolution Data. *Photogrammetric Engineering & Remote Sensing*, 74, 647–659.
- NKONKI-MANDLENI, B., OMOTAYO, A. O., IGHODARO, D. I. & AGBOLA, S. B. 2021. Analysis of the Living Conditions at eZakheleni Informal Settlement of Durban: Implications for Community Revitalization in South Africa. *Sustainability*, 13.
- NYAMEKYE, C., KWOFIE, S., GHANSAH, B., AGYAPONG, E. & BOAMAH, L. A. 2020. Assessing urban growth in Ghana using machine learning and intensity analysis: A case study of the New Juaben Municipality. *Land Use Policy*, 99, 105057.
- ODINDI, J., MHANGARA, P. & KAKEMBO, V. 2012. Remote sensing land-cover change in Port Elizabeth during South Africa's democratic transition. *South African Journal of Science*, 108.
- OGUNRONBI, S., 2014. : The Spatial Planning and Land Use Management Act (SPLUMA).
- OOI, G. L. & PHUA, K. H. 2007. Urbanization and slum formation. *J Urban Health*, 84, i27-34.
- OTUNGA, C., ODINDI, J. & MUTANGA, O. 2014. Land Use Land Cover Change in the fringe of eThekweni Municipality: Implications for urban green spaces using remote sensing. *South African Journal of Geomatics*, 3.
- OWEN, K. K. & WONG, D. W. 2013a. An approach to differentiate informal settlements using spectral, texture, geomorphology and road accessibility metrics. *Applied Geography*, 38, 107-118.
- OWEN, K. K. & WONG, D. W. 2013b. Exploring structural differences between rural and urban informal settlements from imagery: thebasurerosof Cobán. *Geocarto International*, 28, 562-581.
- PALSSON, F., SVEINSSON, J. R., BENEDIKTSSON, J. A. & AANAES, H. 2012. Classification of Pansharpened Urban Satellite Images. *IEEE Journal of Selected Topics in Applied Earth Observations and Remote Sensing*, 5, 281-297.
- PANDIT, V. R. & BHIWANI, R. J. 2015a. Image Fusion in Remote Sensing Applications: A Review. *International Journal of Computer Applications*, 120.
- PARIKH, P., BISAGA, I., LOGGIA, C., GEORGIADOU, M. C. & OJO-AROMOKUDU, J. 2020. Barriers and opportunities for participatory environmental upgrading: Case study of Havelock informal settlement, Durban. *City and Environment Interactions*, 5.
- PARK, H., CHOI, J., PARK, N. & CHOI, S. 2017. Sharpening the VNIR and SWIR Bands of Sentinel-2A Imagery through Modified Selected and Synthesized Band Schemes. *Remote Sensing*, 9, 1080.
- PARNELL, S. & CRANKSHAW, O. 2009. Urban exclusion and the (false) assumptions of spatial policy reform in South Africa.
- PATEL, A., JOSEPH, G., SHRESTHA, A. & FOINT, Y. 2019. Measuring deprivations in the slums of Bangladesh: implications for achieving sustainable development goals. *Housing and Society*, 46, 81-109.

- PATEL, N. N., ANGIULI, E., GAMBA, P., GAUGHAN, A., LISINI, G., STEVENS, F. R., TATEM, A. J. & TRIANNI, G. 2015. Multitemporal settlement and population mapping from Landsat using Google Earth Engine. *International Journal of Applied Earth Observation and Geoinformation*, 35, 199-208.
- PATEL, S. & BAPTIST, C. 2012. Editorial: Documenting by the undocumented. *Environment and Urbanization*, 24, 3-12.
- PELIZARI, P. A., SPRÖHNLE, K., GEIß, C., SCHOEPFER, E., PLANK, S. & TAUBENBÖCK, H. 2018. Multi-sensor feature fusion for very high spatial resolution built-up area extraction in temporary settlements. *Remote Sensing of Environment* 209, 793–807.
- PEREIRA, O. J. R., MELFI, A. J. & MONTES, C. R. 2017. Image fusion of Sentinel-2 and CBERS-4 satellites for mapping soil cover in the Wetlands of Pantanal. *INTERNATIONAL JOURNAL OF IMAGE AND DATA FUSION*, 8 148–172.
- PERSELLO, C. & STEIN, A. 2017. Deep Fully Convolutional Networks for the Detection of Informal Settlements in VHR images. *IEEE GEOSCIENCE AND REMOTE SENSING LETTERS*, 14.
- PHAN, T. N., KUCH, V. & LEHNERT, L. W. 2020. Land Cover Classification using Google Earth Engine and Random Forest Classifier—The Role of Image Composition. *Remote Sensing*, 12.
- PHIRI, D., SIMWANDA, M., SALEKIN, S., NYIRENDA, V., MURAYAMA, Y. & RANAGALAGE, M. 2020. Sentinel-2 Data for Land Cover/Use Mapping: A Review. *Remote Sensing*, 12.
- PONTIUS, R., GAO, Y., GINER, N., KOHYAMA, T., OSAKI, M. & HIROSE, K. 2013. Design and Interpretation of Intensity Analysis Illustrated by Land Change in Central Kalimantan, Indonesia. *Land*, 2, 351-369.
- PONTIUS, R. G., SHUSAS, E. & MCEACHERN, M. 2004. Detecting important categorical land changes while accounting for persistence. *Agriculture, Ecosystems & Environment*, 101, 251-268.
- PRABHU, R. & ALAGU RAJA, R. A. 2018. Urban Slum Detection Approaches from High-Resolution Satellite Data Using Statistical and Spectral Based Approaches. *Journal of the Indian Society of Remote Sensing*, 46, 2033-2044.
- PRABHU, R. & PARVATHAVARTHINI, B. 2021. An enhanced approach for informal settlement extraction from optical data using morphological profile-guided filters: A case study of madurai city. *International Journal of Remote Sensing*, 42, 6688-6705.
- PRABHU, R., PARVATHAVARTHINI, B. & ALAGU RAJA, R. A. 2021a. Slum Extraction from High Resolution Satellite Data using Mathematical Morphology based approach. *International Journal of Remote Sensing*, 42, 172-190.
- PRABHU, R., PARVATHAVARTHINI, B. & ALAGURAJA, A. R. 2021b. Integration of deep convolutional neural networks and mathematical morphology-based postclassification framework for urban slum mapping. *Journal of Applied Remote Sensing*, 15.
- PRABHU, R., UMASREE, S., AVUDAIAMMAL, R. & ALAGU RAJA, R. A. 2017. Urban Slum Extraction using GLCM based Statistical approach from Very High Resolution Satellite data. *2017 Ninth International Conference on Advanced Computing (ICoAC)*.
- PRAPTONO, N. H. & SIRAIT, P. 2013. An Automatic Detection Method for High Density Slums based on Regularity Pattern of Housing using Gabor Filter and GINI Index. *ICACIS*.
- PRATOMO, J., KUFFER, M., MARTINEZ, J. & KOHLI, D. 2017. Coupling Uncertainties with Accuracy Assessment in Object-Based Slum Detections, Case Study: Jakarta, Indonesia. *Remote Sensing*, 9, 1164.

- PU, D. C., SUN, J. Y., DING, Q., ZHENG, Q., LI, T. T. & NIU, X. F. 2020. Mapping Urban Areas Using Dense Time Series of Landsat Images and Google Earth Engine. *The International Archives of the Photogrammetry, Remote Sensing and Spatial Information Sciences*, XLII-3/W10, 403-409.
- PUSHPARAJ, J. & HEGDE, A. V. 2016. Evaluation of pan-sharpening methods for spatial and spectral quality. *Appl Geomat*.
- QU, L. A., CHEN, Z., LI, M., ZHI, J. & WANG, H. 2021. Accuracy Improvements to Pixel-Based and Object-Based LULC Classification with Auxiliary Datasets from Google Earth Engine. *Remote Sensing*, 13, 453.
- QUAN, B., PONTIUS, R. G. & SONG, H. 2019. Intensity Analysis to communicate land change during three time intervals in two regions of Quanzhou City, China. *GIScience & Remote Sensing*, 57, 21-36.
- QUAN, Y., TONG, T., FENG, W., DAUPHIN, G., HUANG, W. & XING, M. 2020. A Novel Image Fusion Method of Multi-Spectral and SAR Images for Land Cover Classification. *Remote Sensing*, 12.
- QUESADA-ROMÁN, A. 2022. Disaster Risk Assessment of Informal Settlements in the Global South. *Sustainability*, 14, 10261.
- RAMOLA, A., SHAKYA, A. K. & VAN PHAM, D. 2020. Study of statistical methods for texture analysis and their modern evolutions. *Engineering Reports*, 2.
- RAO, P., ZHOU, W., BHATTARAI, N., SRIVASTAVA, A. K., SINGH, B., POONIA, S., LOBELL, D. B. & JAIN, M. 2021. Using Sentinel-1, Sentinel-2, and Planet Imagery to Map Crop Type of Smallholder Farms. *Remote Sensing*, 13, 1870.
- RÄSÄNEN, A. & VIRTANEN, T. 2019. Data and resolution requirements in mapping vegetation in spatially heterogeneous landscapes. *Remote Sensing of Environment*, 230, 111207.
- REBA, M. & SETO, K. C. 2020. A systematic review and assessment of algorithms to detect, characterize, and monitor urban land change. *Remote Sensing of Environment* 242.
- ROBERTI DE SIQUEIRA, F., ROBSON SCHWARTZ, W. & PEDRINI, H. 2013. Multi-scale gray level co-occurrence matrices for texture description. *Neurocomputing*, 120, 336-345.
- RODRIGUEZ-GALIANO, V. F., PARDO-IGÚZQUIZA, E., CHICA-OLMO, M., MATEOS, J., RIGOL-SÁNCHEZ, J. P. & VEGA, M. 2012. A comparative assessment of different methods for Landsat 7/ETM+ pansharpening. *International Journal of Remote Sensing*, 33, 6574-6599.
- RODRIGUEZ LOPEZ, J. M., HEIDER, K. & SCHEFFRAN, J. 2017. Frontiers of urbanization: Identifying and explaining urbanization hot spots in the south of Mexico City using human and remote sensing. *Applied Geography*, 79, 1-10.
- RUDIASTUTI, A., FARDA, N. M., RAMDANI, D., WICAKSONO, P. & WIBOWO, S. B. 2021. Mapping built-up land and settlements: a comparison of machine learning algorithms in Google Earth engine. 47.
- RUFIN, P., PICOLI, M., BEY, A. & MEYFROIDT, P. 2022. An operational framework for large-area mapping of active cropland and short-term fallows in smallholder landscapes using PlanetScope data.
- RUIZ HERNANDEZ, I. E. & SHI, W. 2017. A Random Forests classification method for urban land-use mapping integrating spatial metrics and texture analysis. *International Journal of Remote Sensing*, 39, 1175-1198.
- SAMPER, J., SHELBY, J. A. & BEHARY, D. 2020. The Paradox of Informal Settlements Revealed in an ATLAS of Informality: Findings from Mapping Growth in the Most Common Yet Unmapped Forms of Urbanization. *Sustainability*, 12, 9510.

- SANDBORN, A. & ENGSTROM, R. N. 2016. Determining the Relationship between Census Data and Spatial Features Derived from High-Resolution Imagery in Accra, Ghana. *IEEE Journal of Selected Topics in Applied Earth Observations and Remote Sensing*, 9, 1970-1977.
- SANLI, F. B., ABDIKAN, S., ESETLILI, M. T. & SUNAR, F. 2016. Evaluation of image fusion methods using PALSAR, RADARSAT-1 and SPOT images for land use/ land cover classification. *Journal of the Indian Society of Remote Sensing*, 45, 591-601.
- SARP, G. 2014. Spectral and spatial quality analysis of pan-sharpening algorithms: A case study in Istanbul. *European Journal of Remote Sensing*, 47, 19-28.
- SATTERTHWAITE, D., ARCHER, D., COLENBRANDER, S., DODMAN, D., HARDOY, J., MITLIN, D. & PATEL, S. 2020. Building Resilience to Climate Change in Informal Settlements. *One Earth*, 2, 143-156.
- SCHMITT, A., SIEG, T., WURM, M. & TAUBENBÖCK, H. 2018. Investigation on the separability of slums by multi-aspect TerraSAR-X dual-co-polarized high resolution spotlight images based on the multi-scale evaluation of local distributions. *International Journal of Applied Earth Observation and Geoinformation*, 64, 181-198.
- SELVA, M., AIAZZI, B., BUTERA, F., CHIARANTINI, L. & BARONTI, S. 2015b. Hyper-sharpening: A first approach on SIM-GA data. *IEEE Journal of selected topics in applied earth observations and remote sensing*, 8, 3008-3024.
- SHABAT, A. M. & TAPAMO, J.-R. 2017. A comparative study of the use of local directional pattern for texture-based informal settlement classification. *Journal of Applied Research and Technology*, 15, 250-258.
- SHAFIZADEH-MOGHADAM, H., KHAZAEI, M., ALAVIPANAH, S. K. & WENG, Q. 2021. Google Earth Engine for large-scale land use and land cover mapping: an object-based classification approach using spectral, textural and topographical factors. *GIScience & Remote Sensing*, 58, 914-928.
- SHEKHAR, S. 2012. Detecting slums from Quick Bird data in Pune using an object oriented approach. *International archives of the photogrammetry, remote sensing and spatial information sciences*, 39, 519-524.
- SHELESTOV, A., LAVRENIUK, M., KUSSUL, N., NOVIKOV, A. & SKAKUN, S. 2017. Exploring Google Earth Engine Platform for Big Data Processing: Classification of Multi-Temporal Satellite Imagery for Crop Mapping. *Frontiers in Earth Science*, 5.
- SHETTY, S., GUPTA, P. K., BELGIU, M. & SRIVASTAV, S. K. 2021. Assessing the Effect of Training Sampling Design on the Performance of Machine Learning Classifiers for Land Cover Mapping Using Multi-Temporal Remote Sensing Data and Google Earth Engine. *Remote Sensing*, 13.
- SINGH, S. & SRIVASTAVA, D. 2017. GLCM and Its Application in Pattern Recognition. *5th International Symposium on Computational and Business Intelligence*, 2017.
- SOLECKI, W., SETO, K. C. & MARCOTULLIO, P. J. 2013. It's Time for an Urbanization Science. *Environment: Science and Policy for Sustainable Development*, 55, 12-17.
- STARK, T., WURM, M., ZHU, X. X. & TAUBENBÖCK, H. 2020. Satellite-Based Mapping of Urban Poverty With Transfer-Learned Slum Morphologies. *IEEE Journal of Selected Topics in Applied Earth Observations and Remote Sensing* 13, 5251-5263.
- STASOLLA, M. & GAMBA, P. 2008. Spatial Indexes for the Extraction of Formal and Informal Human Settlements From High-Resolution SAR Images. *IEEE Journal Of Selected Topics In Applied Earth Observations And Remote Sensing*, 1.
- STATISTICS, S. 2016. General household survey 2015 statistical release P0318. *Pretoria: Statistics South Africa*.

- STROMANN, O., NASCETTI, A., YOUSIF, O. & BAN, Y. 2019. Dimensionality Reduction and Feature Selection for Object-Based Land Cover Classification based on Sentinel-1 and Sentinel-2 Time Series Using Google Earth Engine. *Remote Sensing*, 12.
- SUHARTINI, N. & JONES, P. 2020. Better Understanding Self-Organizing Cities: A Typology of Order and Rules in Informal Settlements. *Journal of Regional and City Planning*, 31, 237-263.
- TASSI, A., GIGANTE, D., MODICA, G., DI MARTINO, L. & VIZZARI, M. 2021. Pixel- vs. Object-Based Landsat 8 Data Classification in Google Earth Engine Using Random Forest: The Case Study of Maiella National Park. *Remote Sensing*, 13, 2299.
- TASSI, A. & VIZZARI, M. 2020. Object-Oriented LULC Classification in Google Earth Engine Combining SNIC, GLCM, and Machine Learning Algorithms. *Remote Sensing*, 12, 3776.
- TAUBENBÖCK, H., KRAFF, N. J. & WURM, M. 2018. The morphology of the Arrival City - A global categorization based on literature surveys and remotely sensed data. *Applied Geography*, 92, 150-167.
- TAUBENBÖCK, H. & WIESNER, M. 2015. The spatial network of megaregions - Types of connectivity between cities based on settlement patterns derived from EO-data. *Computers, Environment and Urban Systems*, 54, 165-180.
- TAVARES, P. A., BELTRAO, N. E. S., GUIMARAES, U. S. & TEODORO, A. C. 2019. Integration of Sentinel-1 and Sentinel-2 for Classification and LULC Mapping in the Urban Area of Belem, Eastern Brazilian Amazon. *Sensors (Basel)*, 19.
- TEIXEIRA, Z., TEIXEIRA, H. & MARQUES, J. C. 2014. Systematic processes of land use/land cover change to identify relevant driving forces: implications on water quality. *Sci Total Environ*, 470-471, 1320-35.
- TELLMAN, B., EAKIN, H. & TURNER, B. L. 2022. Identifying, projecting, and evaluating informal urban expansion spatial patterns. *Journal of Land Use Science*, 17, 100-112.
- TELUGUNTLA, P., THENKABAIL, P. S., OLIPHANT, A., XIONG, J., GUMMA, M. K., CONGALTON, R. G., YADAV, K. & HUETE, A. 2018. A 30-m landsat-derived cropland extent product of Australia and China using random forest machine learning algorithm on Google Earth Engine cloud computing platform. *ISPRS Journal of Photogrammetry and Remote Sensing*, 144, 325-340.
- TINGZON, I., DEJITO, N., FLORES, R. A., DE GUZMAN, R., CARVAJAL, L., ERAZO, K. Z., CALA, I. E. C., VILLAVECES, J., RUBIO, D. & GHANI, R. 2020. Mapping New Informal Settlements Using Machine Learning and Time Series Satellite Images: An Application in the Venezuelan Migration Crisis. *IEEE /ITU International conference on Artificial Intelligence for Good (AI4G)*, 198-203.IEEE.
- TONG, S., BAO, G., RONG, A., HUANG, X., BAO, Y. & BAO, Y. 2020. Comparison of the Spatiotemporal Dynamics of Land Use Changes in Four Municipalities of China Based on Intensity Analysis. *Sustainability*, 12, 3687.
- TRIANNI, G., ANGIULI, E., LISINI, G. & GAMBÀ, P. 2014. Human settlements from Landsat data using Google Earth Engine. *IN 2014 IEEE Geoscience and Remote Sensing Symposium*, 1473-1476. IEEE.
- UN-HABITAT 2003. The Challenge of Slums-Global Report on Human Settlements. *Earthscan: London, UK*.
- UN-HABITAT 2015. Informal Settlements. *UN-Habitat: New York, NY, USA*, 1-8.
- UN-HABITAT 2016. World Cities Report 2016: Urbanization and Development—Emerging Futures; World Cities Report; UN: Nairobi, Kenya, 2016; ISBN 978-92-1-058281-0.
- UNDP 2018. Human Development Indices and Indicators: 2018 Statistical Update. *UNDP: New York, NY, USA*,.

- UNECE 2012. Informal settlements in countries with economies in transition in the UNECE Region.
- UNITED-NATIONS 2015. The Millennium Development Goals Report 2015. Available online: <http://www.un.org/millenniumgoals/> (accessed on 12 December 2016).
- UNITED-NATIONS 2019. World Urbanization Prospects 2018 *United Nations: New York, NY, USA*,.
- VAIOPOULOS, A. D. & KARANTZALOS, K. 2016. Pansharpening on the Narrow Vnir and Swir Spectral Bands of Sentinel-2. *ISPRS - International Archives of the Photogrammetry, Remote Sensing and Spatial Information Sciences*, XLI-B7, 723-730.
- VAN DEN BERGH, F. 2011. The effects of viewing-and illumination geometry on settlement type classification of quickbird images. . *In International Geoscience and Remote Sensing Symposium. IEEE.*, 1425-1428.
- VAN DER BERG, A., 2017. South Africa's integrated urban development framework and sustainable development goal 11: policy mismatch or success?. *Obiter*, 38(3), pp.557-573.
- VERGNI, L., VINCI, A., TODISCO, F., SANTAGA, F. S. & VIZZARI, M. 2021. Comparing Sentinel-1, Sentinel-2, and Landsat-8 data in the early recognition of irrigated areas in central Italy. *Journal of Agricultural Engineering*, 52.
- VERMA, D., JANA, A. & RAMAMRITHAM, K. 2019. Transfer learning approach to map urban slums using high and medium resolution satellite imagery. *Habitat International*, 88.
- VIVONE, G., ALPARONE, L., CHANUSSOT, J., DALLA MURA, M., GARZELLI, A., LICCIARDI, G. A., RESTAINO, R. & WALD, L. 2015. A Critical Comparison Among Pansharpening Algorithms. *IEEE Transactions on Geoscience and Remote Sensing*, 53, 2565-2586.
- VIZZARI, M. 2022. PlanetScope, Sentinel-2, and Sentinel-1 Data Integration for Object-Based Land Cover Classification in Google Earth Engine. *Remote Sensing*, 14, 2628.
- WANG, J., KUFFER, M. & PFEFFER, K. 2019a. The role of spatial heterogeneity in detecting urban slums. *Computers, Environment and Urban Systems* 73, 95-107.
- WANG, J., KUFFER, M., ROY, D. & PFEFFER, K. 2019b. Deprivation pockets through the lens of convolutional neural networks. *Remote Sensing of Environment*, 234, 111448.
- WANG, Q., SHI, W., LI, Z. & ATKINSON, P. M. 2016a. Fusion of Sentinel-2 images. *Remote Sensing of Environment*, 187, 241-252.
- WANG, T., ZHANG, H., LIN, H. & FANG, C. 2016b. Textural-Spectral Feature-Based Species Classification of Mangroves in Mai Po Nature Reserve from Worldview-3 Imagery. *Remote sensing*, 8.
- WANG, X., LIU, Y., LING, F. & XU, S. 2018. Fine spatial resolution coastline extraction from Landsat-8 OLI imagery by integrating downscaling and pansharpening approaches. *Remote Sensing Letters*, 9, 314-323.
- WEEKS, J. R., HILL, A., STOW, D., GETIS, A. & FUGATE, D. 2007. Can we spot a neighborhood from the air? Defining neighborhood structure in Accra, Ghana. *GeoJournal*, 69, 9-22.
- WEIGAND, M. 2017b. SAR Image Feature Analysis for Slum Detection in Megacities. *Masters thesis. University of Augsburg Faculty of Applied Computer Science Chair of Geoinformatics*.
- WEKESA, B. W., STEYN, G. S. & OTIENO, F. A. O. 2011. A review of physical and socio-economic characteristics and intervention approaches of informal settlements. *Habitat International*, 35, 238-245.

- WILLIAMS, D., MÁÑEZ COSTA, M., CELLIERS, L. & SUTHERLAND, C. 2018b. Informal Settlements and Flooding: Identifying Strengths and Weaknesses in Local Governance for Water Management. *Water*, 10, 871.
- WILLIAMS, D. S., MÁÑEZ COSTA, M., SUTHERLAND, C., CELLIERS, L. & SCHEFFRAN, J. 2019. Vulnerability of informal settlements in the context of rapid urbanization and climate change. *Environment and Urbanization*, 31, 157-176.
- WINTER, S. C., OBARA, L. M. & MCMAHON, S. 2020. Intimate partner violence: A key correlate of women's physical and mental health in informal settlements in Nairobi, Kenya. *PLoS One*, 15, e0230894.
- WU, G. & LIU, Y. 2015. Downscaling Surface Water Inundation from Coarse Data to Fine-Scale Resolution: Methodology and Accuracy Assessment. *Remote Sensing*, 7, 15989-16003.
- WURM, M., STARK, T., ZHU, X. X., WEIGAND, M. & TAUBENBÖCK, H. 2019. Semantic segmentation of slums in satellite images using transfer learning on fully convolutional neural networks. *ISPRS Journal of Photogrammetry and Remote Sensing*, 150, 59-69.
- WURM, M., TAUBENBÖCK, H., WEIGAND, M. & SCHMITT, A. 2017a. Slum mapping in polarimetric SAR data using spatial features. *Remote Sensing of Environment*, 194, 190-204.
- WURM, M., WEIGAND, M., SCHMITT, A., GEIß, C. & TAUBENBÖCK, H. 2017b. Exploitation of textural and morphological image features in Sentinel-2A data for slum mapping. In *2017 Joint Urban Remote Sensing Event (JURSE)*. *IEEE.*, 1-4.
- XIE, Z., PONTIUS JR, R. G., HUANG, J. & NITIVATTANANON, V. 2020. Enhanced Intensity Analysis to Quantify Categorical Change and to Identify Suspicious Land Transitions: A Case Study of Nanchang, China. *Remote Sensing*, 12, 3323.
- XIONG, J., THENKABAIL, P., TILTON, J., GUMMA, M., TELUGUNTLA, P., OLIPHANT, A., CONGALTON, R., YADAV, K. & GORELICK, N. 2017. Nominal 30-m Cropland Extent Map of Continental Africa by Integrating Pixel-Based and Object-Based Algorithms Using Sentinel-2 and Landsat-8 Data on Google Earth Engine. *Remote Sensing*, 9.
- YANG, G., YU, W., YAO, X., ZHENG, H., CAO, Q., ZHU, Y., CAO, W. & CHENG, T. 2021. AGTOC: A novel approach to winter wheat mapping by automatic generation of training samples and one-class classification on Google Earth Engine. *International Journal of Applied Earth Observation and Geoinformation*, 102, 102446.
- YANG, Y., LIU, Y., XU, D. & ZHANG, S. 2017. Use of intensity analysis to measure land use changes from 1932 to 2005 in Zhenlai County, Northeast China. *Chinese Geographical Science*, 27, 441-455.
- YE, S., PONTIUS, R. G. & RAKSHIT, R. 2018. A review of accuracy assessment for object-based image analysis: From per-pixel to per-polygon approaches. *ISPRS Journal of Photogrammetry and Remote Sensing*, 141, 137-147.
- YUAN, Y., LI, B., GAO, X., LIU, H., XU, L. & ZHOU, C. 2015. A method of characterizing land-cover swap changes in the arid zone of China. *Frontiers of Earth Science*, 10, 74-86.
- ZHANG, DONG, LIU, GAO, HU & WU 2019a. Mapping Tidal Flats with Landsat 8 Images and Google Earth Engine: A Case Study of the China's Eastern Coastal Zone circa 2015. *Remote Sensing*, 11, 924.
- ZHANG, J., LI, P. & WANG, J. 2014. Urban Built-Up Area Extraction from Landsat TM/ETM+ Images Using Spectral Information and Multivariate Texture. *Remote Sensing*, 6.

- ZHANG, M., SU, W., FU, Y., ZHU, D., XUE, J., HUANG, J., WANG, W., WU, J. & YAO, C. 2019b. Super-resolution enhancement of Sentinel-2 image for retrieving LAI and chlorophyll content of summer corn. *European Journal of Agronomy*, 111.
- ZHANG, Q., WANG*, J., GONG, P. & SHI, P. 2003. Study of urban spatial patterns from SPOT panchromatic imagery using textural analysis. *International Journal of Remote Sensing*, 24, 4137-4160.
- ZHANG, X. Q. 2016. The trends, promises and challenges of urbanisation in the world. *Habitat International*, 54, 241-252.
- ZHANG, Y. 2004. Understanding Image Fusion. *Photogrammetric Engineering & Remote Sensing*.
- ZHAO, Y., ZHU, W., WEI, P., FANG, P., ZHANG, X., YAN, N., LIU, W., ZHAO, H. & WU, Q. 2022. Classification of Zambian grasslands using random forest feature importance selection during the optimal phenological period. *Ecological Indicators*, 135, 108529.
- ZHENG, H., DU, P., CHEN, J., XIA, J., LI, E., XU, Z., LI, X. & YOKOYA, N. 2017. Performance Evaluation of Downscaling Sentinel-2 Imagery for Land Use and Land Cover Classification by Spectral-Spatial Features. *Remote Sensing*, 9, 1274.
- ZHOU, H., FU, L., SHARMA, R. P., LEI, Y. & GUO, J. 2021. A Hybrid Approach of Combining Random Forest with Texture Analysis and VDVI for Desert Vegetation Mapping Based on UAV RGB Data. *Remote Sens.*, 13.
- ZHOU, J., YAN GUO, R., SUN, M., DI, T. T., WANG, S., ZHAI, J. & ZHAO, Z. 2017. The Effects of GLCM parameters on LAI estimation using texture values from Quickbird Satellite Imagery. *Sci Rep*, 7, 7366.
- ZHOU, P., HUANG, J., PONTIUS, R. G., JR. & HONG, H. 2014. Land classification and change intensity analysis in a coastal watershed of Southeast China. *Sensors (Basel)*, 14, 11640-58.
- ZURQANI, H. A., POST, C. J., MIKHAILOVA, E. A. & ALLEN, J. S. 2019. Mapping Urbanization Trends in a Forested Landscape Using Google Earth Engine. *Remote Sensing in Earth Systems Sciences*, 2, 173-182.